

# Phases of Supersymmetric Gauge Theories on the Three-Sphere

Kazuma Shimizu

*Yukawa Institute for Theoretical Physics, Kyoto University, Kitashirakawa, Oiwakecho, Sakyo-ku,  
Kyoto 606-8502, Japan*

A Dissertation for the degree of Doctor of Philosophy

## Abstract

Three-dimensional supersymmetric gauge theories has been studied in various contexts such as understanding non-perturbative effects of gauge theory. The recent development of localization techniques for supersymmetric field theory enables us to approach its non-perturbative aspects because for some quantities the technique reduces the path integral needed to calculate its expectation value to an ordinary finite-dimensional integral. However, a localization technique usually requires supersymmetric theories to be defined on a compact manifold to avoid infrared divergence. Therefore, the results from localization techniques should not be interpreted by following flat-space intuition, in particular, for non-conformal theories. The purpose of this thesis is to introduce our recent works [2–5] where we found that the results from a localization technique cannot be interpreted by directly following flat-space intuition and discussed them in relation to the flat-space point of view. The results are summarized as follows:

From our results [1–3], it has been expected that in the large  $N$  limit the behavior of the three-sphere partition function of the mass-deformed ABJM theory drastically changes beyond the critical value of the mass. We also found the candidate of the large  $N$  solution which becomes dominant when the mass goes beyond the threshold and investigate physical meanings [4]. This result implies that the gravity dual theory also exhibits such a singular behavior and it is interesting to study the meaning of the threshold from the gravity side.

In my work [5], we investigated the general behavior of the partition function in the infinite mass limit through considering mass-deformed  $\mathcal{N} = 4$  SQCD theory. We found that in the infinite mass limit a point of the flat-space vacuum moduli space dominantly contributes to the partition function and the partition function corresponds to that of the effective theory at the point. This result leads us to understand the problem that which supersymmetric vacua of the theory on flat space survive after coupling the curved background geometry and to shed lights understanding why the partition function of the mass-deformed ABJM theory exhibits such a singular behavior in terms of the flat-space supersymmetric vacua.

# Contents

<b>1</b>	<b>Introduction</b>	<b>4</b>
<b>I</b>	<b>Review of 3d <math>\mathcal{N} = 2</math> gauge theories</b>	<b>8</b>
<b>2</b>	<b>Basic properties of 3d <math>\mathcal{N} = 2</math> gauge theories on flat space</b>	<b>9</b>
2.1	$\mathcal{N} = 2$ supersymmetric gauge theory . . . . .	10
2.1.1	Enhancement of supersymmetry . . . . .	11
2.2	Complex and real mass deformation . . . . .	15
2.3	Vacuum moduli space . . . . .	16
2.4	Review of mass deformed ABJM theory . . . . .	19
2.5	Supersymmetry gauge theory on $S_b^3$ . . . . .	20
2.5.1	Notation for the Elipsoid $S_b^3$ . . . . .	21
2.5.2	Supersymmetric actions on $S_b^3$ . . . . .	22
2.6	Supersymmetric Localization method . . . . .	24
2.6.1	Localization technique for SUSY QFTs . . . . .	24
2.6.2	$S_b^3$ partition function from Coulomb branch localization . . . . .	27
2.6.3	Useful formulas and examples . . . . .	31
<b>II</b>	<b>Aspects of Massive Gauge Theory on The Three-Sphere</b>	<b>35</b>
<b>3</b>	<b>Dominant Point of Coulomb Branch in Infinite Mass Limit</b>	<b>36</b>

3.1	Large $N$ solution and point of Coulomb branch . . . . .	38
3.1.1	SQCD with massless hypermultiplets . . . . .	38
3.1.2	SQCD with massive hypermultiplets . . . . .	41
3.1.3	SQCD with massive and massless hypermultiplets . . . . .	46
3.2	Finite rank SQCD . . . . .	51
3.2.1	With massive hypermultiplets . . . . .	51
3.2.2	With massive and massless hypermultiplets . . . . .	53
3.3	Summary and Discussion . . . . .	56
<b>4</b>	<b>Mass-deformed ABJM theory</b>	<b>59</b>
4.1	General mass deformation of ABJM theory . . . . .	59
4.2	Large $N$ ansatz and Imaginary FI-parameter . . . . .	61
4.2.1	A new derivation of the saddle-point solution for $N^{\frac{3}{2}}$ . . . . .	68
4.3	Large $N$ solution with one massless hypermultiplet . . . . .	75
4.3.1	Partition function of S-dual theory . . . . .	76
4.4	Summary and Discussion . . . . .	82
<b>III</b>	<b>Notes on Large <math>N</math> phases of gauge theories on the ellipsoid</b>	<b>84</b>
<b>5</b>	<b>Saddle-point solution for SUSY breaking phase</b>	<b>85</b>
5.1	Pure $\mathcal{N} = 2$ SUSY Chern-Simons Yang-Mills theory . . . . .	86
5.2	$\mathcal{N} = 2$ SUSY gauge theory with fundamental matter fields . . . . .	90
5.3	$\mathcal{N} = 2$ SUSY gauge theory with adjoint matter fields . . . . .	92
5.4	FI-deformed ABJM theory . . . . .	94
5.4.1	Solutions in large $\zeta/k$ limit . . . . .	94
5.4.2	Any $\zeta/k$ . . . . .	96
5.5	Summary and Discussion . . . . .	97

<b>6</b>	<b>Mass-Deformed ABJM Theory Revisited</b>	<b>99</b>
6.1	Evidence for SUSY breaking . . . . .	100
6.1.1	Criterion for SUSY breaking . . . . .	101
6.2	General deformation with $\zeta_1, \zeta_2 \neq 0$ . . . . .	103
6.2.1	Exact expression for $N = 1, 2$ . . . . .	103
6.2.2	$N \geq 3$ from Monte Carlo Simulation . . . . .	105
6.2.3	Physical origins of the zeroes from Fermi gas formalism . . . . .	109
6.2.4	Conjecture on phase structure in the large- $N$ limit . . . . .	114
6.3	Discussion . . . . .	115
<b>7</b>	<b>Conclusion and Future directions</b>	<b>117</b>
<b>IV</b>	<b>Appendixes</b>	<b>120</b>
<b>A</b>	<b>Appendix for chapter 3</b>	<b>121</b>
A.1	A brief summary of resolvent methods . . . . .	121
A.2	Mixed Chern-Simons terms . . . . .	123
A.3	Convergence bound of matrix models . . . . .	126
<b>B</b>	<b>Appendix for chapter 5</b>	<b>128</b>
B.1	Dominant saddle-point solution . . . . .	128
B.1.1	The dominant saddle-point solutions . . . . .	129
B.1.2	A theory in which confinement solution is dominant . . . . .	131
<b>C</b>	<b>Appendix for Chapter 6</b>	<b>135</b>
C.1	Exact computation of $Z(N, k, 0, \zeta_2)$ . . . . .	135
C.1.1	Exact partition function for finite $(N, k)$ . . . . .	135
C.2	Exact expressions for $Z(N, k, 0, \zeta_2)$ . . . . .	139
C.2.1	Comparison with saddle-point approximation . . . . .	140

# Chapter 1

## Introduction

As represented by the low-energy physics of Quantum ChromoDynamics (QCD), one of the most important problems for modern physics is to obtain knowledge about the strongly coupled theory. This is mainly because of lacking of non-perturbative calculation methods. To approach this problem, we can rely on three-dimensional gauge theories though they do not seem not to be “real” theory in the sense that they are not defined in four-dimensions. There are the following two main reasons why we can rely on three-dimensional gauge theories: The first is that three-dimensional gauge theories are generally more tractable than higher dimensional gauge theories. The second is that in three dimensions, three-dimensional the Yang-Mills term is super-renormalizable since the Yang-Mills couplings have mass dimension and thus, their properties are similar with asymptotic free theories such as QCD. This leads an Abelian gauge theory in three dimensions to be a simple example of a strongly coupled theory. Then, in three dimensions, even for Abelian gauge theory, its low-energy physics is strongly coupled and it can be expected to flow to a non-trivial fixed point [6–8].

We have considered so far advantages of three-dimensional gauge theory comparing with four-dimensional gauge theory. Because three-dimensional gauge theory also includes peculiar properties such as the Chern-Simons theory, which does not exist in four-dimensions, the three-dimensional gauge theory itself can have rich structures. The Chern-Simons theory is a kind of gauge theory and equipped with an integer called as Chern-Simons level instead of a coupling constant. The quantize number connect the Chern-Simons theory with condensed matter physics in the context of quantum Hall effects and so on. In this sense, three-dimensional gauge theory can describe real physical systems.

However, it is still difficult to non-perturbatively analyze three-dimensional gauge theories. Then, we consider supersymmetric theories. One of the advantage of supersymmetry gauge theory is that some physical quantities can be calculated non-perturbatively because almost all

contributions arising from bosonic and fermionic degrees of freedom cancel and only finite contributions can remain. In particular, a localization technique for supersymmetric field theory, which have been developed recently, is a very powerful tool for non-perturbative calculation. For some physical quantities, a localization technique reduces the path integral needed to calculate its expectation value to a finite dimensional ordinary integral. Thus, we can compute the expectation value without perturbative analysis. Moreover, the finite dimensional integral for a three-dimensional gauge theory is simpler than that for a gauge theory in other dimensions in the sense that it does not include an infinite sum arising from solitonic objects such as instantons. Thus, this technique has promoted us to understand non-perturbative phenomena such as dualities.

Another motivation to investigate three-dimensional supersymmetric gauge theories is to understand the M-theory, which is proposed in [9]. The M-theory is a strong candidate of the non-perturbative realization of the string theory, which is defined only perturbatively. Thus, it is important to study and establish the M-theory in order to achieve one of the goals of modern physics, namely completion of the ultimate unified theory of the forces. Recently, a special kind of the supersymmetric Chern-Simons with matter fields theories<sup>†1</sup> has been studied intensively because it is expected to correspond to the world-volume theory of coincided M2-branes. Here, M2-brane is a solitonic object in the eleven dimensional supergravity and is expected to play the important role to understand the M-theory. In particular, the Chern-Simons matter theory proposed by Aharony, Bergman, Jafferis and Maldacena [10] (ABJM theory) is considered to be a world-volume theory of coincided M2-branes on an orbifold singularity.

To apply a localization method to supersymmetric gauge theory, the theory is usually defined on a compact manifold in order to avoid infrared divergence. Then, precisely speaking, the result after localization technique is different from one for the theory on flat space. For conformal theories, when the manifold on which the theory is defined is conformally flat, the result can be interpreted as that for flat space because these can be mapped with each other. Many of the results obtained by employing a localization technique are for superconformal theories. Therefore, this point has not received much attention so far. However, it can be expected that non-conformal theories have richer structures than conformal theories have in the sense that there is an RG flow for a non-conformal theory and it is useful to understand infrared phases.

It is important to connect results from localization technique from non-conformal theory with ones for the flat space theory. For this purpose, it is necessary to specify the properties of the vacuum of the theory on a compact manifold. Generally speaking, the vacuum structure of theory depends on the manifold on which the theory is defined because there are correction

---

<sup>†1</sup>At first, the theory employing the three-algebra was proposed in [22–25], but this theory turned out to describe the world volume theory of two coincided M2-branes.

terms arising from the geometry to the flat space theory. In particular, supersymmetric gauge theories have a moduli space of vacua similar with the vacua of the Higgs fields in the standard model and then, depending on a choice of vacuum, a different phase can be realized in the low-energy region, for example, an interacting conformal phase and a gapped phase and so on. The expectation value from a localization technique should correspond to a flat-space vacuum expectation value by taking the decompactified limit, where the characteristic curvature of a manifold where the theory is defined vanishes.

It is also important to investigate non-conformal supersymmetric theories in the large- $N$ <sup>†2</sup> limit in the sense of the general gauge/gravity correspondence and so on. Three-dimensional supersymmetric gauge theories are also suitable for this purpose because three-dimensional gauge theories have been intensively studied in terms of  $\text{AdS}_4/\text{CFT}_3$ , which is a correspondence between a three-dimensional conformal field theory and the  $\text{AdS}_4$  geometry. In particular, it is natural to expect that the gauge/gravity correspondence can be investigated by deforming a conformal field theory which has a gravity dual with relevant terms. In this context, we should investigate the properties of the theory in the large- $N$  limit because the corresponding object should exist in the gravity side.

Following these research backgrounds, we introduce our work [2–5] where we investigated partition function of the mass-deformed gauge theories and the non-trivial phases are realized in the large- $N$  or the infinite mass limit <sup>†3</sup>.

I investigated the effect of the infinite mass limit to the three-sphere partition function in [5]. This work is motivated by the fact that on the three-sphere, we cannot select a vacuum, then the effective mass seems not to be defined on the round-sphere. In the infinite mass limit, we found that we can determine an effective mass of the matter fields by specifying a point of the flat-space vacuum moduli which contributes dominantly to the partition function. Then, we concluded that the partition function becomes that of an effective theory associated with the point of the flat-space vacuum moduli in this limit.

For the mass-deformed ABJM theories, we found that in the large  $N$  limit, the partition function has a singularity at certain finite value of mass. As a result of successive studies of this theory and related theory in [1–3], we propose that in the large  $N$  limit the supersymmetry is spontaneously broken beyond the above threshold. Though the mass-deformed ABJM theory on flat space has a supersymmetry-preserving vacuum moduli space composed of discrete points, on  $S^3$  metastable vacua can contribute to the partition function of the mass-deformed ABJM theory. This is because the partition function is given by the integration over the parameters describing the vacua. Then, the supersymmetry can be broken spontaneously.

---

<sup>†2</sup>Here,  $N$  typically denotes the rank of the gauge group.

<sup>†3</sup>In [11–18], the phase structure of mass-deformed gauge theories on  $S^3$  is also investigated.



The contents of this thesis is as follows: In part I, we will review the basic properties of a three-dimensional supersymmetric gauge theory. We will attempt to introduce the necessary ingredients for this thesis. However, we will give these ingredients only schematically. When the reader would like to know more information of these things, please read references. In part II, we will introduce our results associated with the partition function of mass-deformed gauge theory. In chapter 3, we will introduce the result in [5]. In chapter 4, we will introduce the results in [1–3] related to the computation of the partition function and the threshold of the saddle-point solution. In part III, we mainly discuss the phase appearing in the large  $N$  limit. In chapter 5, we introduced the result in [4] related to a special kind of saddle-point solution associated with the confinement (supersymmetry breaking) phase. In chapter 6, we will revisit the mass deformed ABJM theory and discuss the large- $N$  phase beyond the threshold through the numerical analysis and results obtained so far and so on.

# Part I

## Review of 3d $\mathcal{N} = 2$ gauge theories

# Chapter 2

## Basic properties of 3d $\mathcal{N} = 2$ gauge theories on flat space

In this thesis, we consider  $\mathcal{N} = 2$  supersymmetric gauge theories<sup>†1</sup>. The symbol  $\mathcal{N}$  denotes the number of generators of the supersymmetry. Because a generator of supersymmetry is fermionic, it should be in “the minimal” spinor representation of the Lorentz group. Here, the word “minimal spinor representation” means that the irreducible representation. This means that the definition of the number of generators of supersymmetry depends on the dimension on which a theory is defined. Because the number of conserved charges of the supersymmetry (supercharges) are same, four-dimensional  $\mathcal{N} = 1$  gauge theories and three-dimensional  $\mathcal{N} = 2$  gauge theories share many of their properties, for example, Seiberg duality [19] and holomorphy and so on. However, three-dimensional  $\mathcal{N} = 2$  gauge theories have some special properties with which four-dimensional  $\mathcal{N} = 1$  gauge theories do not share. Main properties we focus on in this thesis is that they admit a real mass deformation. Because a real mass deformation cannot be given by an expectation value of a chiral multiplet, it cannot be restricted by holomorphy and then, they can trigger the non-trivial phase transition. Moreover, in three dimensions, a Chern-Simons (CS) theory which is a gauge theory different from the Yang-Mills theory

$$S_{\text{CS}} = \frac{k}{4\pi} \int d^3x \text{Tr} \epsilon^{\mu\nu\rho} \left( A_\mu \partial_\nu A_\rho + \frac{2i}{3} A_\mu A_\nu A_\rho \right), \quad (2.0.1)$$

exists. This action is gauge invariant when the Chern-Simons level  $k$  is appropriately quantized depending on the gauge group. The existence of this kind of gauge theory makes three-dimensional gauge theories interesting. In particular, its supersymmetric generalization (su-

---

<sup>†1</sup>Strictly speaking, in this thesis, we mainly focus on  $\mathcal{N} = 4$  and  $\mathcal{N} = 6$  supersymmetric gauge theories. These theories are regarded as a special case of a  $\mathcal{N} = 2$  theory as we will explain later.

persymmetric Chern-Simons theory) plays important roles when we compose the low-energy effective theory of the stack of M2-branes, which will be investigated in this thesis.

## 2.1 $\mathcal{N} = 2$ supersymmetric gauge theory

Here, we introduce basic properties of three-dimensional gauge theories. First, we show supermultiplets corresponding to a vector field and a matter field. An  $\mathcal{N} = 2$  vector multiplet<sup>†2</sup> is composed by a vector field  $A_\mu$ , a Majorana fermion (gaugino)  $\lambda$ , a real scalar  $\sigma$  and an auxiliary field  $D$ . They are in the adjoint representation of the gauge group and often denoted as  $(A_\mu, \lambda, \bar{\lambda}, \sigma, D)$ . Their kinetic term is given by

$$\mathcal{S}_{\text{SYM}} = \frac{1}{g^2} \int d^3x \text{Tr} \left( -\frac{1}{4} F_{\mu\nu} F^{\mu\nu} - i\lambda\gamma^\mu D_\mu \bar{\lambda} - \frac{1}{2} D_\mu \sigma D^\mu \sigma + \frac{1}{2} D^2 - i\lambda[\sigma, \bar{\lambda}] \right), \quad (2.1.1)$$

where  $g^2$  is a Yang-Mills coupling constant and  $D_\mu$  denotes a covariant derivative as

$$D_\mu = \partial_\mu - i[A_\mu, ], \quad (2.1.2)$$

where the  $[A_\mu, ]$  means that the vector fields  $A_\mu$  appropriately act fields depending on its representation of the gauge group. The Lagrangian of the supersymmetric Chern-Simons theory is given by

$$S_{\text{SCS}} = \frac{k}{4\pi} \int d^3x \text{Tr} \epsilon^{\mu\nu\rho} \left( A_\mu \partial_\nu A_\rho + \frac{2i}{3} A_\mu A_\nu A_\rho + i\bar{\lambda}\lambda + 2D\sigma \right), \quad (2.1.3)$$

where  $k$  is a Chern-Simons level. These actions are invariant under the following transformation up to total derivative terms:

$$\delta_Q \sigma = \xi \bar{\lambda} + \bar{\xi} \lambda, \quad (2.1.4)$$

$$\delta_Q A_\mu = -i(\xi \gamma_\mu \bar{\lambda}) + i(\bar{\xi} \gamma_\mu \lambda), \quad (2.1.5)$$

$$\delta_Q D = (\xi \gamma^\mu D_\mu \bar{\lambda}) + (\bar{\xi} \gamma^\mu D_\mu \lambda) - (\xi[\sigma, \lambda]) - (\bar{\xi}[\sigma, \lambda]), \quad (2.1.6)$$

$$\delta_Q \lambda = \frac{i}{2} \gamma^{\mu\nu} \xi F_{\mu\nu} - \gamma^\mu \xi D_\mu \sigma + D\xi, \quad (2.1.7)$$

where  $\xi$  is a complex spinor parameter and  $\bar{\xi}$  is the complex conjugate of  $\xi$ . We can also introduce the Fayet-Iliopolous (FI) term when the gauge group has U(1) part as

$$S_{\text{FI}} = \frac{\zeta}{2\pi} \int d^3x \text{Tr} D, \quad (2.1.8)$$

---

<sup>†2</sup>A vector multiplets are denoted by a vector superfield  $\mathcal{V}(x, \theta, \bar{\theta})$ . A superfield is defined on superspace which is parametrized by both ordinary and Grassmann coordinates  $(x^\mu, \theta, \bar{\theta})$ .

where  $\zeta$  is an FI parameter, which has mass dimension 1 in three dimensions.

Then, we introduce a chiral multiplet as a supersymmetric multiplet corresponding to a matter field. A chiral multiplet consist of a complex scalar  $\phi$ , a complex fermion  $\psi$  and an auxiliary field  $F$ . We can give the multiplet a representation  $R$  of the gauge group. We often denote a chiral multiplet as  $(\phi, \psi, F)^{\dagger 3}$ . The kinetic term of a chiral multiplet with the gauge interaction is given by

$$S_{\text{mat}} = \int d^3x \left[ - (D_\mu \phi_i)^\dagger D^\mu \phi_i + i \psi_i^\dagger \gamma^\mu D_\mu \psi_i + F_i^\dagger F_i - \phi_i^\dagger D \phi + i \sqrt{2} \phi_i^\dagger (\lambda \psi_i) + i \sqrt{2} (\psi_i^\dagger \bar{\lambda}) \phi_i - \phi_i^\dagger \sigma^2 \phi_i - \psi_i^\dagger \sigma \psi_i \right]. \quad (2.1.9)$$

When there are  $N_f$  chiral multiplets, we can consider the interaction term among them in a supersymmetric manner. This interaction is realized by the superpotential  $W(\Phi)$ , which is a holomorphic function of chiral superfields. The interaction among matter fields is given by

$$S_{\text{int}} = \int d^2\theta W(\Phi) + (\text{h.c.}) \quad (2.1.10)$$

The action is invariant under the following infinitesimal transformation:

$$\delta_Q \phi = \sqrt{2} (\xi \psi), \quad (2.1.11)$$

$$\delta_Q \psi = \sqrt{2} \xi F + \bar{\xi} \sigma \phi + \sqrt{2} (\gamma^\mu \bar{\xi})^\alpha D_\mu \phi, \quad (2.1.12)$$

$$\delta_Q F = -\sqrt{2} i (\bar{\xi} \gamma^\mu D_\mu \psi) + \sqrt{2} i (\bar{\xi} \sigma \psi) + \sqrt{2} i (\bar{\xi} \bar{\lambda}) \phi. \quad (2.1.13)$$

Though the action we have introduced so far, a three-dimensional  $\mathcal{N} = 2$  gauge theory is defined as

$$S^{\mathcal{N}=2} = \sum_{\text{gauge}} (S_{\text{YM}} + S_{\text{CS}}) + \sum_{\text{matter}} S_{\text{mat}} + S_{\text{int}}, \quad (2.1.14)$$

where we assume that the gauge group  $G$  is given by a semi-simple Lie group as  $G = \prod_a^M G_a$ ,  $G_a$  is a simple Lie group.

### 2.1.1 Enhancement of supersymmetry

In general, a supersymmetric field theory can have at most 16 supercharges, or it can have  $\mathcal{N} = 8$  in three dimensions. The higher supersymmetry than  $\mathcal{N} = 2$  can be realized by a specific combination of  $\mathcal{N} = 2$  supermultiplets and superpotentials. This is because the R-symmetry can be enhanced by mixing with a global symmetry. In what follows, we will introduce examples of higher supersymmetric fields theories we will investigate in this thesis.

<sup>†3</sup>A chiral multiplet are denoted by a chiral superfields  $\Phi(x, \theta, \bar{\theta})$ .

### Example: $\mathcal{N} = 4$ super QCD theory

The field content of  $U(N)$   $\mathcal{N} = 4$  super QCD with  $N_f$  flavors is as follows: An  $\mathcal{N} = 4$  vector multiplet is composed by a vector multiplet  $\mathcal{V}$  and a chiral multiplet  $\Phi$  in the adjoint representation. An  $\mathcal{N} = 4$  hypermultiplet is a pair of a chiral multiplet in representation  $R$  and that in the conjugate representation  $\bar{R}$  of the gauge group. An  $\mathcal{N} = 4$  vector multiplets and  $N_f$  hypermultiplets in the fundamental representation.

The infrared behavior of this theory is well-studied in [20]. The Infrared property of the  $\mathcal{N} = 4$   $U(N)$  SQCD highly depends on the number of the flavors. In [20], the authors classified the theories depending on their infrared structures: “good”, “ugly” and “bad” theory. They define a “good” theory as a gauge theory in which all the monopole operator obey the unitarity bounds. In this case, the gauge theory is expected to flow to an interacting superconformal fields theory in the IR and the R-symmetry in the IR is the same as that of the UV theory because there are no candidates which are mixed with the UV R-symmetry in the IR. An  $\mathcal{N} = 4$   $U(N)$  SQCD is a good theory when  $N_f \geq 2N$ .

An “ugly” theory is defined as a gauge theory in which the monopole operators satisfy the unitarity bound, but several monopole operators saturate it. An “ugly” theory is also likely to flow to an interacting superconformal field theory with R-symmetry visible in the UV and the decoupled free sector consisting of the monopole operators that saturate the unitarity bound. An  $\mathcal{N} = 4$   $U(N)$  SQCD become an ugly theory when  $N_f = 2N - 1$ .

For a “bad” theory, there are monopole operators with zero or negative R-charge corresponding to the R-symmetry manifest in the UV. Because the monopole operators violate the unitarity bound of the UV R-symmetry, a bad theory may flow to an interacting SCFT, but its R-symmetry is not manifest in the UV because the R-symmetry manifest in the UV theory is mixed in the IR with an accidental symmetry which arises from the decoupled monopole operators. An  $\mathcal{N} = 4$   $U(N)$  SQCD becomes a bad theory when  $N \leq N_f \leq 2N - 2$ <sup>†4</sup>.

These definitions are closely related to the convergence of the  $S^3$  partition function. In particular, the partition function of a “bad” theory is divergent [21]. This might be because the localization methods use the R-symmetry that is manifest in the UV to define the gauge theory on a compact manifold. Thus, we should treat the number of flavors carefully.

---

<sup>†4</sup>Recent progress on “bad” theories in terms of the geometry of the moduli space of vacua is described in [32, 33].

### Example: $\mathcal{N} = 6$ super Chern-Simons matter theory

It was an important open problem to find a superconformal field theory which has  $\mathcal{N} = 8$  supersymmetry in the sense that the theory should correspond to a worldvolume theory of coincided M2-branes. About ten years ago, various successive works started with [22–25] about this problem were done and finally a candidate were proposed in [10]<sup>†5</sup>. It is a the  $U(N)_k \times U(N)_{-k}$  Chern-Simons theory whose field content in the language of  $\mathcal{N} = 2$  supermultiplets is as follows: a  $U(N)_k$  vector multiplet  $\mathcal{V} = (A_\mu, \sigma, \chi, D)$ , a  $U(N)_{-k}$  vector multiplet  $\tilde{\mathcal{V}} = (\tilde{A}_\mu, \tilde{\sigma}, \tilde{\chi}, \tilde{D})$ , two chiral multiplets  $\mathcal{Z}_\alpha = (A_\alpha, \phi_\alpha, F_\alpha)$  in  $(\square, \bar{\square})$  representation under  $U(N)_k \times U(N)_{-k}$  and two chiral multiplets  $\mathcal{W}_{\dot{\alpha}} = (B_{\dot{\alpha}}, \psi_{\dot{\alpha}}, G_{\dot{\alpha}})$  in  $(\bar{\square}, \square)$  representation.<sup>†6</sup> Furthermore, the ABJM theory has superpotential term given as

$$W = \frac{4\pi}{k} \text{Tr}(A_1 B_1 A_2 B_2 - A_1 B_2 A_2 B_1) = \frac{2\pi}{k} \epsilon^{ab} \epsilon^{\dot{a}\dot{b}} \text{Tr}(A_a B_{\dot{a}} A_b B_{\dot{b}}). \quad (2.1.15)$$

This superpotential term is invariant under global symmetry  $SU(2) \times SU(2)$ , which act on  $A_a$  and  $B_{\dot{a}}$  respectively and  $SU(2)$  symmetry which exchanges  $A_a$  with  $(B_{\dot{a}})^\dagger$ . Thus, the supersymmetry can be enhanced to  $\mathcal{N} = 6$ <sup>†7</sup>.

The Lagrangian for this theory is given by

$$S_{\text{ABJM}} = \int d^3x \text{Tr} \left[ \frac{k}{4\pi} \varepsilon^{\mu\nu\rho} (A_\mu \partial_\nu A_\rho + \frac{2i}{3} A_\mu A_\nu A_\rho - \tilde{A}_\mu \partial_\nu \tilde{A}_\rho - \frac{2i}{3} \tilde{A}_\mu \tilde{A}_\nu \tilde{A}_\rho) \right. \\ \left. - \text{Tr}(D_\mu C^I)^\dagger D^\mu C^I - i \text{Tr}(\psi_A)^\dagger \gamma^\mu D_\mu \psi_A - V_{\text{bos}} - V_{\text{fer}} \right], \quad (2.1.16)$$

where we have defined the covariant derivative as

$$D_\mu A_a = \partial_\mu A_a + i A_\mu A_a - i A_a \tilde{A}_\mu \quad (2.1.17)$$

$$D_\mu B_{\dot{a}} = \partial_\mu B_{\dot{a}} + i \tilde{A}_\mu B_{\dot{a}} - i B_{\dot{a}} A_\mu. \quad (2.1.18)$$

We also have employed a  $SU(4)$  covariant notation for the fermion fields by combing fermions  $\zeta_a, \omega_{\dot{a}}$  of chiral multiplets  $A_a$  and  $B_{\dot{a}}$  and defining  $\psi_I$  which have  $SU(4)_R$  index ( $I = 1, 2, 3, 4$ ) as

$$\psi_I = \{\epsilon_{ab} \zeta^b e^{-i\pi/4}, -\epsilon_{\dot{a}\dot{b}} (\omega_{\dot{b}})^\dagger e^{i\pi/4}\}, \quad (\psi_I)^\dagger = \{-\epsilon^{ab} (\zeta^b)^\dagger, \epsilon^{\dot{a}\dot{b}} \omega_{\dot{b}} e^{-i\pi/4}\}, \quad (2.1.19)$$

and for scalar fields we also define as

$$C^I = (A^1, A^2, B_1^\dagger, B_2^\dagger). \quad (2.1.20)$$

<sup>†5</sup>See also [37]

<sup>†6</sup>The (anti-)bi-fundamental chiral multiplets have  $U(1)_R$  charges  $1/2$ .

<sup>†7</sup>The  $\mathcal{N} = 6$  supersymmetry can be write down only on the on-shell formalism so far.

The potential terms are also written as the  $SU(4)_R$  invariant form as

$$V_{\text{fer}} = \frac{2\pi i}{k} \left[ (C^I)^\dagger C^I (\psi_J)^\dagger \psi_J - (\psi_I)^\dagger C^J (C^J)^\dagger \psi_I - 2(C^I)^\dagger C^J (\psi_J)^\dagger \psi_J + 2(\psi_J)^\dagger C^I (C^J)^\dagger \psi_I \right. \\ \left. - \epsilon^{IJKL} (C^I)^\dagger \psi_J (C^K)^\dagger \psi_L + \epsilon_{IJKL} C^I (\psi_J)^\dagger (\psi_K)^\dagger C^L \right] \quad (2.1.21)$$

$$V_{\text{bos}} = \frac{4\pi^2}{3k^2} \left[ C^I (C^I)^\dagger C^J (C^J)^\dagger C^K (C^K)^\dagger - 6C^I (C^J)^\dagger C^J (C^I)^\dagger C^K (C^K)^\dagger \right. \\ \left. + (C^I)^\dagger C^I (C^J)^\dagger C^J (C^K)^\dagger C^K + 4(C^I)^\dagger C^J (C^K)^\dagger C^I (C^J)^\dagger C^K \right]. \quad (2.1.22)$$

We can also find that the Lagrangian (2.1.16) is invariant following  $\mathcal{N} = 6$  supersymmetry transformation:

$$\delta C^I = i\omega^{IJ} \psi_J \quad (2.1.23)$$

$$\delta (C^I)^\dagger = i\psi_J^\dagger \omega_{IJ} \quad (2.1.24)$$

$$\delta \psi_I = -\gamma_\mu \omega_{IJ} D_\mu C^J + \frac{2\pi}{k} \left( -\omega_{IJ} (C^K (C^K)^\dagger) C^J - C^J (C^K)^\dagger C^K + 2\omega_{KL} C^K (C^I)^\dagger C^L \right) \quad (2.1.25)$$

$$\delta (\psi_I)^\dagger = D_\mu (C_J)^\dagger \gamma^\mu \omega^{IJ} + \frac{2\pi}{k} \left( - (C^J)^\dagger C^K (C^K)^\dagger - (C^I)^\dagger C^K (C^J)^\dagger \right) \omega^{IJ} + 2(C^L)^\dagger C^I (C^K)^\dagger \quad (2.1.26)$$

$$\delta A_\mu = -\frac{2\pi}{k} (C^I (\psi_J)^\dagger \gamma_\mu \omega_{IJ} + \omega^{IJ} \gamma_\mu \psi_I (C^J)^\dagger) \quad (2.1.27)$$

$$\delta \tilde{A}_\mu = \frac{2\pi}{k} ((\psi_I)^\dagger C^J \gamma_\mu \omega_{IJ} + \omega_{IJ} \gamma_\mu (C^I)^\dagger \psi_J), \quad (2.1.28)$$

where we have defined  $\omega_{IJ}$  as an antisymmetric fermionic parameter satisfying the following condition:

$$(\omega^{IJ})_\alpha = (\omega_{IJ})_\alpha^*, \quad \omega^{IJ} = \frac{1}{2} \epsilon^{IJKL} \omega_{KL} \quad (2.1.29)$$

This transformation is guaranteed to be  $\mathcal{N} = 6$  since the fermionic parameter  $(\omega_{IJ})$  is in **6** representation of  $SU(4)_R$  and are set to Majorana fermion. We note that the Lagrangian has only  $\mathcal{N} = 6$  supersymmetry apparently, but it is expected that the supersymmetry is enhanced to  $\mathcal{N} = 8$  for  $k = 1, 2$  case including the quantum effects [26–30]. This is consistent with the gravity side because the ABJM theory is dual to  $N$  coincided M2-branes on  $\mathbb{Z}_k$  orbifold singularity and the orbifold break 16 supercharges to 12 supercharges for  $k \neq 1, 2$ .



## 2.2 Complex and real mass deformation

Our interest in this thesis is real mass-deformed theories [31]. Here, we show that two mass parameters which are admitted in three-dimensional supersymmetric gauge theories. A complex mass deformation is given by the superpotential term as

$$\mathcal{L}_{\text{comp}} = \int d^2\theta W(\Phi) + (\text{h.c.}), \quad (2.2.1)$$

where  $W(\Phi) = m_c \tilde{\Phi}\Phi$ .  $\tilde{\Phi}$  is a chiral superfield in the conjugate representation  $\bar{R}$  and then, the combination  $\tilde{\Phi}\Phi$  is gauge-invariant. The corresponding Lagrangian is

$$\mathcal{L}_{\text{comp}} = m_c |\phi|^2 + m_c (\psi\psi) + \bar{m}_c (\psi^\dagger\psi^\dagger) + (\tilde{\phi}, \tilde{\psi} \text{ terms}). \quad (2.2.2)$$

We note that the superpotential is a holomorphic function of  $\Phi$ . This enables us to understand non-perturbative effects of three-dimensional  $\mathcal{N} = 2$  theory in the same manner as the four-dimensional  $\mathcal{N} = 1$  gauge theory. Moreover, by the holomorphy, phase transitions are forbidden. This is because the parameter space is a complex manifold and then, we can avoid the transition point through the codimensions.

Next, we consider a real mass deformation. We can give a real mass parameter to a chiral superfield that has a non-zero charge  $q$  under a global symmetry by introducing the corresponding vector superfield  $V_b$  by

$$\mathcal{L}_{\text{real}} = \int d^4\theta \Phi^\dagger e^{qV_b} \Phi = (q\sigma_b)^2 |\phi|^2 + iq\sigma_b \epsilon^{\alpha\beta} \psi_\alpha \psi_\beta + \dots, \quad (2.2.3)$$

where we define the scalar components of  $V_b$  as  $\sigma_b$  and assume that the chiral superfield  $\Phi$  does not have gauge charges. The real mass deformation is given by replacing the vector superfields  $V$  with the background vector superfield  $V_b$ . This implies that a real mass deformation is obtained by introducing the background gauge fields coupled with the conserved current corresponding to the global symmetry and giving it an expectation value. For the introduced background fields to break the supersymmetry of the theory, the following condition is necessary:

$$\sigma_b = m_r, \quad A_\mu = \lambda = D = 0. \quad (2.2.4)$$

When a chiral superfield is charged under the gauge group, a real mass deformation is given by

$$\mathcal{L}_{\text{real}} = \int d^4\theta \Phi^\dagger e^{V+qV_b} \Phi = \phi^\dagger (\sigma + qm_r)^2 \phi + i(\sigma + qm_r) \epsilon^{\alpha\beta} \psi_\alpha \psi_\beta + \dots \quad (2.2.5)$$

Then, a real mass deformation shift  $\sigma$  by  $qm_r$ . This implies that a real mass deformation shifts the origin of the Coulomb branch. We note that a real mass deformation changes the supersymmetry algebra since the global symmetry has the conserved charge and the charge appear in the supersymmetric algebra as the central charge. We also note that real mass deformations are forbidden in four dimensions since in (2.2.5) the term  $\epsilon^{\alpha\beta} \psi_\alpha \psi_\beta$  cannot exist.

## 2.3 Vacuum moduli space

A generic 3d  $\mathcal{N} = 2$  gauge theory has a moduli space denoting the lowest energy state and it is continuous, not discrete. For quantum theories which have supersymmetry, the lowest state is equivalent to the state preserving the supersymmetry. In this sense, we sometimes call such a moduli space as SUSY vacua. At the classical level, the space is determined by zeros of the scalar potential

$$V = \sum_i (F_i)^\dagger F_i + \frac{1}{2} \text{Tr} D^2 + \sum_i ((\sigma + m_i) \phi_i)^\dagger (\sigma + m_i) \phi_i, \quad (2.3.1)$$

where we consider  $M = 1$  case for simplicity and introduce real mass  $m_i$  employing the  $i$ th  $U(1)$  global symmetry associated with the number of chiral multiplets. With the E.O.M of the auxiliary  $F$  and  $D$ , the vacuum equations are as follows:

$$D^a = -g^a \left( -\sum_i (\phi_i^\dagger T_{R_i}^a \phi_i) + \frac{k}{2\pi} \sigma^a + \frac{\zeta}{2\pi} \right) = 0, \quad a = 1, \dots, \dim G \quad (2.3.2)$$

$$F = -\frac{\partial W(\phi)}{\partial \phi} = 0, \quad (2.3.3)$$

$$\left( \sum_{a=1}^{\dim G} \sigma^a T_{R_i}^a + m_b \right) \phi_i = 0. \quad (2.3.4)$$

As the solution of these equations, we define the three branches as follows:

$$\text{Coulomb branch: } \langle \phi_i \rangle = 0, \quad \langle \sigma \rangle = \sigma_0 \neq 0, \quad (2.3.5)$$

$$\text{Higgs branch: } \langle \phi_i \rangle \neq 0, \quad \langle \sigma \rangle = 0, \quad (2.3.6)$$

$$\text{Mixed branch: } \langle \phi_i \rangle \neq 0, \quad \langle \sigma \rangle \neq 0, \quad (2.3.7)$$

When we introduce real masses, it shifts the origin of the branch. On the Coulomb branch, the gauge group is spontaneously broken in a Coulomb phase  $U(1)^r$ , where  $r$  is the rank of the gauge group because  $\sigma_a$  can be diagonalized by the gauge transformation. This is because the branch is called the Coulomb branch. Next, on the Higgs branch, the gauge group is completely broken. Then, this branch is called the Higgs branch. We would like to argue about the properties of the Coulomb branch for later use. The existence of FI terms leads to lifting the Coulomb branch even at classical level except for  $k \neq 0$ . When the Chen-Simons level  $k$  is non-vanishing, there is an isolated vacuum  $\sigma_I = -\frac{\zeta}{k}$  at least classical level. When  $k = \zeta = 0$ , the Coulomb branch becomes non-compact. On the Coulomb branch, the matter fields charged under the gauge group obtain a real mass by the Higgs mechanism as

$$q_{a,i} \sigma_0, \quad (2.3.8)$$

where  $q_i$  is a charge under the  $i$ th  $U(1)$  group of its Caltan part  $U(1)^r$ . Thus, chiral multiplets with real mass  $m$  become effective massless fields on a specific point of the Coulomb branch where

$$\left( \sum_i q_{a,i} \sigma_{0,i} + m \right) = 0. \quad (2.3.9)$$

This implies that the scalar fields  $\sigma$  is essentially the same as a real mass. What we mentioned so far is a classical argument and we should consider the quantum effect. Generally speaking, the Coulomb branch can be lifted by quantum effect and sometimes SUSY Vacua are completely lifted by quantum effects. In fact, integrating out the massive fermions causes not only ordinary Chern-Simons term, but also mixed Chern-Simons terms which include background gauge fields. This means that the Chern-Simons level and FI-terms can be corrected by the one-loop effects we mentioned above as  $k \rightarrow k_{\text{eff}}$   $\zeta \rightarrow \zeta_{\text{eff}}$ . The correction arising from  $k_{\text{eff}}$  and  $\zeta_{\text{eff}}$  can lift the Coulomb branch.

The Coulomb branch is parametrized by monopole operators  $\mathcal{V}_a$ <sup>†8</sup> defined classically as

$$\mathcal{V}_a = e^{\pm \frac{2\pi}{g^2} (\sigma_a + i\gamma_a)}, \quad (2.3.10)$$

where  $\gamma_a$  is a dual photon defined for  $U(1)$  gauge fields as

$$\partial_\mu \gamma = \epsilon_{\mu\nu\rho} F^{\nu\rho}. \quad (2.3.11)$$

The dual photon is changed under the topological symmetry transformation as

$$\frac{2\pi}{g^2} \gamma \rightarrow \frac{2\pi}{g^2} \gamma + 2\pi, \quad (2.3.12)$$

then, a monopole operator  $\mathcal{V}$  is well-defined under this symmetry. However, it is known that a monopole operator cannot parametrize the whole Coulomb branch after taking quantum effects. The Coulomb branch has singularities and as we across a singularity, it is parametrized by a different parameter. The singularity is interpreted as a fixed point of the monopole operators under the topological symmetry transformation. Then, the singularity can be a root point of the Higgs branch because the matter fields do not have charges under the topological symmetry.

It is known that the SUSY vacua are generally a kähler manifold with singularities. On the singular point, the gauge symmetry is recovered, namely, the W-boson become massless and then, the low-energy effective theory of the gauge theory expected to be an interacting superconformal fields theory. Recently, the relation between singularities of the Coulomb branch and a low-energy effective theory in is argued [32, 33]. In what follows, we introduced  $\mathcal{N} = 2$  SQED as an example for calculating the quantum corrections to the Coulomb branch [34].

---

<sup>†8</sup>For the Chern-Simons theory, the monopole operators are not gauge invariant. Thus, the dressed monopole operator, which is a neutral composite of the monopole operator and the charged matter fields.

### Example of quantum Coulomb branch: $\mathcal{N} = 2$ SQED

We consider the SUSY vacua of three-dimensional  $\mathcal{N} = 2$  SQED with one flavor. The word “flavor” denotes that a pair of chiral multiplets in fundamental and anti-fundamental representation. At the classical level, the Higgs branch is parametrized by the gauge invariant combination, the meson  $M = q\bar{q}$ , where  $q$  ( $\bar{q}$ ) is a scalar component of the chiral multiplet in the fundamental (antifundamental) representation of  $U(1)$  respectively. Then, we would like to consider the Coulomb branch. Because at the classical level, the coulomb brach is parametrized by a monopole operator, it is denoted as  $\mathbb{R} \times S^1_\gamma$  in which  $\sigma$  denotes  $\mathbb{R}$  direction and  $\gamma$  denotes  $S^1_\gamma$  direction. The topological symmetry transformation corresponds to the rotation of  $\gamma$  direction. These two branches are intersected at  $\sigma = M = 0$ , however, the  $U(1)_J$  symmetry act on the Coulomb branch freely while it does not act on the Higgs branch. This contradiction is resolved at the quantum level. In fact, at the semiclassical level, the metric can be calculated as

$$ds^2 = \frac{1}{4} \left( \frac{1}{g^2} + \frac{1}{|\sigma|} \right) d\sigma^2 + \frac{1}{4} \frac{1}{\left( \frac{1}{g^2} + \frac{1}{|\sigma|} \right)} d\gamma^2. \quad (2.3.13)$$

This means that at  $\sigma = 0$ ,  $\gamma$  direction shrinks. Thus, the point is a fixed point of the  $U(1)_J$  symmetry and then the contradiction is resolved.

### Example: $\mathcal{N} = 2$ super Chern-Simons theory

Finally, we would like to introduce  $\mathcal{N} = 2$  supersymmetric Chern-Simons theory as an example of the theory that does not have SUSY vacua at the quantum level. In what follows, we review the argument in [35,36]. The argument is based on the calculation of the Witten index. For the  $U_k(N)$  ( $SU(N)$ )  $\mathcal{N} = 2$  supersymmetric Chern-Simons matter theory with generic real mass parameters, the Witten index  $\text{Tr}(-1)^F$  is given by

$$\text{Tr}(-1)^F = J_G(k'), \quad k' = |k| - N + \frac{1}{2} \sum_f T_2(R_f), \quad (2.3.14)$$

where  $J_G(k')$  is the number of the primary operator of  $U(N)_{k'}$  Wess-Zumino-Witten theory and the summation over  $f$  denotes the contributions from all the fermions of chiral multiplets  $\Phi_f$  in the representation  $R_f$  with  $T_2(R_f)$  being the quadratic index of the representation. Thus, the condition that  $k' < 0$  implies that there are no supersymmetric vacua, namely spontaneously supersymmetry breaking. This condition is consistent with the s-rule arising from D-brane configurations [89,90]. In particular, for  $SU(N)_k$  pure Chern-Simons theory with  $k = N$ , there is only one isolated supersymmetric vacuum at  $\sigma = 0$  and a gapped phase is realized. We note that confinement of electric flux can occur only if the center symmetry  $\mathbb{Z}_N$  acts trivially on

the states, and that requires  $k = N$ . We expect that this vacuum corresponds to the large- $N$  solution we will discuss in chapter 5.

## 2.4 Review of mass deformed ABJM theory

Here, we review the mass-deformed ABJM theory in which  $\mathcal{N} = 6$  supersymmetry of the ABJM theory are preserved at the Lagrangian level [37, 42]. This mass deformation preserves the  $SU(2) \times SU(2) \times U(1) \times \mathbb{Z}_2$  R-symmetry out of original R-symmetry  $SU(4) \times U(1)$  for general Chern-Simons level  $k$ . On-shell formalism, this mass deformation is given by the complex mass deformation as

$$\mathcal{L}_{\text{mass}} = \mu^2 \text{Tr}(C^I (C^I)^\dagger) = \mu^2 \text{Tr}(Q^\alpha (Q^\alpha)^\dagger + R^\alpha (R^\alpha)^\dagger), \quad (2.4.1)$$

where  $\mu$  is a mass parameter. For off-shell formalism, this deformation is given by the FI-deformation as

$$\mathcal{L}_{\text{FI}} = \frac{\zeta}{2\pi} (D + \tilde{D}), \quad \zeta \in \mathbb{R}. \quad (2.4.2)$$

This FI-deformation is favorable for a localization technique because we must use the off-shell formalism of the supersymmetric theory. For this case, this FI term can be canceled by the shift of  $\sigma$  ( $\tilde{\sigma}$ ) by  $\frac{\zeta}{k}$  ( $-\frac{\zeta}{k}$ ) respectively. Thus, these shifts give all matter fields in the ABJM theory the same real mass as that (2.4.1) gives.

This mass deformation change the scalar potential as

$$V = \text{Tr} M^\alpha (M^\alpha)^\dagger + \text{Tr} N^\alpha (N^\alpha)^\dagger, \quad (2.4.3)$$

where we have defined  $M^\alpha$  and  $N^\alpha$  as

$$M^\alpha = \mu Q^\alpha + \frac{2\pi}{k} (2Q^{[\alpha} (Q^\dagger)_{\beta} Q^{\beta]} + R^\beta (R^\dagger)_{\beta} Q^\alpha - Q^\alpha (R^\dagger)_{\beta} R^\beta + 2Q^\beta (R^\dagger)_{\beta} R^\alpha - 2R^\alpha (R^\dagger)_{\beta} Q^\beta) \quad (2.4.4)$$

$$N^\alpha = -\mu R^\alpha + \frac{2\pi}{k} (2R^\alpha (R^\dagger)_{\beta} R^\beta + Q^\beta (Q^\dagger)_{\beta} R^\alpha - R^\alpha (Q^\dagger)_{\beta} Q^\beta + 2R^\beta (Q^\dagger)_{\beta} Q^\alpha - 2Q^\alpha (Q^\dagger)_{\beta} R^\beta), \quad (2.4.5)$$

where we take  $\mu = \frac{2\zeta}{k}$ . Comparing with the original scalar potential, the first term is added by the mass deformation. This term makes the zeros of the scalar potential given by

$$M^\alpha = 0, \quad N^\alpha = 0, \quad (2.4.6)$$

finite solution instead of continuous one. Actually, the non-trivial solution is given by

$$R_\alpha = \begin{pmatrix} A_\alpha^{\ell_1} & & & & & \\ & \ddots & & & & \\ & & A_\alpha^{\ell_k} & & & \\ & & & 0 & & \\ & & & & \ddots & \\ & & & & & 0 \end{pmatrix}, \quad Q_\alpha = \begin{pmatrix} 0 & & & & & \\ & \ddots & & & & \\ & & 0 & & & \\ & & & (A_\alpha^{\ell_{k+1}})^\dagger & & \\ & & & & \ddots & \\ & & & & & (A_\alpha^{\ell_n})^\dagger \end{pmatrix}, \quad (2.4.7)$$

where  $A_\alpha^{\ell_1}$  is defined as

$$A_1^\ell = \sqrt{\frac{\zeta}{\pi}} \begin{pmatrix} 0 & & & & \\ & \ddots & & & \\ & & \sqrt{\ell-2} & & \\ & & & \ddots & \\ & & & & \sqrt{\ell-1} \end{pmatrix}, \quad A_2^\ell = \sqrt{\frac{\zeta}{\pi}} \begin{pmatrix} 0 & \sqrt{\ell-1} & & & \\ & \ddots & \ddots & & \\ & & \ddots & \ddots & \\ & & & \ddots & 1 \\ & & & & 0 \end{pmatrix}, \quad (2.4.8)$$

and  $\ell_k$  is partition of  $N$  satisfying the following relation:

$$\sum_{i=1}^n \ell_i = N, \quad \ell_n \geq \dots \geq \ell_1 \geq 1, \quad (2.4.9)$$

In [40,41], it has been reported that this classical vacua is partially lifted by the quantum effect and  $a$  vacua remain. This implies that the vacuum on which ranks of higgsed gauge groups are less than the Chern-Simons level  $k$  survives.

This mass deformation corresponds to introducing the background flux in the gravity side. It is known that this background flux causes the M-theoretical generalization of the Myers effect [38,39]. The Myers effect is an analogy of the polarization in the Electromagnetism. Namely, the Dp-brane is polarized into D(p+2)-brane with the background flux, which corresponds to the electric flux. In this case, M2-branes are polarized into M5-branes. In fields theory side, the vacuum solution (2.4.7) corresponds to the polarization of the M2-branes into M5-branes in terms of the Fuzzy sphere geometry [42,43].

## 2.5 Supersymmetry gauge theory on $S_b^3$

We have reviewed three-dimensional  $\mathcal{N} = 2$  gauge theories in Minkowski spacetime so far. In this section, we consider that three-dimensional  $\mathcal{N} = 2$  gauge theories on the ellipsoid  $S_b^3$  to apply a localization technique we will introduce later. The ellipsoid is one parameter  $b$  deformation of the round three-sphere. Generally speaking, it is highly non-trivial to put the

theory defined in flat space to a curved manifold  $\mathcal{M}$  because the spinor parameters employed in supersymmetric variations are no longer a constant field. If we just replace the flat theory from the curved one by the following procedure:

$$\eta_{\mu\nu} \rightarrow g_{\mu\nu}, \quad \partial_\mu \rightarrow \nabla_\mu, \quad (2.5.1)$$

in  $\mathcal{L}$  and supersymmetric variations, the theory replaced by this procedure is not supersymmetry on  $\mathcal{M}$  because the term  $\nabla_\mu \epsilon$  breaks the covariance of the corresponding action. Indeed, if we impose the condition  $\nabla_\mu \epsilon = 0$ , the theory can be defined on  $\mathcal{M}$  by the simple procedure mentioned above. However, the condition highly restricts the curved manifold  $\mathcal{M}$ , namely,  $\mathcal{M}$  need to be a Ricchi-flat manifold.

It is known that we do not have to impose such a restriction in order to define a supersymmetric field theory on a curved manifold. A systematic strategy of how to put the theory on the curved manifold is to couple the supersymmetric field theory with supergravity and then to take a rigid limit in which Newton's constant  $G_N \rightarrow 0$  and the supergravity become non-dynamical while taking the metric to a fixed curved manifold, rather than the original flat space. This procedure was proposed in [44]. In this section, we will introduce the result of  $\mathcal{N} = 2$  gauge theory on  $S^3$  and do not enter the detail of the procedure to put the supersymmetric theory on a curved manifold.

### 2.5.1 Notation for the Ellipsoid $S_b^3$

Here, we introduce notation of the geometry and spinor we use in this article. The notation is fundamentally based on [45, 46]. The metric of the ellipsoid  $S_b^3$  is written as

$$d^2s = r^2 (f^2(\vartheta) + b^2 \sin^2 \vartheta d^2\varphi_1 + b^{-2} \cos^2 \vartheta d^2\varphi_2), \quad (2.5.2)$$

where  $\vartheta \in [0, \frac{\pi}{2}]$  and  $\varphi_1, \varphi_2 \in [0, \frac{\pi}{2}]$  and parameter is defined as

$$b = \sqrt{\frac{\tilde{\ell}}{\ell}}, \quad r = \sqrt{\ell\tilde{\ell}}, \quad f(\vartheta) = \sqrt{b^2 \sin^2 \vartheta + b^{-2} \cos^2 \vartheta} \quad (2.5.3)$$

where  $f(\vartheta)$  is allowed to be an any function whose asymptotic form at  $\vartheta = 0, \frac{\pi}{2}$  is  $\ell$  and  $\tilde{\ell}$  respectively and which gives the smooth metric. Thus, the choice of this function is irreverent with the geometry.

This manifold is the hyper surface in  $\mathbb{R}^4$  defined as

$$x_0^2 + x_1^2 + x_2^2 + x_3^2 = 1, \quad (2.5.4)$$

with the metric

$$d^2s = \ell(d^2x_0 + d^2x_1) + \tilde{\ell}(d^2x_2 + d^2x_3). \quad (2.5.5)$$

The orthogonal frame are given by

$$e^1 = rb^{-1} \cos \vartheta d\varphi_2, \quad e^2 = -rb \sin \vartheta d\varphi_1, \quad e^3 = rf(\vartheta) d\vartheta. \quad (2.5.6)$$

This means that the component of the vielbein is explicitly written as

$$\begin{pmatrix} e^1_{\varphi_1} & e^1_{\varphi_2} & e^1_{\vartheta} \\ e^2_{\varphi_1} & e^2_{\vartheta} & e^2_{\varphi_2} \\ e^3_{\varphi_1} & e^3_{\varphi_2} & e^3_{\vartheta} \end{pmatrix} = \begin{pmatrix} 0 & rb^{-1} \cos \vartheta & 0 \\ -rb \sin \vartheta & 0 & 0 \\ 0 & 0 & rf(\vartheta) \end{pmatrix} \quad (2.5.7)$$

The inverse of the vielbein is inverse of the component because this vielbein is diagonal. The killing spinor equations in this manifold are given by

$$\nabla_{\mu} \xi = \frac{1}{2rf(\vartheta)} \gamma_{\mu} \xi, \quad (2.5.8)$$

$$\nabla_{\mu} \bar{\xi} = \frac{1}{2rf(\vartheta)} \gamma_{\mu} \bar{\xi}, \quad (2.5.9)$$

where covariant derivative is defined including the background U(1) gauge field  $V = \frac{1}{2} \left(1 - \frac{b}{f(\theta)}\right) d\varphi_1 + \frac{1}{2} \left(1 - \frac{b^{-1}}{f(\theta)}\right) d\varphi_2$  as

$$\nabla_{\mu} = \partial_{\mu} - \frac{i}{2} \omega_{\mu} + iV_{\mu}. \quad (2.5.10)$$

We note that on the round three-sphere, namely  $b = 1$  case, this U(1) gauge background vanishes. The solution is given by [45]

$$\xi = \frac{1}{\sqrt{2}} \begin{pmatrix} e^{\frac{i}{2}(\varphi_1 + \varphi_2 + \vartheta)} \\ e^{\frac{i}{2}(\varphi_1 + \varphi_2 - \vartheta)} \end{pmatrix}, \quad \bar{\xi} = \frac{1}{\sqrt{2}} \begin{pmatrix} -e^{-\frac{i}{2}(\varphi_1 + \varphi_2 - \vartheta)} \\ e^{-\frac{i}{2}(\varphi_1 + \varphi_2 + \vartheta)} \end{pmatrix}. \quad (2.5.11)$$

## 2.5.2 Supersymmetric actions on $S_b^3$

The Yang-Mills action on  $S_b^3$  for a  $\mathcal{N} = 2$  vector multiplet<sup>†9</sup> is given by

$$S_{\text{YM}} = \frac{1}{g_{\text{YM}}^2} \int_{S_b^3} d^3x \sqrt{g} \text{Tr} \left( \frac{1}{4} F_{\mu\nu} F^{\mu\nu} + \frac{1}{2} D_{\mu} \sigma D^{\mu} \sigma + i \bar{\lambda} \gamma^{\mu} D_{\mu} \lambda + i \bar{\lambda} [\sigma, \lambda] + \frac{1}{2} \left( D + \frac{\sigma}{rf(\vartheta)} \right)^2 - \frac{\bar{\lambda} \lambda}{4rf(\vartheta)} \right), \quad (2.5.12)$$

<sup>†9</sup>In Euclid space, we cannot define a Majorana spinor unlike in Minkowski space time. Thus, for  $\mathcal{N} = 2$  supersymmetry, we consider a gaugino  $\bar{\lambda}$  is not complex conjugate of  $\lambda$ . but indenpedent spinor.



where  $D_\mu = \nabla_\mu - i[A_\mu, \cdot]$ ,  $r$  is the radius of  $S^3$  and  $g$  is the determinant of the metric  $g_{\mu\nu}$ . The supersymmetric Chern-Simons action is given by

$$S_{\text{SCS}} = \int_{S_b^3} d^3x \sqrt{g} \frac{ik}{4\pi} \text{Tr} \left( \frac{1}{\sqrt{g}} \epsilon^{\mu\nu\rho} A_\mu \left( \partial_\nu A_\rho - \frac{2i}{3} A_\nu A_\rho \right) + 2D\sigma + 2\lambda\bar{\lambda} \right), \quad (2.5.13)$$

with quantized level  $k$ . A Fayet-Iliopoulos action is

$$S_{\text{FI}} = \frac{i\zeta}{2\pi} \int_{S_b^3} d^3x \sqrt{g} \text{Tr} \left( D - \frac{\sigma}{rf(\vartheta)} \right), \quad (2.5.14)$$

We find that these actions are invariant under the following supersymmetric variation:

$$\delta A_\mu = -i \left( (\xi \gamma_\mu \bar{\lambda}) + (\bar{\xi} \gamma_\mu \lambda) \right) \quad (2.5.15)$$

$$\delta \sigma = \xi \bar{\lambda} - \bar{\xi} \lambda \quad (2.5.16)$$

$$\delta D = i D_\mu (\xi \gamma^\mu \bar{\lambda} - \bar{\xi} \gamma^\mu \lambda) - \frac{1}{r} \delta \sigma - i (\bar{\xi} [\sigma, \lambda] - \xi [\sigma, \bar{\lambda}]) \quad (2.5.17)$$

$$\delta \lambda = -\xi \left( D + \frac{\sigma}{rf(\vartheta)} \right) + \frac{1}{2} \gamma^{\mu\nu} F_{\mu\nu} \xi + i (D_\mu \sigma) \gamma^\mu \xi \quad (2.5.18)$$

$$\delta \bar{\lambda} = \bar{\xi} \left( D + \frac{\sigma}{rf(\vartheta)} \right) + \frac{1}{2} \gamma^{\mu\nu} F_{\mu\nu} \bar{\xi} - i (D_\mu \sigma) \gamma^\mu \bar{\xi} \quad (2.5.19)$$

We find that the correction terms to the flat space action are given  $\frac{1}{r}$  expansion. This is because the curvature of the curved manifold can be negligible when we focus on sufficiently microscopic physics, namely go to the ultraviolet region.

Next, we consider the kinetic term of the chiral multiplets  $(\phi, \psi, F)$  in the representation  $R$  of the gauge group<sup>†10</sup>. On  $S_b^3$ , we can assign the R-charge  $n$  to the chiral multiplets by adding the background gauge field which couple with R-symmetry current and giving an expectation value  $n$ . Then, the kinetic term of a chiral multiplet on  $S_b^3$  is written as

$$S_{\text{mat}} = \int_{S_b^3} d^3x \sqrt{g} \left( D_\mu \bar{\phi} D^\mu \phi - i \psi \gamma^\mu D_\mu \psi + \bar{F} F - i \bar{\phi} \left( D + \frac{\sigma}{rf(\vartheta)} \right) \phi - 2i \frac{n-1}{rf(\vartheta)} \bar{\phi} \sigma \phi \right) \quad (2.5.20)$$

$$+ \bar{\phi} \left( \sigma^2 - \frac{n(n-2)}{(rf(\vartheta))^2} \right) \phi + i \bar{\psi} \left( -\sigma + \frac{i}{rf(\vartheta)} \left( n - \frac{1}{2} \right) \right) + \sqrt{2} i (\bar{\phi} \lambda \psi + \phi \bar{\lambda} \bar{\psi}), \quad (2.5.21)$$

and the interactions among the multiple chiral multiplets is also given by the superpotential as

$$S_{\text{int}} = \int d^2\theta W(\Phi) + \int d^2\bar{\theta} \bar{W}(\bar{\Phi}). \quad (2.5.22)$$

<sup>†10</sup>We should consider  $\mathcal{N} = 2$  theory for Euclid space. In what follows,  $(\bar{\phi}, \bar{\psi}, \bar{F})$  should be regarded as an independent chiral multiplet in the conjugate representation of  $R$ .

These terms are invariant under the following variation of supersymmetry:

$$\delta\phi = \sqrt{2}\bar{\xi}\psi, \quad (2.5.23)$$

$$\delta\psi = \sqrt{2}\xi F + \sqrt{2}i\left(\sigma - i\frac{n}{rf(\vartheta)}\right)\bar{\xi}\phi - \sqrt{2}i\bar{\xi}D_\mu\phi, \quad (2.5.24)$$

$$\delta F = -\sqrt{2}i\left(\sigma - i\frac{n-2}{rf(\vartheta)}\right)\bar{\xi}\psi + 2i\bar{\xi}\lambda\phi - \sqrt{2}iD_\mu(\bar{\xi}\gamma^\mu\psi). \quad (2.5.25)$$

In particular, by the definition of a superpotential, a superpotential is regarded as the F-term of a gauge invariant chiral multiplet whose R-charge is 2. Then, a supersymmetric variation of (2.5.22) become 0 up to a total derivative term.

The actions we introduced above can be rewritten by the supersymmetric variation as follows:

$$S_{\text{YM}} = \delta_\xi\delta_{\bar{\xi}} \int_{S_b^3} dx^3 \sqrt{g} \left( \bar{\lambda}\lambda - 2D\sigma \right) \quad (2.5.26)$$

$$S_{\text{mat}} = \delta_{\bar{\xi}}\delta_\xi \int_{S_b^3} d^3x \sqrt{g} \left( \bar{\psi}\psi - 2i\bar{\phi}\sigma\phi + \frac{2(n-1)}{rf(\vartheta)}\bar{\phi}\phi \right), \quad (2.5.27)$$

$$S_{\text{int}} = \frac{1}{\sqrt{2}} \int_{S_b^3} d^3x \sqrt{g} \left( \bar{\xi}\delta_\xi\psi_{W(\Phi)} + \xi\delta_{\bar{\xi}}\psi_{W(\bar{\Phi})} \right), \quad (2.5.28)$$

where  $\psi_{W(\Phi)}$  ( $\psi_{W(\bar{\Phi})}$ ) denotes the middle component of the superpotential  $W(\Phi)$  ( $W(\bar{\Phi})$ ), respectively. This  $Q$ -exactness play a crucial role in the derivation of a localization technique.

## 2.6 Supersymmetric Localization method

A notable advantage of the supersymmetric theory is that we can obtain some non-perturbative properties of the theory. First, we introduce the general argument of the localization methods for the path integral and then, we apply it to a three-dimensional  $\mathcal{N} = 2$  gauge theory <sup>†11</sup>.

### 2.6.1 Localization technique for SUSY QFTs

We define the supersymmetric theory on a compact manifold  $\mathcal{M}$ . The expectation value of the BPS operator is given by through the path integral

$$\langle \mathcal{O}_{\text{BPS}} \rangle = \int_{\mathcal{F}} DX \mathcal{O}_{\text{BPS}} e^{-S[X]}, \quad (2.6.1)$$

---

<sup>†11</sup>There are several nice review articles, for example [47]

where  $X$  and  $\mathcal{F}$  represent all fields that the theory have and a total field configuration space respectively. Here, there are no infrared divergences since the the theory is defined on a compact manifold  $\mathcal{M}$ . The action  $S$  and the BPS operator  $\mathcal{O}_{\text{BPS}}$  are invariant ( $Q$ -closed) under the supersymmetric transformation  $\delta_Q$

$$\delta_Q S[X] = 0, \quad \delta_Q \mathcal{O}_{\text{BPS}} = 0. \quad (2.6.2)$$

the supersymmetry transformation  $\delta_Q$  satisfy the following relation:

$$\delta_Q^2 = (\text{Bosonic transformations}), \quad (2.6.3)$$

where the bosonic transformations is associated with the symmetry of the theory such as gauge transformations, translations and so on. The fact that the square of the supersymmetry transformation is vanishing up to symmetry transformation is important for the localization technique. We deform the theory by a  $Q$ -exact functional  $\delta_Q V[X]$  as follows:

$$\langle \mathcal{O}_{\text{BPS}}(t) \rangle = \int_{\mathcal{F}} DX \mathcal{O}_{\text{BPS}} e^{-S[X] - t \delta_Q V[X]}, \quad (2.6.4)$$

where  $t$  is a non-negative deformation parameter and  $V[X]$  is a functional of  $X$  that satisfies

$$\delta_Q^2 V[X] = 0, \quad V[X]|_{\text{Boson}} \geq 0, \quad (2.6.5)$$

where  $V[X]|_{\text{Boson}}$  represents the part composed by only bosonic fields. The original expectation value is recovered by taking  $t = 0$

$$\langle \mathcal{O}_{\text{BPS}} \rangle = \langle \mathcal{O}_{\text{BPS}}(0) \rangle \quad (2.6.6)$$

Moreover, we find that this deformed expectation value does not depend on the parameter  $t$  as follows:

$$\begin{aligned} \frac{d}{dt} \langle \mathcal{O}_{\text{BPS}}(t) \rangle &= - \int_{\mathcal{F}} DX \mathcal{O}_{\text{BPS}} \delta_Q (V[X]) e^{-S[X] - t \delta_Q V[X]} \\ &= - \int_{\mathcal{F}} DX \delta_Q (\mathcal{O}_{\text{BPS}} V[X]) e^{-S[X] - t \delta_Q V[X]} = 0 \end{aligned} \quad (2.6.7)$$

This implies that the expectation values can be evaluated at any values of  $t$ . In particular, when we take  $t$  to infinity, the path integral can be evaluated exactly by the saddle-point approximation associated with the localization parameter  $t$ . Actually, when we take  $t$  to infinite, in the RHS of (2.6.4), we find that the field configurations which satisfy  $\delta_Q V[X] > 0$  do not contribute to the path integral because the integrand of the path integral is  $e^{-\infty}$ . Thus, the path integral is not taken over whole field configuration space  $\mathcal{F}$ , but only the subspace which satisfies  $\delta_Q V[X]|_{\text{boson}} = 0$ .

It is important to which a deformation term  $\delta_Q V[X]$  we select because the saddle-point configuration and the one-loop corrections are determined by  $\delta_Q V[X]$ . One of the canonical choices of such a term is

$$\mathcal{L}_{\text{cano}} = \delta_Q \sum_{\psi} \left( (\delta_Q \psi)^\dagger \psi + \psi^\dagger (\delta_Q \psi^\dagger)^\dagger \right), \quad (2.6.8)$$

where the sum runs over all fermionic fields of the theory. The bosonic part of this term is given by the squares of supersymmetric variations of fermionic fields,

$$\mathcal{L}_{\text{cano}}|_{\text{boson}} = \sum_{\psi} (|\delta_Q \psi|^2 + |\delta_Q \psi^\dagger|^2), \quad (2.6.9)$$

then the saddle-point configuration is determined by the equations.

$$\psi = \psi^\dagger = 0, \quad \delta_Q \psi = \delta_Q \psi^\dagger = 0. \quad (2.6.10)$$

This condition is nothing but BPS condition.

Then, we need to evaluate the effects of the fluctuation around the dominant saddle-point configuration. If we regard the parameter  $t$  as the inverse of the Plank constant  $h$ , the effects of the fluctuation are regarded as the ‘‘loop effects’’ of the  $t = \frac{1}{h}$  expansion. To evaluate the effects, we expand the fields around the saddle-point as

$$X = X_0 + \frac{1}{\sqrt{t}} \delta X, \quad (2.6.11)$$

where  $X_0$  denotes the saddle-point configuration and  $\delta X$  denotes the fluctuation fields. By plugging this into the deformed action, we obtain

$$S[X] - t \delta_Q V[X] = S[X_0] + \frac{1}{2} \frac{\delta^2(\delta_Q V[X])}{\delta X^2} (\delta X)^2 + \mathcal{O}\left(\frac{1}{\sqrt{t}}\right), \quad (2.6.12)$$

where we assume that  $\frac{\delta S[X]}{\delta X}|_{X=X_0} = 0$ <sup>†12</sup>. We can take  $t$  to infinity and then, the ‘‘one-loop’’ part only remains. Finally, the path integral is given by

$$\langle \mathcal{O}_{\text{BPS}}(0) \rangle = \lim_{t \rightarrow \infty} \langle \mathcal{O}_{\text{BPS}}(t) \rangle = \int D X_0 D(\delta X) \mathcal{O}_{\text{BPS}}(X_0) e^{-S[X_0] - \frac{1}{2} \frac{\delta^2(\delta_Q V[X])}{\delta X^2} |_{X=X_0} (\delta X)^2}. \quad (2.6.13)$$

The ‘‘one-loop’’ effect is obtained by the Gaussian integral over the fluctuation fields  $\delta X$  and it is given by the determinant of  $\frac{\delta^2(\delta_Q V[X])}{\delta X^2}$ . Therefore, the path integral in (2.6.4) reduces to

---

<sup>†12</sup>The inequality  $\delta_Q V[X]_{\text{boson}} \geq 0$  means that the saddle-point configuration  $X_0$ , defined  $\frac{\delta S[X]}{\delta X}|_{X=X_0} = 0$ , automatically satisfies  $\delta_Q V[X]|_{\text{boson}} = 0$ . Thus, we consistently assume that the  $X_0$  satisfies  $\frac{\delta S[X]}{\delta X}|_{X=X_0} = 0$

the saddle-point configuration whose dimension is lower than the original one and the action is composed of “classical” action  $S[X_0]$  and “one-loop” corrections associated with  $t$ .

$$\langle \mathcal{O}_{\text{BPS}} \rangle = \int DX_0 \mathcal{O}_{\text{BPS}}(X_0) e^{-S[X_0]} \frac{1}{\text{SDet}[\frac{\delta^2 S[X]}{\delta X^2}]|_{X=X_0}}, \quad (2.6.14)$$

where the one-loop correction is schematically denoted by  $\frac{1}{\text{SDet}[\frac{\delta^2 S[X]}{\delta X^2}]|_{X=X_0}}$ , which is the ratio of the determinants of the operator arising from bosonic and fermionic fluctuation fields respectively. We note that the result (2.6.14) can be regarded as an exact semiclassical approximation with respect to an auxiliary Planck constant  $\hbar = \frac{1}{t}$  of the deformation action  $\delta_Q V[X]$ . Because the original action  $S[X]$  is not weighted  $t$ , it can only contribute to the classical part.

By employing the localization formula, the dimensionality of the path integral reduces. When fields configuration belonging to the localization locus depend on the spacetime, the reduced path integral is still an infinite dimensional integral, namely, the path integral of a lower-dimensional quantum field theory. The desirable case is that the localization locus is composed by the constant field configurations and then the path-integral reduces to a finite dimensional integral of a 0-dimensional quantum fields theory. In this sense, we often called the expectation value given by the finite dimensional integral as a matrix model. In particular, it is known that expectation values of various BPS operators of supersymmetric gauge theories in various dimensions are given by a matrix model by employing localization methods [21, 48–50, 53–55] and so on.

We note that when there are multiple conserved supercharges  $Q_i$ , we need to fix a supercharge  $Q_{i_0}$  in order to run the procedure of the localization methods. Depending on the choice of a supercharge, a set of the BPS operator  $\mathcal{O}_{\text{BPS}}$  is determined and a deformation term  $\delta_Q V[X]$  can differ, which need not be canonical one. A choice of a deformation term  $\delta_Q V[X]$  affect the localization saddle-point locus and then the one-loop corrections. This change of the localization scheme generally leads to apparently different forms of the localization formula. However, The final answers in different localization schemes must coincide because the differences are  $Q$ -exact terms and then they cannot contribute to the path integral. In this thesis, we employ one of the localization scheme, which is the so-called Coulomb branch localization. Another localization scheme, which is called Higgs branch localization, is also well-known [55–57].

## 2.6.2 $S_b^3$ partition function from Coulomb branch localization

In this section, we apply a localization method we reviewed in the previous section to the 3d  $\mathcal{N} = 2$  gauge theory. A theory needs to be defined on a compact manifold  $\mathcal{M}$  to be applied localization technique. In this thesis, we apply the localization methods to 3d  $\mathcal{N} = 2$  gauge

theory defined on  $\mathcal{M} = S_b^3$  introduced in the previous section 2.5.2. Looking back the argument on localization methods, we should choose the localization deformation term  $\delta_Q V[X]$  associated with a specific supersymmetry charge  $Q$ . Fortunately, we found that in (2.5.26) and (2.5.27), the kinetic terms of vector and chiral multiplets are rewritten as a form  $\delta_Q V[X]$ . We often use the kinetic terms as a localization term and find that the localization locus is given by the same condition as that of the canonical choice of  $\delta_Q V[X]$  introduced in the previous section. In this section, we introduced the formula of  $S_b^3$  partition function given by a matrix model and will not enter the detailed argument on the derivation of one-loop corrections. The detailed derivation is given by [45, 46].

We consider a gauge theory with gauge group  $G = \prod_{a=1}^r G_a$  and  $N_0$  chiral multiplets in the representation  $R$  of  $G$ . The corresponding vector multiplets to  $G_a$  is denoted as  $(A_{a\mu}, \lambda_a, \bar{\lambda}_a, D_a)$  with the label  $a$  associated with  $a$ -th gauge group. The  $N_0$  chiral multiplets is denoted as  $(\phi_{i\ell_0}, \psi_{i\ell_0}, F_{i\ell_0})$  with two indices  $i, \ell_0$  associated with the representation  $R$  and  $N_0$ , respectively. The localization locus given by the solution of the equations

$$\lambda_a = \bar{\lambda}_a = 0, \quad \delta_Q \lambda = \delta_Q \bar{\lambda}_a = 0, \quad (2.6.15)$$

$$\psi_{i\ell_0} = \bar{\psi}_{i\ell_0} = 0, \quad \delta_Q \psi_{i\ell_0} = \delta_Q \bar{\psi}_{i\ell_0} = 0. \quad (2.6.16)$$

is as follows:

$$\sigma_a = \sigma_{0a}, \quad (\sigma_{0a}: \text{constant matrix}), \quad (2.6.17)$$

$$D_a = -\frac{1}{rf(\vartheta)} \sigma_{0a}, \quad (\text{Other fields}) = 0. \quad (2.6.18)$$

This implies that the path integral reduces to an integration over the whole constant matrices, which is in the adjoint representation of  $G$ . By employing the gauge transformation, we can make the constant matrix  $\sigma_{0a}$  a diagonal matrix as

$$\sigma_{0a} = \text{diag}(\sigma_{0a,1}, \dots, \sigma_{0a,r_a}). \quad (2.6.19)$$

and then, the integration variables of the matrix integral can be changed to the diagonal elements with accompanied with the Vandermonde determinant as

$$\int_{\mathcal{F}} DX \rightarrow \prod_{a=1}^M \frac{1}{|W(G_a)|} \prod_{i=1}^{r_a} \left( \int d\sigma_{0a,i} \right) \prod_{a=1}^M \prod_{\alpha \in \Delta_+^a} \pi (\alpha(\sigma_{0a}))^2. \quad (2.6.20)$$

Therefore, the expectation values are written by the integration over the diagonal  $U(1)$ s part of  $\sigma_a$ , namely, they are represented by the contributions from the whole classical Coulomb phase of the theory with the generic point of the Coulomb branch. Then, this localization scheme is called Coulomb branch localization <sup>†13</sup>.

<sup>†13</sup>In what follows, all parameters which have mass dimensions will appear as a dimensionless form by the radius  $r$ . We will set  $r$  to 1 for simplicity.

By substituting the localization locus for the action, the classical action arises only from Chern-Simons terms and FI terms as

$$S_{\text{SCS}} = \sum_{a=1}^M \frac{ik_a}{4\pi} \int_{S^3} d^3x \sqrt{g} \text{Tr} (-2f(\vartheta) \sigma_{0a}^2) = -i\pi \sum_{a=1}^M k_a \sum_{i=1}^{r_a} (\sigma_{0a,i}^2), \quad (2.6.21)$$

$$S_{\text{FI}} = \sum_{a=1}^M \frac{i\zeta_a}{2\pi} \int_{S^3} d^3x \sqrt{g} \text{Tr} \left( -2 \frac{\sigma_{0a}}{f(\vartheta)} \right) = -2\pi i \sum_{a=1}^M \sum_{i=1}^{r_a} (\zeta_a r) (\sigma_{0a,i}). \quad (2.6.22)$$

Then, we would like to introduce one-loop correction which arise from the localization deformation terms, which are kinetic terms of the vector and chiral multiplets in this case. Here, we make a rough sketch of the derivation of the one-loop correction. In fact, we can evaluate  $\text{SDet}[\frac{\delta^2 S[X]}{\delta X^2}]|_{X=X_0}$  because the eigenvalues of the kinetic operator  $\frac{\delta^2 S[X]}{\delta X^2}|_{X=X_0}$ , which is composed of covariant derivative terms and interaction terms with  $\sigma_{a0}$  in this case, are denoted by indices which label the eigenvalues of the representation of the isometry group of  $S_b^3$ . Thus, the fluctuation fields can be expanded by the harmonic functions and then, the gaussian integral over the fluctuation fields can be done. Then,  $\text{SDet}[\frac{\delta^2 S[X]}{\delta X^2}]|_{X=X_0}$  can be represented by an infinite product of the eigenvalues of the kinetic operator  $\frac{\delta^2 S[X]}{\delta X^2}|_{X=X_0}$ . While almost all the contributions from the modes of the harmonic function expansion between the paired bosonic and fermionic degree of freedom by the supersymmetry, an infinite series of of the eigenvalues still remain arising from unpaired bosonic and fermionic degree of freedoms. Then, we would like to give the result in [45]. For a vector multiplets, the one-loop contributions are given by <sup>†14</sup>

$$Z_{1\text{-loop}}^{\text{vec}}(\sigma_{a0}) = \prod_{\alpha \in \Delta_+^a} \prod_{n>0} \left( \frac{n^2}{\ell^2} + (\alpha(\sigma_{0a}))^2 \right) \left( \frac{n^2}{\tilde{\ell}^2} + (\alpha(\sigma_{0a}))^2 \right) \quad (2.6.23)$$

$$= \prod_{\alpha \in \Delta_+^a} \frac{\sinh \pi b \alpha(\sigma_{0a}) \sinh \pi b^{-1} \alpha(\sigma_{0a})}{(\pi \alpha(\sigma_{0a}))^2}, \quad (2.6.24)$$

where  $\Delta_+^a$  denotes a set of the positive root of the Lie algebra of  $G_a$ . We note that the denominator is nothing but the Vandermonde determinant and exactly cancel a factor in (2.6.20).

For a chiral multiplets in the representation  $R$  and  $\hat{R}$  of gauge group  $G$  and of the global symmetry group  $\hat{G}$  with R-charge  $r$ <sup>†15</sup>, the one-loop correction is determined as

$$Z_{1\text{-loop}}^{\text{mat}}(\sigma_0) = \frac{\prod_{m,n \geq 0} \det_{R, \hat{R}}(mb + nb^{-1} - \frac{Q(r-2)}{2} + i(\sigma_0 + \hat{\sigma}))}{\prod_{m,n \geq 0} \det_{R, \hat{R}}(mb + nb^{-1} + \frac{Qr}{2} - i(\sigma_0 + \hat{\sigma}))} \quad (2.6.25)$$

<sup>†14</sup>The infinite product is divergent and should be regularized. In terms of the Physics, this divergence corresponds to an ultraviolet divergence. It is usually defined in the zeta function regularisation.

<sup>†15</sup>This is slight abuse of notation since we have employed “ $r$ ” as the radius of the ellipsoid. However, since the radius has been set to 1, “ $r$ ” denotes the R-charge.

$$= \prod_{\rho, \hat{\rho}} s_b \left( \frac{iQ(1-r)}{2} - (\rho(\sigma_0) + \hat{\rho}(\hat{\sigma})) \right), \quad Q = \frac{b+b^{-1}}{2}, \quad (2.6.26)$$

where we define  $\sigma_0$  as a diagonal matrix  $\text{diag}(\sigma_{01}, \sigma_{02}, \dots, \sigma_{0r})$ . We note that we can regard the part in (2.6.25)

$$m \equiv \rho(\sigma) + \hat{\rho}(\hat{\sigma}) \quad (2.6.27)$$

as effective real mass  $m(\sigma)$  of a chiral multiplet. This is because we can regard  $\rho(\sigma)$  is real mass arising from the higgs mechanism on a generic point of the Coulomb branch  $\sigma_0$  and  $\hat{\rho}(\hat{\sigma})$  is a real mass arising from introducing a background vector multiplet that couple with the symmetry current of a global symmetry.

Consequently, the corresponding  $S_b^3$  partition function for a given 3d  $\mathcal{N} = 2$  gauge theory is obtained by producing the classical part with the one-loop part as

$$Z^{S_b^3}(\hat{\sigma}, k, \zeta) = \prod_{a=1}^M \frac{1}{|W(G_a)|} \prod_{i=1}^{r_a} \left( \int d\sigma_{0a,i} \right) Z_{1\text{-loop}}(\sigma_0, \hat{\sigma}) Z_{\text{classical}}(\sigma_0, k, \zeta), \quad (2.6.28)$$

where we define

$$Z_{\text{classical}}(\sigma_0, k, \zeta) = e^{-S_{\text{SCS}} - S_{\text{FI}}}, \quad (2.6.29)$$

$$Z_{\text{one-loop}}(\sigma_0, \hat{\sigma}) = \prod_{a=1}^M \prod_{\alpha \in \Delta_+^a} \sinh \pi b \alpha(\sigma_{0a}) \sinh \pi b^{-1} \alpha(\sigma_{0a}) \prod_{\rho, \hat{\rho}} s_b \left( \frac{iQ(1-r)}{2} - (\rho(\sigma_0) + \hat{\rho}(\hat{\sigma})) \right). \quad (2.6.30)$$

We note that an expectation value does not depend on the Yang-Mills coupling because the Yang-Mills term is  $Q$ -exact and then, it cannot contribute to the expectation values. In particular, a  $S_b^3$  partition function without any real mass parameter denotes the infrared fixed point of the gauge theory obtained as  $g \rightarrow \infty$  even though its derivation depends only on the ultraviolet definition of the gauge theory. In fact, between two gauge theories which flow to the same IR fixed point, namely they are a pair associated with the Seiberg like duality, it is confirmed that their partition functions coincide in many cases [21, 58, 59]. The localization methods have played an important role in consistency checks of dualities.

Then, we would like to argue on the partition function for a real mass-deformed theory. Because the partition function has mass parameters, the partition function cannot represent some infrared fixed point of some gauge theory. Then, we may interpret the deformed partition function denoting the theory obtained by adding the fixed point theory to which the undeformed theory flows to the real mass deformation term. If there are no spontaneously symmetry breaking



of the global symmetry of the gauge theory, the infrared fixed point theory has the same global symmetry. Then, we can deform the fixed point theory by real mass parameter by introducing the background vector multiplets which couple with the current of the global symmetry. Thus, when  $m = 0$ , the partition function denote the fixed point theory and it also may denote another fixed point theory when we take  $m$  to infinity.

We introduce the localization formula for a partition function, namely, in case that  $\mathcal{O}_{\text{BPS}} = 1$  in (2.6.14) so far. To calculate the expectation value  $\mathcal{O}_{\text{BPS}}$ , all we have to do is to insert it evaluated at the localization locus in (2.6.28). For example, a supersymmetric Wilson-loop in representation  $R$  on  $S^1$  at  $\theta = 0$  defined as

$$W_R(\theta = 0) \equiv \text{Tr}_R \text{P exp} \oint_{\theta=0} (iA + \sigma dl), \quad (2.6.31)$$

is also evaluated at the saddle-point inserting the Wilson loop becomes

$$W_R(\theta = 0)|_{\text{saddle}} = \text{Tr}_R(e^{2\pi \frac{\sigma}{b}}). \quad (2.6.32)$$

in the finite dimensional integral in (2.6.28).

### 2.6.3 Useful formulas and examples

In the previous section, we introduced the finite integral formula denoting an expectation value. Generally, it has the all non-perturbative effects of the gauge theory in some sense. However, it is still difficult to do the integral exactly for given parameters because the integrand is a complex form. Fortunately, For specific theories, which have high supersymmetry, the integrand often reduces to a simple form by employing the formulas about the double sine function  $s_b$ . In this section, we introduce useful formulas of the double sine function and find that the integrand becomes the more simple form for the specific case.

The function  $s_b$  is a double sine function. We introduce some properties of the function studied in [60,61]. The double sine function  $s_b(x)$  satisfies

$$s_b(z) = s_{b^{-1}}(z), \quad s_b(z)s_b(-z) = 1, \quad (2.6.33)$$

and the expansion around  $\text{Re}(z) = \infty$ :

$$i \log s_b(z) = -\frac{\pi z^2}{2} - \frac{\pi}{24}(b^2 + b^{-2}) + \sum_{l=1}^{\infty} \frac{(-1)^{l-1}}{l} \left( \frac{e^{-2\pi l b z}}{2 \sin(\pi l b^2)} + \frac{e^{-2\pi l z/b}}{2 \sin(\pi l b^{-2})} \right), \quad (2.6.34)$$

and around  $\text{Re}(z) = -\infty$ :

$$i \log s_b(z) = \frac{\pi z^2}{2} + \frac{\pi}{24}(b^2 + b^{-2}) + \sum_{l=1}^{\infty} \frac{(-1)^l}{l} \left( \frac{e^{2\pi l b z}}{2 \sin(\pi l b^2)} + \frac{e^{2\pi l z/b}}{2 \sin(\pi l b^{-2})} \right). \quad (2.6.35)$$

For the vector like matters, the 1-loop factor becomes

$$\left( \prod_{w \in R} s_b \left( \frac{iQ}{2} (1-r) - w(\sigma) \right) \right) \left( \prod_{w \in R} s_b \left( \frac{iQ}{2} (1-r) + w(\sigma) \right) \right) = \prod_{w \in R} D_{-iQ(1-r)/2}(w(\sigma)), \quad (2.6.36)$$

where

$$D_\alpha(x) \equiv \frac{s_b(x - \alpha)}{s_b(x + \alpha)}. \quad (2.6.37)$$

This function satisfies

$$D_\alpha(x) = D_\alpha(-x). \quad (2.6.38)$$

We also define

$$D_b(x) \equiv D_{-iQ/4}(x). \quad (2.6.39)$$

When  $|\text{Im}(x)| < \frac{|\text{Re}Q|}{2}$ ,  $\log D_b(x)$  has the following integral form:

$$\log D_b(x) = \int_{\mathbb{R}+i0} \frac{dt \sinh\left(\frac{Qt}{2}\right) \cos(2xt)}{2t \sinh(bt) \sinh(b^{-1}t)}. \quad (2.6.40)$$

For round three-sphere  $S^3$  case, it is useful to introduce the following function  $\ell(x)$  defined in [51]:

$$\ell(x) = -x \log(1 - e^{2\pi ix}) + \frac{i}{2} \left( \pi x^2 + \frac{1}{\pi} \text{Li}_2(e^{2\pi ix}) \right) - \frac{\pi i}{12} \quad (2.6.41)$$

The double sine function  $s_b(x)$  with  $b = 1$  is written by  $\ell(z)$  as

$$\log s_b(iz) = \ell(z). \quad (2.6.42)$$

When  $b = 1$ , (2.6.36) become drastically simple as

$$\prod_{w \in R} D_1(w(x)) = \prod_{w \in R} \frac{1}{2 \cosh(\pi w(x))}. \quad (2.6.43)$$

In what follows, we introduce simple examples of the partition function using above formulas.

### Example: Free massive chiral multiplet

For a chiral multiplet with R-charge  $r$  and real mass  $m$ , the partition function is given by

$$Z_{\text{free}}(r, m) = s_b \left( \frac{iQ(1-r)}{2} - im \right). \quad (2.6.44)$$

Then, for two chiral multiplets with R-charge  $r$  and real mass  $\pm m$  respectively, the partition function

$$Z_{\text{free}}(r, m) = s_b \left( \frac{iQ(1-r)}{2} - im \right) s_b \left( \frac{iQ(1-r)}{2} + im \right) = D_{-\frac{iQ(1-r)}{2}}(m). \quad (2.6.45)$$

When  $r = \frac{1}{2}$  and  $b = 1$ , the partition function has the following simple form:

$$Z_{\text{free}}(m) = \frac{1}{2 \cosh \pi m} \quad (2.6.46)$$

### Example: $\mathcal{N} = 2$ SQED and check of mirror symmetry

three-dimensional  $\mathcal{N} = 2$  SQCD with  $N_f$  flavors and an FI term  $\zeta$  denote the U(1) Yang-Mills theory with  $N_f$  pairs of massive chiral multiplets in fundamental representation and in anti-fundamental representation with real mass  $m$ <sup>†16</sup>. The partition function is given by

$$Z_{\text{SQED}} = \int_{-\infty}^{\infty} d\sigma e^{2\pi i \zeta \sigma} s_b \left( \frac{iQ(1-r_1)}{2} + \sigma - m \right) s_b \left( \frac{iQ(1-r_2)}{2} - \sigma - m \right) \quad (2.6.47)$$

and the integral over  $\sigma$  is exactly done by the Ramanujan's integral identity

$$\begin{aligned} Z_{\text{SQED}} = & e^{-\frac{i\pi}{12}(1+Q^2)} e^{-i\pi\zeta\left(\frac{iQ(r_1-r_2)}{2}\right)} s_b \left( \frac{iQ(1-(r_1+r_2))}{2} + 2m \right) \\ & \times s_b \left( \zeta - \frac{iQ(1-(r_1+r_2))}{2} + m \right) s_b \left( -\zeta - \frac{iQ(1-(r_1+r_2))}{2} + m \right). \end{aligned} \quad (2.6.48)$$

When  $r_1 = r_2$ , this result reflect in the fact that SQED flows to the XYZ model composed three free chiral multiplet  $X, Y$  and  $Z$  with the superpotential  $W = XYZ$  in the IR [65] in the sense that

$$Z_{\text{SQED}} = Z_{XYZ}. \quad (2.6.49)$$

In the RHS of (2.6.48), three double sine functions correspond to free chiral multiplets  $X, Y, Z$ . In fact, this is an example of the consistency check of a infrared duality in three-dimensional supersymmetric field theories through  $S_b^3$  partition functions.

---

<sup>†16</sup>it seems that tbecaus there are two U(1) global symmetries as the maximal subgroup we can introduce two real mass parameter  $m_1$  and  $m_2$ . However, one parameter of the real mass parameters cancel by shifting  $\sigma$ . Generally speaking, the real mass parameter corresponds to the diagonal part of the global symmetry group.

## Example: $\mathcal{N} = 4$ SQCD with massive hypermultiplets

### Vector multiplet

We only consider  $U(N)$  gauge theories in this paper. The one-loop contribution of the vector multiplets is given by

$$Z_{1\text{-loop}}^{\text{vec}}(\sigma) = \prod_{i<j}^N \frac{4 \sinh^2 \pi(\sigma_i - \sigma_j)}{\pi^2(\sigma_i - \sigma_j)^2}, \quad (2.6.50)$$

where the denominator cancels against the Vandermonde determinant, which appears when we choose the diagonal gauge of  $\sigma$ .

### Matter multiplet

Here, we consider following two mass deformations: In case (i), we give a real mass  $m$  to  $\frac{N_f}{2}$  flavors while we give a real mass  $-m$  to the remaining  $\frac{N_f}{2}$  flavors<sup>†17</sup>. This breaks each  $SU(N_f)$  of the global symmetry  $SU(N_f) \times SU(N_f)$  down to  $SU(\frac{N_f}{2}) \times SU(\frac{N_f}{2})$ . The total one-loop contribution is given by

$$Z_{1\text{-loop}}^{\text{mat}}(\sigma) = \prod_{i=1}^N (D_b(\sigma_i + m) D_b(\sigma_i - m))^{\frac{N_f}{2}} \prod_{i=1}^N \frac{1}{2 (\cosh \pi(\sigma_i + m) 2 \cosh \pi(\sigma_i - m))^{\frac{N_f}{2}}}. \quad (2.6.51)$$

In case (ii), we give  $\frac{N_f}{3}$  flavors a real mass  $m$  while we give other  $\frac{N_f}{3}$  flavors a real mass  $-m$ . Then, we keep the remaining  $\frac{N_f}{3}$  flavors massless. This real mass assignment breaks each of the  $SU(N_f)$  global symmetries of the matter fields down to  $SU(\frac{N_f}{3}) \times SU(\frac{N_f}{3}) \times SU(\frac{N_f}{3})$ <sup>†18</sup>. The total one-loop contribution of the chiral multiplets is given by

$$Z_{1\text{-loop}}^{\text{mat}}(\sigma) = \prod_{i=1}^N (D_b(\sigma + m) D_b(\sigma - m) D_b(x))^{\frac{N_f}{3}} \prod_{i=1}^N \frac{1}{(2 \cosh \pi(\sigma_i + m) 2 \cosh \pi(\sigma_i - m) 2 \cosh \pi \sigma_i)^{\frac{N_f}{3}}}. \quad (2.6.52)$$

---

<sup>†17</sup>We assume that  $\frac{N_f}{2}$  is an integer.

<sup>†18</sup>We assume that  $\frac{N_f}{3}$  is an integer.

## Part II

# Aspects of Massive Gauge Theory on The Three-Sphere

# Chapter 3

## Dominant Point of Coulomb Branch in Infinite Mass Limit

In this chapter, we investigate  $S^3$  partition functions of real mass-deformed  $\mathcal{N} = 4$  U( $N$ ) SQCD in the infinite mass limit<sup>†1</sup>. For example, if we give real masses to enough matter multiplets of a “good” theory for it to become a “bad” theory after the massive matter fields decouple, it could naively be thought that the massive matter multiplets will decouple from the theory. Thus, it is interesting to investigate what happens to this partition function in the infinite mass limit. In particular, a partition function of a “bad” theory is divergent.<sup>†2</sup> This means that our interest is to determine which hypermultiplets become effectively massless or massive in the infinite mass limit on the three-sphere. When a theory is defined on flat space, we must choose a vacuum in order to determine decoupling of matter fields. However, we cannot select a vacuum for the theories on the three-sphere. In particular, we will apply the Coulomb branch localization scheme to calculate the  $S^3$  partition function and this is given by the integration over the classical Coulomb branch parameters in flat space. Therefore, it is difficult to determine whether or not the massive multiplets will decouple when we take the infinite mass limit.

It is highly non-trivial to determine which points dominantly contribute to a  $S^3$  partition function in the infinite mass limit because all points of the Coulomb branch can contribute to it, including generic points and singular ones. The singular points have special meanings in the sense that whole or a part of W-bosons become massless on that point. Namely, the gauge group is recovered. As an example, let us consider U(2)  $\mathcal{N} = 4$  SQCD with  $\frac{N_f}{2}$  pairs

---

<sup>†1</sup>The infinite mass limit of the matrix model of 3d gauge theories is also considered in [59, 66–69] in the context of finding new examples of Seiberg-like dualities [31, 70]. This is because in the infinite mass limit the matter fields can decouple from the theory and a phase transition can occur.

<sup>†2</sup>The magnetic theory of a “bad” theory in terms of the Seiberg-like duality is considered as a good theory [67].

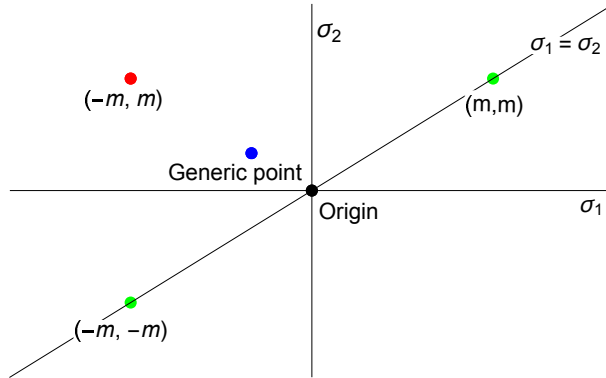


Figure 3.1: This figure schematically shows the real parts of the two classical Coulomb branch parameters of  $U(2)$   $\mathcal{N} = 4$  SQCD with  $\frac{N_f}{2}$  pairs of hypermultiplets with real mass  $\pm m$ . There are some special points where new massless degrees of freedom appear or the gauge symmetry is enhanced to  $U(2)$ . Here, we assume that  $\sigma_2 \geq \sigma_1$  due to the Weyl symmetry of  $U(2)$ . (This figure is cited from my paper [5].)

of hypermultiplets with real mass  $\pm m$ . In Figure 3, we show that the real parts of the two classical Coulomb branch parameters have some special points denoted by colored dots. When we take a generic point of the Coulomb branch (blue dot), the low-energy effective theory is  $U(1) \times U(1)$  with massive matter fields and W-bosons while on a specific point, such as green or red points, the effective theory has  $\frac{N_f}{2}$  or  $N_f$  massless hypermultiplets, respectively. The origin (black dot) is also special in the sense that the gauge symmetry is enhanced to  $U(2)$ . These special points may be likely to dominantly contribute to the partition function. However, we cannot determine which points dominantly contribute to the partition function so far.

First, we focus on the solution of the saddle-point equation because the solution corresponds to a classical Coulomb branch point and in the large  $N$  limit it gives a dominant contribution to the  $S^3$  partition function. Hence, in the large  $N$  limit, we can determine which massive matter fields decouple as well as which theory will appear as an effective theory on the point of the Coulomb branch which corresponds to the solution.

Then, we would like to determine the dominant which points of the Coulomb branch become dominant even in the finite  $N$  and the infinite mass limit. The dominant point should exist and then the partition function becomes that of an effective theory because the infinite mass limit corresponds to the decompactified limit ( $r_{S^3} \rightarrow \infty$ )<sup>†3</sup> and in flat space we must choose a

---

<sup>†3</sup>Mass parameters  $m$  necessarily appear as a combination with the radius of the three-sphere  $r_{S^3}$  as  $mr_{S^3}$ . Therefore we cannot distinguish between the infinite mass limit and the decompactified limit. In our convention we take  $r_{S^3}$  to 1.

vacuum. From the solution of the saddle-point, we determine the mechanism of the vacuum selection in the infinite mass limit, rather than the large  $N$  limit. We deduce the dominant point of the Coulomb branch from the large  $N$  analysis and verify it for the partition function for small rank  $N$ . We also confirm that the effective theory is the same as that we deduced. Therefore, we conclude that this vacuum selection does not require the large  $N$  limit, rather than just the infinite mass limit.

We study the two types of the mass-deformed  $\mathcal{N} = 4$   $U(N)$  SQCD. For the first one, there are only massive matter fields with real mass  $\pm m$  and for the second one, there are massive and massless matter fields. The first deformation is simple and suitable for studying the case in which the mass deformation of a good theory leads to a bad theory after decoupling of the matter fields. The second deformation is simple and suitable for investigating the case where a good theory arise from the mass deformation of a good theory after the massive matter fields simply decouple from the theory.

The rest of this chapter is organized as follows: In Section 3.1, we solve the saddle-point equation of  $\mathcal{N} = 4$  SQCD with massless or massive matter fields and investigate the theory that appears in the infinite mass limit. In Section 3.2, we calculate the partition function for finite rank SQCDs and evaluate the leading part in the infinite mass limit. In Section 3.3 we present a conclusion and discussion. In Appendix A.1, we introduce the techniques of the resolvent methods utilized in this paper. In Appendix A.2, we explain mixed Chern-Simons terms which appear in the infinite mass limit as one-loop effects. Then, we attempt to interpret what happens in the infinite mass limit in terms of these mixed Chern-Simons terms. In Appendix A.3, we discuss the convergent bound of the matrix model and reconsider the matrix model of the effective theory in the infinite mass limit from the viewpoint of its convergence bound.

## 3.1 Large $N$ solution and point of Coulomb branch

### 3.1.1 SQCD with massless hypermultiplets

In this subsection, we solve the saddle-point equation of  $U(N)$  SQCD with massless hypermultiplets and FI parameter. In particular in this section, we consider imaginary FI terms. This is in preparation for the latter part of this paper, where such terms appear as one-loop effects when we take the infinite mass limit, namely in the form of certain mixed Chern-Simons terms. The solution is given as an eigenvalue density function  $\rho(x)$ , which determines the large  $N$



behavior of the theory. The partition function is written as

$$Z = \frac{1}{N!} \int \prod_{i=1}^N dx_i \frac{e^{\pi\zeta \sum_i x_i} \prod_{i<j} 4 \sinh^2(\pi(x_i - x_j))}{\prod_i \left(2 \cosh \pi(x_i)\right)^{N_f}}, \quad (3.1.1)$$

It is generally difficult to calculate this partition function exactly. Fortunately, the leading part in the large  $N$  limit can be evaluated by the saddle-point approximation. Namely, the  $N$  dimensional integration are evaluated by substituting the solution of the saddle-point equation into the integrand as

$$Z = \int d^N x e^{-S[x]} \xrightarrow{N \rightarrow \infty} e^{-S[x]}|_{\text{saddle}}, \quad (3.1.2)$$

where the RHS represents that the integrand is evaluated at the solution of the saddle-point equation into. For this theory, the saddle-point equation is given by

$$0 = \zeta + N_f \tanh(\pi x_i) - 2 \sum_{j \neq i} \coth \pi(x_i - x_j). \quad (3.1.3)$$

Assuming that the eigenvalues become dense in the large  $N$  limit, we take the continuous limit as follows:

$$\frac{i}{N} \rightarrow s \in [0, 1], \quad x_i \rightarrow x(s), \quad \frac{1}{N} \sum_{i=1}^N \rightarrow \int ds. \quad (3.1.4)$$

The leading part of this saddle-point equation is given by a singular integral equation<sup>†4</sup>

$$0 = \eta + \xi \tanh \pi(x) - 2 \left( \text{P} \int dy \rho(y) \coth \pi(x - y) \right), \quad (3.1.5)$$

where we also took  $N_f$  to be infinite with

$$\xi \equiv \frac{N_f}{N}, \quad \eta \equiv \frac{\zeta}{N}, \quad (3.1.6)$$

finite and introduced the density function  $\rho(x)$  defined as

$$\frac{ds}{dx} \equiv \rho(x), \quad (3.1.7)$$

---

<sup>†4</sup>We denote a principal value integral as

$$\text{P} \int dx.$$

with the following normalization condition:

$$\int_I dx \rho(x) = 1. \quad (3.1.8)$$

This means that we regard the values of the eigenvalues denoted by  $x$  as constituting the fundamental variables. The density function  $\rho(x)$  counts the number of the eigenvalues which exist between  $x$  and  $x + dx$ . In order to solve the equation (3.1.5), it is useful to employ the resolvent methods. In Appendix A.1, a brief summary of the resolvent methods is provided. Before solving the equation, we define the variables  $X$  and  $Y$  as

$$e^{2\pi x} \equiv X, \quad e^{2\pi y} \equiv Y \quad (3.1.9)$$

and also define the resolvent  $\omega(X)$  and the potential  $V'(x)$  as

$$\omega(X) \equiv 2 \int_I dy \rho(y) \frac{e^{\pi(x-y)} + e^{-\pi(x-y)}}{e^{\pi(x-y)} - e^{-\pi(x-y)}} = 2 \int_I dy \rho(y) \frac{X + Y}{X - Y} = 2 \left( 1 + \int_{\mathcal{C}} \frac{dY}{\pi} \frac{\rho(y)}{X - Y} \right), \quad (3.1.10)$$

$$V'(x) \equiv \eta + \frac{X - 1}{X + 1} \xi, \quad (3.1.11)$$

where  $I$  and  $\mathcal{C}$  represent the intervals  $[x_{\min}, x_{\max}]$  and  $[b, a]$  respectively. The resolvent is determined from the analyticity and the one-cut solution of the resolvent is given by (A.1.14) as

$$\omega(X) = \eta + \xi \left( \frac{X - 1}{X + 1} - \frac{2\sqrt{(X - a)}\sqrt{(X - b)}}{(X + 1)\sqrt{(1 + a)(1 + b)}} \right) = \eta + \omega_0(X; 1; a, b), \quad (3.1.12)$$

For later convenience, we have introduced the following function  $\omega_0$ :

$$\omega_0(X; A; a, b) = \xi \left( \frac{X - A}{X + A} - \frac{2A\sqrt{(X - a)}\sqrt{(X - b)}}{(X + A)\sqrt{(1 + a)(1 + b)}} \right). \quad (3.1.13)$$

Then, the solution  $\rho(x)$  defined on  $[b, a]$  is given by (A.1.8) as

$$\rho(x) = \frac{\xi}{(X + 1)} \sqrt{\frac{(X - b)(a - X)}{(1 + a)(1 + b)}}. \quad (3.1.14)$$

where  $a$  and  $b$  are determined from the equation describing the asymptotic behavior of  $\omega(X)$  at  $X = 0$  and  $\infty$ :

$$\frac{\eta}{\xi} = \frac{1 - \sqrt{ab}}{\sqrt{(1 + b)(1 + a)}}, \quad (3.1.15)$$

$$1 - \frac{2}{\xi} = \frac{1 + \sqrt{ab}}{\sqrt{(1 + b)(1 + a)}}. \quad (3.1.16)$$

Because an FI term breaks the  $\mathbb{Z}_2$  symmetry under which  $x_i \rightarrow -x_i$  in the saddle-point equation,  $a$  and  $b$  do not satisfy the condition  $ab = 1$ . The solutions of (3.1.15) and (3.1.16) are given by

$$a = \frac{-4 + 4\xi + \xi^2 - \eta^2 + 4\sqrt{(\xi - 1)(\xi^2 - \eta^2)}}{(-2 + \xi + \eta)^2}, \quad b = \frac{-4 + 4\xi + \xi^2 - \eta^2 - 4\sqrt{(\xi - 1)(\xi^2 - \eta^2)}}{(-2 + \xi + \eta)^2}. \quad (3.1.17)$$

From (3.1.15) and (3.1.16), we find that the solution only exists when

$$\xi \geq 2 + |\eta|. \quad (3.1.18)$$

This condition is equivalent to the condition that the matrix model converges in the large  $N$  limit. In Appendix A.3, we will discuss the convergence bound of the matrix model of SQCDs.

Here, we argue on the relation between this large  $N$  solution and a point of the classical Coulomb branch. The equation (3.1.17) implies that when we take  $r_{S^3}$  to infinity,  $x_{\min}$  and  $x_{\max}$  become 0 because the edges of the interval given by  $a = e^{2\pi r_{S^3} x_{\max}}$  and  $b = e^{2\pi r_{S^3} x_{\min}}$ , where the radius is recovered as  $x \rightarrow x r_{S^3}$ . Thus, the saddle-point solution becomes condensed to 0 in this limit. Because taking the radius to infinity corresponds to considering the theory on a flat space, this solution corresponds to the origin of the Coulomb branch in flat space. On this point, the theory at the deep IR of the RG flow expected to be an interacting superconformal field theory because the W-bosons become massless on the point. Thus, it is expected that the sphere partition function of SQCD with massless hypermultiplets always represents that of the non-trivial SCFT. Here, we note that we use the terminology ‘‘Coulomb branch’’ as that associated with a flat space, not the three-sphere. Generally, the Coulomb branch associated with flat space and that associated with the three-sphere is completely different. In this thesis, we would like to claim that the saddle-point solution corresponds to a point of the Coulomb branch associated with flat space in the decompactified limit.

### 3.1.2 SQCD with massive hypermultiplets

In this subsection, we consider  $U(N)$  SQCD with  $N_f$  pairs of chiral multiplets with real mass  $m$  and the partition function is given as follows (2.6.51):

$$Z = \frac{1}{N!} \int \prod_{i=1}^N dx_i \frac{\prod_{i<j} 4 \sinh^2(\pi(x_i - x_j))}{\prod_i \left( 2 \cosh \pi(x_i + m) 2 \cosh \pi(x_i - m) \right)^{\frac{N_f}{2}}}. \quad (3.1.19)$$

When  $m = 0$ , this partition function becomes that of  $U(N)$  with  $N_f$  massless fundamental hypermultiplets. If the massive matter multiplets decouple, the partition function is not well

defined because the theory become a bad theory. In what follows, we confirm that in the infinite mass limit the partition function does not diverge and its leading part in the infinite mass limit may correspond to the partition function of a effective theory.

The saddle-point equation for the above matrix model is written as

$$2 \sum_i \coth \pi(x_i - x_j) = \frac{N_f}{2} \left( \tanh \pi(x_i + m) + \tanh \pi(x_i - m) \right), \quad (3.1.20)$$

and in the continuous limit this becomes

$$4 \left( \text{P} \int dy \rho(y) \coth \pi(x - y) \right) = \xi \left( \tanh \pi(x + m) + \tanh \pi(x - m) \right), \quad (3.1.21)$$

Then, the resolvent  $\omega(X)$  and potential  $V'(x)$  are defined as

$$\omega(X) = 4 \int dy \rho(y) \frac{X + Y}{X - Y} = 4 \left( 1 + \int \frac{dY}{\pi} \frac{\rho(y)}{X - Y} \right), \quad (3.1.22)$$

$$V'(x) = \xi \left( \frac{X - M^{-1}}{X + M^{-1}} + \frac{X - M}{X + M} \right), \quad (3.1.23)$$

where we have defined  $M$  instead of  $m$  as

$$M \equiv e^{2\pi m}. \quad (3.1.24)$$

Then, the saddle-point equation is solved by analytic properties (A.1.14) of the resolvent as

$$\omega(X) = \omega_0(X; M; a, b) + \omega_0(X; M^{-1}; a, b), \quad (3.1.25)$$

and the density function through the discontinuity equation on the branch cut (A.1.8) as

$$\rho(x) = \frac{\xi}{2} \left[ \frac{M \sqrt{(a - X)(X - b)}}{(X + M) \sqrt{(M + a)(M + b)}} + \frac{M^{-1} \sqrt{(a - X)(X - b)}}{(X + M^{-1}) \sqrt{(M^{-1} + a)(M^{-1} + b)}} \right]. \quad (3.1.26)$$

The constants  $a$  and  $b$  are detemined by the symmetry under the simultaneous change of signs of all eigenvalues and asymptotic behavior when  $X = 0$ :

$$-4 = 2\xi \left( -1 + \frac{1}{\sqrt{(M + a)(M + \frac{1}{a})}} + \frac{1}{\sqrt{(M^{-1} + a)(M^{-1} + \frac{1}{a})}} \right), \quad (3.1.27)$$

and the solution  $a$  is given by

$$a = \frac{2(\xi - 1)(M^2 + 1) + M\xi^2 + 2(M + 1)\sqrt{(\xi - 1)(\xi - 1 + M^2(\xi - 1) + M(\xi^2 - 2\xi + 2))}}{M(\xi - 2)^2}. \quad (3.1.28)$$

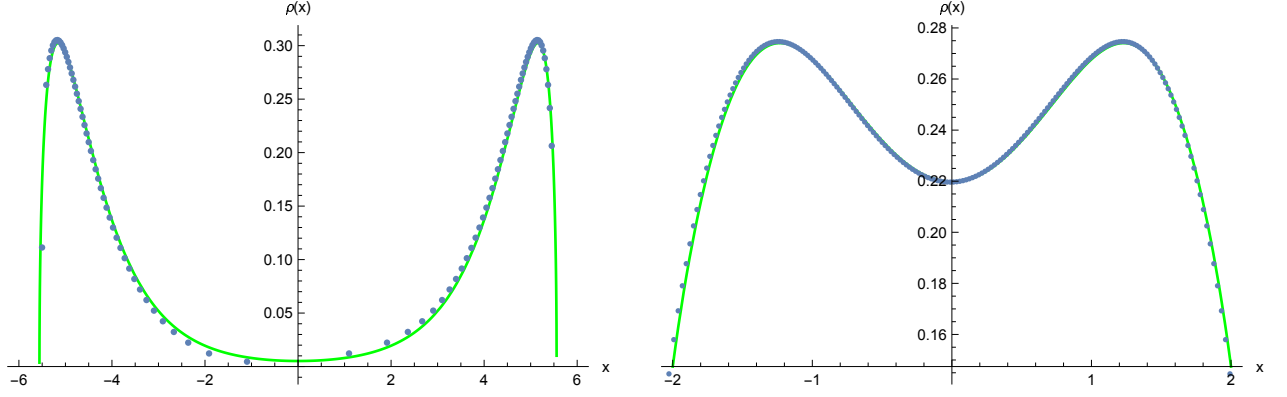


Figure 3.2: These figures show the numerical solution (blue dots) and analytic solutions for  $\rho(x)$  (green line). The left utilizes the parameter  $(N, N_f, m) = (100, 2000, 2)$ , and the right one is for parameter  $(N, N_f, m) = (200, 800, 0.5)$ . There is relation between the numerical  $x_{\text{num}}$  and exact  $x_{\text{exa}}$  values as  $\pi x_{\text{exa}} = x_{\text{num}}$ . (These figures are cited from my paper [5].)

This equation immediately implies that  $a$  exists when  $\xi \geq 2$ . This implies that this type of mass deformation does not affect the bound of the existence of the solution.

In the infinite mass limit, it can naively be thought that this theory becomes a bad theory, and its partition function diverges. However, this argument is not correct in the following sense: The partition function of this massive SQCD theory corresponds to that of an effective theory on a point of the Coulomb branch associated with the solution of the saddle-point equation. The density function shows that the eigenvalues corresponding to the solution gather around  $\pm m$ , which is showed in Figure 3.2. This implies that the solution of the saddle-point equation corresponds to the following point of the Coulomb branch:

$$\sigma = \left( \begin{array}{c|c} -m \mathbf{1}_{\frac{N}{2} \times \frac{N}{2}} & \mathbf{0} \\ \hline \mathbf{0} & m \mathbf{1}_{\frac{N}{2} \times \frac{N}{2}} \end{array} \right). \quad (3.1.29)$$

In fact, this argument is confirmed as follows: We assume that the eigenvalues are separated as

$$x_i = \begin{cases} m - \lambda_i & (i = 1, \dots, \frac{N}{2}), \\ -m - \tilde{\lambda}_i & (i = \frac{N}{2} + 1 \dots N), \end{cases} \quad (3.1.30)$$

where we also assume that  $\lambda_i$  and  $\tilde{\lambda}_i$  are independent on  $m$ . For the first  $\frac{N}{2}$  eigenvalues, the saddle-point equations (3.1.20) are written as

$$0 = -2 \sum_{j \neq i} \coth \pi (\lambda_i - \lambda_j) - 2 \sum_j \coth \pi (\lambda_i - \tilde{\lambda}_j - 2m) + \frac{N_f}{2} \left( \tanh \pi \lambda_i + \tanh \pi (\lambda_i - 2m) \right)$$

$$\rightarrow 0 = N \left( \frac{N_f}{2N} - 1 \right) + 2 \sum_{j \neq i}^{\frac{N}{2}} \coth \pi (\lambda_i - \lambda_j) - \frac{N_f}{2} \tanh \pi \lambda_i, \quad (3.1.31)$$

where we took the infinite mass limit in the second line. It is worth noting that the first term in the second line can be interpreted as the gauge-R mixed Chern-Simons term [62–64] induced by integrating out the massive gauginos and complex fermions of chiral multiplets. Then, for the latter  $\frac{N}{2}$  eigenvalues, the saddle-point equation in the large mass limit is

$$0 = N \left( 1 - \frac{N_f}{2N} \right) + 2 \sum_{j \neq i}^{\frac{N}{2}} \coth \pi (\tilde{\lambda}_i - \tilde{\lambda}_j) - \frac{N_f}{2} \tanh \pi \tilde{\lambda}_i. \quad (3.1.32)$$

The equations (3.1.31) and (3.1.32) imply that in the infinite mass limit the partition function (3.1.19) becomes <sup>†5</sup>

$$Z \sim Z_{\text{Massive}}(m) \int d^{\frac{N}{2}} \lambda \frac{e^{\pi N \left( \frac{N_f}{2N} - 1 \right) \sum_i \lambda_i} \prod_{i < j} (2 \sinh \pi (\lambda_i - \lambda_j))^2}{\prod_i (2 \cosh \pi \lambda_i)^{\frac{N_f}{2}}} \\ \times \int d^{\frac{N}{2}} \tilde{\lambda} \frac{e^{-\pi N \left( \frac{N_f}{2N} - 1 \right) \sum_i \tilde{\lambda}_i} \prod_{i < j} (2 \sinh \pi (\tilde{\lambda}_i - \tilde{\lambda}_j))^2}{\prod_i (2 \cosh \pi \tilde{\lambda}_i)^{\frac{N_f}{2}}}, \quad (3.1.33)$$

because the saddle-point equation of this is equivalent to (3.1.31) and (3.1.32). The factor  $Z_{\text{Massive}}(m)$  arises from the contribution of decoupled free massive degrees of freedom. We can evaluate  $Z_{\text{Massive}} \sim M^{-\frac{N}{2}(N_f - N)}$  by substituting (3.1.30) for (3.1.19). This matrix model represents SQCD theories with the two  $U(\frac{N}{2})$  gauge group,  $\frac{N_f}{2}$  fundamental hypermultiplets, and an FI parameter  $\pm N \left( 1 - \frac{N_f}{2N} \right)$ . <sup>†6</sup> We will argue that FI terms and the sector of decoupled free massive degree of freedoms can be interpreted as induced mixed Chern-Simons term through one-loop effect of the massive fermions in Appendix A.2.

Then, we verify our assumptions by comparing the density function of the effective theory (3.1.33) with that of the original theory (3.1.19) in the infinite mass limit. First, we consider the density function of SQCD with massive hypermultiplets (3.1.26) in the infinite mass limit. In order to focus on the peak of the density function around  $+m$ , we redefine  $X$  as  $X = MZ$  and assume that  $Z$  is order  $\mathcal{O}(M^0)$ . This redefinition corresponds to simultaneous shifting  $x_i$  by  $m$ . We consider the expansion of  $a$  (3.1.28) and  $\rho$  around  $m = \infty$ . It is given by

$$a = \alpha M + \mathcal{O}(M^0), \quad \alpha \equiv \frac{4(\xi - 1)}{(\xi - 2)^2}, \quad (3.1.34)$$

<sup>†5</sup>The overall factor of the matrix model cannot be determined in this procedure.

<sup>†6</sup>To be precise, the FI parameter is given by  $\frac{1}{r_{S^3}} \left( 1 - \frac{N_f}{2N} \right)$  if we recover the radius of  $S^3$  because in a 3d theory an FI parameter has mass dimension 1.

$$\rho(x) = \frac{\xi}{2(Z+1)} \sqrt{\frac{Z(\alpha-Z)}{1+\alpha}} + \mathcal{O}(M^{-1}), \quad (3.1.35)$$

where  $Z \in [0, \alpha]$  in the infinite mass limit. We compare this with the solution for the saddle-point equation of  $\lambda$  part (3.1.31) because  $\lambda$  part corresponds to a part of the massive SQCD in which the eigenvalues are concentrated on  $+m$ . The solution of its saddle-point equation (3.1.31) is given by applying the result in Section 3.1.1. In this case,  $a$ ,  $b$  and  $\rho(x)$  are obtained as

$$a = \alpha, \quad b = 0, \quad (3.1.36)$$

$$\rho(z) = \frac{\xi}{2(Z+1)} \sqrt{\frac{Z(\alpha-Z)}{1+\alpha}}, \quad Z \equiv e^{2\pi z}, \quad (3.1.37)$$

where the additional factor of  $\frac{1}{2}$  arises from the fact that the effective theory has two  $U(\frac{N}{2})$  gauge groups and the normalization condition should be taken as

$$\int_I \frac{dZ}{2\pi Z} \rho(z) = \frac{1}{2}. \quad (3.1.38)$$

The density functions (3.1.35) and (3.1.37) are completely equivalent. Next, we should consider the part around  $-m$ . Here, in order to focus on the part, we rewrite  $X$  as  $X = M^{-1}Z$  in (3.1.26) and the density function in this limit can be written as

$$\rho(x) = \frac{\xi}{2(Z+1)} \sqrt{\frac{Z - \frac{1}{\alpha}}{1 + \frac{1}{\alpha}}} + \mathcal{O}(M^{-1}), \quad (3.1.39)$$

where  $Z$  is defined on an interval  $[\frac{1}{\alpha}, \infty]$ . Then, we should compare this with the solution of  $\tilde{\lambda}$  part of (3.1.33). The solution is given by applying the result of 3.1.1 to (3.1.32) as

$$a = \infty, \quad b = \frac{1}{\alpha}, \quad (3.1.40)$$

with the density function

$$\rho(z) = \frac{\xi}{2(Z+1)} \sqrt{\frac{Z - \frac{1}{\alpha}}{1 + \frac{1}{\alpha}}}. \quad (3.1.41)$$

This is the same as (3.1.39). Thus, we conclude that SQCD with  $N_f$  massive hypermultiplets, as studied here, becomes two SQCDs in the infinite mass limit: each theory is a  $U(\frac{N}{2})$  SQCD with  $\frac{N_f}{2}$  massless hypermultiplets and the FI term  $\zeta = \pm iN(\frac{2N_f}{N} - 1)$ . This result implies that if the mass deformation naively leads to a bad theory, the sphere partition function actually becomes that of a specific effective theory. This is because a specific point of the Coulomb branch dominantly contributes to the partition function in the infinite mass limit. This result also suggests that a mass-deformed theory cannot be employed for the UV regularization of a bad theory. In Section 3.2, we will verify our claim through the exact calculation of the partition function of finite  $N$  cases.

### 3.1.3 SQCD with massive and massless hypermultiplets

In the previous subsection, we made all matter fields massive. Here, we consider an SQCD theory with both massive and massless matter fields. The number of massless matter fields will change the asymptotic behavior of the partition function in the infinite mass limit since the existence of sufficient matter fields makes the partition function convergent.

We think of  $U(N)$  SQCD with  $\frac{N_f}{3}$  pairs of massive hypermultiplets with  $\pm m$  and  $\frac{N_f}{3}$  massless hypermultiplets.<sup>†7</sup> The partition function for this theory is given by (2.6.52)

$$Z = \frac{1}{N!} \int \prod_{i=1}^N dx_i \frac{\prod_{i<j} 4 \sinh^2(\pi(x_i - x_j))}{\prod_i \left( 2 \cosh \pi(x_i + m) 2 \cosh \pi(x_i - m) 2 \cosh \pi(x_i) \right)^{\frac{N_f}{3}}}. \quad (3.1.42)$$

The saddle-point equation is

$$2 \sum_{j \neq i}^N \coth \pi(x_i - x_j) = \frac{N_f}{3} (\tanh \pi(x_i + m) + \tanh \pi(x_i - m) + \tanh \pi x_i), \quad (3.1.43)$$

and in the continuous limit, this equation is rewritten as

$$6 \left( \mathbb{P} \int_{\mathcal{C}} dy \coth \pi(x - y) \right) = \xi \left( \tanh \pi(x + m) + \tanh \pi(x - m) + \tanh \pi x \right). \quad (3.1.44)$$

In this case, the resolvent  $\omega(X)$  and potential  $V'(x)$  are defined as

$$\omega(X) = 6 \int dy \rho(y) \frac{X + Y}{X - Y} = 6 \left( 1 + \int \frac{dY}{\pi} \frac{\rho(y)}{X - Y} \right), \quad (3.1.45)$$

$$V'(x) = \xi \left( \frac{X - 1}{X + 1} + \frac{X - M}{X + M} + \frac{X - M^{-1}}{X + M^{-1}} \right), \quad (3.1.46)$$

where  $M = e^{2\pi m}$ . The resolvent is determined by its analytic properties and obtained from (A.1.14) as

$$\omega(X) = \omega_0 \left( X; 1; a, \frac{1}{a} \right) + \omega_0 \left( X; M; a, \frac{1}{a} \right) + \omega_0 \left( X; M^{-1}; a, \frac{1}{a} \right), \quad (3.1.47)$$

where  $b$  is determined as  $\frac{1}{a}$  because of the symmetry of the saddle-point equation under the simultaneous changing the sign of the eigenvalues. Then, the cut  $\mathcal{C} = [\frac{1}{a}, a]$  is determined by the following asymptotic equation:

$$-\frac{6}{\xi} = -3 + \frac{2}{\sqrt{(1+a)(1+\frac{1}{a})}} + \frac{2}{\sqrt{(M+a)(M+\frac{1}{a})}} + \frac{2}{\sqrt{(M^{-1}+a)(M^{-1}+\frac{1}{a})}}. \quad (3.1.48)$$

<sup>†7</sup>Here, We assume that  $\frac{N_f}{3}$  is an integer.



There are generally no explicit forms of the solution because this equation corresponds to an octic equation in  $a$ . However we can obtain the solution numerically or in the infinite mass limit.

The density function for this case is determined by (A.1.8) as

$$\rho(x) = \frac{\xi}{3} \left[ \frac{M\sqrt{(a-X)(X-\frac{1}{a})}}{(X+M)\sqrt{(M+a)(M+\frac{1}{a})}} + \frac{M^{-1}\sqrt{(a-X)(X-\frac{1}{a})}}{(X+M^{-1})\sqrt{(M^{-1}+a)(M^{-1}+\frac{1}{a})}} + \frac{\sqrt{(a-X)(X-\frac{1}{a})}}{(X+1)\sqrt{(1+a)(1+\frac{1}{a})}} \right]. \quad (3.1.49)$$

Then, we argue that the leading behavior of the partition function in the infinite mass limit depends on the number of the matter fields. First, when  $\frac{N_f}{3} \geq 2N$ , the partition function is still well-defined even if all massive matter fields decouple from the theory. This implies that the limit in which mass goes to infinity and the integrals of the matrix model are commutative<sup>†8</sup>. In this case, all massive matter fields simply decouple and the remaining theory is  $U(N)$  SQCD with  $\frac{N_f}{3}$  massless matter fields. This situation is reflected in the equation (3.1.48) in the sense that the equation becomes the same as (3.1.16) for the case with  $\frac{N_f}{3}$  flavors and  $b = \frac{1}{a}$ . To confirm this fact, we assume that the solution does not depend on  $M$  when we take  $m$  to infinity. Then, the equation becomes

$$3 - \frac{6}{\xi} = \frac{2}{\sqrt{(1+a)(1+\frac{1}{a})}}. \quad (3.1.51)$$

This implies that the solution of (3.1.48), which does not depend on mass  $m$  can exist when  $\frac{N_f}{3} \geq 2N$  while the constant solution cannot exist in the infinite mass limit when  $\frac{N_f}{3} < 2N$ . The numerical analysis of (3.1.48) supports the existence of such a solution. Indeed, the density function becomes the same as that of  $U(N)$  gauge theory with  $\frac{N_f}{3}$  massless hypermultiplets. Therefore, we conclude that in this case, all the massive hypermultiplets simply decouple from the theory because the origin of the Coulomb branch become dominant in the infinite mass limit.

---

<sup>†8</sup>In this work, we focus only on the leading part of the mass infinite limit. Namely, when there exist finite constants  $\alpha$  and  $\beta$  such that the relation

$$\lim_{M \rightarrow \infty} \left( \int_{-\infty}^{\infty} dx f(x, M) M^\alpha \right) = \int_{-\infty}^{\infty} dx \lim_{M \rightarrow \infty} (f(x, M) M^\alpha) = \beta, \quad (3.1.50)$$

is satisfied for  $f(x, M)$ , which is a function of  $x$  and  $M$ , we say that the infinite integral and the limit of  $M$  are commutative.

Next, we consider the case  $\frac{N_f}{3} < 2N$ . the solution  $a$  have to be proportional to  $M$  in the infinite mass limit and then, we find that the density function has three peaks: around the origin and  $x = \pm m$ . We illustrate the behavior of the density function  $\rho(x)$  in Figure 3.3. We would like to study the effective theory in the infinite mass limit that appears in this situation by analyzing the density function. First, we should know how the gauge group  $U(N)$  is broken. Because the density function has three peaks, it is expected that the gauge group  $U(N)$  is broken into three parts. Thus, we assume that

$$U(N) \rightarrow U(N_1) \times U(N_2) \times U(N_3), \quad (N_1 + N_2 + N_3 = N). \quad (3.1.52)$$

Each rank of the three gauge groups is determined by the numbers of eigenvalues around each peak. Since the density function  $\rho(x)$  counts the number of the eigenvalues between  $x$  and  $x + dx$ , what we should do to count the numbers of the eigenvalues that exist around each peak is to integrate the corresponding density function over the corresponding peak. Then, we can determine each rank of the three gauge group.

First, we would like to determine a solution proportional to  $M$ . In the infinite mass limit, the equation (3.1.48) becomes with the assumption  $a = M\beta$ .

$$1 - \frac{2}{\xi} = \frac{2}{3\sqrt{(1+\beta)}}, \quad (3.1.53)$$

then we can immediately determine  $\beta$  as

$$\beta = \frac{(5\xi - 6)(-\xi + 6)}{9(\xi - 2)^2}. \quad (3.1.54)$$

In order to study the behavior of the density function around  $x = m$ , we redefine  $X$  using an order  $\mathcal{O}(M^0)$  variable  $Z$  as  $X = MZ$ . When  $m \rightarrow \infty$ , the density function (3.1.49) becomes

$$\rho(x) \xrightarrow{m \rightarrow \infty} \rho_+(z) \equiv \frac{\xi}{3(Z+1)} \sqrt{\frac{Z(\beta - Z)}{1 + \beta}}, \quad Z \equiv e^{2\pi z}, \quad (3.1.55)$$

where  $Z \in [0, \beta]$ . Next, we investigate the density function around the peak at  $x = -m$  by redefining  $X$  as  $X = M^{-1}Z$  in (3.1.49). By the same calculation as in (3.1.37), this becomes

$$\rho(x) \xrightarrow{m \rightarrow \infty} \rho_-(z) \equiv \frac{\xi}{3(Z+1)} \sqrt{\frac{Z - \frac{1}{\beta}}{1 + \frac{1}{\beta}}}, \quad (3.1.56)$$

where  $Z \in [\frac{1}{\beta}, \infty]$ . Finally, we study the density function around  $x = 0$ . To focus on this part of the density function, we regard  $X$  as order  $\mathcal{O}(M^0)$ . Then, in the infinite mass limit, the density function becomes

$$\rho(x) \xrightarrow{m \rightarrow \infty} \rho_0(z) \equiv \frac{\xi\sqrt{Z}}{3(Z+1)}, \quad (3.1.57)$$

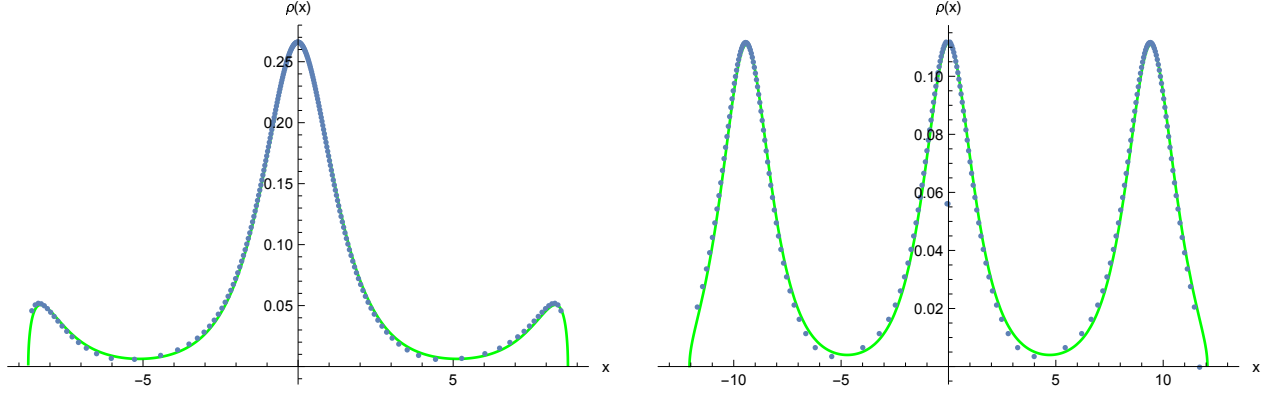


Figure 3.3: These figure shows the density function  $\rho(x)$  (3.1.49) (green line) and the numerical one from the saddle-point equation (blue dots). The left and right figures correspond to  $(N, N_f, m) = (200, 1000, 3)$  and  $(200, 420, 3)$  respectively. There are relation between the numerical values  $x_{\text{num}}$  and exact values  $x_{\text{exa}}$  as  $\pi x_{\text{exa}} = x_{\text{num}}$ . (These figures are cited from my paper [5].)

where  $Z$  takes value  $\in [0, \infty]$ . In order to determine  $N_1$ ,  $N_2$  and  $N_3$ , we employ (3.1.55), (3.1.56) and (3.1.57), respectively. We obtain the following relation:

$$\int_0^\beta \frac{dZ}{2\pi Z} \rho_+(z) = \frac{6 - \xi}{12}, \quad (3.1.58)$$

$$\int_{\frac{1}{\beta}}^\infty \frac{dZ}{2\pi Z} \rho_-(z) = \frac{6 - \xi}{12}, \quad (3.1.59)$$

$$\int_0^\infty \frac{dZ}{2\pi Z} \rho_0(z) = \frac{\xi}{6}. \quad (3.1.60)$$

This result implies that the gauge group  $U(N)$  is broken into the following:

$$N_1 = \frac{\xi}{6}N, \quad N_2 = N_3 = \frac{6 - \xi}{12}N, \quad (3.1.61)$$

where we assume that  $\frac{\xi}{6}N$  and  $\frac{6 - \xi}{12}N$  are integers. This implies that in the infinite mass limit, the theory becomes a effective theory on a point of the Coulomb branch as

$$\sigma = \left( \begin{array}{c|c|c} -m \mathbf{1}_{N_2 \times N_2} & & \\ \hline & \mathbf{0}_{N_1 \times N_1} & \\ \hline & & m \mathbf{1}_{N_2 \times N_2} \end{array} \right). \quad (3.1.62)$$

We assume that eigenvalues are separated as

$$x_i = \begin{cases} -m - \lambda_i^1, & (i = 1, \dots, N_2), \\ \lambda_i^2, & (i = N_2 + 1, \dots, N_1 + N_2), \\ m - \lambda_i^3 & (i = N_1 + N_2 + 1, \dots, N). \end{cases} \quad (3.1.63)$$

Through a similar calculation in the previous subsection, the saddle-point equation is rewritten in the following three parts under the assumption:

$$0 = 2N \left( \frac{6 + \xi}{12} - \frac{\xi}{3} \right) + 2 \sum_{j \neq i}^{N_2} \coth \pi (\lambda_i^1 - \lambda_j^1) - \frac{N_f}{3} \tanh \pi \lambda_i^1, \quad (i = 1, \dots, N_2), \quad (3.1.64)$$

$$0 = 2 \sum_{j \neq i}^{N_1} \coth \pi (\lambda_i^2 - \lambda_j^2) - \frac{N_f}{3} \tanh \pi \lambda_i^2, \quad (i = 1, \dots, N_1) \quad (3.1.65)$$

$$0 = -2N \left( \frac{6 + \xi}{12} - \frac{\xi}{3} \right) + 2 \sum_{j \neq i}^{N_2} \coth \pi (\lambda_i^3 - \lambda_j^3) - \frac{N_f}{3} \tanh \pi \lambda_i^3, \quad (i = 1, \dots, N_2). \quad (3.1.66)$$

These equations imply that the partition function (3.1.19) in the infinite mass limit becomes the following matrix model:

$$\begin{aligned} Z = & Z_{\text{massive}}(m) \int d^{N_2} \lambda^2 \frac{e^{2\pi N \left( \frac{\xi}{3} - \frac{6+\xi}{12} \right) \sum_i \lambda_i^2} \prod_{i < j} (2 \sinh \pi (\lambda_i^2 - \lambda_j^2))^2}{\prod_i (2 \cosh \pi \lambda_i^2)^{\frac{N_f}{3}}} \\ & \times \int d^{N_2} \lambda^3 \frac{e^{-2\pi N \left( \frac{\xi}{3} - \frac{6+\xi}{12} \right) \sum_i \lambda_i^3} \prod_{i < j} (2 \sinh \pi (\lambda_i^3 - \lambda_j^3))^2}{\prod_i (2 \cosh \pi \lambda_i^3)^{\frac{N_f}{3}}} \int d^{N_1} \lambda^1 \frac{\prod_{i < j} (2 \sinh \pi (\lambda_i^1 - \lambda_j^1))^2}{\prod_i (2 \cosh \pi \lambda_i^1)^{\frac{N_f}{3}}}. \end{aligned} \quad (3.1.67)$$

There are FI terms associated with two  $U(N_2)$  gauge group, which also arise from the gauge-R-symmetry mixed Chern-Simons term. The  $U(N_1)$  part has no FI terms since there are pairs of mixed Chern-Simons terms which have opposite overall signs corresponding to those of the masses of the effectively massive fermions. The decoupled massive free sector can be estimated by  $Z_{\text{Massive}}(m) \sim M^{-\frac{N_f N(6+\xi)}{36}}$  by substituting (3.1.63) for (3.1.42).

In fact, we can confirm that the three density functions in the infinite mass limit are the same as those obtained from (3.1.64), (3.1.65) and (3.1.66). First, the solution of (3.1.64) is obtained from (3.1.14) and (3.1.17) as

$$a = \infty, \quad \rho(z) = \frac{\xi \sqrt{Z}}{3\pi(Z+1)}, \quad (3.1.68)$$

where  $Z \in [0, \infty]^{\dagger 9}$ . This density function is the same as  $\rho_0(z)$ . Next, we consider the solution of (3.1.65). We obtain the solution from the equations (3.1.17) as

$$a = \infty, \quad b = \frac{(\tilde{\xi} - 2)^2}{4(\tilde{\xi} - 1)} = \frac{1}{\beta}, \quad \tilde{\xi} \equiv \frac{4\xi}{6 - \xi}, \quad (3.1.69)$$

---

<sup>†9</sup>Here we assume that  $\frac{Z}{a}$  is zero since when we scale  $Z = a\tilde{Z}$ ,  $\rho(z)$  is  $\mathcal{O}(\frac{1}{a})$  and only the order  $\mathcal{O}(a^0)$  part of  $Z$  can contribute to  $\rho(z)$ .

and the density function is

$$\rho(z) = \frac{6 - \xi}{12} \frac{\tilde{\xi}}{(Z + 1)} \sqrt{\frac{Z - \frac{1}{\beta}}{1 + \frac{1}{\beta}}} = \frac{\xi}{3(Z + 1)} \sqrt{\frac{Z - \frac{1}{\beta}}{(1 + \frac{1}{\beta})}}, \quad (3.1.70)$$

where  $Z \in [\frac{1}{\beta}, \infty]$ . This coincides with  $\rho_-(z)$ . Finally, we consider the solution of (3.1.66) obtained in the same manner as that of (3.1.65) as

$$a = \frac{4(\tilde{\xi} - 1)}{(\tilde{\xi} - 2)^2} = \beta, \quad b = 0, \quad (3.1.71)$$

and

$$\rho(z) = \frac{6 - \xi}{12} \frac{\tilde{\xi}}{(Z + 1)} \sqrt{\frac{Z(\beta - Z)}{1 + \beta}} = \frac{\xi}{3(Z + 1)} \sqrt{\frac{Z(\beta - Z)}{1 + \beta}}. \quad (3.1.72)$$

This density function is the same as  $\rho_+(z)$ . We note that the normalization condition of each density function is set such that they correspond to each rank of the gauge groups (3.1.61). We conclude that the partition function (3.1.42) becomes that (3.1.67) in the infinite mass limit. The result so far suggests that the massive multiplets cannot always simply decouple from the theory. In other words, a partition function of a “good” theory cannot become that of a “bad” theory after the massive matter fields decouple although a partition function of a “good” theory can become that of a specific “good” theory after simply decoupling of the massive matter multiplets. A notable result is that the gauge group of the effective theory depends on the number of flavors.

## 3.2 Finite rank SQCD

For SQCD cases, partition functions can be actually calculated at least for a sufficiently low rank of the gauge group. In this section, through exact results, we confirm exact results that our argument for the effective theory is true even in case of finite  $N$ . Furthermore, we reveal what happens in the infinite mass limit for theories that are not covered by our argument in the large  $N$  limit.

### 3.2.1 With massive hypermultiplets

#### U(1) SQED

The partition function of SQED with massive matter fields is given by

$$Z_{\text{U}(1)}^{N_f} = \int_{-\infty}^{\infty} dx \frac{1}{(2 \cosh \pi(x + m) 2 \cosh \pi(x - m))^{\frac{N_f}{2}}}. \quad (3.2.1)$$

This model is considered in [15] with an FI term. In this case, the theory may not become the effective theory expected from the previous section because  $\frac{N_f}{2}$  is not integer. Thus, it is interesting to know what happens in this case when  $m \rightarrow \infty$ . The exact result for any  $N_f$  is given in terms of the hypergeometric function as [15]

$$Z_{\text{U}(1)}^{N_f} = \frac{\Gamma(\frac{N_f}{2})}{2^{\frac{N_f}{2}} \sqrt{2\pi} \Gamma(\frac{N_f}{2} + \frac{1}{2}) (\cosh 2\pi m + 1)^{\frac{N_f}{2} - \frac{1}{2}}} {}_2F_1\left(\frac{1}{2}, \frac{1}{2}, \frac{N_f}{2} + \frac{1}{2}; \frac{1}{2}(1 - \cosh 2\pi m)\right), \quad (3.2.2)$$

and its leading part in the infinite mass limit is written as

$$Z_{\text{U}(1)}^{N_f} \xrightarrow{m \rightarrow \infty} \frac{1}{\pi} \frac{\log M}{M^{\frac{N_f}{2}}}, \quad M \equiv e^{2\pi m}. \quad (3.2.3)$$

This is a strange result in the sense of our argument so far because a decoupled sector, which is the only part depending on mass in the mass infinite limit, does not have such a term. Therefore, we cannot determine what the effective theory is in this case from our previous argument.

## U(2) SQCD

The partition function for this theory is following:

$$Z_{\text{U}(2)}^{N_f} = \frac{1}{2!} \int_{-\infty}^{\infty} dx \int_{-\infty}^{\infty} dy \frac{4 \sinh^2 \pi(x-y)}{(2 \cosh \pi(x+m) 2 \cosh \pi(x-m) 2 \cosh \pi(y+m) 2 \cosh \pi(y-m))^{\frac{N_f}{2}}}, \quad (3.2.4)$$

and the results for small  $N_f$  are summarized in the following table.

$N_f = 4$	$N_f = 6$	$N_f = 8$	$N_f = 10$
$\frac{1}{(2\pi)^2 M^2}$	$\frac{1}{(4\pi)^2 M^4}$	$\frac{1}{(6\pi)^2 M^6}$	$\frac{1}{(8\pi)^2 M^8}$

Table 3.1: The leading part of  $Z_{\text{U}(2)}^{N_f}$  when  $m \rightarrow \infty$ .

These results show that in the infinite mass limit, our expectation obtained from the large  $N$  calculation is valid since the following relation is verified:

$$Z_{\text{Massive}} Z_{\text{U}(1) \times \text{U}(1)} = \frac{4 \sinh^2(2\pi m)}{(2 \cosh 2\pi m)^{N_f}} \int_{-\infty}^{\infty} dx \frac{e^{\pi(2 - \frac{N_f}{2})x}}{(2 \cosh \pi x)^{\frac{N_f}{2}}} \int_{-\infty}^{\infty} dx \frac{e^{-\pi(2 - \frac{N_f}{2})x}}{(2 \cosh \pi x)^{\frac{N_f}{2}}}$$

$$\xrightarrow{m \rightarrow \infty} \frac{1}{((N_f - 2)\pi)^2 M^{(N_f - 2)}}, \quad (3.2.5)$$

where two integrals represent a  $U(1) \times U(1)$  theory and the pre-factor  $Z_{\text{massive}}$  denotes the decoupled massive free sector, for which the denominator arises from massive hypermultiplets and the numerator arises from vector multiplets. the gauge group  $U(2)$  can be broken down  $U(1) \times U(1)$  since  $\frac{N}{2}$  is an integer. In this case, we also find that the leading part of partition functions are equal with a partition function of corresponding effective theory including the overall factor, which cannot be determined from the large  $N$  analysis.

### U(3) SQCD

The partition function for this case is written as

$$Z_{U(3)}^{N_f} = \frac{1}{3!} \int_{-\infty}^{\infty} dx dy dz \frac{4 \sinh^2 \pi(x - y) 4 \sinh^2 \pi(x - z) 4 \sinh^2 \pi(y - z)}{(2 \cosh \pi(x \pm m) 2 \cosh \pi(y \pm m) 2 \cosh \pi(z \pm m))^{\frac{N_f}{2}}}, \quad (3.2.6)$$

where we have defined the following notation:

$$2 \cosh \pi(X \pm Y) \equiv 2 \cosh \pi(X + Y) 2 \cosh \pi(X - Y). \quad (3.2.7)$$

The results for small  $N_f$  are summarized in the following table:

$N_f = 6$	$N_f = 8$	$N_f = 10$	$N_f = 12$
$\frac{\log M}{16\pi^3 M^5}$	$\frac{\log M}{144\pi^3 M^8}$	$\frac{\log M}{576\pi^3 M^{11}}$	$\frac{\log M}{1600\pi^3 M^{14}}$

Table 3.2: The leading part of  $Z_{U(3)}^{N_f}$  when  $m \rightarrow \infty$

In this case, it may not also be possible that the partition function of effective theories is divided into a superconformal field theory sector and a massive free sector for the same reason as in the  $U(1)$  case, namely, that  $\frac{N}{2}$  is not an integer.

### 3.2.2 With massive and massless hypermultiplets

#### U(1) SQED

This case is trivial because the limit that takes mass to infinity is commutative with the infinite integral. Massive matter fields simply decouple from the theory and the remaining theory is

SQED with  $\frac{N_f}{3}$  massless hypermultiplets. In fact, the following relation is valid:

$$\tilde{Z}_{\text{U}(1)}^{N_f} = \int_{-\infty}^{\infty} dx \frac{1}{(2 \cosh \pi x 2 \cosh \pi(x+m) 2 \cosh \pi(x-m))^{N_f/3}} \xrightarrow{m \rightarrow \infty} \left(\frac{1}{M}\right)^{N_f/3} \tilde{Z}_{\text{U}(1)}^{N_f}|_{m=0},$$

where for  $\mathcal{N} = 4$  U( $N$ ) SQCD with a massless flavors part,  $\tilde{Z}_{\text{U}(N)}^{N_f}|_{m=0}$  can be calculated for  $N_f \geq 2N$  [71, 72] as

$$\tilde{Z}_{\text{U}(N)}^{N_f}|_{m=0} = \frac{1}{N!} \frac{1}{(2\pi)^N} \prod_{k=0}^{N-1} \frac{\Gamma(k+2) \left(\Gamma\left(\frac{N_f}{2} - N + k + 1\right)\right)^2}{\Gamma(N_f - N + k + 1)}. \quad (3.2.8)$$

## U(2) SQCD

In what follows, we present the exact calculation of the partition function of U(2) SQCD

$$\tilde{Z}_{\text{U}(2)}^{N_f} = \frac{1}{2!} \int_{-\infty}^{\infty} dx dy \frac{4 \sinh^2 \pi(x-y)}{(2 \cosh \pi(x \pm m) 2 \cosh \pi(y \pm m) 2 \cosh \pi x 2 \cosh \pi y)^{N_f/3}}. \quad (3.2.9)$$

The results for small  $N_f$  are summarized in the following table:

$N_f = 3$	$N_f = 6$	$N_f = 9$	$N_f = 12$
$\frac{1}{4M}$	$\frac{(\log M)^2}{4\pi^2 M^4}$	$\frac{1}{32M^6}$	$\frac{1}{48\pi^2 M^8}$

Table 3.3: The leading part of  $\tilde{Z}_{\text{U}(2)}^{N_f}$  when  $m \rightarrow \infty$ .

When  $N_f = 3$ , we can deduce the effective theory as follows:

$$Z_{\text{Massive}} Z_{\text{U}(1) \times \text{U}(1)} = \frac{4 \sinh^2 2\pi m}{(2 \cosh 2\pi m 2 \cosh \pi m)^2} \left( \int_{-\infty}^{\infty} dx \frac{1}{2 \cosh \pi x} \right)^2 \xrightarrow{m \rightarrow \infty} \frac{1}{4M}. \quad (3.2.10)$$

This means that the effective theory appears when we chose the point of the Coulomb branch as

$$\sigma = \begin{pmatrix} -m \\ m \end{pmatrix}, \quad (3.2.11)$$

in the sense of theories on the flat space. Our previous expectation cannot be applied to this case because  $\frac{\xi}{6}N$  and  $\frac{12-\xi}{12}N$  are not integers, nevertheless a  $\log M$  term does not appear in the infinite mass limit unlike the case with only massive matter fields. The effective theory can be deduced. When  $N_f = 6$ , a  $\log M$  term appears and the effective theory may not be U(1)  $\times$  U(1).



It is also notable that whether or not a  $\log M$  appears depends on the number of flavors. When  $N_f \geq 9$ , the infinite mass limit is commutative with the integral. Thus, the result is trivial<sup>†10</sup>. This implies that the  $\frac{2NN_f}{3}$  massive matter fields simply decouple by choosing the origin of the Coulomb branch since the remaining theory is a good theory. Namely, in the infinite mass limit, the partition function is written as

$$\tilde{Z}_{\text{U}(2)}^{N_f} \xrightarrow{m \rightarrow \infty} \left(\frac{1}{M}\right)^{\frac{2N_f}{3}} \tilde{Z}_{\text{U}(2)}^{\frac{N_f}{3}}|_{m=0}. \quad (3.2.12)$$

### U(3) SQCD

For this case, the partition function is given by

$$\tilde{Z}_{\text{U}(3)}^{N_f} = \frac{1}{3!} \int_{-\infty}^{\infty} \frac{4 \sinh^2 \pi(x-y) 4 \sinh^2 \pi(x-z) 4 \sinh^2 \pi(y-z) dx dy dz}{(2 \cosh(\pi x) 2 \cosh(\pi y) 2 \cosh(\pi z) 2 \cosh \pi(x \pm m) 2 \cosh \pi(y \pm m) 2 \cosh \pi(z \pm m))^{\frac{N_f}{3}}}. \quad (3.2.13)$$

For small  $N_f$ , the results are summarized in the following table:

$N_f = 6$	$N_f = 9$	$N_f = 12$	$N_f = 15$
$\frac{1}{(2\pi)^3 M^4}$	$\frac{9}{2^{12} M^8}$	$\frac{(\log M)^2}{48\pi^3 M^{12}}$	$\frac{1}{2^{13} M^{15}}$

Table 3.4: The leading part of  $\tilde{Z}_{\text{U}(3)}^{N_f}$  when  $m \rightarrow \infty$ .

For  $N_f = 6$  case, the gauge group  $\text{U}(3)$  is broken into  $\text{U}(1) \times \text{U}(1) \times \text{U}(1)$  and then, each  $\text{U}(1)$  SQCD has two massless fundamental hypermultiplets. This theory is expected from the large  $N$  analysis because  $\frac{\xi}{6}N$  and  $\frac{12-\xi}{6}N$  are integers. Actually, the partition function becomes

$$\begin{aligned} Z_{\text{Massive}} Z_{\text{U}(1) \times \text{U}(1) \times \text{U}(1)} &= \frac{(4 \sinh^2 \pi m)^2 4 \sinh^2 2\pi m}{(2 \cosh \pi m)^4 (2 \cosh 2\pi m)^6} \left( \int_{-\infty}^{\infty} dx \frac{1}{(2 \cosh \pi x)^2} \right)^3 \\ &\xrightarrow{m \rightarrow \infty} \frac{1}{(2\pi)^3 M^4}. \end{aligned} \quad (3.2.14)$$

When  $N_f = 9$ , this means that  $\frac{\xi}{6}N$  and  $\frac{12-\xi}{12}N$  are not integers. Therefore, we cannot simply apply the result from the large  $N$  analysis to this case. Nevertheless, we can guess that the

---

<sup>†10</sup>Exactly speaking, the matrix converges when  $2N - 2 \leq \frac{N_f}{3}$ . In the large  $N$  limit the order one part is neglected.

effective theory will be a  $U(1) \times U(1) \times U(1)$  gauge theory in which each  $U(1)$  SQED has three massless hypermultiplets. The partition function of the effective theory is given by

$$Z_{\text{massive}} Z_{U(1) \times U(1) \times U(1)} = \frac{(4 \sinh^2 \pi m)^2 (4 \sinh^2 2\pi m)}{(2 \cosh 2\pi m)^6 (2 \cosh \pi m)^{12}} \left( \int_{-\infty}^{\infty} dx \frac{e^{-2\pi x}}{(2 \cosh \pi x)^3} \right)^2 \int_{-\infty}^{\infty} dx \frac{1}{(2 \cosh \pi x)^3} \xrightarrow{m \rightarrow \infty} \frac{9}{2^{12} M^8}, \quad (3.2.15)$$

and this is the same as  $\tilde{Z}_{U(3)}^{N_f=9}$ . Unlike the  $N_f = 6$  case, two of the three  $U(1)$  theory have an imaginary FI term arising from one-loop effects of massive fermions. Thus, in the case of  $N_f = 6, 9$ , we conclude that the IR effective theory corresponds to the theory on a non-trivial Coulomb branch point

$$\sigma = \begin{pmatrix} m & & \\ & 0 & \\ & & -m \end{pmatrix}, \quad (3.2.16)$$

in the sense of theories in flat space.

When  $N_f = 12$ , a  $\log M$  term appears and then, we do not have any interpretations of the effective theory. we would like to note that a  $\log M$  term appears when  $\frac{N_f}{3} = 2N - 2$ , where  $N_f = 2N - 2$  is the threshold for a “bad” theory of  $\mathcal{N} = 4$   $U(N)$  SQCD with  $N_f$  flavors. When  $N_f \geq 15$ , massive multiplets simply decouple in the infinite mass limit because we can change the order of the limit of the mass and the integrals. Indeed, the following relation is valid:

$$\tilde{Z}_{U(3)}^{N_f} \xrightarrow{m \rightarrow \infty} \left( \frac{1}{M} \right)^{\frac{3N_f}{3}} \tilde{Z}_{U(3)}^{\frac{N_f}{3}} \Big|_{m=0}, \quad (3.2.17)$$

and this relation implies the trivial Coulomb branch point

$$\sigma = \begin{pmatrix} 0 & & \\ & 0 & \\ & & 0 \end{pmatrix}. \quad (3.2.18)$$

dominantly contributes to the partition function.

### 3.3 Summary and Discussion

It is known that three-dimensional supersymmetric SQCD theories flow to different phases in the deep IR depending on the number of matter multiplets. Hence, it is interesting that we give infinite mass to matter multiplets in order to decouple them and then investigate the

effects including non-perturbative effects. In particular, a supersymmetric localization method is a powerful tool which allowed us to exactly calculate several observables. Thus, through a round three-sphere partition function, we studied the effect in the infinite mass limit. In this chapter, we consider the following two types of deformations: (i) only massive matter fields, and (ii) massive and massless matter fields. To determine which matter hypermultiplets decouple from theory, we must select a vacuum (in this thesis we only consider the Coulomb branch), which can give matter fields real mass by the Higgs mechanism in the sense of theories on flat space. Because a three-sphere partition function is written in terms of integrals over the Coulomb branch, it seemed that we cannot determine effective real masses of matter fields and then which matter fields decouple. To specify a dominant point of the Coulomb branch, we focused on the solution of the saddle-point equation. This is because it not only corresponds to a point of the Coulomb branch, but also determine the leading behavior of the partition function in the large  $N$  limit. Therefore, we could investigate decoupling of matter fields and the effective theory by the following solution in the large  $N$  limit. Finally, for finite-rank SQCD, we confirmed that in the infinite mass limit an effective theory on a non-trivial point of the Coulomb branch appears through the exact calculation of the partition function.

In case (i), we can naively think that if we consider a theory at the trivial Coulomb branch and take mass to infinity, then, all massive matter fields decouple from the theory and its partition function diverges. However, in fact, this argument was not valid since the limit with respect to real mass is not commutative with the integrals of the matrix model. Then, we found that the density function, which shows a configuration of the solution, is distributed in two separated regions: one is concentrated around  $m$  and the other around  $-m$ . This means that in the infinite mass limit the gauge group  $U(N)$  is broken down to  $U(\frac{N}{2}) \times U(\frac{N}{2})$  with  $N_f$  massless hypermultiplets and FI terms. Even for cases of finite  $N$ , this expectation obtained from the large  $N$  analysis may be true except when  $\frac{N}{2}$  is not an integer.

In case (ii), the behavior of the partition function depends on the number of the massless flavors. When  $\frac{N_f}{3} > 2N - 2$ , the limit with respect to real mass is commutative with the integrals and the massive matter fields simply decouple from the theory. This implies that the origin of the Coulomb branch dominantly contributes to the partition function. On the other hand, in case that  $\frac{N_f}{3} \leq 2N - 2$ , we found that the gauge group is broken into three parts and each rank of gauge group depends on the number of flavors. Through the results in cases of finite  $N$ , we confirmed that a non-trivial effective theory appears in the infinite mass limit except in a few cases.

Let us comment on more general mass deformations. In this chapter, we considered above two mass deformations. In fact, we can consider more general mass deformations of  $\mathcal{N} = 4$   $U(N)$  SQCD as long as mass deformations preserve  $\mathcal{N} = 4$  supersymmetry because the large

$N$  analysis with resolvent methods can be applied to the general mass deformations. We can expect the result for the more general mass-deformed theories from our results. In fact, our results suggest that the number of real mass parameters corresponds to that of peaks of the density function and the number of flavors which have the same real mass is associated with the rank of the gauge groups which the original gauge group is spontaneously broken into.

Finally, we would like to comment on the F-theorem. In our analysis, it can be verified that the free energies of many theories are divided into two parts in the infinite mass limit as

$$F \rightarrow F_{\text{SCFT}} + F_{\text{Massive}}, \quad (3.3.1)$$

where  $F_{\text{SCFT}}$  is the mass-independent part of the free energy, which can be regarded as that of a superconformal field theory and  $F_{\text{Massive}}$  denotes the sector of free massive multiplets.  $F_{\text{Massive}}$  is proportional to  $m$  and we can counter it by a local-counter term, which corresponds the Einstein-Hilbert action of  $S^3$  [62]. In this setting, we expect that

$$F_{\text{UV}} > F_{\text{SCFT}}, \quad (3.3.2)$$

where  $F_{\text{UV}}$  is the free energy when  $m = 0$  because it can naively be considered that the limit  $m \rightarrow \infty$  corresponds to flowing to the deep IR and  $m = 0$  corresponds to a UV limit<sup>†11</sup>. Indeed this relation is valid at least in our results in Section 3.2. We would like to note that there are exceptional theories, whose partition functions exhibit  $\log M$  behavior in the infinite mass limit, and these theories cannot be interpreted as in (4.2.41) because the leading behavior of the partition function can be evaluated by substituting the dominant point of the Coulomb branch for the action. Therefore, contributions from the points of the Coulomb branch (at most countable) cannot cause the logarithmic factors. It may be possible that the logarithmic factors arise from the contributions of the uncountably infinite points of the Coulomb branch, namely, the moduli is remaining.

---

<sup>†11</sup>we can regard that the characteristic energy scale  $E_0$  is determined as  $\frac{1}{r_{S^3}}$  and then  $m/E_0 \rightarrow \infty$  and  $m/E_0 \rightarrow 0$  corresponds to the UV and IR limit respectively.

# Chapter 4

## Mass-deformed ABJM theory

This chapter is organized as follows. In Section 4.1, we show that the matrix model expression of the three-sphere partition function resulting from the localization. Before we provide our main results, we also provide the solution to the saddle-point equation for the imaginary mass, as an easy example of HKPT' ansatz. Then, in Section 2.2.5, we solve the saddle-point equation for real mass parameter and show that the solution is not valid beyond the certain value of the mass parameter. In Section 4.3, we consider the mass-deformation for  $\zeta_1 = 0$ . We find that the saddle-point solution does not have any singularities at a finite value of  $\zeta_2$  unlike that for the real FI-deformed case. In Section 4.4, we conclude with some discussion about the threshold of the eigenvalues distributions and comments on the relation between it and the next chapter.

### 4.1 General mass deformation of ABJM theory

In this section, we review some basic facts on the mass-deformed ABJM theory on  $S^3$ . The field content of the ABJM theory consists of, in the 3d  $\mathcal{N} = 2$  SUSY notation, a  $U(N)_k$  vector multiplet  $\mathcal{V} = (A_\mu, \sigma, \chi, D)$ , a  $U(N)_{-k}$  vector multiplet  $\tilde{\mathcal{V}} = (\tilde{A}_\mu, \tilde{\sigma}, \tilde{\chi}, \tilde{D})$ , two chiral multiplets  $\mathcal{Z}_\alpha = (A_\alpha, \phi_\alpha, F_\alpha)$  in  $(\square, \bar{\square})$  representation under  $U(N)_k \times U(N)_{-k}$  and two chiral multiplets  $\mathcal{W}_{\dot{\alpha}} = (B_{\dot{\alpha}}, \psi_{\dot{\alpha}}, G_{\dot{\alpha}})$  in  $(\bar{\square}, \square)$  representation.<sup>†1</sup> Here the vector multiplets obey the Chen-Simons action with level  $\pm k$ , while the action for the chiral multiplets consists of the superpotential together with the following minimal coupling to the vector multiplets

$$S_{\text{kin}} = \int d^3x \sqrt{g} \text{Tr} \left[ |D_\mu A_a|^2 + |D_\mu W_{\dot{a}}|^2 + \frac{3}{4r_{S^3}^2} (|A_a|^2 + |W_{\dot{a}}|^2) \right. \\ \left. + \frac{1}{r_{S^3}} |\sigma A_a - A_a \tilde{\sigma}|^2 + i(\bar{A}^a D A_a - A_a \tilde{D} \bar{A}^a) \right]$$

---

<sup>†1</sup>The (anti-)bi-fundamental chiral multiplets have  $U(1)_R$  charges  $1/2$ .

$$+ \frac{1}{r_{S^3}} |\tilde{\sigma} B_{\dot{a}} - B_{\dot{a}} \sigma|^2 + i(\bar{B}^{\dot{a}} \tilde{D} B_{\dot{a}} - B_{\dot{a}} D \bar{B}^{\dot{a}}) \Big] + (\text{fermions}). \quad (4.1.1)$$

We can introduce a mass by turning on a background vector multiplet  $\mathcal{V}^{(\text{bgd})} = (A_{\mu}^{(\text{bgd})}, \sigma^{(\text{bgd})}, \chi^{(\text{bgd})}, D^{(\text{bgd})})$  of a global symmetry in the following supersymmetric configuration<sup>†2</sup> [73]

$$A_{\mu}^{(\text{bgd})} = 0, \quad \sigma^{(\text{bgd})} = \delta, \quad \chi^{(\text{bgd})} = 0, \quad D^{(\text{bgd})} = -\delta. \quad (4.1.2)$$

where we have set the radius of  $S^3$  to  $r_{S^3} = 1$ . Here we turn on the background multiplets of the flavor symmetries  $U(1)_1 \times U(1)_2 \times U(1)_3$  commuting with the  $\mathcal{N} = 2$  supersymmetry under which the chiral multiplets are charged<sup>†3</sup> as in table 4.1. The background gauge fields also minimally couples to the chiral multiplets in the same way as (4.1.1), hence it modifies the action as

$$\begin{aligned} S \rightarrow S + \int \sqrt{g} \text{Tr} \Big[ & \left( \frac{\delta^1}{2} + \frac{\delta^2}{2} + \frac{\delta^3}{2} \right) (-i|A_1|^2 - 2(\bar{A}^1 \sigma A_1 - \bar{A}^1 A_1 \tilde{\sigma})) + \left( \frac{\delta^1}{2} + \frac{\delta^2}{2} + \frac{\delta^3}{2} \right)^2 |A_1|^2 \\ & + \left( \frac{\delta^1}{2} - \frac{\delta^2}{2} - \frac{\delta^3}{2} \right) (-i|A_2|^2 - 2(\bar{A}^2 \sigma A_2 - \bar{A}^2 A_2 \tilde{\sigma})) + \left( \frac{\delta^1}{2} - \frac{\delta^2}{2} - \frac{\delta^3}{2} \right)^2 |A_2|^2 \\ & + \left( -\frac{\delta^1}{2} + \frac{\delta^2}{2} - \frac{\delta^3}{2} \right) (-i|B_1|^2 - 2(\bar{B}^1 \tilde{\sigma} B_1 - \bar{B}^1 B_1 \sigma)) + \left( -\frac{\delta^1}{2} + \frac{\delta^2}{2} - \frac{\delta^3}{2} \right)^2 |B_1|^2 \\ & + \left( -\frac{\delta^1}{2} - \frac{\delta^2}{2} + \frac{\delta^3}{2} \right) (-i|B_2|^2 - 2(\bar{B}^2 \tilde{\sigma} B_2 - \bar{B}^2 B_2 \sigma)) + \left( -\frac{\delta^1}{2} - \frac{\delta^2}{2} + \frac{\delta^3}{2} \right)^2 |B_2|^2 \Big]. \quad (4.1.3) \end{aligned}$$

Then, we introduce  $\delta^i$  ( $i = 1, 2, 3$ ) as the vacuum expectation values of the background vector multiplets  $\mathcal{V}^{(\text{bgd}, i)}$  for  $U(1)_i$ . In this chapter, we select  $\delta^i$  as

$$\delta^1 = \frac{2(\zeta_1 + \zeta_2)}{k}, \quad \delta^2 = \frac{2(\zeta_1 - \zeta_2)}{k}, \quad \delta^3 = 0, \quad (4.1.4)$$

so that  $\zeta_1, \zeta_2$  are regarded as real mass parameters for chiral multiplets as  $m_1 = 2\zeta_1/k$  for  $\mathcal{Z}_1, \mathcal{W}_2$  and  $m_2 = 2\zeta_2/k$  for  $\mathcal{Z}_2, \mathcal{W}_1$ . We note that first, we will investigate FI-deformed ABJM theory, which corresponds to the case  $\delta^2 = 0$  as follows: The background gauge fields uniformly gives the mass to both of  $A_{\alpha}, \bar{B}^{\dot{\alpha}}$  in (4.1.3) and then can be absorbed into the shift as  $(\sigma, D, \tilde{\sigma}, \tilde{D}) \rightarrow (\sigma, D, \tilde{\sigma}, \tilde{D}) + (-\pi\zeta/k, \pi\zeta/k, \pi\zeta/k, -\pi\zeta/k)$  with  $\zeta = (\zeta_1 + \zeta_2)/2$ . Finally, the Fayet-Illiopoulos terms arise from the Chern-Simons term by the above redefinition of the fields.

<sup>†2</sup>This type of mass is usually called real mass. We can also add “complex mass” by adding quadratic terms in superpotential but it is known that  $S^3$  partition function of general 3d  $\mathcal{N} = 2$  theory is independent of complex mass.

<sup>†3</sup>These charges are denoted as  $h_4, h_1, h_2$  in [26], respectively. These  $U(1)$  symmetries are a part of non-Abelian R-symmetry in higher SUSY language.

	U(1) <sub>1</sub>	U(1) <sub>2</sub>	U(1) <sub>3</sub>
Z <sub>1</sub>	$\frac{1}{2}$	$\frac{1}{2}$	$\frac{1}{2}$
Z <sub>2</sub>	$\frac{1}{2}$	$-\frac{1}{2}$	$-\frac{1}{2}$
W <sub>1</sub>	$-\frac{1}{2}$	$\frac{1}{2}$	$-\frac{1}{2}$
W <sub>2</sub>	$-\frac{1}{2}$	$-\frac{1}{2}$	$\frac{1}{2}$

Table 4.1: Charges of the U(1)<sub>1</sub> × U(1)<sub>2</sub> × U(1)<sub>3</sub> flavor symmetry.

Applying the localization method [50–52] to this theory, the sphere partition function of the mass-deformed ABJM theory is given by the following matrix model [74]

$$Z = \frac{1}{(N!)^2} \int \frac{d^N \lambda}{(2\pi)^N} \frac{d^N \tilde{\lambda}}{(2\pi)^N} e^{\frac{ik}{4\pi} \sum_i (\lambda_i^2 - \tilde{\lambda}_i^2)} \frac{\prod_{i \neq j}^N 2 \sinh \frac{\lambda_i - \lambda_j}{2} \cdot 2 \sinh \frac{\tilde{\lambda}_i - \tilde{\lambda}_j}{2}}{\prod_{i,j=1}^N 2 \cosh \frac{\lambda_i - \tilde{\lambda}_j - 4\pi\zeta_1/k}{2} \cdot 2 \cosh \frac{\lambda_i - \tilde{\lambda}_j - 4\pi\zeta_2/k}{2}}. \quad (4.1.5)$$

## 4.2 Large $N$ ansatz and Imaginary FI-parameter

In this section, before going on to the real mass deformation, we shall investigate the case with pure imaginary FI-parameter

$$\zeta = -i\xi, \quad \xi \in \mathbb{R}. \quad (4.2.1)$$

as an example of an ansatz proposed in [75] (HKPT ansatz) to solve the large  $N$  saddle-point of the equation. Though this FI deformation is equivalent to that for the  $R$ -charge deformation of the ABJM theory studied in [51, 74] (see also [63]), it is useful to consider gauge theories of which the large  $N$  free energy exhibits a special behavior like as the  $N^{\frac{3}{2}}$  behavior of the ABJM theory for a demonstration of the general ideas in the evaluation of the free energy in the large  $N$  limit. Interestingly, the results for mass deformed ABJM theory and its “analytically continued” version we consider here are substantially different in various ways, contrary to the naive expectation.

Employing (4.2), for the mass-deformed ABJM theory, the partition function is given by the following finite dimensional integral

$$Z(N) = \frac{1}{(N!)^2} \prod_{i=1}^N \int d\lambda_i d\tilde{\lambda}_i e^{-f(\lambda, \tilde{\lambda})}, \quad (4.2.2)$$

where the action  $f(\lambda, \tilde{\lambda})$  is written as

$$f(\lambda, \tilde{\lambda}) = \pi i k \left( \sum_{i \geq 1} \lambda_i^2 - \sum_{i \geq 1} \tilde{\lambda}_i^2 \right) - 2\pi i \zeta \left( \sum_{i \geq 1} \lambda_i + \sum_{i \geq 1} \tilde{\lambda}_i \right)$$

$$- \sum_{i>j} \log 4 \sinh^2 \pi(\lambda_i - \lambda_j) - \sum_{i>j} \log 4 \sinh^2 \pi(\tilde{\lambda}_i - \tilde{\lambda}_j) + \sum_{i,j \geq 1} \log 4 \cosh^2 \pi(\lambda_i - \tilde{\lambda}_j), \quad (4.2.3)$$

In the large  $N$  limit, the partition function can be evaluated with the saddle-point approximation. The saddle-point equations are given by

$$\begin{aligned} 0 &= \frac{\partial f(\lambda, \tilde{\lambda})}{\partial \lambda_i} = 2\pi i k \lambda_i - 2\pi i \zeta - 2\pi \sum_{j \neq i} \coth \pi(\lambda_i - \lambda_j) + 2\pi \sum_j \tanh \pi(\lambda_i - \tilde{\lambda}_j), \\ 0 &= \frac{\partial f(\lambda, \tilde{\lambda})}{\partial \tilde{\lambda}_i} = -2\pi i k \tilde{\lambda}_i - 2\pi i \zeta - 2\pi \sum_{j \neq i} \coth \pi(\tilde{\lambda}_i - \tilde{\lambda}_j) - 2\pi \sum_j \tanh \pi(\lambda_j - \tilde{\lambda}_i). \end{aligned} \quad (4.2.4)$$

The free energy  $F = -\log Z(N)$  can be evaluated by the saddle-point configuration

$$F \approx f(\lambda, \tilde{\lambda})|_{\text{saddle}}. \quad (4.2.5)$$

We note that the saddle-point configurations is generally complex although  $\lambda_i$  and  $\tilde{\lambda}_i$  are real in the integration contours in (4.2.2).

### Analytical solution in large $N$ limit

In the case of pure imaginary FI parameter, we can find the solution to the saddle-point equations (4.2.4) in the large  $N$  limit by evaluating the equations up to  $\mathcal{O}(N^0)$ . As we discuss above we set

$$\lambda_i = \left( \tilde{\lambda}_i \right)^*. \quad (4.2.6)$$

Moreover, we shall assume that

$$\lambda_i = N^\alpha x_i + i y_i, \quad \tilde{\lambda}_i = N^\alpha x_i - i y_i, \quad (4.2.7)$$

with  $x_i$  and  $y_i$  being of order  $\mathcal{O}(N^0)$ . We have introduced a factor  $N^\alpha$  to denote the growth of the real part of eigenvalues and then, the scaling exponent  $\alpha$  will be determined later.<sup>†4</sup>

In the large  $N$  limit, we can define continuous functions  $x(s), y(s) : [0, 1] \rightarrow \mathbb{R}$  to replace  $x_i$  and  $y_i$  as

$$x_i = x\left(\frac{i}{N}\right), \quad y_i = y\left(\frac{i}{N}\right). \quad (4.2.8)$$

---

<sup>†4</sup>Although there is no proof that there are no solutions without the assumption, we believe this assumption is valid for the solution which gives the lowest free energy configurations, based on numerical calculations.



Here we have ordered the eigenvalues so that  $x(s)$  is a strictly increasing function. It is reasonable to take the real part of the eigenvalues  $x$  as the fundamental variable rather than  $s$  and to denote the imaginary part  $y$  as a function of  $x$ . Then, we introduce the eigenvalue density  $\rho(x)$  associated with the real part of the eigenvalues as

$$\rho(x) = \frac{ds}{dx} \quad (4.2.9)$$

which is normalized as

$$\int_I dx \rho(x) = 1. \quad (4.2.10)$$

This means that

$$\sum_i (\cdots)_i \rightarrow N \int_I dx \rho(x) (\cdots)(x). \quad (4.2.11)$$

Here  $I$  is the support where the eigenvalues are defined and we shall assume it to be a single finite interval  $I = [a, b]$ . In this continuum limit, the saddle-point equations (4.2.4) become

$$0 = -ik(N^\alpha x + iy(x)) + \xi + N \left( \text{P} \int_I dx' \rho(x') \coth \pi [(x - x')N^\alpha + i(y(x) - y(x'))] \right) - N \left( \text{P} \int_I dx' \rho(x') \tanh \pi [(x - x')N^\alpha + i(y(x) + y(x'))] \right). \quad (4.2.12)$$

We regard the integral whose integrand has a singular point at  $x = x'$  as the principal value integral. Now to solve the saddle-point equation (4.2.12) implies to find functions  $y(x)$  and  $\rho(x)$  which satisfy (4.2.12) and the normalization (4.2.10).

Then, to obtain the leading part of the saddle-point equation, we expand the last two terms in (4.2.12) including the integration over  $x'$ . Because the arguments of  $\coth$  and  $\tanh$  are scaled by  $N^\alpha$ , this can be evaluated by approximating them by the sign of the real part of the arguments and by the integration by parts. First, we notice the following expansion formulas

$$\begin{aligned} \tanh(z) &= \begin{cases} 1 - 2 \sum_{n=1}^{\infty} (-1)^{n-1} e^{-2nz} & (\text{Re}(z) \geq 0) \\ -1 + 2 \sum_{n=1}^{\infty} (-1)^{n-1} e^{2nz} & (\text{Re}(z) < 0) \end{cases}, \\ \coth(z) &= \begin{cases} 1 + 2 \sum_{n=1}^{\infty} e^{-2nz} & (\text{Re}(z) \geq 0) \\ -1 - 2 \sum_{n=1}^{\infty} e^{2nz} & (\text{Re}(z) < 0) \end{cases}. \end{aligned} \quad (4.2.13)$$

The leading terms in (4.2.13) arise from the sign function approximation. In the two integrals, these leading factors are precisely canceled together as follows:

$$\begin{aligned}
& N \int_I dx' \rho(x') \coth \pi [(x - x')N^\alpha + i(y(x) - y(x'))] \\
& \quad - N \int_I dx' \rho(x') \tanh \pi [(x - x')N^\alpha + i(y(x) + y(x'))] \\
& \sim N \int_I dx' \rho(x') \operatorname{sgn}(x - x') - N \int_I dx' \rho(x') \operatorname{sgn}(x - x') = 0.
\end{aligned} \tag{4.2.14}$$

Because the real part of the arguments grows with  $N^\alpha$ , the contributions from the remaining terms  $e^{-2nz}$  in (4.2.13) are exponentially suppressed in large  $N$  limit and do not contribute to the  $1/N$  expansion except for the contributions from the integration near  $z \sim 0$ , which give  $1/N^\alpha$  corrections. These terms in (4.2.13) can be evaluated by separating the integration interval into  $x > x'$  and  $x < x'$  and integrating by parts

$$\begin{aligned}
& N \int_I dx' \rho(x') \coth \pi [(x - x')N^\alpha + i(y(x) - y(x'))] \\
& \quad - N \int_I dx' \rho(x') \tanh \pi [(x - x')N^\alpha + i(y(x) + y(x'))] \\
& = -2iN^{1-\alpha} \rho(x) \sum_{n=1}^{\infty} \frac{(-1)^{n-1}}{\pi n} \sin(4n\pi y(x)) - N^{1-2\alpha} \dot{\rho}(x) \sum_{n=1}^{\infty} \frac{(-1)^{n-1}}{\pi^2 n^2} \cos(4n\pi y(x)) \\
& \quad - N^{1-2\alpha} \dot{\rho}(x) \sum_{n=1}^{\infty} \frac{1}{\pi^2 n^2} + 2N^{1-2\alpha} \rho(x) \dot{y}(x) \sum_{n=1}^{\infty} \frac{(-1)^{n-1}}{\pi n} \sin(4n\pi y(x)) + \mathcal{O}(N^{1-3\alpha}),
\end{aligned} \tag{4.2.15}$$

where we have used the following formula

$$\int_a^b g(x) e^{Ax+iy(x)} dx = \sum_{\ell=0}^{\infty} \frac{(-1)^\ell}{A^{\ell+1}} \left[ \frac{d^\ell}{dx^\ell} (g(x) e^{iy(x)}) e^{Ax} \right]_a^b \tag{4.2.16}$$

with  $A$  an arbitrary constant. In this case,  $A$  denotes a  $N^\alpha$  factor and this formula implies the  $1/N^\alpha$  expansion. Here, we have kept the terms up to  $\mathcal{O}(N^{1-2\alpha})$  since these terms will be the leading contributions.

Substituting (4.2.15) for the saddle-point equation (4.2.12), Finally, we obtain two equations from the real part and the imaginary part as the leading part in the  $1/N$  expansion of the saddle-point equation as

$$\begin{cases}
(\text{imaginary part}) = 0 & \rightarrow -kN^\alpha x - 4N^{1-\alpha} \rho(x) y(x) = 0, \\
(\text{real part}) = 0 & \rightarrow ky(x) + \xi - N^{1-2\alpha} \dot{\rho}(x) \left[ \frac{1}{4} - 4y^2(x) \right] + 4N^{1-2\alpha} \rho(x) y(x) \dot{y}(x) = 0,
\end{cases} \tag{4.2.17}$$

where dot “.” denotes the abbreviation for the differential with respect to  $x$ . Here, we have used the following Fourier series expansion formulas:

$$\sum_{n=1}^{\infty} \frac{(-1)^{n-1}}{n^2} \cos(4\pi ny) = \frac{\pi^2}{12} - 4\pi^2 y^2, \quad \text{for } -\frac{1}{4} \leq y \leq \frac{1}{4}, \quad (4.2.18)$$

$$\sum_{n=1}^{\infty} \frac{(-1)^{n-1}}{n} \sin(4\pi ny) = 2\pi y, \quad \text{for } -\frac{1}{4} \leq y \leq \frac{1}{4}. \quad (4.2.19)$$

If the function  $y(x)$  does not satisfy  $-\frac{1}{4} \leq y(x) \leq \frac{1}{4}$ , (4.2.17) is no longer correct. The formulas can be generalized considering the periodicity of the trigonometric functions although we will not consider this here. In order to obtain a non-trivial solution, we should balance the scalings of all terms in each equation of (4.2.17). From this condition, the scaling exponent is determined as

$$\alpha = \frac{1}{2}. \quad (4.2.20)$$

Here, we note that the non-local saddle-point equations (4.2.12) have reduced to the local differential equations (4.2.17). This is because the non-local part of the equation vanishes under the assumption  $\lambda_i = \tilde{\lambda}_i^*$ , as we have seen in (4.2.14).

The saddle-point equations can be solved by

$$y(x) = -\frac{kx}{4(4\xi x + C)}, \quad (4.2.21)$$

$$\rho(x) = 4\xi x + C, \quad (4.2.22)$$

where  $C$  is an integration constant which is determined from the normalization condition (4.2.10) as

$$C = \frac{1}{b-a} - 2\xi(b+a). \quad (4.2.23)$$

Formally, the solution (4.2.22) implies that  $y(x)$  diverges at  $x = -\frac{C}{4\xi}$ , and the density  $\rho(x)$  is negative for  $x < -\frac{C}{4\xi}$ . This situation obviously contradicts to the notion of the eigenvalue density. Here, we assume that these points are excluded from the support  $I$ . The support is determined by the extremization of the free energy consistently with the assumption, as we will see in the next section.

## Leading behavior of free energy

Employing the solution (4.2.22) obtained in the last section, the free energy in the large  $N$  limit (4.2.3) can be evaluated. The free energy is evaluated as a function of the edges of the support

$(a, b)$ . As in the case of the ABJM theory, The support  $(a, b)$  is determined by the condition extremizing the free energy under the variation of  $a$  and  $b$ .

We shall start with the continuum limit of the free energy (4.2.3) as

$$\begin{aligned}
f(\lambda, \tilde{\lambda}) = & -4N^{\frac{3}{2}}\pi k \int_I dx x \rho(x) y(x) - 4N^{\frac{3}{2}}\pi \xi \int_I dx \rho(x) x \\
& - 2N^2 \text{Re} \int_I dx \int_I dx' \rho(x) \rho(x') \log 2 \sinh N^{\frac{1}{2}}\pi [(x - x') + i(y(x) - y(x'))] \\
& + 2N^2 \int_I dx \int_I dx' \rho(x) \rho(x') \log 2 \cosh N^{\frac{1}{2}}\pi [(x - x') + i(y(x) + y(x'))]. \quad (4.2.24)
\end{aligned}$$

The last two double integrations can be evaluated in the parallel way as in the last section, with the help of the formulas obtained by integrating (4.2.13)

$$\begin{aligned}
\log 2 \cosh(z) = & \begin{cases} z + \sum_{n=1}^{\infty} \frac{(-1)^{n-1} e^{-2nz}}{n} & (\text{Re}(z) \geq 0) \\ -z + \sum_{n=1}^{\infty} \frac{(-1)^{n-1} e^{2nz}}{n} & (\text{Re}(z) < 0) \end{cases}, \\
\log 2 \sinh(z) = & \begin{cases} z - \sum_{n=1}^{\infty} \frac{e^{-2nz}}{n} & (\text{Re}(z) \geq 0) \\ -z - \sum_{n=1}^{\infty} \frac{e^{2nz}}{n} \pm i\pi & (\text{Re}(z) < 0) \end{cases}. \quad (4.2.25)
\end{aligned}$$

The contributions to the free-energy arising from the first terms in (4.2.25) are again canceled, and this implies that the double integration terms in the free energy no longer exist in the large  $N$  limit. The contributions from the second terms in (4.2.25) can be evaluated by the integration by parts with the formula (4.2.16) and the integration by parts as

$$2\pi N^{2-\frac{1}{2}} \int_I dx \left[ \frac{1}{4} - 4y^2(x) \right] \rho^2(x), \quad (4.2.26)$$

where we have applied the formula (4.2.18) to the summation over  $n$ . In this case, we should keep the terms up to  $N^{\frac{3}{2}}$  because the Chern-Simons terms and FI terms are already of order  $\mathcal{O}(N^{\frac{3}{2}})$  for  $\alpha = \frac{1}{2}$ .

Substituting (4.2.26) for (4.2.24) and performing the single integrations for the solution (4.2.22), we obtain

$$\frac{f}{\pi N^{\frac{3}{2}}} = \frac{k^2(b^3 - a^3)}{6} \left( 1 - \frac{16\xi^2}{k^2} \right) + \frac{1}{2(b-a)} - 2\xi(b+a) + 2\xi^2(b+a)^2(b-a). \quad (4.2.27)$$

For the free energy to have a local minimum in terms of  $(a, b)$ , the deformation  $\xi$  has to satisfy the inequality

$$1 - \frac{16\xi^2}{k^2} > 0. \quad (4.2.28)$$

Inside this region, the values of  $a$  and  $b$  are uniquely determined as<sup>†5</sup>

$$a = -\frac{1}{\sqrt{2k}}\left(1 - \frac{4\xi}{k}\right), \quad b = \frac{1}{\sqrt{2k}}\left(1 + \frac{4\xi}{k}\right), \quad (4.2.30)$$

where the free energy is evaluated as

$$F = \frac{\sqrt{2k}}{3}\pi N^{\frac{3}{2}}\left(1 - \frac{16\xi^2}{k^2}\right). \quad (4.2.31)$$

Substituting these values of  $(a, b)$  into the solution (4.2.22), we obtain the solution as

$$y(x) = -\frac{kx}{4\left[4\xi x + \sqrt{\frac{k}{2}}\left(1 - \frac{16\xi^2}{k^2}\right)\right]}, \quad (4.2.32)$$

$$\rho(x) = 4\xi x + \sqrt{\frac{k}{2}}\left(1 - \frac{16\xi^2}{k^2}\right). \quad (4.2.33)$$

Here we note that the solution is indeed consistent with the bound  $-\frac{1}{4} \leq y(x) \leq \frac{1}{4}$  we have assumed and the positivity of  $\rho(x)$  on the support  $(a, b)$ .

Before closing this section, let us comment on the results obtained in [74] where the ABJM theory was deformed by assigning the non-canonical  $R$ -charges  $\Delta$  to the bifundamental matter fields  $A_i$  and  $B_i$ . Our solution (4.2.22) and (4.2.31) corresponds to the special case of their results (See section 5 in [74]) with the parameters  $\Delta_{A_1} = \Delta_{A_2} = \frac{1}{2} + \frac{2\xi}{k}$ ,  $\Delta_{B_1} = \Delta_{B_2} = \frac{1}{2} - \frac{2\xi}{k}$  and  $\Delta_m = 0$ . The dual gravity solution corresponding to this field theory result was also constructed [73].

In the next section, we will consider the case of real mass with the similar method used here. The naive guess is that the free energy and the eigenvalue distribution in the mass deformed ABJM theory would be obtained by simply replacing  $\xi \rightarrow i\zeta$  and assuming  $\zeta \in \mathbb{R}$ . Such an ‘‘analytic continuation’’ of the parameter, however, is not allowed generally. Our result will suggest that the large  $N$  limit breaks the holomorphy in the sense that the solution is valid only in the certain region of the parameter.

We also have obtained the large  $N$  saddle-point solution for the real FI-deformation by a generalization of the HKPT ansatz [1]. However, there are several subtle points for the HKPT

---

<sup>†5</sup>So far we have not considered the other non-local constraint the following by integrating the real part of the saddle-point equation (4.2.12)

$$k \int_a^b dx \rho(x) y(x) + \xi = 0, \quad (4.2.29)$$

which should have been considered before the variation of the free energy. The solutions  $(a, b)$  (4.2.30) indeed satisfy this condition.

ansatz: First, we must determine the domain where the density function is defined by the minimization condition for the free energy. This means that the large  $N$  saddle-point solution cannot be determined only by the saddle-point equation and the minimization condition is necessary. The second one is that the assumption we employ to use the formula of Fourier expansion (4.2.18) seems to be somehow ad hoc. For a simple theory like as the ABJM theory, indeed, we can confirm that the solution is consistent with the assumptions after solving saddle-point equation and calculating the free energy. In general case, the consistency check is hard to do. Intrinsically, the saddle-point solution including the integral constant and the domain should be completely determined only by the saddle-point equation. Thus, we attempt to search another way and found a new ansatz in [2] in which the solution is determined by the saddle-point equation, including the boundary conditions which is missed in the approach introduced here. We will introduce the methods in the next section.

### 4.2.1 A new derivation of the saddle-point solution for $N^{\frac{3}{2}}$

We also take the continuous limit and impose the following ansatz on the eigenvalues:

$$\begin{aligned}\lambda(s) &= \sqrt{N}z_1(s) + z_2(s), \\ \tilde{\lambda}(s) &= \sqrt{N}z_1(s) - z_2(s),\end{aligned}\tag{4.2.34}$$

where  $z_1$  and  $z_2$  are  $N$  independent and arbitrary complex-valued functions of  $s$ .<sup>†6</sup> In what follows, we will not introduce the density function instead of the previous section and treat the eigenvalues as a function of the continuous valuable  $s$ .

Note that the transformation

$$\tilde{\lambda}(s) \rightarrow \tilde{\lambda}(-s),\tag{4.2.36}$$

only changes the ordering of the  $U(N)$  index of the  $\tilde{\lambda}$ , thus the gauge symmetry. This means that the configuration  $\{\lambda(s), \tilde{\lambda}(s)\}$  is equivalent to  $\{\lambda(s), \tilde{\lambda}(-s)\}$  under this symmetry. Then, we can find that the new ansatz (4.2.34) includes the ansatz taken in [1] for pure imaginary  $\zeta$  and for real  $\zeta$  with this gauge transformation (4.2.36).

Due to the above gauge symmetry, we always take  $\text{Re}(z_1(s))$  a monotonically increasing function with respect to  $s$ . We also assume that the complex functions  $z_1(s)$  and  $z_2(s)$  are

---

<sup>†6</sup>We can generalize this ansatz while keeping the large  $N$  scaling of the free energy  $f \sim N^{3/2}$  unchanged to

$$\begin{aligned}\lambda(s) &= \sqrt{N}z_1(s) + z_2(s), \\ \tilde{\lambda}(s) &= \sqrt{N}z_1(s) + z_3(s).\end{aligned}\tag{4.2.35}$$

However, this generalized ansatz is reduced to (4.2.34) by an  $\mathcal{O}(N^{-1/2})$ -shift of  $z_1(s)$ .

piecewise continuous in  $0 \leq s \leq 1$  for this choice of the ordering. We believe that the form (4.2.34) is the most general form which gives  $N^{\frac{3}{2}}$  behavior of the free energy, but there are no theoretical supports for this belief. However, a highly non-trivial cancellation of  $\mathcal{O}(N^2)$  and  $\mathcal{O}(N^{\frac{5}{2}})$  terms in the free energy make the free energy exhibit the  $N^{\frac{3}{2}}$  behavior. This cancelation prevents us to find other possible ansatzes difficult.

Then, we evaluate the free energy for the assumptions (4.2.34). The Chern-Simons term, which is proportional to  $k$ , and the FI term, which is proportional to  $\zeta$ , are immediately evaluated as

$$4i\pi k N^{\frac{3}{2}} \int ds \left( z_1 z_2 - \frac{\zeta}{k} z_1 \right). \quad (4.2.37)$$

The one-loop factor in the free energy is written as ,

$$\begin{aligned} -N^2 \int_0^1 ds' \int_{s'}^1 ds & \left( \log \left( 4 \sinh^2 \left( \sqrt{N} \pi (z(s) + w_-(s)) \right) 4 \sinh^2 \left( \sqrt{N} \pi (z(s) - w_-(s)) \right) \right) \right. \\ & \left. - \log \left( 4 \cosh^2 \left( \pi \left( \sqrt{N} z(s) + w_+(s) \right) \right) 4 \cosh^2 \left( \pi \left( \sqrt{N} z(s) - w_+(s) \right) \right) \right) \right) \end{aligned} \quad (4.2.38)$$

where we define

$$z(s) = \sqrt{N} (z_1(s) - z_1(s')), \quad (4.2.39)$$

$$w_{\pm}(s) = z_2(s) \pm z_2(s'), \quad (4.2.40)$$

with a fixed  $s'$ . we will use the decomposition

$$\begin{aligned} \int ds \log(\sinh^2(z)) &= 2 \int ds \operatorname{sgn}(R(s)) z \\ &+ \int_{R(s)>0} ds \log(\sinh^2(z) e^{-2z}) + \int_{R(s)<0} ds \log(\sinh^2(z) e^{2z}), \end{aligned} \quad (4.2.41)$$

where  $R(s)$  is a real function, and the decomposition for cosh is obtained by replacing sinh by cosh in (4.2.41). We take  $R(s) = \operatorname{Re}(z(s))$  in this case. Then, we can find that the terms linear in  $z$  cancel each other:

$$\begin{aligned} N^2 \pi \int_0^1 ds' \int_{s'}^1 ds \operatorname{Re}(z(s)) & \left( \left( \sqrt{N} z(s) + w_+(s) \right) + \left( \sqrt{N} z(s) - w_+(s) \right) \right. \\ & \left. - \left( \sqrt{N} z(s) + w_-(s) \right) - \left( \sqrt{N} z(s) - w_-(s) \right) \right) = 0. \end{aligned} \quad (4.2.42)$$

The leading contribution can arises from the neighborhood of the point  $s = s'$  because the contributions can evaluated as about  $\mathcal{O}(e^{-N})$  when  $s \neq s'$  and cannot contribute to the leading

part in the large  $N$  expansion. The remaining terms arising from the neighborhood of  $s = s'$  can be evaluated by employing the following formulas (here dot  $\cdot$  is the abbreviation for  $\frac{d}{ds}$ ):

$$\int_{s_0} ds \log(1 \pm e^{-2y(s)}) \sim \frac{1}{\sqrt{N}\dot{u}(s)|_{s=s_0}} \int_{C_+} dt \log(1 \pm e^{-2y(s)}), \quad (4.2.43)$$

$$\int^{s_0} ds \log(1 \pm e^{2y(s)}) \sim \frac{1}{\sqrt{N}\dot{u}(s)|_{s=s_0}} \int_{C_-} dt \log(1 \pm e^{2y(s)}), \quad (4.2.44)$$

for  $\dot{u}(s)|_{s=s_0} > 0$  where

$$y(s) = \sqrt{N}u(s) + v(s), \quad (4.2.45)$$

and  $u(s_0) = 0$ . The arguments of the integrand are varied vary largely even when  $s$  is slightly change around  $s = s'$  because  $z(s)$  is proportional to  $\sqrt{N}$ . Thus, we have assumed that  $u(s)$  extends to infinity even in the neighborhood of  $s = s'$ . This means that the integral contours  $C_{\pm}$  also are regarded as the half-starlight line from  $\pm 2z_2(s)$  towards  $z(\frac{1}{2})$  respectively.  $\dot{z}_1(s)$  can be replaced by  $\dot{z}_1(s')$  and we can take  $w_- = 0$ ,  $w_+ = 2z_2(s')$ . Then, the one-loop parts of the free energy is evaluated as

$$\begin{aligned} & N^{\frac{3}{2}} \int ds' \frac{1}{\pi \dot{z}_1(s')} \left( -4 \int_0^{\infty} dt \log(\sinh(t)e^{-t}) \right. \\ & \left. + 2 \int_{2\pi z_2(s')}^{\infty} dt \log(\cosh(t)e^{-t}) + 2 \int_{-2\pi z_2(s')}^{\infty} dt \log(\cosh(t)e^{-t}) \right) \\ & = N^{\frac{3}{2}} \int ds' \frac{2}{\pi \dot{z}_1(s')} \left( -2 \int_0^{\infty} dt \log\left(\frac{\sinh(t)}{\cosh(t)}\right) + \int_{2\pi z_2(s')}^0 dt \log\left(\frac{\cosh(t)e^{-t}}{\cosh(t)e^t}\right) \right) \\ & = N^{\frac{3}{2}} \int ds' \frac{1}{\pi \dot{z}_1(s')} \left( \frac{1}{2}\pi^2 + 2(2\pi z_2(s'))^2 \right), \end{aligned} \quad (4.2.46)$$

where we have assumed  $\dot{z}_1(s') > 0$  and there is no singularities in  $t$ -plane and we can deform the contour  $C_{\pm}$ . However, there are singularities of the integrand where the cosh factors vanish. We can find that if the relation

$$-\frac{1}{4} < \text{Im}(z_2) - \text{Re}(z_2) \frac{\text{Im}(\dot{z}_1)}{\text{Re}(\dot{z}_1)} < \frac{1}{4}, \quad (4.2.47)$$

is satisfied, we can deform the contour. If this is not the case, we should shift  $z_2 \rightarrow z_2 + in/2$ , where  $n$  is an integer, to satisfy the condition (4.2.47). Including the correction term  $h$ , we finally evaluate the free energy as

$$f = 4\pi N^{\frac{3}{2}} \int ds \left( ikz_1(s)z_2(s) - i\zeta z_1(s) + \frac{2}{\dot{z}_1(s)} \left( \frac{1}{16} + (z_2(s) + ih)^2 \right) \right), \quad (4.2.48)$$

where  $h \in \mathbb{Z}/2$  such that the condition

$$-\frac{1}{4} < \text{Im}(z_2) - \text{Re}(z_2) \frac{\text{Im}(\dot{z}_1)}{\text{Re}(\dot{z}_1)} + h < \frac{1}{4}, \quad (4.2.49)$$



is satisfied.<sup>†7</sup>

In the above derivation of the free energy  $f$  (4.2.48), the assumption that  $\text{Re}(z_1)$  is monotonically increasing <sup>†8</sup> is crucial. This assumption is violated when the real part of the eigenvalue distribution is a double-valued function of  $s$ . In this case, (4.2.48) should include the correction term arising from the cross terms such as  $\log \sinh \pi(\lambda_i - \lambda_j)$  with  $\lambda_i$  and  $\lambda_j$  in two different segments with overlapping shades.

Here, we will argue that such a double-valued configuration cannot be the saddle-point solution. First, we suppose that the values of  $\text{Im}(z_1)$  are different for  $s$  and  $s'$  where  $\text{Re}(z_1(s) = z_1(s'))$  and denote the difference as  $\text{Im}(\Delta z_1)$ . We can evaluate the cross terms again using the formula (4.2.43) and (4.2.44), but with the contour  $C_{\pm}$  extended by a straight line  $[\pm v(s_0), \pm v(s_0) + i\pi\sqrt{N}\text{Im}(\Delta z_1(s_0))]$ . Since the integration of  $\log(\cosh(t)e^{-t})$  over  $\pi i$  vanishes, the contribution of  $\text{Im}(\Delta z_1)$  to the free energy depends on the remainder of  $\sqrt{N}\text{Im}(\Delta z_1)$  divided by 1 and then oscillate as  $N$  varies. This implies that the profile functions will not converge in the large  $N$  limit and thus, the  $N \rightarrow \infty$  will be ill-defined. To obtain a well-defined large  $N$  limit, we should impose the condition that  $\text{Im}(\Delta z_1) = 0$  on the profile function as an ansatz. In this case, however, the original saddle-point equation will not be solved by the variational problem, as the degrees of freedom of the variations will be fewer than those for the smooth eigenvalue distributions for multiple segments. The above argument means that there are no solutions with overlapping segments, at least, if we assume that the free energy exhibits  $N^{3/2}$ . Below we will consider only the solution without overlapping segments.

The saddle-point equations are given by the variation of the free energy with respect to  $z_1$  and  $z_2$  in this case. That associated with  $z_1$  is given by

$$0 = ikz_2(s) - i\zeta + 2\frac{\partial}{\partial s} \left( \frac{1}{\dot{z}_1(s)^2} \left( \frac{1}{16} + (z_2(s) + ih)^2 \right) \right). \quad (4.2.51)$$

We note that because the free energy includes a derivative of  $z_1$ , we should solve the following boundary condition as a part of the saddle-point equation:

$$0 = \frac{1}{\dot{z}_1(s)^2} \left( \frac{1}{16} + (z_2(s) + ih)^2 \right) \Big|_{\text{boundary}}, \quad (4.2.52)$$

---

<sup>†7</sup>Note that

$$\text{Im}(z_2) - \text{Re}(z_2) \frac{\text{Im}(\dot{z}_1)}{\text{Re}(\dot{z}_1)} + h = \frac{\text{Im}((z_2 + ih)\bar{\dot{z}}_1)}{\text{Re}(\dot{z}_1)} = -k|\dot{z}_1|^2 \frac{\text{Re}(z_1)}{4\text{Re}(\dot{z}_1)}. \quad (4.2.50)$$

Thus, if  $z_2 + ih \rightarrow \pm i/4$ , then  $\frac{\text{Im}((z_2 + ih)\bar{\dot{z}}_1)}{\text{Re}(\dot{z}_1)} \rightarrow \pm 1/4$ , which is the edge of the bound (4.2.49).

<sup>†8</sup>This condition is satisfied when the eigenvalues are rearranged so that the profile functions are piecewise continuous in  $s$

and the saddle-point equation associated with  $z_2$  is given by

$$0 = ikz_1(s) + 4\frac{1}{\dot{z}_1(s)}(z_2(s) + ih), \quad (4.2.53)$$

which is rewritten as

$$z_2(s) + ih = -i\frac{k}{4}z_1(s)\dot{z}_1(s) = -i\frac{k}{8}\frac{\partial}{\partial s}(z_1(s))^2. \quad (4.2.54)$$

These implies that

$$\begin{aligned} 0 &= \frac{k^2}{8}(z_1(s))^2 - i(\zeta + ikh)(s - s_0) + \frac{2}{\dot{z}_1(s)^2} \left( \frac{1}{16} + (z_2(s) + ih)^2 \right) \\ &= -i(\zeta + ikh)(s - s_0) + \frac{1}{8\dot{z}_1(s)^2}, \end{aligned} \quad (4.2.55)$$

where  $s_0$  is a complex integration constant. Therefore, we obtain the solution as

$$z_1(s) = g\sqrt{s - s_0} + z_0, \quad \dot{z}_1(s) = g\frac{1}{2\sqrt{s - s_0}}, \quad (4.2.56)$$

$$z_2(s) + ih = -i\frac{kg^2}{8} - iz_0g\frac{k}{8\sqrt{s - s_0}}, \quad (4.2.57)$$

where  $z_0$  is the integration constant and

$$g = \frac{1}{\sqrt{2i(\zeta + ikh)}}. \quad (4.2.58)$$

we note that because  $z_1(s)$  should be defined on the single segment of  $s$  and a continuous function, we defined  $\sqrt{s - s_0}$  as a continuous function of  $s$  although we allowed the overall sign ambiguity. This overall sign should be determined by requiring that  $z_1$  should be a monotonically increasing function of  $s$ .

To obtain solutions, we have to determine the locations of the boundary points and integration constant  $z_0$  and the solutions must satisfy the condition (4.2.49) everywhere. We would like to emphasize that for general types of  $\zeta$ , above discussions are also valid. In fact, we can find the solutions for the pure imaginary  $\zeta$  and undeformed case also are included in the above solutions.

Then, we assume that  $\zeta$  is real and there is only one segment in the eigenvalue distributions. We can always choose  $s_0 = ic$  where  $c$  is real by shifting  $s$ . Because there is one segment, the boundary points is written as  $s = s_b$  and  $s = s_b + 1$ . Then, the boundary condition is written as

$$(z_2 + ih)|_{s=s_b} = \gamma_1 \frac{i}{4}, \quad (4.2.59)$$

$$(z_2 + ih)|_{s=s_b+1} = -\gamma_1 \frac{i}{4}, \quad (4.2.60)$$

where  $\gamma_1$  satisfies the condition  $(\gamma_1)^2 = 1$  representing a choice of the boundary values,<sup>†9</sup> which lead (assuming  $\zeta \neq 0$ )

$$\frac{kz_0}{\sqrt{s_b - ic}} = -2\gamma_1 \frac{1}{g} - kg, \quad (4.2.61)$$

$$\frac{kz_0}{\sqrt{s_b + 1 - ic}} = 2\gamma_1 \frac{1}{g} - kg. \quad (4.2.62)$$

We can determine  $z_0$  from these boundary conditions:

$$1 = \left( -\frac{1}{\left(\frac{2}{g} + \gamma_1 kg\right)^2} + \frac{1}{\left(\frac{2}{g} - \gamma_1 kg\right)^2} \right) (kz_0)^2 = \frac{8\gamma_1 k (kz_0)^2}{\left(\frac{4}{g^2} - k^2 g^2\right)^2}, \quad (4.2.63)$$

which also lead

$$s_b - ic = \frac{\gamma}{8k} \left( \frac{2}{g} - \gamma_1 kg \right)^2. \quad (4.2.64)$$

Thus, we find

$$s_b = -\frac{1}{2} - \gamma_1 \left( h + \frac{1}{16} \frac{h}{m^2 + h^2} \right), \quad (4.2.65)$$

$$c = \gamma_1 m \left( -1 + \frac{1}{16} \frac{1}{m^2 + h^2} \right). \quad (4.2.66)$$

In what follows, we will confirm that the solution is indeed a continuous function of  $s$ . First, we define the following parameters:

$$m \equiv \frac{\zeta}{k} \quad (4.2.67)$$

$$m_c \equiv m + ih, \quad (4.2.68)$$

$$s' \equiv \gamma_1 \left( s - s_b - \frac{1}{2} \right), \quad (4.2.69)$$

thus, we determine

$$s' = -\frac{\gamma_1}{2} \quad \text{for } s = s_b, \quad (4.2.70)$$

$$s' = \frac{\gamma_1}{2} \quad \text{for } s = s_b + 1. \quad (4.2.71)$$

---

<sup>†9</sup>The other possibility is  $z_1(s) = g\sqrt{s} + z_0$  ( $s = [0, 1]$ ) which satisfies  $z_1(s=0) = \infty$  and  $z_0$  is fixed by the boundary condition at  $s = 1$ . However, considering  $s \gg 1$ , we see that for the condition (4.2.49)  $\text{Re}(z_0) = 0$  is needed. This is not satisfied for generic  $\zeta/k$ , for example, with  $h = 0$ ,  $z_0 = 0$  means  $\frac{\zeta}{k} = \frac{1}{4}$ .

Then, we find

$$z_1 = \frac{1}{\sqrt{-2\gamma_1 k}} \left( \sqrt{\left(\frac{1}{16m_c^2} - 1\right) + i\frac{s'}{m_c}} - 4\gamma_2 \left(m_c + \frac{1}{16m_c}\right) \right), \quad (4.2.72)$$

and

$$\dot{z}_1 = \frac{i\gamma_1}{2m_c\sqrt{-2\gamma_1 k}} \frac{1}{\sqrt{\left(\frac{1}{16m_c^2} - 1\right) + i\frac{s'}{m_c}}}, \quad (4.2.73)$$

which leads

$$z_2 + ih = -\frac{1}{16m_c} + \gamma_2 \frac{1}{4} \frac{1 + \frac{1}{16m_c^2}}{\sqrt{\left(\frac{1}{16m_c^2} - 1\right) + i\frac{s'}{m_c}}}. \quad (4.2.74)$$

Here, we introduced  $\gamma_2$  which satisfies  $(\gamma_2)^2 = 1$  for the sign ambiguity of  $z_0$ . The boundary condition  $z_2 + ih = \pm i/4$  means that

$$\sqrt{\left(\frac{1}{16m_c^2} - 1\right) + i\frac{s'}{m_c}} \Big|_{s'=\mp\gamma_1/2} = \gamma_2 \left(\frac{1}{4m_c} \mp i\gamma_1\right), \quad (4.2.75)$$

at the boundaries.<sup>†10</sup> This condition implies  $\gamma_2$  is determined by fixing the overall sign in the l.h.s. of (4.2.75). Furthermore, we will find that for  $m > \frac{1}{4}$ , these conditions are not consistent with the continuity of the factor  $\sqrt{D}$  where

$$D = \left(\frac{1}{16m_c^2} - 1\right) + i\frac{s'}{m_c}, \quad (4.2.77)$$

for  $s'$ .

As we will see below,  $\text{Re}(D)$  is always negative for  $m > \frac{1}{4}$ . Then, the phase  $e^{i\theta} = \sqrt{D}/|\sqrt{D}|$  satisfies the condition that  $\frac{\pi}{4} < \theta < \frac{3\pi}{4}$  or  $-\frac{3\pi}{4} < \theta < -\frac{\pi}{4}$  while for  $m \leq \frac{1}{4}$ ,  $-\frac{\pi}{4} < \theta < \frac{\pi}{4}$  or  $\frac{3\pi}{4} < \theta < \frac{5\pi}{4}$ . This range of the phase for  $m > \frac{1}{4}$  conflict with two boundary conditions (4.2.59) and (4.2.60) imposing  $\text{Im}(\sqrt{D})$  to have different signs at the two boundaries. In fact, for  $h = 0$ , we easily find that  $\text{Re}(D)$  is always negative. Even for  $h \neq 0$ , we can see that

$$\text{Re}(D) = \frac{1}{16|m_c|^4} \left( (\text{Re}(m_c))^2 - (\text{Im}(m_c))^2 - 16|m_c|^4 - 16|m_c|^2 \text{Im}(m_c)s' \right) \quad (4.2.78)$$

<sup>†10</sup>The condition is only for the sign because

$$\left(\frac{1}{16m_c^2} - 1\right) - i\gamma\frac{1}{2m_c} = \left(\frac{1}{4m_c} - i\gamma\right)^2, \quad (4.2.76)$$

for  $\gamma^2 = 1$ .

$$\leq \frac{1}{16|m_c|^4} \left( (\operatorname{Re}(m_c))^2 - (\operatorname{Im}(m_c))^2 - 16|m_c|^4 + 8|m_c|^2 |\operatorname{Im}(m_c)| \right) < 0, \quad (4.2.79)$$

where we have used  $|s'| \leq \frac{1}{2}$  and  $|\operatorname{Im}(m_c)| = |h| \geq \frac{1}{2}$ . Therefore, there are no solutions for  $m > \frac{1}{4}$ .

We can also confirm that no solutions exist for  $m \leq \frac{1}{4}$  and  $h \neq 0$  because

$$(\operatorname{Re}(m_c))^2 - (\operatorname{Im}(m_c))^2 = m^2 - h^2 < 0, \quad (4.2.80)$$

$$-|m_c|^4 + |m_c^2 h s'| < |m_c|^2 (-(m^2 + h^2) + |h/2|) < 0, \quad (4.2.81)$$

where we have used  $|h| \geq \frac{1}{2}$ , which implies  $\operatorname{Re}(D) < 0$  using (4.2.78). Therefore, only the possibility is for  $m \leq \frac{1}{4}$  and  $h = 0$ . For this case, we see that for  $\gamma_1 = -1$ ,  $\operatorname{Re}(\dot{z}_1) = 0$  at  $s' = 0$ . Thus, this solution violates the condition (4.2.49) and we should set  $\gamma_1 = 1$ . The solution is given by

$$z_1 = \frac{1}{\sqrt{-2k}} \left( \sqrt{\left( \frac{1}{16m^2} - 1 \right) + i \frac{s'}{m}} - 4\gamma_2 \left( m + \frac{1}{16m} \right) \right), \quad (4.2.82)$$

where the sign ambiguity of the  $\sqrt{\left( \frac{1}{16m^2} - 1 \right) + i \frac{s'}{m}}$  is fixed by requiring  $\operatorname{Re}(\dot{z}_1) \geq 0$  because we have arranged the ordering of eigenvalues such that  $z_1(s)$  is an increasing function of  $s$ .

Finally, we will consider the solution defined on multiple segments. The real part of such a solution should not intersect each other because of the extra interactions as explained before. Then, the solutions are denoted as a sum of the single segment solutions with  $N_a$  eigenvalues where  $\sum_a N_a = N$ . However, the unique single segment solutions for  $m < \frac{1}{4}$  with different  $N$  always have an eigenvalue such that  $\operatorname{Re}(\lambda) = 0$  and then the monotonicity of the function is not maintained. Thus, there are no multiple-segments solutions.<sup>†11</sup> We conclude there is a unique solution for  $m = \frac{\zeta}{k} < \frac{1}{4}$ , and no solutions for  $m > \frac{1}{4}$ .

### 4.3 Large $N$ solution with one massless hypermultiplet

It is unfamiliar for a large  $N$  saddle-point solution to have a singularity. For example, there is no singularity for the large  $N$  saddle-point solution obtained in Section 3.1. It seems that for a general mass-deformed ABJM theory, the large- $N$  saddle-point solution always has a singularity. However, we can find a specific mass deformation for which a large- $N$  saddle-point

---

<sup>†11</sup>So far, we have neglected a possibility that the solutions with different  $h$  which have the same  $z_1$  and  $z_2$  at a boundary. However, this is not possible because the cancellation of the boundary term requires that  $(z_2 + ih)^2$  also should be same at the boundary.

solution does not have a singularity<sup>†12</sup>. It is the case in which one massless hypermultiplet and massive hypermultiplet exist taking  $\zeta_1 = 0$ . Therefore, it is reasonable to expect that the physical situation is very different among mass deformations which exhibit the singular behavior and does not. We expect that the singular behavior arises from the physical situation and we will discuss in the next part.

### 4.3.1 Partition function of S-dual theory

Before investigating the mass-deformation, we introduce the S-dual representation of the partition function, which we practically use in what follows and chapter 5. It is simply obtained by rewriting the original partition function 4.1.5. The computation is essentially the same as those in the Fermi gas formalism for the ABJM theory [76]. Let us start with the integral (4.1.5). Changing the integral variables as  $\lambda \rightarrow \lambda/k + \pi(\zeta_1 + \zeta_2)$  and  $\tilde{\lambda} \rightarrow \tilde{\lambda}/k - \pi(\zeta_1 + \zeta_2)$ , we find

$$Z = \frac{1}{(N!)^2} \int \frac{d^N \lambda}{(2\pi k)^N} \frac{d^N \tilde{\lambda}}{(2\pi k)^N} e^{\frac{i}{4\pi k} \sum_i (\lambda_i^2 - \tilde{\lambda}_i^2) + \frac{i\zeta}{k} \sum_i (\lambda_i + \tilde{\lambda}_i)} \frac{\prod_{i<j}^N (2 \sinh \frac{\lambda_i - \lambda_j}{2k})^2 \prod_{i<j}^N (2 \sinh \frac{\tilde{\lambda}_i - \tilde{\lambda}_j}{2k})^2}{\prod_{i,j=1}^N \prod_{\pm} 2 \cosh \frac{\lambda_i - \tilde{\lambda}_j \pm \mu}{2k}}, \quad (4.3.1)$$

where

$$\zeta = \frac{\zeta_1 + \zeta_2}{2}, \quad \mu = 2\pi(\zeta_1 - \zeta_2). \quad (4.3.2)$$

Then, we rewrite the one-loop determinant into a pair of determinants of  $N \times N$  matrices by using the Cauchy determinant formula

$$\frac{\prod_{i<j}^N 2 \sinh \frac{x_i - x_j}{2} \prod_{i<j}^N 2 \sinh \frac{y_i - y_j}{2}}{\prod_{i,j=1}^N 2 \cosh \frac{x_i - y_j}{2}} = \det_{i,j} \frac{1}{2 \cosh \frac{x_i - y_j}{2}}, \quad (4.3.3)$$

and then,  $Z$  is rewritten as

$$Z = \frac{1}{(N!)^2} \int \frac{d^N \lambda}{(2\pi k)^N} \frac{d^N \tilde{\lambda}}{(2\pi k)^N} e^{\frac{i}{4\pi k} \sum_i (\lambda_i^2 - \tilde{\lambda}_i^2) + \frac{i\zeta}{k} \sum_i (\lambda_i + \tilde{\lambda}_i)} \det_{i,j} \frac{1}{2 \cosh \frac{\lambda_i - \tilde{\lambda}_j + \mu}{2k}} \det_{i,j} \frac{1}{2 \cosh \frac{\lambda_i - \tilde{\lambda}_j - \mu}{2k}}. \quad (4.3.4)$$

Then, we use the formula

$$\frac{1}{N!} \int d^N x \det_{i,j} f_i(x_j) \det_{i,j} g_i(x_j) = \det_{i,j} \int dx f_i(x) g_j(x). \quad (4.3.5)$$

---

<sup>†12</sup>We can calculate exactly for finite  $N$  case. The detail is written in app.C.2

and obtain the following expression for the partition function

$$Z = \frac{1}{N!} \int \frac{d^N \lambda}{(2\pi)^N} \det_{i,j} f(\lambda_i, \lambda_j), \quad (4.3.6)$$

where

$$f(x, y) = \int \frac{dz}{2\pi} e^{\frac{i}{4\pi k} x^2 + \frac{i\zeta}{k} x} \frac{1}{2k \cosh \frac{x-z-\mu}{2k}} e^{-\frac{i}{4\pi k} z^2 + \frac{i\zeta z}{k}} \frac{1}{2k \cosh \frac{z-y-\mu}{2k}}. \quad (4.3.7)$$

We can see that the partition function takes the form of the partition function of 1d  $N$  particle non-interacting Fermi gas if we regard  $f(\lambda', \lambda'')$  as the matrix element of a one-particle density matrix  $\langle \lambda | \hat{\rho} | \lambda' \rangle$  with position eigenstates  $|\cdot\rangle$

$$Z = \frac{1}{N!} \int \frac{d^N x}{(2\pi)^N} \det_{i,j} \langle x_i | \hat{\rho} | x_j \rangle, \quad (4.3.8)$$

where<sup>†13</sup>

$$\hat{\rho} = e^{\frac{i}{4\pi k} \hat{q}^2 + \frac{i\zeta}{k} \hat{q}} \frac{e^{\frac{i\mu}{2\pi k} \hat{p}}}{2 \cosh \frac{\hat{p}}{2}} e^{-\frac{i}{4\pi k} \hat{q}^2 + \frac{i\zeta}{k} \hat{q}} \frac{e^{\frac{i\mu}{2\pi k} \hat{p}}}{2 \cosh \frac{\hat{p}}{2}}. \quad (4.3.9)$$

Furthermore, we can rewrite the parts represented as determinant by the Fourier transformation

$$\frac{1}{2 \cosh p} = \frac{1}{\pi} \int dx \frac{e^{\frac{2i}{\pi} px}}{2 \cosh x}, \quad (4.3.10)$$

and by doing the Fresnel integral with respect to both of  $\lambda$  and  $\tilde{\lambda}$ . Then, employing the above Fourier transformation and Cauchy determinant formula inversely, we finally obtain the following another equivalent representation of the partition function<sup>†14</sup>:

$$Z(N, k, \zeta_1, \zeta_2) = \frac{1}{N!} \int \frac{d^N x}{(2\pi k)^N} \prod_{i=1}^N \frac{e^{\frac{2i\zeta_1}{k} x_i}}{2 \cosh \frac{x_i}{2}} \frac{\prod_{i<j}^N (2 \sinh \frac{x_i - x_j}{2k})^2}{\prod_{i,j=1}^N 2 \cosh \frac{x_i - x_j + 4\pi\zeta_2}{2k}}. \quad (4.3.13)$$

<sup>†13</sup>See (C.1.8) for the notation for the 1d quantum mechanics.

<sup>†14</sup>These computations can be interpreted in terms of the Fermi gas formalism. It is obvious from (4.3.8) that the partition function is invariant under any similarity transformation of the density matrix  $\hat{\rho}$ . We can simplify  $\hat{\rho}$  by the similarity transformation  $\hat{\rho} \rightarrow e^{-\frac{i}{4\pi k} \hat{p}^2 - \frac{i\zeta}{k} \hat{p}} \hat{\rho} e^{\frac{i}{4\pi k} \hat{p}^2 + \frac{i\zeta}{k} \hat{p}}$  as

$$\hat{\rho} = \frac{e^{\frac{2i\zeta_1}{k} \hat{q}}}{2 \cosh \frac{\hat{q}}{2}} \frac{e^{\frac{2i\zeta_2}{k} \hat{p}}}{2 \cosh \frac{\hat{p}}{2}}, \quad (4.3.11)$$

whose matrix element is

$$\langle x | \hat{\rho} | y \rangle = \frac{e^{\frac{2i\zeta_1}{k} x}}{2 \cosh \frac{x}{2}} \frac{1}{2k \cosh \frac{x-y+4\pi\zeta_2}{2k}}. \quad (4.3.12)$$

Applying the Cauchy determinant formula (4.3.3) reversely to  $\det_{i,j} \langle x_i | \hat{\rho} | x_j \rangle$  in the Fermi gas formalism (4.3.8) with this new  $\hat{\rho}$ , we finally obtain the S-dual representation for the partition function (4.3.13).

For  $k = 1$  and  $\zeta_1 = \zeta_2 = 0$ , this latter expression denotes the partition function of the  $\mathcal{N} = 8$   $U(N)$  Yang-Mills theory coupled with a fundamental hypermultiplet, which is dual to the ABJM theory under the S-dual transformation in the type IIB brane setup. Due to this reason, we simply refer to (4.3.13) as the S-dual representation even for general  $(k, \zeta_1, \zeta_2)$ .

We note that the integration in the S-dual representation (4.3.13) is absolutely convergent while the representation (4.1.5) is not and its convergence is guaranteed by the rapidly oscillating factors. In the sense of the convergence, the S-dual representation is much more suitable for the Monte Carlo simulation than the original one (4.1.5). By employing the Monte Carlo simulation of (4.3.13), we will find a notable behavior of the partition function: the partition function vanishes at some finite values of  $\zeta_1, \zeta_2$ , which was not observed in the undeformed case or the case of the R-charge deformation ( $\zeta_1, \zeta_2 \in i\mathbb{R}$ ).

In what follows, we investigate the case with  $\zeta_1 = 0$ . We can find a solution to the saddle-point equation for the partition function in the S-dual representation (4.3.13) while we could not find any large- $N$  solution of the saddle-point equation of (4.1.5) for  $\zeta_1 = 0$ .

### saddle-point analysis in the large- $N$ limit

Here, we evaluate the partition function in the large- $N$  limit

$$N \rightarrow \infty, \quad \text{with fixed } (k, \zeta_2). \quad (4.3.14)$$

In this limit, we can evaluate the partition function with the saddle-point approximation. To perform the saddle-point analysis, we first introduce the action for the matrix model  $S_{\text{eff}}$  by

$$Z = \frac{1}{N!} \int \frac{d^N x}{(2\pi k)^N} e^{-S_{\text{eff}}(x)} \quad (4.3.15)$$

where

$$\begin{aligned} S_{\text{eff}}(x) = & -\frac{2i\zeta_1}{k} \sum_{i=1}^N x_i + \sum_{i=1}^N \log \left( 2 \cosh \frac{x_i}{2} \right) \\ & - \sum_{i<j}^N \log \left( 2 \sinh \frac{x_i - x_j}{2k} \right)^2 + \sum_{i,j=1}^N \log \left( 2 \cosh \frac{x_i - x_j + 4\pi\zeta_2}{2k} \right). \end{aligned} \quad (4.3.16)$$

We rearrange the eigenvalues  $x_i$  such that  $x_{i+1} \geq x_i$  by the permutation symmetry. We also take the continuous limit taken in the previous section.

We look for saddle-point solutions by the same approach taken in the previous section 4.2.1 which has been used to derive  $\mathcal{O}(N^{\frac{3}{2}})$  behaviors of free energies, rather than the traditional



approach applied for matrix models in the planar limit.<sup>†15</sup> This is achieved by the following ansatz

$$x(s) = \sqrt{N}z(s), \quad (4.3.17)$$

with an  $N$ -independent real<sup>†16</sup> function  $z(s)$ , and perform the large- $N$  expansion of  $S_{\text{eff}}(x)$  to reduce the saddle-point equation to the true leading order. It is easy to write down the leading part for the first and second terms in (4.3.16) in the continuous limit:

$$-\frac{2i\zeta_1}{k} \sum_{i=1}^N x_i + \sum_{i=1}^N \log \left( 2 \cosh \frac{x_i}{2} \right) = N^{\frac{3}{2}} \int_{-\frac{1}{2}}^{\frac{1}{2}} ds \left( -\frac{2i\zeta_1 z}{k} + \frac{|z|}{2} \right) + \mathcal{O}(N). \quad (4.3.18)$$

We can also expand the third and fourth terms in (4.3.16) respectively using the same techniques as that we employed in the previous section to evaluate the leading part of  $S_{\text{eff}}$ . First, we rewrite these terms as

$$\begin{aligned} -\sum_{i<j}^N \log \left( 2 \sinh \frac{x_i - x_j}{2k} \right)^2 &= -\frac{N^2}{2} \int ds ds' \log \left( 2 \sinh \frac{\sqrt{N}(z - z')}{2k} \right)^2 \\ &= \frac{N^2}{2} \int ds ds' \left[ \text{sgn}(z - z') \frac{\sqrt{N}(z - z')}{k} + \log \left( 1 - e^{-\sqrt{N} \left| \frac{z-z'}{k} \right|} \right)^2 \right], \end{aligned} \quad (4.3.19)$$

and<sup>†17</sup>

$$\begin{aligned} \sum_{i,j}^N \log \left( 2 \cosh \frac{x_i - x_j + 4\pi\zeta_2}{2k} \right) \\ = N^2 \int ds ds' \left[ \text{sgn}(z - z') \frac{\sqrt{N}(z - z')}{2k} + \log \left( 1 + e^{-\text{sgn}(z-z') \frac{\sqrt{N}(z-z') + 4\pi\zeta_2}{k}} \right) \right]. \end{aligned} \quad (4.3.20)$$

where  $z'$  is the abbreviation for  $z(s')$ . We note that the  $\mathcal{O}(N^{5/2})$  terms, which are the first terms in (4.3.19) and (4.3.20), are canceled and only the second terms remain. Then, as we follows the same procedure as that we employed in Section 4.2.1, we use the formula in the large- $N$  limit (4.2.43) and (4.2.44)<sup>†18</sup>. Through these formulas, the second terms in (4.3.19)

<sup>†15</sup>The traditional approach was taken in [81, 82] for  $\zeta_1 = 0 = \zeta_2$  identifying 't Hooft coupling with  $N/N_f$  where  $N_f$  denotes an additional power put on the cosh (For our case,  $N_f = 1$ ).

<sup>†16</sup>In our actual analysis, we have looked for solutions with complex  $z(s)$  under the ansatz (4.3.17) but we have found only a real solution as a result. Because of this, we take  $z(s)$  to be real for simplicity in the main context. Precisely speaking, we should take the variation  $\frac{\delta S_{\text{eff}}}{\delta z(s)}$  with  $z(s) \in \mathbb{C}$  before taking  $z(s) \in \mathbb{R}$ . This causes a new constraint  $\frac{\delta S_{\text{eff}}}{\delta \text{Im}(z(s))} = 0$  in addition to (4.3.24) and (4.3.25); nevertheless the final result (4.3.27) remains the same.

<sup>†17</sup>Note that odd functions of  $z - z'$  do not contribute.

<sup>†18</sup>The condition that this evaluation is valid is following [2]:

$$-\frac{1}{4} < \text{Im}(w) - \text{Re}(w) \frac{\text{Im}(\dot{v})}{\text{Re}(\dot{v})} < \frac{1}{4}.$$

and (4.3.20) can be evaluated as

$$\begin{aligned}
& 2kN^{\frac{3}{2}} \int \frac{ds'}{\dot{z}_1(s')} \left[ -2 \int_0^\infty dt \log(1 - e^{-2t}) + \int_{\frac{2\pi\zeta_2}{k}}^\infty dt \log(1 + e^{-2t}) + \int_{-\frac{2\pi\zeta_2}{k}}^\infty dt \log(1 + e^{-2t}) \right] \\
&= \frac{\pi^2 k N^{\frac{3}{2}}}{2} \left( 1 + \frac{16\zeta_2^2}{k^2} \right) \int \frac{ds'}{\dot{z}_1(s')}. \tag{4.3.21}
\end{aligned}$$

Putting the above evaluation together, we find the following large- $N$  expansion for the effective action

$$S_{\text{eff}} = N^{3/2} \int ds F(z, \dot{z}) + \mathcal{O}(N), \tag{4.3.22}$$

with

$$F(z, \dot{z}) = \left[ -\frac{2i\zeta_1 z}{k} + \frac{|z|}{2} + \frac{\pi^2 k}{2} \left( 1 + \frac{16\zeta_2^2}{k^2} \right) \frac{1}{\dot{z}} \right]. \tag{4.3.23}$$

Then, this implies that the integration (4.3.15) is dominated in the large- $N$  limit by the saddle-point configuration satisfying the following equation of motion

$$0 = \frac{\delta F(z, \dot{z})}{\delta z(s)} = \frac{\partial F}{\partial z} - \frac{d}{dt} \frac{\partial F}{\partial \dot{z}} = -\frac{2i\zeta_1}{k} + \frac{\text{sgn}(z)}{2} - \frac{d}{ds} \left[ -\frac{\pi^2 k}{2} \left( 1 + \frac{16\zeta_2^2}{k^2} \right) \frac{1}{\dot{z}^2} \right] \tag{4.3.24}$$

together with the boundary condition

$$0 = \frac{\partial F}{\partial \dot{z}} = -\frac{\pi^2 k}{2} \left[ \left( 1 + \frac{16\zeta_2^2}{k^2} \right) \frac{1}{\dot{z}^2} \right]_{\text{boundary}}. \tag{4.3.25}$$

First, let us consider the case for  $\zeta_1 = 0$ . First of all the equation of motion (4.3.24) has the following two local solutions depending on  $\text{sgn}(z)$

$$\begin{aligned}
z^{(+)}(s) &= \sqrt{2\pi^2 k \left( 1 + \frac{16\zeta_2^2}{k^2} \right)} \left( z_b^{(+)} - \sqrt{2(s_b - s)} \right), \quad (\text{sgn}(z) = +1) \\
z^{(-)}(s) &= -\sqrt{2\pi^2 k \left( 1 + \frac{16\zeta_2^2}{k^2} \right)} \left( z_b^{(-)} - \sqrt{2(s_b + s)} \right), \quad (\text{sgn}(z) = -1)
\end{aligned} \tag{4.3.26}$$

where  $s_b$  and  $z_b$  are integration constants.<sup>†19</sup> The bulk solution would be obtained by connecting these solutions appropriately and determining the integration constants so that  $z(s)$  satisfies the boundary condition  $\dot{z}(s) = \pm\infty$  (4.3.25) at every point. We note that both of  $z^{(\pm)}(s)$  satisfies  $\dot{z}^{(\pm)}(s) = \infty$  at only a single point  $s = s_b$  and  $z^{(+)}$  and  $z^{(-)}$  must be glued at the zero of the functions because we have assumed that the solution is differentiable at every point. These

In this case, this condition is satisfied.

<sup>†19</sup>We have excluded the other two solutions by the condition  $\dot{z}(s) \geq 0$ .

lead the solution to be defined on a single segment by the following argument: If we split the support  $-1/2 < s < 1/2$  into segments by the points of discontinuity,  $z(s)$  on each segment must be given as a smooth junction of  $z^{(-)}(s)$  and  $z^{(+)}(s)$ . Since  $z^{(+)}(s)$  cannot be followed by  $z^{(-)}(s)$  due to the assumption that  $z(s)$  is monotonically increasing, we conclude that the solution has a single junction of  $z^{(-)}(s)$  with  $s_b = -1/2$  ( $-1/2 < s < s_0$ ) and  $z^{(+)}(s)$  with  $s_b = 1/2$  ( $s_0 < s < 1/2$ ), which are connected at some  $s_0$ . The remaining constants  $s_0, z_b$  are determined from  $z^{(-)}(s_0) = z^{(+)}(s_0) = 0$  as  $s_0 = 0, z_b = 1$  (for both domain). Consequently, we obtain the following unique solution as the saddle-point configuration:

$$z(s) = \text{sgn}(s) \sqrt{2\pi^2 k \left(1 + \frac{16\zeta_2^2}{k^2}\right)} \left(1 - \sqrt{1 - 2|s|}\right). \quad (4.3.27)$$

In the language of the eigenvalue density, this solution corresponds to

$$\rho(z) = \frac{ds}{dz} = \frac{1}{\sqrt{2\pi^2 k \left(1 + \frac{16\zeta_2^2}{k^2}\right)}} \left(1 - \frac{|z|}{\sqrt{2\pi^2 k \left(1 + \frac{16\zeta_2^2}{k^2}\right)}}\right). \quad (4.3.28)$$

Substituting this solution to (4.3.22), we find that the partition function in the large- $N$  limit is given as

$$-\log Z|_{\zeta_1=0} \approx \frac{\pi\sqrt{2k}}{3} \sqrt{1 + \frac{16\zeta_2^2}{k^2}} N^{\frac{3}{2}}. \quad (4.3.29)$$

For  $\zeta_1 \neq 0$ , we could not solve the saddle-point equation with the ansatz employed here because the solution cannot satisfy the boundary condition (4.3.25) because of the existence of the imaginary term  $\frac{2i\zeta_1}{k}$  in (4.3.24). However, the partition function with  $\zeta_1 = 0, \zeta_2 \neq 0$  and that with  $\zeta_1 \neq 0, \zeta_2 = 0$  is the same because the partition function is invariant under exchanging  $\zeta_1$  and  $\zeta_2$ . This fact may suggest that even when  $\zeta_2 = 0, \zeta_1 \neq 0$ , there exists the solution of the saddle-point equation in large- $N$  limit and the free energy can be evaluated by the saddle-point approximation.

## 4.4 Summary and Discussion

In this chapter, we studied the mass deformed ABJM theory in the large  $N$  limit with finite value  $(k, \zeta_1, \zeta_2)$ , using the saddle-point approximation for the matrix model. We obtained the saddle-point equation assuming a new ansatz including the boundary condition as the saddle-point equation we propose [2]. In particular, the second one has solved the problems that some assumptions apparently are not included in the saddle-point equation by regarding them the boundary conditions.

Our result for the ABJM theory deformed by an FI-term suggests that the large  $N$  solution of the saddle-point equation is valid only when  $\frac{\zeta}{k} < \frac{1}{4}$  in our convention. This also implies that the free energy is no longer proportional to  $N^{\frac{3}{2}}$  beyond the critical value. It is not clear that what is a correct solution for  $\frac{\zeta}{k} > \frac{1}{4}$ . One possibility is that it is the solution with  $f \sim N^2$  we will show in the next part, which implies that the free energy seems to jump between  $\frac{\zeta}{k} < \frac{1}{4}$  and  $\frac{\zeta}{k} > \frac{1}{4}$ . However, for finite  $N$ , the partition function (4.2.2) will be continuous with respect to  $\frac{\zeta}{k}$ , hence so is the free energy  $f$ . This does not rule out the discontinuous change of the scaling exponent of the free energy  $N^{\frac{3}{2}} \rightarrow N^2$  in the large  $N$  limit while the finite  $N$  correction can make the free energy smooth around the critical value. Indeed, our solution for which the free energy exhibiting the order  $N^{\frac{3}{2}}$  singular at  $\frac{\zeta}{k} = \frac{1}{4}$ , thus it is not valid very near the point. We expect that the analysis very near  $\frac{\zeta}{k} = \frac{1}{4}$  including finite  $N$  effects makes the free energy smooth.

It seems that for the general mass deformation, the large  $N$  saddle-point solution has a singularity at a finite mass parameter. Indeed, we found that the large  $N$  saddle-point solution for the case  $\zeta_1 = 0$  can be obtained in the S-dual representation and it does not have a singularity at finite  $\zeta_2$ . Thus, we expect that the singularity reflects in some physical origin.

Another important property of the FI-deformed ABJM theory is that it will describe the M2-M5 system. Indeed, in the classical analysis [42], the supersymmetric vacua are found to be discrete and given by a configuration which is a generalization of the fuzzy sphere to a fuzzy  $S^3$  which describes the M5-brane [42, 83]. Remember the result of chapter 3 that the solution of the saddle-point equation associated with a point of the Coulomb branch can become dominant. This implies that in the infinite mass region, the corresponding point of the Vacuum moduli space is no longer realized in the large  $N$  limit. Then, we cannot deny the possibility that another solution for which the free energy exhibits  $N^{\frac{3}{2}}$  behavior becomes dominant. However, because we could not find such a solution with our general ansatz, it is likely that the solution associated with a metastable vacuum becomes dominant <sup>†20</sup>. This scenario is also supported

---

<sup>†20</sup>More generally speaking, it is subtle that the partition function in the infinite mass limit can always be identified with that of an effective theory.

by the fact that the supersymmetric vacuum moduli space of the mass-deformed ABJM theory is composed of discrete points, but the integration of the matrix model is taken over the all Coulomb branch parameter including non-supersymmetric vacua.

In the next part, we argue on the large  $N$  solution corresponding to the supersymmetry breaking phase. We investigate several examples which can exhibit spontaneously supersymmetry breaking and the similar properties with confinement in the large  $N$  limit. Then, we show the solution for supersymmetry breaking exists in the mass deformed ABJM theory and argue on its supersymmetry breaking in the large  $N$  limit.

## Part III

# Notes on Large $N$ phases of gauge theories on the ellipsoid

# Chapter 5

## Saddle-point solution for SUSY breaking phase

In this chapter, we study a phase which can be realized in the large- $N$  limit of  $\mathcal{N} = 2$  gauge theories, using the localization technique for various theories on the ellipsoid, which interpolates the sphere and the flat space compactified on  $S^1$ . Due to the large- $N$  limit, we can evaluate the matrix model integral by the saddle-point approximation and find a large- $N$  saddle-point solution for a gauge theory (with massive matter fields which transform as the adjoint representation of the gauge group). The free energy evaluated by this solution exhibits the vanishing typical order  $\mathcal{O}(N^2)$  arising from the degrees of freedom of gluons in  $1/N$  expansion except for the contributions from the decoupling matter fields. This implies that  $\mathcal{O}(N^2)$  gluons are confined. We also find that the solution is consistent with the exact results of  $\mathcal{N} = 2$  SUSY Chern-Simons theory believed to be in a SUSY breaking phase.

We also investigate the expectation value of a supersymmetric Wilson loop on the ellipsoid for the solution and show that it vanishes in the leading order in  $1/N$  expansion. In the flat limit of the ellipsoid, a Wilson loop can be regarded as a (supersymmetric generalized) Polyakov loop since this loop wraps around the  $S^1$  in  $S^1 \times \mathbb{R}^2$ . Because the usual Polyakov loop is the order parameter of this symmetry, we can expect that the supersymmetric Wilson loop (2.6.31) also is the order parameter of the center symmetry because the center symmetry does not act the scalar in it and the supersymmetric Wilson loop is expected to be transformed under the symmetry as the non-supersymmetric Wilson-loop. We note that only the  $\mathbb{R}^2$  is the non-compact space, thus there are no spontaneous breaking of symmetries if  $N$  is finite. However, we take the large- $N$  limit of the theory and thus symmetries can be broken spontaneously. Therefore, we will call the phase with  $\langle W_R \rangle = 0$  “confinement phase” although it is only meaningful for the large- $N$  limit.

The remaining of this chapter is organized as follows: In section 1,2 and 3, we investigate large- $N$  solutions of several kinds of gauge theories and show that there exists the solution corresponding to supersymmetry breaking phase. In section 4, we summarize this paper and discuss some problems. In appendix B, we discuss which solution is dominant in the large- $N$  limit. We introduce the theory whose saddle-point equation has at least two types of solutions. We investigate when the solution in the SUSY breaking phase tends to become the dominant one.

## 5.1 Pure $\mathcal{N} = 2$ SUSY Chern-Simons Yang-Mills theory

First, we study the Chern-Simons Yang-Mills theory without chiral multiplets<sup>†1</sup>. The action  $S$  for the matrix model is

$$S(\sigma) = i\pi k \sum_{i=1}^N \sigma_i^2 - 2\pi i\zeta \sum_{i=1}^N \sigma_i - \frac{1}{2} \sum_{i,j=1, i>j}^N (\log 4 \sinh(\pi b(\sigma_i - \sigma_j)) + \log 4 \sinh(\pi b^{-1}(\sigma_i - \sigma_j))) + N \log N, \quad (5.1.1)$$

up to a constant.<sup>†2</sup> In particular, for  $k = 0$ , the matrix integral is not convergent and the theory is the pure  $\mathcal{N} = 2$  SUSY Yang-Mills theory which has the runaway type effective potential [86]. The saddle-point equation is written down as

$$0 = \frac{\partial S(\sigma)}{\partial \sigma_j} = 2i\pi k \sigma_j - 2i\pi \zeta - b\pi \sum_{k \neq j} \coth \pi b(a_j - a_k) - b^{-1}\pi \sum_{k \neq j} \coth \pi b^{-1}(a_j - a_k). \quad (5.1.2)$$

In this chapter, we consider the special class of the ellipsoids which have

$$b = \sqrt{\frac{p}{q}}, \quad (5.1.3)$$

where  $p, q \in \mathbb{Z}$ . For these special values, we can find large- $N$  solutions corresponding to the supersymmetry breaking phase<sup>†3</sup>.

---

<sup>†1</sup>In this case, although the integrations over  $a_i$  diverge, even for non-zero  $k$  without a precise regularization. We will analyze them assuming the regularization is done. In fact, we can introduce the imaginary part of the Chern-Simons-level for the integrals to converges and finally take it to zero. The existence of this imaginary part of the Chern-Simons-level does not change the solution of the saddle-point equation because the solution we will consider does not depend on the Chern-Simons-level. In the recent works [84,85], it was shown that we can take the contour so that the integrations of the matrix models converge.

<sup>†2</sup>We have approximated  $\log N! \approx N \log N$ .

<sup>†3</sup>It is interesting to extend the solution without this condition on  $b$ . It is also interesting to find the reason why this condition should be imposed. We will argue this point in Section 5.5.



Extending the solution given in [2], the solution is determined as

$$a_j = i \left( \frac{j}{N} - c \right) \sqrt{pq} M, \quad (5.1.4)$$

where  $M = \mathbb{Z}_{>0}$  and  $c = \frac{N+1}{2N}$ . We note that the constant is taken  $c$  to satisfy  $\sum_{j=1}^N a_j = 0$ . Then, the saddle-point equation in the large- $N$  limit becomes

$$0 = b \int_0^1 dy \cot \pi p(x - y) + b^{-1} \int_0^1 dy \cot \pi q(x - y), \quad (5.1.5)$$

where we have taken the continuous limit in which we replace the discrete valuable  $j$  and the summation of it from continuous ones  $x$  and the integral over  $x$  as

$$\frac{j}{N} \rightarrow x \in [0, 1], \quad \frac{1}{N} \sum_{j=1}^{N-1} \rightarrow \int_0^1 dx. \quad (5.1.6)$$

The integrals are defined as the principal value integral because the zero of the sinh is not included in (5.1.1)<sup>†4</sup>. Here, the Chern-Simons term and the FI term were neglected in the large- $N$  limit because  $k$  and  $\zeta$  are finite. Then, indeed, the integrations over  $y$  in (5.1.5) vanish for any  $x$  because the integration of the cot over the period vanishes since  $p, q$  are integers<sup>†5</sup>.

The expectation value of a Wilson loop at  $\theta = 0$  for the fundamental representation is evaluated in the leading order in the large  $N$  limit as

$$\langle W \rangle \approx e^{-\pi i q} \sum_{j=1}^N \exp \left( 2\pi i \frac{j}{N} q \right) = 0, \quad (5.1.7)$$

where we neglected the sub-leading term which will be  $\mathcal{O}(N^0)$ . This implies that a theory is in the confining phase, at least in the large  $b$  limit which can be taken, for example, by taking  $q = 1$  and  $p \rightarrow \infty$ .

The free energy is evaluated for the solution (5.1.4) as

$$F = 0 \cdot N^2 + \mathcal{O}(N), \quad (5.1.8)$$

because

$$\frac{N^2}{4} \int_{1 \geq x > y \geq 0} dx dy \left[ \log \sin^2 \pi p(x - y) + \log \sin^2 \pi q(x - y) \right] = 0. \quad (5.1.9)$$

---

<sup>†4</sup>Here we assumed  $pq$  and  $N$  are coprime.

<sup>†5</sup>For this solution, there are infinitely many discrete moduli,  $a_j = i \left( \frac{j}{N} - c + n(j) \right) \sqrt{pq} M$  where  $n(j)$  is an  $\mathcal{O}(N^0)$  integer, which do not change the values of the free energy and the Wilson loop [2]. The summation over these may not affect the large  $N$  results although these could be important to obtain  $Z = 0$ , which is expected for the theory in the SUSY breaking, through the Chern-Simons term.

This result also implies that this theory is in the confining phase because the vanishing  $\mathcal{O}(N^2)$  term corresponds to confinement of gluons and other fields. We also note that at the saddle-point,  $\sigma$  is pure imaginary. This would be related to the expectation value of a usual Polyakov loop because the combination of the gauge field  $iA_\mu$  and  $\sigma$  appears in the supersymmetric Wilson loop.

We have considered the large- $N$  limit of the  $\mathcal{N} = 2$  supersymmetric Chern-Simons Yang-Mills theory, however, even for finite  $N$  the partition function and the Wilson loop have been obtained by doing the integration. Under a certain regularization, the partition function for the  $\mathcal{N} = 2$  supersymmetric  $SU(N)$  Chern-Simons theory on the round three-sphere can be explicitly computed as [50]

$$|Z_{\text{Chern-Simons}}| = \frac{2^{N(N-1)/2}}{k^{N/2}} \prod_{m=1}^{N-1} \left| \sin^{N-m} \left( \frac{\pi m}{k} \right) \right| = \frac{1}{k^{N/2}} \prod_{1 \leq j < l \leq N} \left| 2 \sin \left( \frac{\pi(l-j)}{k} \right) \right|, \quad (5.1.10)$$

which is the same as the one for the bosonic Chern-Simons theory with the level  $k - N$ . This result is the same for the theory even on the ellipsoid as expected from the fact that the Chern-Simons theory is topological. The expectation value of a supersymmetric Wilson loop of the fundamental representation was also computed as [50]

$$\langle W \rangle \sim \prod_{1 \leq j < l \leq N} \frac{\sin \left( \frac{\pi(l-j+\delta_{1,j}-\delta_{1,l})}{k} \right)}{\sin \left( \frac{\pi(l-j)}{k} \right)} = \frac{\sin \left( \frac{\pi N}{k} \right)}{\sin \left( \frac{\pi}{k} \right)} \quad (5.1.11)$$

where we neglected the phase factor which is related to the framing dependence.

For  $N > k$ , this partition function (5.1.10) becomes zero and this is related to the spontaneous symmetry breaking of SUSY Chern-Simons theory as we reviewed in Part I. Although the partition function is vanishing, the expectation value of a supersymmetric Wilson loop, which is normalized by the partition function, is not diverging<sup>†6</sup> and  $\mathcal{O}(N^0)$  for the large  $N$  limit with finite  $k (\neq 1)$ , which is the same as for the large  $N$  solution<sup>†7</sup>. On the other hand, the free energy is divergent for  $N > k$ , which seems to be different from the large  $N$  solution for the confinement phase. However, below we will argue that in the large  $N$  expansion the free energy  $-\log |Z_{\text{Chern-Simons}}|$  is consistent with that for the large  $N$  solution. Thus, we expect that the large  $N$  solution corresponds to a SUSY breaking phase.

---

<sup>†6</sup>There may be Nambu-Goldstone fermion zero modes which make the partition function vanishes. It is expected that the Wilson loop does not include these zero modes and the contributions of the zero modes are canceled.

<sup>†7</sup>For  $k \rightarrow 1$ , we find  $\langle W \rangle \sim N$ . Thus, for  $k = 1$ , the large  $N$  solution does not seem to correspond to the pure Chern-Simons theory.

Now we will evaluate the (5.1.10) in the large- $N$  limit and compare it to the saddle-point approximation by the confinement solution. We take logarithm of (5.1.10) and take continuous limit by the following replacements of the discrete index  $m$  and the summation:

$$\frac{m}{N} \rightarrow x \in [0, 1], \quad \frac{1}{N} \sum_{m=1}^{N-1} \rightarrow \int_0^1 dx. \quad (5.1.12)$$

Then, the large  $N$  leading part of the logarithm of (5.1.10) is written as

$$\frac{F(t)}{N^2} \equiv -\frac{\log |Z_{\text{Chern-Simons}}|}{N^2} \sim -\int_{0 \leq y < x \leq 1} dx dy \log \left| 2 \sin \frac{\pi(x-y)}{t} \right| \quad (5.1.13)$$

$$= -\int_0^1 dx (1-x) \log \left| 2 \sin \frac{\pi x}{t} \right|, \quad (5.1.14)$$

where  $N$  is infinite while keeping  $\frac{k}{N} = t$  finite <sup>†8</sup>. In the first line, the RHS is the same as (5.1) except for  $1/t$  factor. We can find that there are infinite zeros of (5.1.14) as a function of  $t$  at  $t = \frac{1}{n}$ ,  $n \in \mathbb{Z}$  and no singularities for  $t > 0$ . The behavior of (5.1.14) is shown in the figure 5.1 and we can see that  $\frac{F(t)}{N^2} \rightarrow 0$  when  $t \rightarrow 0$ . This is consistent with the large  $N$  solution with finite  $k$ . We would like to emphasize that in this large  $N$  analysis it may be impossible to recover the singular behavior where  $k$  is an integer.

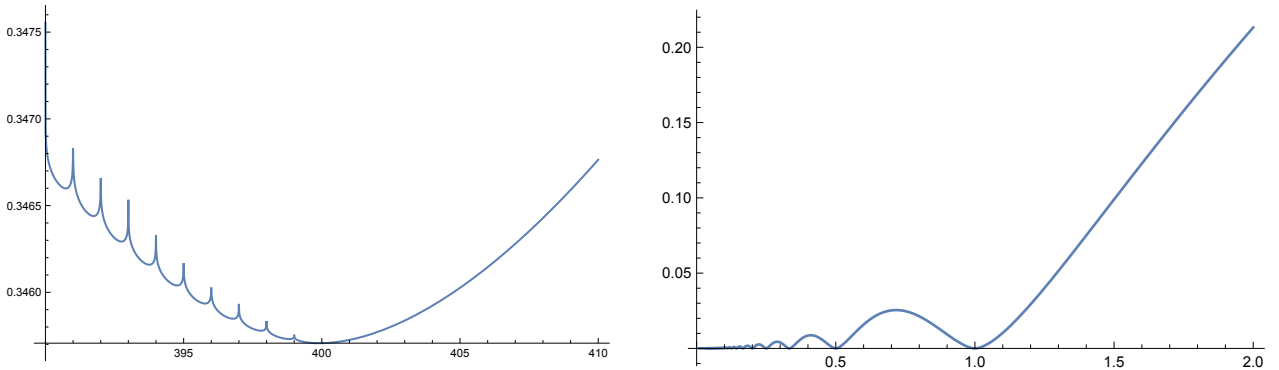


Figure 5.1: The left figure shows the numerical plot of  $-\log |Z_{\text{Chern-Simons}}|$  divided by  $N^2$  with  $N = 400$ . The horizontal axis corresponds to  $k \in [390, 410]$  as real value. The function is diverging when  $k < N$  and  $k$  is integer. The right figure shows (5.1.14) as a function of  $t$ . The zeros only appear in  $t \leq 1$  region. (These figures are cited from our paper [4].)

Finally, we will comment on the numerical results on the large  $N$  solution in the 't Hooft limit. In the region  $k \ll N$ , the solution is indeed the confinement solution we discussed above

<sup>†8</sup>In [91, 92], the authors discuss this free energy of the pure Chern-Simons theory in the 't Hooft limit. They argue that when  $t < 1$  the integrand of the free energy has a logarithmic branch cut on a part of the integral interval and the integral is ill-defined. However, in this time, we only consider the absolute value of the partition function and then its singular properties does not change. The integrand of (5.1.14) is well-defined even when  $t < 1$ .  $t$  is a inverse 't Hooft coupling.

because the Chern-Simons term can be ignored. In the region  $k \gg N$ , we found the solution also in [2] and the distribution of  $a_j$  lie on a line in the complex plane. The numerical result suggests that as  $k$  decreases and goes beyond to  $N$ , the imaginary part of the saddle-point solution tends to become a double-valued function as a function of the real part. The confinement solution (5.1.4) seems to be also a double-valued function including the real part of the confinement solution, which is  $\mathcal{O}(\frac{1}{N})$  and ignored <sup>†9</sup>. These similarities also suggest that the confinement solution corresponds to a SUSY breaking phase.

## 5.2 $\mathcal{N} = 2$ SUSY gauge theory with fundamental matter fields

In this section, we consider the  $N_f$  non-chiral pair of chiral multiplets  $(Q_a, \tilde{Q}^a)$  in the fundamental and the anti-fundamental representations of the gauge group  $G$  and  $a$  is a flavor index which runs from 1 to  $N_f$ . The total global symmetry is  $U(N_f) \times U(N_f)$  and we will introduce the mass  $m_a$  for the  $a$ -th flavor by gauging  $U(1)^{N_f}$  part of flavor symmetry as usual [52] <sup>†10</sup>. Since the center symmetry  $\mathbb{Z}_N$  does not exist, the argument about the confinement we used so far is not available.

For this theory, we have

$$S(a) = i\pi k \sum_{i=1}^N \sigma_i^2 - 2\pi i \zeta \sum_{i=1}^N \sigma_i - \frac{1}{2} \sum_{i,j=1, i>j}^N (\log 4 \sinh(\pi b(\sigma_i - \sigma_j)) + \log 4 \sinh(\pi b^{-1}(\sigma_i - \sigma_j))) - \sum_{a=1}^{N_f} \sum_{i=1}^N (\log s_b(\alpha + m_a - \sigma_i) + \log s_b(\alpha - m_a + \sigma_i)) + N \log N, \quad (5.2.1)$$

where

$$\alpha = \frac{iQ(1-r)}{2}. \quad (5.2.2)$$

In the large  $N$  limit, for  $N_f = \mathcal{O}(N^0)$ , the matter parts do not contribute to the saddle-point equation. Thus, the previous result (5.1.4) without matter fields is valid for this case although the  $\mathcal{O}(N)$  part of the free energy  $F$  is changed.

---

<sup>†9</sup>The real part of the solution was considered in the appendix of [2].

<sup>†10</sup>When we take the gauge group  $G=U(N)$ , we take the overall  $U(1)$  symmetry of  $U(N)$  to cancel one of the flavor mass. This means that when the Chern-Simons level and FI parameter is vanishing, we can always make one hypermultiplet massless. We do not consider such a case.

For  $N_f = \mathcal{O}(N)$ , the saddle-point equation has the following extra terms:

$$- \sum_{a=1}^{N_f} \frac{\partial}{\partial \sigma_i} (\log s_b(\alpha + m_a - \sigma_i) + \log s_b(\alpha - m_a + \sigma_i)), \quad (5.2.3)$$

which will make a solution completely different from the previous one and may reflect in the general fact that definitions of the confinement phase are ambiguous<sup>†11</sup> for the theory with the matter fields in the fundamental representations. However, for the large mass limit  $e^{-2\pi b^{\pm 1}|m_a|} \ll 1$ , these extra terms in the action are approximated to

$$\begin{aligned} & -i \frac{\pi}{2} \sum_{a=1}^{N_f} \sum_{i=1}^N \text{sign}(m_a) ((\alpha + m_a - (\sigma_i))^2 - (\alpha - m_a + (\sigma_i))^2) \\ & = -2\pi i \alpha \sum_{a=1}^{N_f} \sum_{i=1}^N \text{sgn}(m_a) (m_a - \sigma_i), \end{aligned} \quad (5.2.4)$$

thus, the action in this limit is written as

$$\begin{aligned} S(a) & \approx -\frac{1}{2} \sum_{i,j=1, i>j}^N (\log 4 \sinh(\pi b(\sigma_i - \sigma_j)) + \log 4 \sinh(\pi b^{-1}(\sigma_i - \sigma_j))) + N \log N \\ & + i\pi k \sum_{i=1}^N \left( \sigma_i - \frac{1}{k} \tilde{\zeta} \right)^2 - 2\pi i \alpha N \sum_{a=1}^{N_f} |m_a| - i \frac{\pi}{k} \tilde{\zeta}^2, \end{aligned} \quad (5.2.5)$$

where

$$\tilde{\zeta} = \zeta - \alpha \sum_{a=1}^{N_f} \text{sgn}(m_a). \quad (5.2.6)$$

This action is the same form as the one without the matter fields. Thus, by shifting the U(1) part of  $\sigma_i$  in the solution (5.1.4), the saddle-point solution is obtained as

$$\sigma_j = i \left( \frac{j}{N} - c \right) \sqrt{pq} M + \frac{\tilde{\zeta}}{k}, \quad (5.2.7)$$

The Wilson loop vanishes also because the shift changes the overall phase only. Note that for the SU( $N$ ) gauge theory, (5.2.5) with  $\tilde{\zeta} = 0$  is correct.

Without the vector multiplets, in the large mass limit we obtain the action (5.2.5). Naively considering, by choosing  $\tilde{\zeta} = 0$  and subtracting the contribution of the decoupled massive matter fields from the action, the result of the pure  $\mathcal{N} = 2$  super Yang-Mills Chern-Simons

---

<sup>†11</sup>The center symmetry is explicitly broken by the matter fields and the Wilson loop will not obey the area law by the pair creations.

theory is recovered. This implies that this solution corresponds to the origin of the Coulomb branch and simply the massive multiplets decouple. Because this point does not maintain the supersymmetry, which is a metastable vacuum, we conclude that the confinement solution corresponds to a supersymmetry breaking phase in the large  $N$  limit. However, as we mentioned in chapter 3, whether the solution introduced in this chapter can become dominant is non-trivial. As will be discussed in the appendix for the adjoint matter fields, we need to choose the coupling constants to realize the solution for the confinement phase for this theory with fundamental matter field although we do not explicitly do this.

### 5.3 $\mathcal{N} = 2$ SUSY gauge theory with adjoint matter fields

Next, we consider the  $N_a$  chiral multiplets of the adjoint representation of the gauge group  $G^{\dagger 12}$ . We will introduce the mass  $m_a$  for the adjoint chiral multiplets. Then, the action for the matrix model is written as

$$\begin{aligned}
S(\sigma) = & i\pi k \sum_{i=1}^N \sigma_i^2 - 2\pi i \zeta \sum_{i=1}^N \sigma_i - \frac{1}{2} \sum_{i,j=1, i>j}^N (\log 4 \sinh(\pi b(\sigma_i - \sigma_j)) + \log 4 \sinh(\pi b^{-1}(\sigma_i - \sigma_j))) \\
& + N \log N - \sum_{a=1}^{N_a} \sum_{i,j=1}^N \log s_b(\alpha + m_a - (\sigma_i - \sigma_j)). \tag{5.3.1}
\end{aligned}$$

Comparing with the pure Chern-Simons Yang-Mills case, additional terms in the saddle-point equations are

$$\sum_{a=1}^{N_a} \sum_{j \neq i}^N \frac{\partial}{\partial a_i} (\log s_b(\alpha + m_a - (a_i - a_j)) - \log s_b(\alpha + m_a - (a_j - a_i))) \tag{5.3.2}$$

where  $x = \frac{j}{N}$ . We will expand  $\log s_\alpha$  using (2.6.34) and (2.6.35).

Then, the matter fields contribute to the action as

$$-i \frac{\pi}{2} \sum_{a=1}^{N_a} \sum_{i,j=1}^N \text{sgn}(m_a) \left( (\alpha + m_a - (\sigma_i - \sigma_j))^2 + \frac{(Q^2 - 2)}{12} - \frac{2}{\pi} H(\text{sgn}(m_a)(\alpha + m_a - (\sigma_i - \sigma_j))) \right), \tag{5.3.3}$$

---

<sup>†12</sup>When  $G$  is  $SU(N)$  case, the matrix model of the gauge theory with gauge group  $G$  with  $N_a \geq 2$  converges. However,  $G = U(N)$  case, the matrix model with any  $N_a$  diverges because the integrand depends only through the difference of the integral variables as  $\sigma_i - \sigma_j$ . Generally, the condition that the determinant is one makes the matrix model converge depending on the  $N_a$ .

where

$$H(z) = \sum_{l=1}^{\infty} \frac{(-1)^{l-1}}{l} \left( \frac{e^{-2\pi lbz}}{2 \sin(\pi lb^2)} + \frac{e^{-2\pi lz/b}}{2 \sin(\pi lb^{-2})} \right). \quad (5.3.4)$$

Now, we assume that

$$\sum_{a=1}^{N_a} \text{sgn}(m_a) = 0, \quad (5.3.5)$$

to solve the saddle-point equations.

In what follows, we will show that

$$a_j = 2i \left( \frac{j}{N} - c \right) \sqrt{pq}M, \quad (5.3.6)$$

is a solution of the saddle-point equation for the theory with the adjoint matter fields<sup>†13</sup>. We see that the terms including  $H'(x)$  vanish because  $H(x)$  is the periodic function with the period  $2i\sqrt{pq}$ , i.e.  $H(x + 2i\sqrt{pq}) = H(x)$ , which can be seen from  $\sqrt{pq} = qb = p/b$ , and then,

$$\sum_{j \neq i}^N H' \left( \text{sgn}(m_a) \left( \alpha + m_a \pm i \frac{\sqrt{pq}M}{N} (i - j) \right) \right) = \sum_{\ell=1}^{N-1} H' \left( \text{sgn}(m_a) \left( \alpha + m_a \pm i \frac{\sqrt{pq}M}{N} \ell \right) \right). \quad (5.3.7)$$

We can also see that the remaining terms are canceled each others:

$$\sum_{a=1}^{N_a} \text{sgn}(m_a) \left( \alpha + m_a + 2i \frac{\sqrt{pq}M}{N} \sum_{j \neq i}^N (i - j) - (\alpha + m_a) + 2i \frac{\sqrt{pq}M}{N} \sum_{j \neq i}^N (i - j) \right) = 0. \quad (5.3.8)$$

Therefore, (5.3.6) is the large  $N$  saddle-point solution. The leading part of the Wilson loop in the fundamental representation vanishes in the large  $N$  limit as for the pure Chern-Simons Yang-Mills case. We can also evaluate the free energy and find that  $F = 0 \cdot N^2 + \mathcal{O}(N)$  where we used the periodicity of the function  $H(z)$  like as (5.3.7).

For this theory with fundamental matter fields, there is another large  $N$  solution as discussed in the appendix. To realize the confinement phase, we need to tune the parameters as we will see in the appendix.

---

<sup>†13</sup>There is an additional factor 2 in (5.3.6) compared with the pure Yang-Mills case. This is because  $H(x)$  contains  $e^{\pi b^{\pm 1}x}$  instead of  $e^{2\pi b^{\pm 1}x}$  for  $\sinh^2(\pi b^{\pm 1}x)$ . If  $(1 + b^{\pm 2})(1 - r) = m_{\pm}$  where  $m_{\pm} \in \mathbb{Z}$ , we can show that this factor 2 can be dropped, although these mean  $b = 2r = m_{\pm} = 1$  for  $r > 0$ .

## 5.4 FI-deformed ABJM theory

In this section, we study the confinement solution of the mass-deformed ABJM theory for  $\zeta_1 = \zeta_2 = \zeta$  in the limit  $N \rightarrow \infty$  with the Chern-Simons levels  $k$  kept finite. The solution is different from the solution for which the free energy exhibits  $N^{\frac{3}{2}}$  behavior.

### 5.4.1 Solutions in large $\zeta/k$ limit

First, we consider the case  $\zeta/k \gg 1$ . The saddle-point equations further (4.2.4) are simplified in this regime. Here, we take the reality condition and an ansatz as follows:

$$\lambda_i = -\tilde{\lambda}_j^* \quad (5.4.1)$$

$$\lambda_j = \frac{\zeta}{k} + i\frac{N}{k} + u_j + iv_j. \quad (5.4.2)$$

where we assume that  $u_j$  and  $v_j$  are of  $\mathcal{O}(N^0)$ . Shifting the eigenvalues in the real part by  $\frac{\zeta}{k}$  cancels the term  $-2\pi i\zeta$ , while the last terms in the saddle-point equations (4.2.4) are approximated as

$$\sum_{j=1}^N \tanh \pi(\lambda_i - \tilde{\lambda}_j) = N + \mathcal{O}(e^{-\frac{4\pi\zeta}{k}}), \quad (5.4.3)$$

which is canceled by the shift in the imaginary part of the eigenvalues. The equation finally obtained are up to sub-leading correction of  $\zeta$

$$-kv_i - \sum_{\substack{j=1 \\ (j \neq i)}}^N \frac{\sinh 2\pi(u_i - u_j)}{\cosh 2\pi(u_i - u_j) - \cos 2\pi(v_i - v_j)} = 0, \quad (5.4.4)$$

$$ku_i + \sum_{\substack{j=1 \\ (j \neq i)}}^N \frac{\sin 2\pi(v_i - v_j)}{\cosh 2\pi(u_i - u_j) - \cos 2\pi(v_i - v_j)} = 0, \quad (5.4.5)$$

where we write down the real and imaginary part of the saddle-point equation separately. The free energy (4.2.3) also is simplified in this limit as

$$f = 2N \log N + \frac{4\pi N^2 \zeta}{k} + \delta f + \mathcal{O}(e^{-\frac{4\pi\zeta}{k}}) \quad (5.4.6)$$

with

$$\delta f = -4\pi k \sum_{i=1}^N u_i v_i - \sum_{\substack{i,j=1 \\ (i \neq j)}}^N \log \left[ 2 \left( \cosh 2\pi(u_i - u_j) - \cos 2\pi(v_i - v_j) \right) \right]. \quad (5.4.7)$$



We note that the equations (5.4.4) and (5.4.5) are in the same form as the saddle-point equations for the pure Chern-Simons theory, which were analyzed in 5.1. In that sense the correction  $\delta f$  in the free energy corresponds to the free energy of the pure Chern-Simons theory in the large- $N$  limit.

### Large- $N$ solution

With the ansatz (5.4.2), the solution of the saddle-point equations is the following:

$$u_j = 0 + \frac{1}{N}g\left(\frac{j}{N}\right), \quad v_j = \frac{j}{N} + n(j) + \Delta + \mathcal{O}\left(\frac{1}{N}\right). \quad (5.4.8)$$

Here  $g(s)$  is some function and  $\Delta$  is a constant both of which being of  $\mathcal{O}(N^0)$ , while  $n(j)$  is some integer which can be different for each  $j$ . Indeed, after the substitution of these expressions the real part of the saddle-point equation (5.4.4) is of  $\mathcal{O}(N^0)$ , while the  $\mathcal{O}(N)$  part of the imaginary part of the saddle-point equations (5.4.5) vanishes due to the following identity

$$\sum_{\substack{j=1 \\ (j \neq i)}}^N \frac{\sin \frac{2\pi(i-j)}{N}}{1 - \cos \frac{2\pi(i-j)}{N}} = 0. \quad (5.4.9)$$

Hence, (5.4.8) solves the saddle-point equations up to  $\mathcal{O}(N^0)$  corrections.

Then, we evaluate the free energy  $\delta f$  for this solution. The second term is obviously of  $\mathcal{O}(N^0)$ . Approximating the cosine hyperbolic factor by 1 we can compute the third term exactly as

$$-\sum_{\substack{i,j=1 \\ (i \neq j)}}^N \log \left[ 2 \left( \cosh 2\pi(u_i - u_j) - \cos 2\pi(v_i - v_j) \right) \right] \approx -N \log \prod_{i=1}^{N-1} 2 \left[ 1 - \cos \frac{2\pi i}{N} \right] = -2N \log N. \quad (5.4.10)$$

Hence the free energy in the large  $N$  limit is

$$f \approx \frac{4\pi N^2 \zeta}{k} + \mathcal{O}\left(\frac{1}{N}\right), \quad (5.4.11)$$

with the solution,

$$\lambda_j \approx \frac{\zeta}{k} + i \left( \frac{N}{k} + \frac{j}{N} - \frac{1}{2} \right), \quad (5.4.12)$$

where we have fixed the values of  $\Delta$  and  $n(j)$  as  $\Delta = -\frac{1}{2}$  and  $n(j) = 0$ .

We note that  $N \log N$  term arising from the Weyl group of  $U(N) \times U(N)$  cancels the contributions from the one-loop part (5.4.10). The remaining  $N^2$  factor can be interpreted as the

contributions from decoupled free hypermultiplets. Because there are  $N \times N$  hypermultiplets in the ABJM theory, from (2.6.46) we can derive the above result. On the other hand, after integrating out the matter multiplets in the mass deformed ABJM theory, the pure Chern-Simons theory remains. This is the reason why the saddle-point equations for the shifted eigenvalues  $u_i + iv_i$  (5.4.4) and (5.4.5) can be interpreted as that for this reduced theory.

## Wilson loops

Then, we attempt to compute the expectation values of a supersymmetric Wilson loops (2.6.31). We consider the Wilson loop associated with  $U(N)_k$  gauge group in  $U(N)_k \times U(N)_{-k}$ . By substituting the saddle-point configuration (5.4.2) with (5.4.8), we obtain

$$\langle W_{\square}(C) \rangle = \frac{1}{N} e^{\pi(\frac{\zeta}{k} + i\frac{N}{k})} \sum_{j=1}^N \exp\left[\frac{2\pi i j}{N} + \mathcal{O}(N^{-1})\right]. \quad (5.4.13)$$

Similarly, the Wilson loop for  $U(N)_{-k}$  can be written as

$$\langle \widetilde{W}_{\square}(C) \rangle = \frac{1}{N} e^{\pi(-\frac{\zeta}{k} + i\frac{N}{k})} \sum_{j=1}^N \exp\left[\frac{2\pi i j}{N} + \mathcal{O}(N^{-1})\right]. \quad (5.4.14)$$

When we neglect the  $\mathcal{O}(N^{-1})$  deviations in the exponent, the leading part of the right-hand side vanishes in both cases.

### 5.4.2 Any $\zeta/k$

Below we will consider the limit  $N \rightarrow \infty$  with both  $k$  and  $\zeta$  kept finite. We will show that for any finite  $\zeta/k$ , there is a solution which is a simple generalization of the solution obtained in the last section and has the same expression for the free energy  $f \sim \frac{4\pi N^2 \zeta}{k}$  in the large- $N$  limit.

Let us begin with the small generalization of the ansatz in the last section (5.4.12) ( $\lambda_i = x_i + iy_i$ )

$$x_i = \frac{\zeta}{k} + \frac{1}{N} g\left(\frac{i}{N}\right), \quad y_i = \frac{N}{k} + \frac{i}{N} + \Delta + \frac{1}{N} h\left(\frac{i}{N}\right). \quad (5.4.15)$$

with  $g(s)$  and  $h(s)$  some functions and  $\Delta$  some real constant, both being of  $\mathcal{O}(N^0)$ . Indeed, we can solve the saddle-point equation with the help of the following trivial generalization of the identities (5.4.9):

$$\sum_{j=1}^N \frac{\sin \frac{2\pi(i-j)}{N}}{a + \cos \frac{2\pi(i-j)}{N}} = 0, \quad (a \notin (-1, 1)). \quad (5.4.16)$$

Similarly,  $\mathcal{O}(N)$  terms in the real part of the saddle-point equation vanish due to

$$\sum_{j=1}^N \frac{1}{\cosh b + \cos \frac{2\pi(i-j)}{N}} = \frac{N}{\sinh b}. \quad (b > 0) \quad (5.4.17)$$

We can also solve the  $\mathcal{O}(N^0)$  part of the saddle-point equations to determine  $(f(s), g(s), \Delta)$ , though they are irrelevant to the leading part of the free energy. The computation is parallel to those in the large  $\zeta$  limit and displayed in [2].

The free energy  $f$  for this solution also takes the same form as in the case of the large  $\zeta$  limit. In the large- $N \rightarrow \infty$ , the relevant terms to the free energy are following:

$$\begin{aligned} f(\lambda) &\approx N \log N - \sum_{\substack{i,j=1 \\ (i \neq j)}}^N \log 2 \left[ 1 - \cos \frac{2\pi(i-j)}{N} \right] + \sum_{i,j=1}^N \log \left[ \cosh \frac{4\pi\zeta}{k} + \cos \frac{2\pi(i-j)}{N} \right] \\ &= \frac{4\pi\zeta N^2}{k} + \mathcal{O}(N \log N). \end{aligned} \quad (5.4.18)$$

To obtain the second line, it is convenient to take the continuous limit in which the summation is replaced with the integration over  $s \sim \frac{i}{N}$ . The  $\mathcal{O}(N \log N)$  denotes correction terms due to the difference between the integrations and the original discrete summation.

## 5.5 Summary and Discussion

In this chapter, we have studied the properties of the confinement solution which we discovered in [2] and the theory which has that type of the solution. First, we have considered theories on  $S_b^3$  for supersymmetric Wilson loops to be regarded as the (generalized) Polyakov loop by taking  $b \rightarrow \infty$  limit in the sense that  $S_b^3$  become locally  $S^1 \times \mathbb{R}^2$  and the supersymmetric Wilson loop is wrapping on the  $S^1$ . In the large- $N$  limit, a supersymmetric Wilson loop in the fundamental representation can be evaluated with the solution of the saddle-point equation. We showed that various gauge theories have the special kind of solution. With this solution, the expectation value of Wilson loop is vanishing in the large- $N$  limit. Thus, we call the solution as a confinement solution in the sense that this Wilson loop can be regarded as the generalized Polyakov loop. We expect that this solution corresponds to the spontaneously SUSY breaking phase <sup>†14</sup>. This result is somewhat surprising in the sense that although  $\mathbb{Z}_N$  symmetric configurations for the non-vanishing gauge fields give the vanishing Polyakov loop, the localization technique reduces the path integral variables to the integrations over the constant scalars where the gauge fields

---

<sup>†14</sup>One reason for this expectation is that this solution only valid in the region  $N \gg k$ . This is consistent with the fact that the SUSY breaking phase may be gapped and confined [35].

are fixed to zero. We also note that in our solution, the nonzero imaginary scalars values are similar to the  $\mathbb{Z}_N$  symmetric configurations for the gauge fields. The scalars and gauge fields are combined and regarded as a complex variable in a supersymmetric Wilson loop, then this may lead to the vanishing (generalized) Polyakov loop.

One of the interesting future work is to consider the large- $N$  solution for the confinement phase in a theory on the Seifert manifold [84, 85]. Indeed, we expect that this solution for the confinement phase exists even for a theory on the Seifert manifold also by the following reasons. In the 1-loop part of the twisted index of the Seifert manifold, the holonomy  $a$  along the  $S^1$  fiber direction and the scalar field of the vector multiplet  $\sigma$  are combined into a complex scalar in which  $a$  and  $\sigma$  are real and imaginary part respectively. Moreover, the 1-loop part is periodic under the constant shift of the holonomy which is regarded as the large gauge transformation and essentially equivalent to the action of the center symmetry. Then, it is also periodic under the shift of the imaginary part of  $\sigma$  because this also gives the same constant shift of the complex scalar. Thus, the large- $N$  solution for the confinement phase exists as for the theory on the ellipsoid  $S_b^3$ . We emphasize that if there is no non-trivial one-cycle, the holonomy  $a$  does not exist, however, for the Seifert manifold with a non-trivial fundamental group, the large- $N$  solution associated with the confinement phase is regarded as just the usual symmetric configuration of the Polyakov loop for the confinement phase. This might explain our observation that the large- $N$  solution for the theory on the squashed  $S^3$  may exist only when a square of the squashed parameter  $b$  is a rational number because the partition function for a theory on the ellipsoid with the rational squashing parameter is represented by the one on a Seifert manifold. It will be interesting to investigate the large- $N$  solution of the theory on a Seifert manifold further and the corresponding gravity solutions [87, 88].<sup>†15</sup>

We also note that we found that the mass deformed ABJM theory has the large  $N$  solution whose free energy is proportional to  $N^{\frac{3}{2}}$  and it is valid when  $\frac{\zeta}{k} < \frac{1}{4}$ . In the next chapter, we will argue that when  $\frac{\zeta}{k} \geq \frac{1}{4}$ , the mass deformed ABJM theory is expected to be in a SUSY breaking phase in the large- $N$  limit and the confinement solution is a candidate which becomes dominant in this region. This might reflect in the naive expectation that the pure Chern-Simons theory in a SUSY breaking phase appears if all massive bi-fundamental hypermultiplets decouple. Thus, we expect that the theory is in a SUSY breaking phase and the confinement solution can be relevant in the large- $N$  limit when  $\frac{\zeta}{k} \geq \frac{1}{4}$ .

---

<sup>†15</sup>We would like to thank a referee of our paper [4] for suggesting a relation between our solution and the theory on Seifert manifolds.

# Chapter 6

## Mass-Deformed ABJM Theory Revisited

First, we would like to clarify relation between results introduced so far and this chapter. As we have mentioned, the theory with the R-charge deformation is formally identical to the mass deformation with pure imaginary mass parameters  $\zeta_1, \zeta_2 \in i\mathbb{R}$  at the level of the localization formula (4.1.5). Therefore, it seems that the results for the real masses were simply obtained by an analytic continuation of the ones for the R-charge deformations or equivalently imaginary masses. Indeed, our result will show that the statement is true only in a small region of the mass parameters, but we claim that this is true for small  $\zeta_1, \zeta_2$  otherwise this is not. However, the behaviors of the partition function are completely different from that for the real mass deformation. The partition function diverges because when one of  $\zeta_1, \zeta_2$  reaches  $\zeta_i = \pm \frac{ik}{4}$ , the integration runs over the pole of the integrand. On the other hand, the partition function never vanishes for real masses since the integrand has no poles. Furthermore, the shape of the phase boundary is different from that for the R-charge deformation. In particular, the result in 4.3 has told us that if  $\zeta_1 = 0$  the matrix model does not encounter any phase transition regardless of the value of  $\zeta_2$ . Though the understanding is not complete, we suspect that this phase boundary particular for the real masses is related to the convergence property of the large- $N$  expansion, which is completely different for  $\zeta_1, \zeta_2 \in i\mathbb{R}$  and  $\zeta_1, \zeta_2 \in \mathbb{R}$ . We will elaborate this point in Section 6.2.3 in terms of the result [77].

Combining the results in chapter 3, it is likely that the supersymmetric vacua do not become dominant in the infinite mass limit and metastable vacua contribute to the partition function. One possible phase realized in the large  $N$  limit outside the phase boundary is that mentioned in chapter 5. Then, in this chapter, we have obtained the exact expressions<sup>†1</sup> for  $Z(N, k, 0, \zeta_2)$

---

<sup>†1</sup>The exact expression for  $N = 1, 2$  and general  $\zeta_1, \zeta_2$  was obtained in [104].

and numerical results for  $Z(N, k, \zeta_1, \zeta_2)$  with finite  $N \geq 3$ , and the large- $N$  expressions. We expect that in the large  $N$  limit, the mass-deformed ABJM theory on the three-sphere is in supersymmetry breaking phase outside of the above phase boundary. We argue that point in this chapter from the numerical result for finite  $N$  result and the result we discussed so far in this thesis.

## 6.1 Evidence for SUSY breaking

In this section, we explain why we expect the SUSY breaking of the mass deformed ABJM theory on  $S^3$  in the large- $N$  limit at some finite  $(\zeta_1, \zeta_2)$  and explain our criterion for the SUSY breaking which we will examine in the following sections.

First, in the case of  $\zeta_1 = \zeta_2 = \zeta$ , there is a large- $N$  saddle-point solution for the original matrix model (4.1.5) which exist only for  $0 \leq \frac{\zeta}{k} < \frac{1}{4}$  [2]. This solution is smoothly connected with the saddle-point solution of the massless ABJM theory [75] as  $m \rightarrow \infty$  and exhibit the  $N^{3/2}$ -law of the free energy:

$$-\log Z = \frac{\pi\sqrt{2k}}{3} \left(1 + \frac{16\zeta^2}{k^2}\right) N^{3/2}. \quad (6.1.1)$$

However, this saddle-point solution becomes singular in the  $\frac{\zeta}{k} \rightarrow \frac{1}{4}$  limit. There is another large- $N$  solution for any value of  $\zeta$ . The free energy of this solution is proportional to  $N^2$  and this solution may correspond to a confinement vacuum.<sup>†2</sup> Although it would be possible that there are other solutions,<sup>†3</sup> these results strongly indicate a phase transition at  $\frac{\zeta}{k} \rightarrow \frac{1}{4}$  in the large  $N$  limit.

We expect that this phase transition comes from a supersymmetry breaking as follows. We take the mass very large, i.e.  $\frac{\zeta}{k} \gg 1$ , then, at least naively, the hypermultiplets become heavy and decouple from the vector multiplets. The remaining  $\mathcal{N} = 2$  SUSY pure Chern-Simons theory will be in supersymmetry breaking phase as shown in [35, 90], and at the same time be in the confinement phase in the large- $N$  limit. This perspective is consistent with the above large- $N$  solutions. However, for the mass deformed ABJM theory, the Witten index was computed to be non-zero in [40, 41]. As we reviewed in the previous review part, this theory has

---

<sup>†2</sup>This statement is not precise because the Chern-Simons interaction remains and theory may be in a gapped phase. Nevertheless, we will call the confinement phase for such case also. Note that here we take  $k/N \rightarrow 0$  limit, thus the Chern-Simons interaction will be ignored for the leading order in the large- $N$  limit and the Yang-Mills term always induced by the renormalization flow. We also note that the  $\mathcal{N} = 2$  SUSY pure Yang-Mills theory does not have SUSY vacua.

<sup>†3</sup>From some numerical methods, we have not been able to find any solution other than the two solutions.

discrete supersymmetric vacua which are characterized by the fuzzy  $S^3$  solutions, which denote dielectric M5-branes. Although the contribution to the index for the trivial vacuum, where all the scalar fields are zero, vanishes as in the pure supersymmetric Chern-Simons theory for  $N > k$ , other vacua can give the non-zero contributions to the index. This result seems to contradict with the above argument of the supersymmetry breaking. However, this result is for the theory on  $T^3$ , not on  $S^3$ . For the  $\mathcal{N} = 2$  SUSY theory on  $S^3$ , there are mass terms for the chiral multiplets proportional to the curvature of  $S^3$ . The mass term will lift all of the vacua except the trivial vacuum at the origin classically.<sup>†4</sup> Thus, the result of [40, 41] on the Witten index does not exclude the possibility that the mass deformed ABJM theory on  $S^3$  has the supersymmetry breaking phase in the large  $N$ .<sup>†5</sup> Here note that we do not take the large volume limit.

### 6.1.1 Criterion for SUSY breaking

By now, we have denoted the definition of a spontaneous SUSY breaking on  $S^3$ . Usually, a spontaneous supersymmetry breaking means that there are no states with zero energy of the theory. For  $S^3$ , we cannot define states with an appropriate Hamiltonian and time, thus we cannot apply this definition to our case. Instead of this definition for a spontaneously SUSY breaking, the spontaneous breaking of a symmetry  $\hat{Q}$  can be defined as  $\exists \mathcal{O}$  s.t.  $\langle 0 | [\hat{Q}, \hat{\mathcal{O}}] | 0 \rangle \neq 0$ . In the path-integral formalism, this corresponds to

$$Q \text{ is spontaneously broken} \stackrel{\text{def}}{\iff} \exists \mathcal{O} \text{ s.t. } \langle Q\mathcal{O} \rangle \neq 0, \quad (6.1.2)$$

where the condensation is the order parameter of the spontaneously symmetry breaking. Note that this definition is valid for the theory with enough number of non-compact space directions, in which the notion of vacuum is meaningful, otherwise,  $\langle Q\mathcal{O} \rangle$  corresponds to  $\text{Tr}[\hat{Q}, \hat{\mathcal{O}}]$ ,<sup>†6</sup> not to  $\langle 0 | [\hat{Q}, \mathcal{O}] | 0 \rangle$ . Because  $Q$  is a symmetry generator which behaves well, we expect that  $\langle Q\mathcal{O} \rangle = 0$  ( $\text{Tr}[Q, \mathcal{O}] = 0$ ) is trivial identity because of the invariance of path integral measure (cyclic invariance of  $\text{Tr}$ ).<sup>†7</sup> For example, for SUSY quantum mechanics case, the invariance of the Witten

<sup>†4</sup>We expect that the energy of the possible metastable SUSY breaking vacuum is proportional to  $\zeta$  and the free energy will be proportional to  $\zeta r_{S^3}$ . The extra contribution by the curvature induced mass term to the free energy for the fuzzy sphere solutions will also be proportional to  $\zeta r_{S^3}$  because the size of the fuzzy sphere grows as  $\zeta$  grows. Of course, this is not valid except the weak coupling limit and the phase of the theory can be non-trivial.

<sup>†5</sup>Here, we assume that the theory is regarded as a deformation of the ABJM theory on  $S^3$  for a small  $\zeta/k$  case. For an enough large  $\zeta/k$  case, we think that the curvature effect of  $S^3$  is almost negligible, but still remains. This picture will lead the SUSY breaking scenario explained here.

<sup>†6</sup>For the SUSY, it corresponds to  $\text{Tr}(-1)^{\hat{F}} \{ \hat{Q}, \hat{\mathcal{O}} \} = \text{Tr}(-1)^{\hat{F}} [\hat{Q}, \hat{\mathcal{O}}]$ .

<sup>†7</sup>In the case of  $Q = \text{SUSY}$ ,  $Q\mathcal{O}$  is such as  $F$ -term and  $D$ -term. Unfortunately, we cannot compute  $\langle F \rangle$  or  $\langle D \rangle$  by using the supersymmetry localization. We can compute  $\langle \int F \rangle$  and  $\langle \int D \rangle$ , but they are trivially zero. This is

index implies that  $\text{Tr}[(-1)^{\hat{F}}\hat{Q}, \hat{Q}^\dagger] \sim \text{Tr}(-1)^{\hat{F}}\hat{H} = 0$ . Thus, the definition of (6.1.2) is meaningful for the theory with some space with enough number of non-compact directions. In order to apply this definition to our case, we need to take the large volume limit or large- $N$  limit in which extra dimensions can effectively appear. When supersymmetry is spontaneously broken, there should exist a massless Goldstone fermion in the theory which makes the supersymmetric partition function  $Z$  vanished.

We take a large- $N$  limit and the SUSY breaking can be meaningful. Thus, we need a criterion of the SUSY breaking in the large- $N$  limit from a finite  $N$  result. For the theory in which the Witten index can be defined,  $Z = 0$  denotes the necessary condition for the SUSY breaking for the finite volume. For the other theories also, we expect that the massless Goldstone fermion makes  $Z = 0$ . Indeed, for a superconformal theory on  $S^3$ , the theory can break the SUSY if  $Z = 0$  because the radius of  $S^3$  is not physical. As an example of such theories is Chern-Simons matter theory and discussed in [58, 91–93]. For our case, the theory is not conformal, but we take the large- $N$  limit. Thus, we regard  $Z = 0$  as a criterion of the SUSY breaking.<sup>†8</sup> <sup>†9</sup> We emphasize that  $Z = 0$  does not always mean SUSY breaking as in the Witten index. However, for our case, interpreting  $Z = 0$  as SUSY breaking is the most natural possibility because the mass deformed ABJM theory on  $S^3$  will be smoothly connected to the pure SUSY CS theory in the large mass limit whose SUSY is broken for  $k \leq N$ .

In the following sections, we will see further supporting arguments for the SUSY breaking phase for the mass deformed ABJM theory on  $S^3$  using the S-dual representation of the matrix model. Here, we will summarize these arguments for the SUSY breaking shortly. The S-dual representation of the matrix model (for  $k = 1$ ) is obtained from the  $U(N)$  Yang-Mills theory with an adjoint and fundamental matter fields where  $\zeta_1$  and  $\zeta_2$  corresponds to the FI term and the mass for the adjoint matter in the S-dual representation, respectively. Because of the FI term and the mass term included at the same time, the supersymmetry will be broken spontaneously at the origin of the Coulomb branch which will be favored by the mass terms induced from the curvature of  $S^3$ . Moreover, for  $\zeta_1 = 0$ , we expect that because the FI term vanishes, the SUSY will not be broken. Indeed, for this case, as we seen, we constructed a large- $N$  solution for any value of  $\zeta_2$ , thus there was no critical mass for this case. This is consistent with the above picture.

---

consistent with the fact that there is no SUSY breaking for the theory on  $S^3$  with  $N$  finite.

<sup>†8</sup>In the gravity dual, the SUSY is gauged and the theory is described by supergravity. In supergravity, there are massless fermions, however, there are no zero modes around the SUSY vacuum which is an asymptotic  $AdS_4$  background. In a SUSY breaking vacuum, some fermions near the boundary have zero modes.

<sup>†9</sup>As an analogy to the case with bosonic zero modes, an appropriate analysis would be to add an explicit-SUSY-breaking deformation to kill the zero modes and see what happens in the limit of zero deformation. In this approach, however, we cannot use the result of the localization.



In order to investigate further, we will compute the partition function  $Z$  for finite  $N$  exactly and numerically using the Monte Carlo method for various points of  $(\zeta_1, \zeta_2)$ . With some finite values of  $N$ , we computed  $Z$  and the computed values of  $Z$  are consistent with the large- $N$  solutions for  $\zeta_1 = \zeta_2 < \frac{k}{4}$  and  $\zeta_1 = 0$  even though the employed values of  $N$  is not so large. These actual computations of  $Z$  for finite  $N$  show that as  $Z$  is a decreasing and oscillating function of  $\zeta_1$ , thus  $Z = 0$  is realized for some values of  $\zeta_i$ . We will associate this zero with the SUSY breaking in the large- $N$  limit. Furthermore, when we increase  $N$  with other parameters fixed, the smallest value of  $\zeta_i$  which gives  $Z = 0$  tends to decreasingly approach to the critical point of the large- $N$  solution. Therefore, the extrapolation of this to the large- $N$  limit is consistent with the SUSY breaking picture above at least within our calculation.

## 6.2 General deformation with $\zeta_1, \zeta_2 \neq 0$

In this section, we consider the case for  $\zeta_1, \zeta_2 \neq 0$ . Note that this may affect the sign of the partition function because the integrand of (4.3.13) for  $\zeta_1 \neq 0$  has the oscillation factor  $e^{\frac{2i\zeta_1}{k} \sum_i x_i}$  in contrast to the  $\zeta_1 = 0$  case, where the integrand was positive semi-definite. Therefore the partition function may be negative or zero depending on the parameters  $(N, k, \zeta_1, \zeta_2)$ . In this section, we will see that the zeroes appear also for finite  $(\zeta_1, \zeta_2)$ .

In this case, we could not find a solution to the saddle-point equation. The technique for small integers  $k, N$  in app. C.1.1 is not applicable either. Nevertheless, we can evaluate the partition function exactly for  $N = 1, 2$ , which suggest the partition function has zeroes as a function of  $\zeta_1, \zeta_2$  only for  $(N, k) = (2, 1), (2, 2)$ . We argue a possible interpretation for this zeroes. We further conjecture the zeroes for general  $k, N$ , and provide positive evidence from the numerical computation of the partition function for  $N \geq 3$ .

### 6.2.1 Exact expression for $N = 1, 2$

In this subsection, we review the exact results for  $N = 1, 2$  obtained in [104].<sup>†10</sup> The relation (C.1.3) between the partition function and  $\text{Tr} \widehat{\rho}^n$  is correct also for general  $\zeta_1$  if we take  $\widehat{\rho}$  as

$$\langle x | \widehat{\rho} | y \rangle = \frac{e^{\frac{2i\zeta_1}{k} x}}{2 \cosh \frac{x}{2}} \frac{1}{2k \cosh \frac{x-y+4\pi\zeta_2}{2k}}. \quad (6.2.1)$$

---

<sup>†10</sup>The notation in [104] is related to ours through the relation

$$Z_{\text{ours}}(N, k, \zeta_1, \zeta_2) = 2^{-2N} Z_{\text{Russo-Silva}}(N, k, m_1 = -4\pi\zeta_2/k, \zeta_2 = -4\pi\zeta_1/k).$$

For  $N = 1$ , the partition function is simply determined by  $Z(1, k, \zeta_1, \zeta_2) = \text{Tr } \hat{\rho}$ , which can be exactly obtained as

$$Z(1, k, \zeta_1, \zeta_2) = \int_{-\infty}^{\infty} \frac{dx}{2\pi} \frac{e^{\frac{2i\zeta_1 x}{k}}}{2 \cosh \frac{x}{2}} \frac{1}{2k \cosh \frac{2\pi\zeta_2}{k}} = \frac{1}{4k \cosh \frac{2\pi\zeta_1}{k} \cosh \frac{2\pi\zeta_2}{k}}. \quad (6.2.2)$$

For  $N = 2$ , we need to determine  $\text{Tr } \hat{\rho}^2$ , which is obtained by the following two dimensional integration

$$\text{Tr } \hat{\rho}^2 = \int_{-\infty}^{\infty} \frac{dx}{2\pi} \frac{dy}{2\pi} \frac{e^{\frac{2i\zeta_1(x+y)}{k}}}{16k^2 \cosh \frac{x}{2} \cosh \frac{y}{2} \cosh \frac{x-y+4\pi\zeta_2}{2k} \cosh \frac{x-y-4\pi\zeta_2}{2k}}. \quad (6.2.3)$$

By changing the integration variables  $x, y$  to  $x_{\pm} = x \pm y$ , we can do the  $x_+$ -integration and it leads to the following integration over  $x_-$

$$\text{Tr } \hat{\rho}^2 = \frac{1}{16\pi k^2 \sin \frac{4\pi\zeta_1}{k}} \int_{-\infty}^{\infty} dx_- \frac{\sin \frac{2\zeta_1 x_-}{k}}{\sin \frac{x_-}{2} \cosh \frac{x_-+4\pi\zeta_2}{2k} \cosh \frac{x_- - 4\pi\zeta_2}{2k}}. \quad (6.2.4)$$

For  $k \in \mathbb{Z}_+$ , this integral can be evaluated by an integral with the same integrand of which integral contour is set to a rectangular whose corners are  $x_- = (-\infty, \infty, \infty + 2\pi ik, -\infty + 2\pi ik)$  [103, 104], and we obtain

$$\text{Tr } \hat{\rho}^2 = \frac{1}{8k^2 \sinh \frac{4\pi\zeta_1}{k} \cosh^2 \frac{2\pi\zeta_2}{k} (1 - (-1)^k \cosh 4\pi\zeta_1)} \left[ \sum_{n=1}^{k-1} \frac{(-1)^n \sin^2 \frac{\pi n}{k} \sinh \frac{4\pi\zeta_1 n}{k}}{\cosh \frac{2\pi\zeta_2 + i\pi n}{k} \cosh \frac{2\pi\zeta_2 - i\pi n}{k}} + R_k \right], \quad (6.2.5)$$

where

$$R_k = \begin{cases} (-1)^{\frac{k-1}{2}} \frac{k \coth \frac{2\pi\zeta_2}{k} \cosh \frac{2\pi\zeta_1}{k}}{\cosh 2\pi\zeta_2} \sin \frac{8\pi\zeta_1\zeta_2}{k} & \text{for odd } k \\ (-1)^{\frac{k}{2}+1} \frac{k \coth \frac{2\pi\zeta_2}{k} \sinh \frac{2\pi\zeta_1}{k}}{\sinh 2\pi\zeta_2} \cos \frac{8\pi\zeta_1\zeta_2}{k} & \text{for even } k \end{cases}. \quad (6.2.6)$$

For example, the final results for  $k = 1, 2, 3, 4$  are explicitly determined as

$$\begin{aligned} Z(2, 1, \zeta_1, \zeta_2) &= \frac{\sin 8\pi\zeta_1\zeta_2}{8 \sinh 4\pi\zeta_1 \sinh 4\pi\zeta_2 \cosh 2\pi\zeta_1 \cosh 2\pi\zeta_2}, \\ Z(2, 2, \zeta_1, \zeta_2) &= \frac{\sin^2 2\pi\zeta_1\zeta_2}{8 \sinh^2 2\pi\zeta_1 \sinh^2 2\pi\zeta_2}, \\ Z(2, 3, \zeta_1, \zeta_2) &= \frac{1}{24(\cosh \frac{4\pi\zeta_1}{3} + \cosh \frac{8\pi\zeta_1}{3})(\cosh \frac{4\pi\zeta_2}{3} + \cosh \frac{8\pi\zeta_2}{3})} \left( 2 - \frac{\sin \frac{8\pi\zeta_1\zeta_2}{3}}{\sinh \frac{2\pi\zeta_1}{3} \sinh \frac{2\pi\zeta_2}{3}} \right), \\ Z(2, 4, \zeta_1, \zeta_2) &= \frac{1}{128 \sinh^2 \pi\zeta_1 \sinh^2 \pi\zeta_2} \left( 1 - \frac{1}{\cosh \pi\zeta_1} - \frac{1}{\cosh \pi\zeta_2} + \frac{\cos 2\pi\zeta_1\zeta_2}{\cosh \pi\zeta_1 \cosh \pi\zeta_2} \right). \end{aligned} \quad (6.2.7)$$

We easily see from these results that the partition function for  $(N, k) = (2, 1), (2, 2)$  has zeroes at finite  $(\zeta_1/k, \zeta_2/k)$ .

Remembering the results in Part II, the partition function in the infinite mass limit can be interpreted as the massive free part and the superconformal part. Here, we would like to investigate the infinite mass limit of the above partition function. First, we focus on the case for  $(N, k) = (2, 3)$ . In the infinite mass limit in which  $\zeta_1, \zeta_2 \rightarrow \infty$ , the leading part of the partition function is evaluated as

$$Z(2, 3, \zeta_1, \zeta_2) = \frac{1}{3(M_1 M_2)^{\frac{4}{3}}} + \mathcal{O}\left(\frac{1}{(M_1 M_2)^{\frac{4}{3}}}\right), \quad (6.2.8)$$

where we have defined

$$M_1 = e^{2\pi\zeta_1}, \quad M_2 = e^{2\pi\zeta_2}. \quad (6.2.9)$$

This result implies that the origin of the Coulomb branch dominantly contributes to the partition function because this result is the same as the partition function in which the massive multiplets simply decouple from the theory

$$\begin{aligned} Z_{\text{decoupled}} &= \\ &= \frac{1}{2^4 \cosh^4\left(\frac{2\pi\zeta_1}{3}\right) 2^4 \cosh^4\left(\frac{2\pi\zeta_2}{3}\right)} \int \frac{d\lambda^2}{2!} \int \frac{d\tilde{\lambda}^2}{2!} e^{3\pi i(\lambda^2 - \tilde{\lambda}^2)} \prod_{i>j}^2 4 \sinh^2 \pi (\lambda_i - \lambda_j) \prod_{i>j}^2 4 \sinh^2 \pi (\tilde{\lambda}_i - \tilde{\lambda}_j) \\ &\sim \frac{1}{3} \frac{1}{(M_1 M_2)^{\frac{4}{3}}}, \end{aligned} \quad (6.2.10)$$

where we have employed the formula (5.1.10). The same thing happens to the case for  $(N, k) = (2, 4)$ . However, it does not in the case for  $(N, k) = (2, 2)$  and  $(2, 1)$ . This may be because the theory is in a supersymmetry breaking phase for these case as we reviewed. The result cannot be obtained simply assuming that the dominant point of the Coulomb branch is the origin. Then, we expect that the dominant point of the Coulomb branch will be the confinement solution through the analysis here is for finite  $N$  and the confinement solution includes the imaginary part.

### 6.2.2 $N \geq 3$ from Monte Carlo Simulation

In this subsection, through numerical analysis, we would like to provide evidence that the partition function has zeroes at finite  $(\zeta_1/k, \zeta_2/k)$  also for  $N \geq 3$ . For this purpose, we apply (Markov chain) Monte Carlo method to the  $S$ -dual representation of the partition function (4.3.13):

$$Z(k, N, \zeta_1, \zeta_2) = \frac{1}{N!} \int \frac{d^N x}{(2\pi k)^N} e^{-S(k, N, \zeta_1, \zeta_2; x)}, \quad (6.2.11)$$

where

$$\begin{aligned}
S(k, N, \zeta_1, \zeta_2; x) &= - \sum_{i < j}^N \log \left( 2 \sinh \frac{x_i - x_j}{2k} \right)^2 + \sum_{i, j=1}^N \log \left( 2 \cosh \frac{x_i - x_j + 4\pi\zeta_2}{2k} \right) \\
&+ \sum_{i=1}^N \log \left( 2 \cosh \frac{x_i}{2} \right) - \log \cos \left( \frac{2\zeta_1}{k} \sum_{i=1}^N x_i \right). \tag{6.2.12}
\end{aligned}$$

## Algorithm

First, we shall explain our algorithm. There are two subtleties when we apply the Monte Carlo method to our problem. The first subtlety, which will not be problematic as explained below, is that Monte Carlo simulation can calculate only “expectation values” or equivalently ratio of two functions rather than  $Z$  itself. The second one is that the Boltzmann weight  $e^{-S}$  is not positive semi-definite for  $\zeta_1 \neq 0$  and hence cannot be regarded as a probability.

We treat these subtleties as follows. We consider the ratio, rather than  $Z$  itself

$$Z_{\text{MC}}(N, k, \zeta_1, \zeta_2) = \frac{Z(N, k, \zeta_1, \zeta_2)}{Z(N, k, 0, \zeta_2)} = \left\langle \cos \left( \frac{2\zeta_1}{k} \sum_{i=1}^N x_i \right) \right\rangle_{\zeta_1=0}, \tag{6.2.13}$$

where  $\langle \mathcal{O}(x) \rangle_{\zeta_1=0}$  represents the expectation value of  $\mathcal{O}(x)$  under the action  $S(N, k, \zeta_1 = 0, \zeta_2)$ . Then, we evaluate the ratio<sup>†11</sup> by Hybrid Monte Carlo simulation<sup>†12</sup> by taking samples generated with the probability  $\sim e^{-S}|_{\zeta_1=0}$ . We note that to study the ratio is sufficient for our purpose since  $Z(N, k, 0, \zeta_2)$  is real positive and we are interested only in the sign of the partition function.<sup>†13</sup> Since we take samples of the oscillating function, whose frequency of the oscillation is determined by  $\zeta_1/k$ , in general, more statistics are required for larger  $\zeta_1/k$  to obtain precise approximations. The reason why we employ the  $S$ -dual representation (4.3.13) is that it has much milder oscillation than the original matrix model (4.1.5) as in [105].

## Results

Then, we would like to show numerical results for the ratio  $Z_{\text{MC}}$  (6.2.13), which has the same sign as the partition function  $Z(N, k, \zeta_1, \zeta_2)$  itself. Fig. 6.1 plots  $Z_{\text{MC}}$  for  $(N, k, \zeta_2) = (4, 1, 1)$

<sup>†11</sup>This is the so-called reweighting method.

<sup>†12</sup>The application to a similar system is explained in app. A of [105].

<sup>†13</sup>Of course we can also compute  $Z(N, k, \zeta_1, \zeta_2)$  itself by combining  $Z_{\text{MC}}(N, k, \zeta_1, \zeta_2)$  with  $Z(N, k, 0, \zeta_2)$  computed in another way. For example, we know the exact values of  $Z(N, k, 0, \zeta_2)$  for various  $(N, k, \zeta_2)$  obtained in sec. (C.1.1) and Monte Carlo simulation of  $Z(N, k, 0, \zeta_2)$  is much easier than the  $\zeta_1 \neq 0$  case if we use the algorithm in [105].

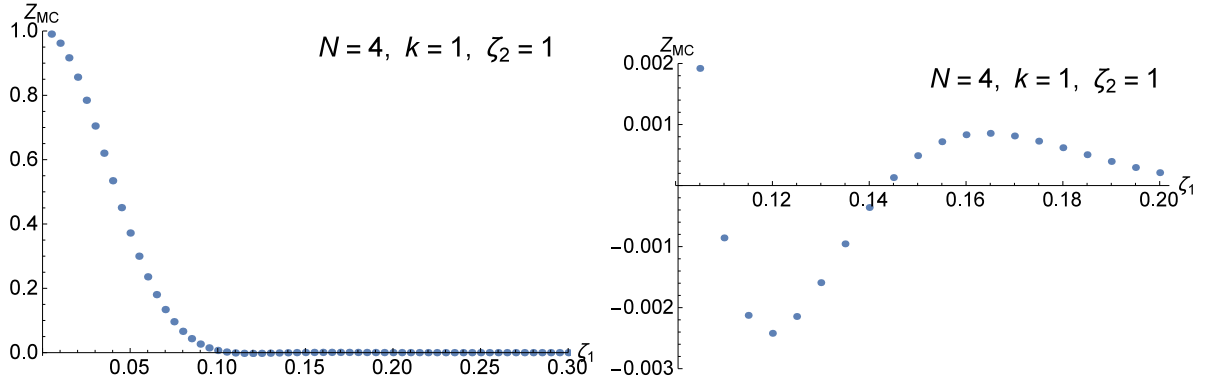


Figure 6.1: The ratio (6.2.13) computed by Monte Carlo simulation is plotted against  $\zeta_1$  for  $(N, k, \zeta_2) = (4, 1, 1)$ . The right panel is the zoom-up of the left panel around the negative peak of the partition function. (These figures are cited from our paper [3])

as a function of  $\zeta_1$ . In these results, the statistical errors are estimated by Jackknife method although they are practically almost invisible in the figures. The right figure of fig. 6.1 is the zoomup of the left figure in the range  $\zeta_1 \in [0.1, 0.2]$ . From the right figure, we can find that the partition function takes negative values when  $\zeta_1 = 0.110, 0.115, \dots, 1.14$  even if we take into account the errors. Therefore, we claim that there is a zero of the partition function and the zero are located at  $0.105 < \zeta_1 < 0.110$ .

We also have found similar results for other values of  $(N, k, \zeta_2)$  whose plots are shown in fig. 6.2. These figures show that the partition function also has the zeroes at finite  $\zeta_1/k$  for various  $(N, k, \zeta_2)$ . We note that we sometimes encounter subtle cases. For example, in the case of  $(N, k, \zeta_2) = (4, 2, 1)$  shown in the right-bottom of fig. 6.2, the minimum is consistent with both positive and negative  $Z$  within the numerical errors.<sup>†14</sup> It can be expected that this type of behavior will appear when the partition function is positive semidefinite but has zeroes as in the case of  $(N, k) = (2, 2)$  of which analytic result is given in the second line of (6.2.7). For this kind of cases, any numerical simulation with nonzero errors cannot lead to the existence of zeroes because numerical values at the zeroes must be consistent with all the possible signs of  $Z$  within errors. Therefore, for this type of cases, all things we can do by numerical simulation are to confirm that points consistent with  $Z = 0$  exist. For all values of  $(N \geq 2, k, \zeta_2)$  which we have analyzed, we have confirmed that there exists at least one value of  $\zeta_1$  consistent with the zeroes of  $Z$  within errors. For the cases for which we have conformed existence of first zeroes of  $Z$ , bounds on the zeroes are shown in tables 6.1, 6.2 and 6.3 for fixed  $(k, \zeta_2)$  (see also tab. 6.4 for  $Z_{MC}$  at the first negative peaks and their errors). We also estimate their locations

<sup>†14</sup>Similar behaviors have been observed for  $(N, k, \zeta_2) = (3, 1, 1), (4, 2, 2), (5, 2, 1), (5, 2, 2)$ .

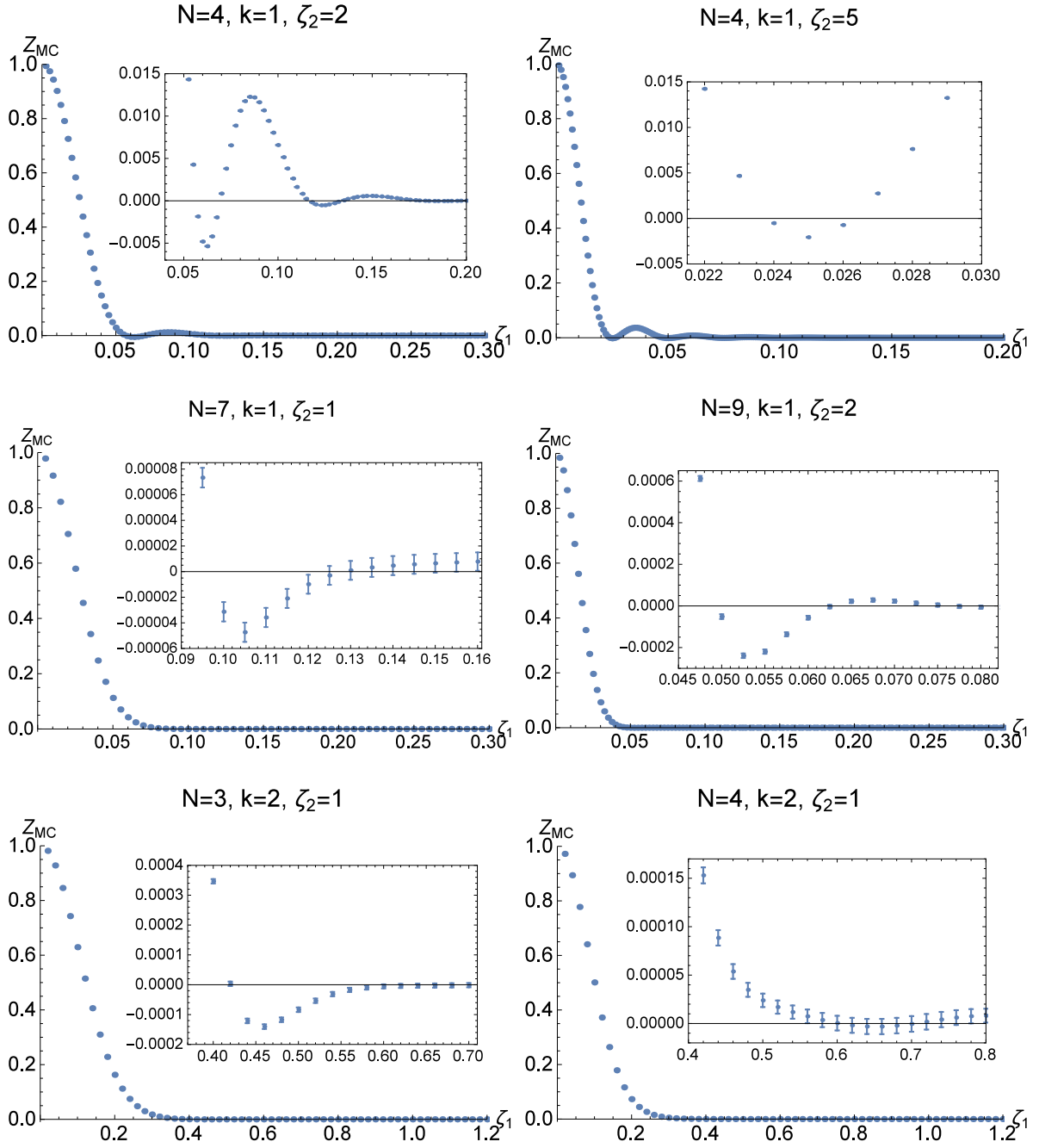


Figure 6.2: The numerical plots of  $Z_{MC}$  as functions of  $\zeta_1$  for various  $(N, k, \zeta_2)$  with their zoomups around the minima. (These figures cited from our paper [3]. )

$N$	Bounds on the zeroes	Estimate of the zeroes
2	$\zeta_1 = 0.125$	$\zeta_1 = 0.125$
4	$0.105 < \zeta_1 < 0.11$	$\zeta_1 = 0.108084 \pm 0.000016$
5	$0.105 < \zeta_1 < 0.11$	$\zeta_1 = 0.105249 \pm 0.000041$
7	$0.095 < \zeta_1 < 0.1$	$\zeta_1 = 0.0975822_{-0.0003715}^{+0.0004201}$
9	$0.085 < \zeta_1 < 0.095$	$\zeta_1 = 0.0898839_{-0.0004039}^{+0.0003752}$

Table 6.1: Bounds on first zeroes of the partition function and estimate of their precise locations by interpolating functions for  $(k, \zeta_2) = (1, 1)$ . The value for  $N = 2$  is the exact value.

$N$	Bounds on the zeroes	Estimate of the zeroes
2	$\zeta_1 = 0.0625$	$\zeta_1 = 0.0625$
4	$0.055 < \zeta_1 < 0.0575$	$\zeta_1 = 0.0565766 \pm 0.0000060$
5	$0.0525 < \zeta_1 < 0.055$	$\zeta_1 = 0.0543974 \pm 0.0000068$
7	$0.05 < \zeta_1 < 0.0525$	$\zeta_1 = 0.0518753_{-0.0000320}^{+0.0000324}$
9	$0.0475 < \zeta_1 < 0.05$	$\zeta_1 = 0.0496673_{-0.0000677}^{+0.0000700}$

Table 6.2: Bounds and estimate of first zeroes of the partition function for  $(k, \zeta_2) = (1, 2)$ .

by constructing<sup>†15</sup> interpolating functions of all the data points of  $Z_{MC}$  for fixed  $(N, k, \zeta_2)$  and finding zeroes of the interpolating functions. Then, we will discuss implications of these values in sec. 6.2.4.

### 6.2.3 Physical origins of the zeroes from Fermi gas formalism

In this subsection, we discuss the physical origins of the zeroes of the partition function. By applying Fermi gas formalism, we attempt to investigate which effects trigger the zeros of  $Z$ . We emphasize that some techniques in the Fermi gas formalism are not available for  $\zeta_1 \neq 0$  because the Hamiltonian is not Hermitian. However, there exists a technique which is still available, which is a formal  $\hbar$ -expansion of  $\text{Tr}\widehat{\rho}^n$  through Wigner transformation where  $\text{Tr}\widehat{\rho}^n$  is described as a phase-space integration of a function whose explicit form can be determined by acting differential operators on  $\rho(q, p)$ . In this technique, the problem is reduced to the computation of a perturbative series of the explicit two-dimensional integral with respect to  $\hbar$

---

<sup>†15</sup>This can be done by the command “Interpolation” in Mathematica. The values without “ $\pm$ ” are first zeroes of the interpolating functions for the average values of  $Z_{MC}$ . The values including “ $\pm$ ” describe zeroes of interpolating functions for the average values plus/minus the errors.

$N$	Bounds on the zeroes	Estimate of the zeroes
2	$\zeta_1 = 0.025$	$\zeta_1 = 0.025$
4	$0.0023 < \zeta_1 < 0.024$	$\zeta_1 = 0.0238516 \pm 0.0000102$
5	$0.023 < \zeta_1 < 0.024$	$\zeta_1 = 0.023177 \pm 0.000007$
7	$0.022 < \zeta_1 < 0.023$	$\zeta_1 = 0.022638^{+0.000042}_{-0.000039}$
9	$0.021 < \zeta_1 < 0.023$	$\zeta_1 = 0.0218204^{+0.0000247}_{-0.0000241}$

Table 6.3: Bounds and estimate of first zeroes of  $Z$  for  $(k, \zeta_2) = (1, 5)$ .

$N$	$\zeta_2$	$\zeta_1$	$Z_{\text{MC}}$	Errors
4	1	0.12	-0.00242055	$7.70257 \times 10^{-6}$
	2	0.0625	-0.00536328	0.0000115859
	5	0.025	-0.00206855	0.000035207
5	1	0.115	-0.000807839	$7.76448 \times 10^{-6}$
	2	0.06	-0.00579732	0.0000125459
	5	0.025	-0.00481262	0.000036708
7	1	0.105	-0.0000473376	$7.52208 \times 10^{-6}$
	2	0.055	-0.000501799	0.0000102382
	5	0.035	-0.00411775	0.000018267
9	1	0.1	-0.0000167033	$2.0722 \times 10^{-6}$
	2	0.0525	-0.000239292	0.0000109368
	5	0.035	-0.00176051	0.0000142852

Table 6.4:  $Z_{\text{MC}}$  at the first negative peaks and their statistical errors for various  $(N, \zeta_2)$  with  $k = 1$ .

with no relation to the hermiticity of the Hamiltonian. This analysis has been already done in [77] for imaginary  $(\zeta_1, \zeta_2)$  in the context of the R-charge deformation and then, we can apply the results to our case simply by taking analytic continuation in [77] assuming the parameter  $\zeta_1$  and  $\zeta_2$  are sufficiently small for the singular behavior not to appear.<sup>†16</sup> First, we compute  $\text{Tr} \widehat{\rho}^n$  approximated in this way and then, we can obtain the grand potential  $J(\mu)$  by the following Mellin-Barnes expression

$$J(\mu) = - \int_{\epsilon - i\infty}^{\epsilon + i\infty} \frac{dt}{2\pi i} \Gamma(t) \Gamma(-t) \mathcal{Z}(t) e^{t\mu} \quad (0 < \epsilon < 1), \quad (6.2.14)$$

<sup>†16</sup>This analysis was done in sec. 4 of [77]. The result in our notation can be obtained by taking  $p \rightarrow 1$ ,  $q \rightarrow 1$ ,  $\xi \rightarrow \frac{4i}{k} \zeta_1$  and  $\eta \rightarrow \frac{4i}{k} \zeta_2$ .



where  $\mathcal{Z}(t) = \text{Tr} \widehat{\rho}^t$  and the canonical partition function determined by  $J(\mu)$  as

$$Z(N) = \int d\mu e^{J(\mu) - \mu N}. \quad (6.2.15)$$

The  $\hbar$ -expansion of  $\mathcal{Z}(n)$  takes the form

$$\mathcal{Z}(n) = \sum_{s=0}^{\infty} \hbar^{2s-1} \mathcal{Z}_{2s}(n) + \mathcal{O}(e^{-\frac{n}{\hbar}}) \quad (6.2.16)$$

where the second term denotes non-perturbative effects of the  $\hbar$ -expansion which we are ignoring. The large- $N$  behavior of  $Z(N)$  can be derived by the large- $\mu$  expansion of  $J(\mu)$ , which are determined as follows:

$$J(\mu) = J^{\text{pert}}(\mu) + \mathcal{O}\left(e^{-\frac{2\mu}{1 \pm 4i\zeta_1/k}}, e^{-\frac{2\mu}{1 \pm 4i\zeta_2/k}}, e^{-\mu}\right) + \mathcal{O}\left(e^{-\frac{n}{\hbar}\mu}\right), \quad (6.2.17)$$

where we define

$$J_{\text{pert}}(\mu) = \frac{C(\zeta_1, \zeta_2, k)}{3} \mu^3 + B(\zeta_1, \zeta_2, k) \mu + A(\zeta_1, \zeta_2, k). \quad (6.2.18)$$

We would like to make several comments. First, the  $\hbar$ -expansions for the coefficients  $C$  and  $B$  are terminated at leading and sub-leading orders respectively:

$$\begin{aligned} C &= \frac{2}{\pi^2 k (1 + 16\zeta_1^2/k^2) (1 + 16\zeta_2^2/k^2)}, \\ B &= \frac{\pi^2 C}{3} - \frac{1}{6k} \left( \frac{1}{1 + 16\zeta_1^2/k^2} + \frac{1}{1 + 16\zeta_2^2/k^2} \right) + \frac{k}{24}. \end{aligned} \quad (6.2.19)$$

The coefficient  $A$  are corrected by all order contributions and it has been conjectured in [77] that the exact answer for  $A$  is determined by

$$A = \frac{1}{4} \left[ A_{\text{ABJM}}(k + 4i\zeta_1) + A_{\text{ABJM}}(k - 4i\zeta_1) + A_{\text{ABJM}}(k + 4i\zeta_2) + A_{\text{ABJM}}(k - 4i\zeta_2) \right], \quad (6.2.20)$$

where [99, 105]

$$A_{\text{ABJM}}(k) = \frac{2\zeta(3)}{\pi^2 k} \left( 1 - \frac{k^3}{16} \right) + \frac{k^2}{\pi^2} \int_0^\infty dx \frac{x}{e^{kx} - 1} \log(1 - e^{-2x}). \quad (6.2.21)$$

If the approximation by  $J_{\text{pert}}(\mu)$  is valid, then the canonical partition function is approximated as follows:

$$Z \simeq Z_{\text{pert}}, \quad Z_{\text{pert}} = \int d\mu e^{J_{\text{pert}}(\mu) - \mu N} = e^A C^{-\frac{1}{3}} \text{Ai} \left[ C^{-\frac{1}{3}} (N - B) \right]. \quad (6.2.22)$$

Then, we can evaluate the large  $N$  limit of  $Z(N)$  and it exhibits  $N^{\frac{3}{2}}$  behavior as <sup>†17</sup>

$$-\log Z = \frac{2}{3}C^{-1/2}N^{3/2} + \mathcal{O}(N^{1/2}) = \frac{\pi\sqrt{2k}}{3} \sqrt{\left(1 + \frac{16\zeta_1^2}{k^2}\right) \left(1 + \frac{16\zeta_2^2}{k^2}\right)} N^{3/2} + \mathcal{O}(N^{1/2}), \quad (6.2.23)$$

which agrees with (4.3.29) for  $\zeta_1 = 0$  and the result of [2] for  $\zeta_1 = \zeta_2 = \zeta$ .

The second term in (6.2.17) is non-perturbative corrections of the large- $\mu$  expansion whose exponents can be explicitly derived by the  $\hbar$ -expansion (6.2.16). These corrections for the massless case have been interpreted as membrane instanton effects whose type IIA picture is D2-branes wrapping (warped)  $\mathbb{RP}^3$  in  $AdS_4 \times \mathbb{CP}^3$  [106]. The third term in (6.2.17) denotes the non-perturbative correction of the  $\hbar$ -expansion in (6.2.16). However, their exponents cannot be determined by the above arguments. In [77], it has been conjectured that the exponent for imaginary  $(\zeta_1, \zeta_2)$  is given by

$$\mathcal{O}\left(e^{-\frac{4\mu}{k(1\pm 4i\zeta_1/k)(1\pm 4i\zeta_2/k)}}\right) \quad (\text{double signs correspond}). \quad (6.2.24)$$

These corrections for the massless case have been identified with worldsheet instanton effects arising from fundamental strings wrapping  $\mathbb{CP}^1$  [107].

Assuming approximation by the perturbative part  $J_{\text{pert}}(\mu)$  in the large- $\mu$  expansion (6.2.18) is valid, or equivalently the canonical partition function is well approximated by (6.2.22), The second term in (6.2.18) is always exponentially suppressed for any  $(\zeta_1, \zeta_2)$  and therefore we can ignore the second term in the large- $N$  limit. As we find in what follows, the third term which arises from non-perturbative effects of the  $\hbar$ -expansion can break the perturbation. We assume that the exponent of the third term for real  $(\zeta_1, \zeta_2)$  should be the same as the naive analytic continuation of the one for imaginary  $(\zeta_1, \zeta_2)$  in the domain on which the partition function is holomorphic with respect to  $(\zeta_1, \zeta_2)$ . Then, we have the following correction in (6.2.18) for real  $(\zeta_1, \zeta_2)$ :

$$\mathcal{O}\left(e^{-\frac{4\mu}{k(1\pm 4i\zeta_1/k)(1\pm 4i\zeta_2/k)}}\right) = \mathcal{O}\left(e^{-\frac{4\mu}{k(1+16\zeta_1^2/k^2)(1+16\zeta_2^2/k^2)} \left[1 - \frac{16\zeta_1\zeta_2}{k^2} \mp \frac{4i(\zeta_1+\zeta_2)}{k}\right]}\right), \quad (6.2.25)$$

where the double signs are in the same order. This implies that this correction is no longer exponentially suppressed for

$$\frac{\zeta_1\zeta_2}{k^2} \geq \frac{1}{16}, \quad (6.2.26)$$

and the estimation of the grand potential  $J(\mu)$  by  $J_{\text{pert}}(\mu)$  is not valid in this region. This also implies that the holomorphy of the partition function with respect to  $(\zeta_1, \zeta_2)$  is no longer

---

<sup>†17</sup>In the large- $N$  limit, the  $\mu$ -integral is dominated by  $\mu = \sqrt{\frac{N-B}{C}}$ . Therefore, the non-perturbative effects in (6.2.17) contribute to  $Z$  like  $\sim \mathcal{O}(e^{-\sqrt{kN}})$ ,  $\mathcal{O}(e^{-\sqrt{N/k}})$ .

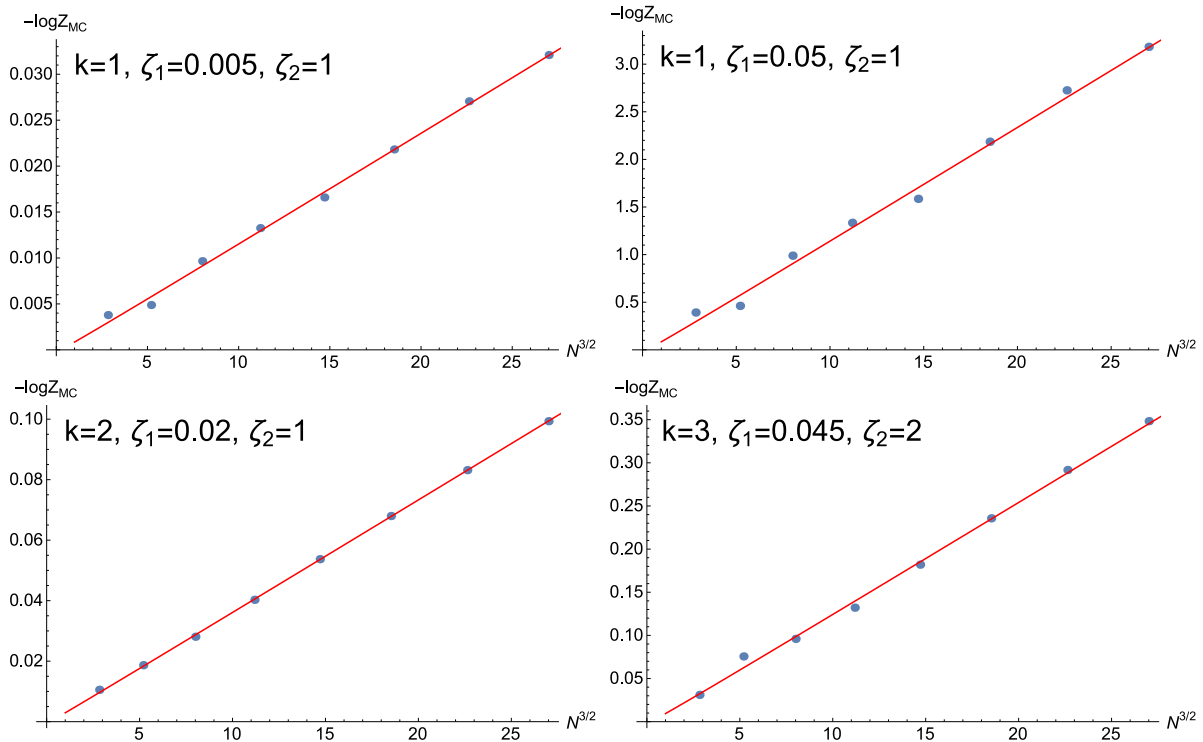


Figure 6.3: The quantity  $-\log Z_{\text{MC}}$  with  $Z_{\text{MC}}(N, k, \zeta_1, \zeta_2) = \frac{Z(N, k, \zeta_1, \zeta_2)}{Z(N, k, 0, \zeta_2)}$  is plotted against  $N^{3/2}$  for  $\frac{\zeta_1 \zeta_2}{k^2} < \frac{1}{16}$ . The symbols are the numerical results obtained by the Monte Carlo simulation. The red line denotes the result computed by the Airy function formula (6.2.22), namely  $-\log \frac{Z_{\text{pert}}(N, k, \zeta_1, \zeta_2)}{Z_{\text{pert}}(N, k, 0, \zeta_2)}$ . (These figures are cited from our paper [3].)

valid in the region (6.2.26) at least in the large- $N$  limit. If we take the large- $N$  limit first, in the domain  $\frac{\zeta_1 \zeta_2}{k^2} \geq \frac{1}{16}$  the free energy is very likely different from (6.2.23) obtained by analytic continuation to real  $(\zeta_1, \zeta_2)$ .

We emphasize that the above estimate is consistent with our numerical results obtained in sec. 6.2.2. In fig. 6.3, we compare the ratio  $Z_{\text{MC}}(N, k, \zeta_1, \zeta_2) = \frac{Z(N, k, \zeta_1, \zeta_2)}{Z(N, k, 0, \zeta_2)}$  obtained numerically with the one computed by the approximation (6.2.22) for some cases where we expect (6.2.22) to be good approximation. From the plots, we can see that our numerical results are nicely approximated with the Airy function formula (6.2.22) and exhibit the  $N^{3/2}$ -law. Here, we explicitly present only the four cases, but we have observed similar results for various other values of  $(k, \zeta_1, \zeta_2)$  satisfying  $\frac{\zeta_1 \zeta_2}{k^2} < \frac{1}{16}$ . Figure 6.4 describes similar plots for  $\frac{\zeta_1 \zeta_2}{k^2} \geq \frac{1}{16}$  where (6.2.22) is expected not to be valid due to the correction (6.2.25). We also emphasize that in contrast to fig. 6.3, it can be seen that the numerical results do not agree with (6.2.22) and no longer exhibit the  $N^{3/2}$ -law. We have also found similar behaviors for various other values of  $(k, \zeta_1, \zeta_2)$  with  $\frac{\zeta_1 \zeta_2}{k^2} \geq \frac{1}{16}$ . Thus, our numerical results support our expectation that the

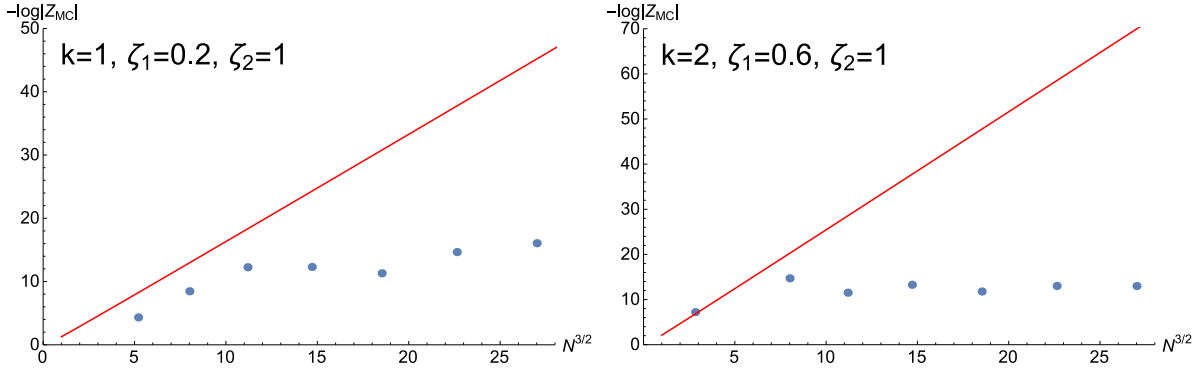


Figure 6.4: Similar plots to fig. 6.3 for  $\frac{\zeta_1\zeta_2}{k^2} \geq \frac{1}{16}$ . (These figures are cited from our paper [3])

approximation by (6.2.22) is valid for  $\frac{\zeta_1\zeta_2}{k^2} < \frac{1}{16}$  and a different phase can be realized outside of the region.

## 6.2.4 Conjecture on phase structure in the large- $N$ limit

Here, we discuss the phase structure of the mass deformed ABJM theory in the large- $N$  limit. We shall recall the results obtained so far by the various methods:

- In the case of  $\zeta_1 = \zeta_2 = \zeta$ , the partition function in the representation (4.1.5) has been analyzed by the saddle-point method in Section 2 of Part II as reviewed in sec. 6.1. The saddle-point configuration exhibits the  $\mathcal{O}(N^{3/2})$  behavior of the free energy and becomes singular at  $\zeta/k = 1/4$ .
- In sec. 4.3.1, we constructed the saddle-point solution for  $\zeta_1 = 0$  in the  $S$ -dual representation, which gives the  $\mathcal{O}(N^{3/2})$  free energy (4.3.29). This behavior is consistent with the exact results for finite  $N$  obtained in sec. C.1.1. We note that we can obtain the result for  $\zeta_1 \neq 0, \zeta_2 = 0$  by the replacement  $\zeta_2 \rightarrow \zeta_1$  in (4.3.29) since the partition function is symmetric under  $\zeta_1 \leftrightarrow \zeta_2$ .
- In sec. 6.2.1, we showed the exact results for  $N = 1, 2$  and arbitrary  $(k, \zeta_1, \zeta_2)$  obtained in [104]. we saw that the partition function for  $N = 2$  has the zeroes at finite  $(\zeta_1, \zeta_2)$  while the one for  $N = 1$  does not.
- In sec. 6.2.2, we have performed the Monte Carlo simulation for higher  $N$ . The numerical result showed that the partition function has zeroes at finite  $(\zeta_1, \zeta_2)$  given  $(N, k)$ . The bounds and estimates on the zeroes given in tables 6.1, 6.2 and 6.3. These results have

implied that the first zeroes do not increase by  $N$ . It is reasonable to expect that the partition function becomes zero at some finite  $(\zeta_1, \zeta_2)$  also in the large- $N$  limit.

- In sec. 6.2.3, we have argued when one can trust the approximation in terms of the perturbative grand potential (6.2.18) in the Fermi gas formalism, which gives the  $\mathcal{O}(N^{3/2})$  free energy in the large- $N$  limit. We have found that the approximation is reliable for  $\frac{\zeta_1 \zeta_2}{k^2} < \frac{1}{16}$  while in the other regime  $\frac{\zeta_1 \zeta_2}{k^2} \geq \frac{1}{16}$ , the expected non-perturbative effects (6.2.25) of the  $\hbar$ -expansion are no longer exponentially suppressed. We emphasize that for  $\zeta_1 = \zeta_2 = \zeta$ , the approximation becomes invalid at  $\zeta/k = 1/4$ . The same condition has appeared as that introduced in the previous section.

Considering the above results, we propose the following scenario

- For small  $(\zeta_1, \zeta_2)$ , the large- $N$  free energy exhibits the  $N^{3/2}$  behavior whose explicit expression is given by (6.2.23). We expect that this formula is valid for  $\frac{\zeta_1 \zeta_2}{k^2} < \frac{1}{16}$ , and becomes invalid for  $\frac{\zeta_1 \zeta_2}{k^2} \geq \frac{1}{16}$ .
- The partition function vanishes at some finite values of  $(\zeta_1, \zeta_2)$ . We expect that this occurs at the boundary of the validity of (6.2.23):  $\frac{\zeta_1 \zeta_2}{k^2} = \frac{1}{16}$ . We interpret this as the SUSY breaking at this point.

Our results strongly support the first point by the saddle-point analysis for  $\zeta_1 = \zeta_2$  in [2] and Fermi gas analysis in sec. 6.2.3. Then, we attempt to provide further evidence for the second point. Tables 6.1, 6.2 and 6.3 show that locations of the first zero decrease slowly as  $N$  increases. Therefore, it is plausible that the first zeroes in the large- $N$  limit are at some finite values of  $(\zeta_1, \zeta_2)$ . However, it would be nontrivial whether or not the first zero in the large- $N$  limit coincides with our expected bound  $\frac{\zeta_1 \zeta_2}{k^2} = \frac{1}{16}$ . Thus, we performed consistency checks of this through fitting analysis of our numerical data in [3].

Moreover, the correlation between the supersymmetry breaking and the singularity in the saddle-point approximation was argued for the pure Chern-Simons theory [92, 108]. Hence it would be more than just a minimal scenario for our theory to relate the singularity in the saddle-point approximation with the supersymmetry breaking. It would be interesting to test this conjecture by studying the partition function for larger  $N$  in future.

## 6.3 Discussion

In this chapter, we have interpreted the singular behavior of the mass deformed ABJM theory on the three-sphere at the finite value of the mass. Based on the argument in sec. 6.1, we expect

that this theory exhibits spontaneous supersymmetry breaking in large- $N$  limit at  $\zeta_1 = \zeta_2 = k/4$ . To gain evidence for this conjecture we have analyzed the partition function of the mass deformed ABJM theory for finite  $k$  and  $N$  by using the Monte Carlo simulation. As a result, we have found that the partition function vanishes at some finite values of  $\zeta_1, \zeta_2$ . The numerical results also indicate that the zeroes exist for general  $N$ , and that the locus of the first zero stays finite as  $N$  increases. These observations are consistent with the expectation at the end of sec. 6.1 from the large- $N$  supersymmetry breaking. We also found a saddle-point solution for a new slice  $\zeta_1 = 0$  by using the S-dual representation of the matrix model. In contrast to the situation for  $\zeta_1 = \zeta_2$  this solution exists for an arbitrary value of  $\zeta_2$ . This is again consistent with our argument in sec. 6.1 where the supersymmetry breaking does not occur in this case. Our result would shed new light to the phase structure of the mass deformed ABJM theory in the M-theory limit, which was unclear in the previous works [1, 2].

Another direction is to improve the algorithm of the numerical simulation. In this paper, we have treated the oscillation factor of (4.3.13) in the quite naive way where we just regard the factor as the observable in the system with  $\zeta_1 = 0$ . In this approach, we need much more statistics than simulations without oscillating factors so that the simulation at large- $N$  becomes harder. It is nice if one can find a more appropriate algorithm such as complex Langevin method and Lefschetz thimble.

# Chapter 7

## Conclusion and Future directions

In this thesis, we have summarized our successive works [2–5], in which we have mainly studied the partition function in the large  $N$  or the infinite mass limit employing the localization methods. We have found that the partition function exhibits non-trivial behaviors.

We have discussed decoupling of massive matter fields in the infinite mass limit. We have found that in the infinite mass limit a point of the Coulomb branch dominantly contributes to the partition function and decoupling of matter fields and an effective theory can be determined with respect to this point. We note that the definition of the Coulomb branch employed here is valid only on flat space, not on the three-sphere. In my work [5], we conclude that we specify the vacuum and an interacting superconformal phase (with decoupled massive free theories) are realized for some theories in the infinite mass limit. Our result implies that the massive good theory cannot be employed as a UV regularization of a bad theory because in the infinite mass limit a dominant point of the Coulomb branch is selected such that the mass-deformed good theory become a good theory as an effective theory. Therefore, it is still difficult an open problem in this research field to investigate a bad theory from localization methods.

We have also discussed that for theories whose supersymmetric vacua is composed of discrete points, such as a pure Chern-Simons theory and mass-deformed ABJM theory, the ellipsoid partition function can exhibit the supersymmetry breaking phase in the large  $N$  limit since the partition function is represented by the integration over the parameter describing its vacua including the metastable one. It is important to interpret this result in terms of the gravity side in the sense of understanding of the gauge/gravity correspondence. A real mass deformation corresponds to a flux background in the gravity side. In particular, the gravity dual of the mass-deformed ABJM theory on flat space and of R-charge-deformed ABJM theory have been studied [39, 73]. In our work, we could not obtain enough knowledge about the meaning of this phenomenon in the gravity side. We hope that the gravity dual corresponding to our case and

the singular structure at the threshold are found and some interesting results will be discovered.

We also have argued the phases which can be realized in the large  $N$  limit by the saddle-point analysis and found a special kind of solution of saddle-point equation. The confinement-like phase realized with the saddle-point solution we obtained may be related to supersymmetry breaking phase with considering the result [35, 36]. We note that because the theories we consider in this thesis defined on the ellipsoid, the spontaneous symmetry breaking can make sense in the large  $N$  or the decompactified limit.

Lastly, we would like to conclude this thesis by giving some comments on the analysis using a localization technique. Localization techniques are very powerful tools to compute quantities non-perturbatively. To apply this, we should define the theory on a compact manifold to subtract IR divergence. Then, it is subtle to identify the obtained result with that on flat space except for a superconformal field theory on a conformally flat manifold. Thus, in our successive works, we have attempted to interpret the results of mass-deformed theories in terms of the language of theories on flat space.



# Acknowledgement

First of all, I would like to thank my Ph.D supervisor Hiroshi Kunitomo for helping me through my Ph.D course. I also thank my second supervisor Seiji Terashima for teaching me how to research, presentation of work and the series of collaborations in research. I am grateful to Shigeki Sugimoto for carefully reading my draft and giving me fruitful comments. Our works introduced in this thesis is based on the valuable discussions with Nosaka Tomoki, Masazumi Honda, Shuichi Yokoyama and Takaya Miyamoto, who will also work with me at the same company from next April. I have spent very interesting time with my colleagues, seniors and juniors and I would like to thank all of them. Finally, we would like to thank my parents for their support and giving me the opportunity o study in Ph.D course in Yukawa Institute for Theoretical Physiscs in Kyoto University.

**Part IV**

**Appendixes**

# Appendix A

## Appendix for chapter 3

### A.1 A brief summary of resolvent methods

In this section, we give brief review of resolvent methods and further details of the calculation of a density function in this paper. We follow the argument on resolvent method for the Chern-Simons matrix model in [109–111]. First, we assume that the eigenvalues become dense in the large  $N$  limit and we can take the continuous limit as follows:

$$\frac{i}{N} \rightarrow s \in [0, 1], \quad x_i \rightarrow x(s), \quad \frac{1}{N} \sum_{i=1}^N \rightarrow \int ds. \quad (\text{A.1.1})$$

We define the density function  $\rho(x)$  as

$$\rho(x) \equiv \frac{ds}{dx}, \quad (\text{A.1.2})$$

and impose the normalization condition on it as

$$\int_I \rho(x) = 1, \quad (\text{A.1.3})$$

where  $I$  is an interval on which  $\rho(x)$  is defined. In this thesis, we consider only the following type of the saddle-point equation, given as a singular integral equation:

$$\alpha \left( \text{P} \int_I dy \rho(y) \coth \pi(x - y) \right) = V'(x), \quad (\text{A.1.4})$$

where  $\alpha$  is a constant. It is useful for us to define  $X = e^{2\pi x}$  and  $Y = e^{2\pi y}$  as in this case various techniques are available. The saddle-point equation is written as

$$\alpha \left( 1 + \text{P} \int_{\mathcal{C}} \frac{dY}{\pi} \frac{\rho(y)}{X - Y} \right) = V'(x), \quad (\text{A.1.5})$$

where  $X \in \mathcal{C} = [b, a]$ . We define an auxiliary function  $\omega(Z)$  as

$$\omega(X) \equiv \alpha \left( 1 + \int_{\mathcal{C}} \frac{dY}{\pi} \frac{\rho(y)}{X - Y} \right). \quad (\text{A.1.6})$$

This function is defined on all of the complex plane except on  $\mathcal{C}$ , where  $\omega(X)$  has a discontinuity when we across the interval  $\mathcal{C}$ . The function satisfies the following properties:

$$\lim_{X \rightarrow 0} \omega(X) = -\alpha, \quad \lim_{X \rightarrow \infty} \omega(X) = \alpha, \quad (\text{A.1.7})$$

$$\rho(x) = -\frac{1}{2\alpha i} \lim_{\epsilon \rightarrow 0} (\omega(X + i\epsilon) - \omega(X - i\epsilon)), \quad X \in \mathcal{C}, \quad (\text{A.1.8})$$

$$V'(x) = \frac{1}{2} \lim_{\epsilon \rightarrow 0} (\omega(X + i\epsilon) + \omega(X - i\epsilon)), \quad X \in \mathcal{C}. \quad (\text{A.1.9})$$

Then, we would like to give a proof of (A.1.8) and (A.1.9), which arise from the discontinuity of  $\omega(X)$ . We obtain the following relation by changing the integral contour:

$$\int_{\mathcal{C}} \frac{dY}{\pi} \frac{\rho(y)}{X + i\epsilon - Y} = \left( \int_b^{X-\epsilon} + \int_{X+\epsilon}^a \right) \frac{dY}{\pi} \frac{\rho(y)}{X - Y} + \int_{C_\epsilon^-} \frac{dY}{\pi} \frac{\rho(y)}{X - Y}, \quad (X \in \mathcal{C}), \quad (\text{A.1.10})$$

where  $C_\epsilon^-$  is a circle with radius  $\epsilon$  around  $Y = X$  in the lower half plane, which is oriented counterclockwise. From the definition of the principal value integral and the residue theorem, we finally obtain

$$\lim_{\epsilon \rightarrow 0} \omega(X + i\epsilon) = \alpha \left( 1 + \text{P} \int_{\mathcal{C}} \frac{dY}{\pi} \frac{\rho(y)}{X - Y} - i\rho(x) \right), \quad (\text{A.1.11})$$

$$\lim_{\epsilon \rightarrow 0} \omega(X - i\epsilon) = \alpha \left( 1 + \text{P} \int_{\mathcal{C}} \frac{dY}{\pi} \frac{\rho(y)}{X - Y} + i\rho(x) \right). \quad (\text{A.1.12})$$

Therefore, the equations (A.1.8) and (A.1.9) are proved.

From the analyticity<sup>†1</sup>, the resolvent is given by

$$\omega(X) = \oint_C \frac{dZ}{2\pi i} \frac{V'(z)}{X - Z} \frac{\sqrt{(X-a)}\sqrt{(X-b)}}{\sqrt{(Z-a)}\sqrt{(Z-b)}}, \quad Z = e^{2\pi z}, \quad (\text{A.1.13})$$

where  $C$  is a circle which encloses  $\mathcal{C}$ . This implies that the density function is determined once the potential  $V'(z)$  is given. When  $n_i$  degree poles  $X_{0i}$ , ( $i = 1, \dots, n_0$ ) of  $V'(x)$  exist outside of  $\mathcal{C}$ , we can deform the integral contour  $\mathcal{C}$  to infinity and pick up the poles  $Z = X$  and  $Z = X_{0i}$ , ( $i = 1, \dots, n_0$ ). Thus, the resolvent is determined as

$$\omega(X) = - \oint_{\infty} \frac{dZ}{2\pi i} \frac{V'(z)}{X - Z} \frac{\sqrt{(X-a)}\sqrt{(X-b)}}{\sqrt{(Z-a)}\sqrt{(Z-b)}}$$

---

<sup>†1</sup>We should consider the resolvent  $\omega(X)$  such that its branch cut is on  $[b, a]$  and it satisfies the asymptotic equations (A.7). Then, we should take the resolvent  $\omega(X)$  that has the product of the square root  $\sqrt{X-a}\sqrt{X-b}$ , not  $\sqrt{(X-a)(X-b)}$  because indeed,  $\sqrt{(X-a)(X-b)}$  has the branch cut on  $[b, a]$ , but does not satisfy the asymptotic behavior at  $X \rightarrow 0$

$$= V'(x) - \sum_{i=1}^{n_0} \text{Res} \left( \frac{V'(z)}{X-Z} \frac{\sqrt{(X-a)}\sqrt{(X-b)}}{\sqrt{(Z-a)}\sqrt{(Z-b)}}, X_{0i} \right). \quad (\text{A.1.14})$$

To determine the cut  $\mathcal{C}$ , we simply solve the equation (A.1.7) with the resolvent  $\omega(X)$  obtained in (A.1.14).

## A.2 Mixed Chern-Simons terms

It is known that the various Chern-Simons terms exist in three dimensions, which do not consist only of dynamical gauge fields, but also of background fields which couple with a current of a global symmetry of the theory, which we call mixed Chern-Simons term. These Chern-Simons terms are induced in the infinite mass limit because there are one-loop effects by integrating out massive fermions charged under the corresponding symmetries. In particular, on  $S^3$  we can consider a background vector field that couple with the R-symmetry current and Chern-Simons terms including the background field. These terms are important to understand what remains in the partition function after taking the infinite mass limit [62–64]. Mixed Chern-Simons terms that will appear are flavor-R and gauge-R mixed Chern-Simons terms given by

$$S_{\text{CS}}^{\text{FR}} \sim \frac{k_{\text{FR}}}{2\pi} \int_{S^3} \sqrt{g} d^3x (\sigma_f + iD_f), \quad (\text{A.2.1})$$

$$S_{\text{CS}}^{\text{GR}} \sim \frac{k_{\text{GR}}}{2\pi} \text{Tr} \int_{S^3} \sqrt{g} d^3x (\sigma + iD), \quad (\text{A.2.2})$$

where  $\sigma_f$  and  $D_f$  represent the scalar and auxiliary fields of the background vector superfields, respectively. Here, we only write parts that contribute to the partition function after applying localization methods. The induced Chern-Simons levels are given by integrating out a Majorana fermion  $\psi$  as

$$k_{\psi}^{\text{FR}} = \frac{\Delta_{\psi}}{2} \text{sgn}(M_{\psi}) \sum_{\mathbf{f}} q_{\psi, \mathbf{f}}, \quad (\text{A.2.3})$$

$$k_{\psi}^{\text{GR}} = \frac{\Delta_{\psi}}{2} \text{sgn}(M_{\psi}) \sum_i q_{\psi, i}, \quad (\text{A.2.4})$$

where  $q_f$ ,  $q_g$  and  $\Delta$  correspond to flavor, gauge and R charges respectively. Furthermore,  $M_{\psi}$  is an effective mass of the fermions at a point of the Coulomb branch. The effective mass is written as  $M_{\psi} = \sum_{\mathbf{f}} q_{\mathbf{f}} \sigma_{\mathbf{f}} + \sum_i q_i \sigma_i$ , where  $i$  labels the U(1) gauge groups on the Coulomb branch.

We use the terms (A.2.1) and (A.2.2) after applying a localization technique. These are given by

$$e^{S_{\text{CS}}^{\text{FR}}} = e^{2\pi k_{\text{FR}} \sigma_f}, \quad (\text{A.2.5})$$

$$e^{S_{\text{CS}}^{\text{GR}}} = e^{2\pi k_{\text{GR}}\sigma}, \quad (\text{A.2.6})$$

where the supersymmetric configuration of the background fields and the localization locus are required:

$$D_f = -i\sigma_f, \quad D = -i\sigma, \quad (\text{Other fields}) = 0. \quad (\text{A.2.7})$$

The real mass is given by the expectation value of the background field  $\sigma_f = m$ . Thus, the flavor-R Chern-Simons terms (A.2.1) induced in the infinite mass limit corresponds to the contributions from the free massive degrees of freedom. The induced gauge-R Chern-Simons term (A.2.2) corresponds to FI terms and contributions from massive degrees of freedom when we shift  $\sigma$  by  $m$ .

As an example, we attempt to derive the decoupled free massive sector of the partition function and FI terms of U(2) SQCD described in Section 3.2.1 from induced Chern-Simons terms<sup>†2</sup>. We assume that the classical Coulomb branch parameters  $(\sigma_1, \sigma_2)$  are written as  $(-m - \delta\sigma_1, m - \delta\sigma_2)$ . Then, the gauge group U(2) is broken down to  $U(1)_L \times U(1)_R$ . The effective mass and charges of the massive gauginos and Majorana fermions of chiral multiplets<sup>†3</sup> are summarized in Table A.1<sup>†4</sup>.

	effective mass	U(1) <sub>R</sub>	U(1) <sub>L</sub> × U(1) <sub>R</sub>
$\lambda_+$	$\sigma_1 - \sigma_2$	1	(1, -1)
$\lambda_-$	$\sigma_2 - \sigma_1$	1	(-1, 1)
$\psi_{1\pm}$	$\pm m + \sigma_1$	$-\frac{1}{2}$	(1, 0)
$\psi_{2\pm}$	$\pm m + \sigma_2$	$-\frac{1}{2}$	(0, 1)
$\tilde{\psi}_{1\pm}$	$\pm m - \sigma_1$	$-\frac{1}{2}$	(-1, 0)
$\tilde{\psi}_{2\pm}$	$\pm m - \sigma_2$	$-\frac{1}{2}$	(0, -1)

Table A.1: The effective mass, R-charge and gauge charge of the fermions under  $U(1) \times U(1)$ . Here,  $\lambda_{\pm}$  denote gauginos and  $\psi$  ( $\tilde{\psi}$ ) is a Majorana fermion in the chiral multiplet in the fundamental (anti-fundamental) representation.

The contributions of massive gauginos to induced Chern-Simons terms as follows:

$$\lambda_+ : e^{\pi\Delta_\lambda \text{sign}(-2m - \delta\sigma_1 + \delta\sigma_2)(-m - \delta\sigma_1 - (-\delta\sigma_2 + m))} \quad (\text{A.2.8})$$

<sup>†2</sup>We would like to thank Masazumi Honda for giving me useful comments and discussion on this point.

<sup>†3</sup>three-dimensional  $\mathcal{N} = 2$  vector and chiral multiplet have a Majorana fermion on the on-shell formalism instead of a complex fermion on the off-shell formalism.

<sup>†4</sup>An  $\mathcal{N} = 4$  gauge theory has a chiral multiplet in the adjoint representation of the gauge group. It seems that we must consider the contributions from the chiral multiplets. However, because the canonical R-charge of the chiral multiplet is 1, the R-charge of the fermion component is 0 and it does not contribute to gauge-R mixed Chern-Simons level.

$$\lambda_- : e^{\pi\Delta_\lambda \text{sign}(2m+\delta\sigma_1-\delta\sigma_2)(-(-m-\delta\sigma_1)+(-\delta\sigma_2+m))}. \quad (\text{A.2.9})$$

Thus, total contributions of massive gauginos when  $m \rightarrow \infty$  are determined as

$$e^{2\pi\Delta_\lambda(2m+\delta\sigma_1-\delta\sigma_2)}. \quad (\text{A.2.10})$$

The first term can be interpreted as the massive free part and the second and third terms are induced FI terms associated with  $U(1)_L$  and  $U(1)_R$ .

The contributions of the massive matter fermions are summarized as follows:

$$\psi_{1-} : e^{\pi\Delta_\psi \text{sgn}(-2m-\delta\sigma_1)(-2m-\delta\sigma_1)} \quad (\text{A.2.11})$$

$$\psi_{2+} : e^{\pi\Delta_\psi \text{sgn}(2m-\delta\sigma_2)(2m-\delta\sigma_2)} \quad (\text{A.2.12})$$

$$\tilde{\psi}_{1+} : e^{\pi\Delta_\psi \text{sgn}(2m+\delta\sigma_1)(2m+\delta\sigma_1)} \quad (\text{A.2.13})$$

$$\tilde{\psi}_{2-} : e^{\pi\Delta_\psi \text{sgn}(-2m+\delta\sigma_2)(-2m+\delta\sigma_2)}. \quad (\text{A.2.14})$$

Then, the total contribution of the massive matter fermions to the induced Chern-Simons term is given by

$$e^{\pi\frac{N_f}{2}\Delta_\psi(8m+2\delta\sigma_1-2\delta\sigma_2)}. \quad (\text{A.2.15})$$

The first term can be interpreted as contributions from the massive free sector and the second and third can be interpreted as FI terms. Then, we conclude that in this case the total contributions from the free massive sectors when  $m \rightarrow \infty$  is given by

$$e^{2m\pi(2-N_f)}, \quad (\text{A.2.16})$$

and total induced FI terms are given by

$$e^{\pi\left(2-\frac{N_f}{2}\right)\delta\sigma_1}, \quad \text{for } U(1)_L, \quad (\text{A.2.17})$$

$$e^{-\pi\left(2-\frac{N_f}{2}\right)\delta\sigma_2}, \quad \text{for } U(1)_R. \quad (\text{A.2.18})$$

These results are same as those obtained in Section 3.2.1 from the calculation of the matrix model. Thus, the effects that appear in the infinite mass limit in the matrix model can indeed be regarded as induced mixed Chern-Simons terms. The result can easily be generalized to other theories in this paper. These consequences are not surprising because one-loop parts of the vector and chiral multiplets in the matrix model must inherit such one-loop effects after integrating out massive fermions.

### A.3 Convergence bound of matrix models

In this section, we discuss the convergence of the matrix models. The convergence bound of the matrix model of SQCD was first discussed in [59]. In [112], it is also pointed out that the convergence bound is indistinguishable from the unitarity bound of the monopole operator in the Veneziano limit.

We consider the convergence of the matrix model introduced in (3.1.1):

$$Z = \frac{1}{N!} \int \prod_{i=1}^N dx_i \frac{e^{\pi\zeta \sum_i x_i} \prod_{i<j} 4 \sinh^2(\pi(x_i - x_j))}{\prod_i \left(2 \cosh \pi(x_i)\right)^{N_f}}. \quad (\text{A.3.1})$$

To investigate whether the integral is convergent, it is sufficient to know the asymptotic behavior of the integrand when we take one of the integral valuables  $|x_i| \rightarrow \infty$ . Therefore, we focus on  $x_1$  and study the asymptotic behavior of the integrand. When  $|x_1| \rightarrow \infty$ , the part of the integrand related to convergence is evaluated as

$$e^{\pi|x_1|(\text{sign}(x_1)\zeta+2(N-1)-N_f)}. \quad (\text{A.3.2})$$

Thus, for the matrix model to converge the relation

$$|\zeta| + 2(N - 1) - N_f < 0 \quad (\text{A.3.3})$$

must hold. This threshold corresponds to the condition that the solution of the saddle-point equation in (3.1.1) in the large  $N$  limit exists. We note that the partition function of the effective theories (3.1.33) and (3.1.67) satisfy the above relation and converge. In fact, each matrix model narrowly satisfies the convergence bound. For example, for the case of (3.1.33), the left-hand side of the bound (A.3.3) is  $-2$ , which does not depend on any parameter. Therefore, This implies that the convergence of the matrix model restricts the theory that appears in the infinite mass limit. In fact, in the subsection 3.1.2 we assume that the solution of the saddle-point equation where the gauge group  $U(N)$  is broken down to  $U(N_1) \times U(N_2)$  ( $N_1 > N_2$ )<sup>†5</sup> is allowed. Then, the convergence bound of the partition function corresponding to the effective theory is given by

$$0 > \frac{N_f}{2} - 2N_2 + 2(N_1 - 1) - \frac{N_f}{2} = 2(N_1 - N_2) - 2, \quad (\text{A.3.4})$$

$$0 > \left| \frac{N_f}{2} - 2N_1 \right| + 2(N_1 - 1) - \frac{N_f}{2}. \quad (\text{A.3.5})$$

---

<sup>†5</sup>We assume this situation without loss of generality.



The first line is not satisfied when  $N_1 > N_2$ . Therefore, only the case that  $N_1 = N_2$  is allowed owing to the convergence of the matrix model of the effective theory<sup>†6</sup>. By the same argument concerning the convergence bound, we can also understand why  $N_1$ ,  $N_2$  and  $N_3$  satisfy the relation (3.1.61).

---

<sup>†6</sup>We would like to thank Tomoki Nosaka for pointing out and discussing this point.

# Appendix B

## Appendix for chapter 5

### B.1 Dominant saddle-point solution

We have studied the large  $N$  saddle-point solution associated with the confining phase. In general, if there are solutions of the saddle-point equation, then we should determine which solution will really give the dominant contribution to the partition function in the large  $N$  limit. In this appendix, we will focus on  $SU(N)$  SUSY Chern-Simons Yang-Mills theory with  $N_f$  adjoint massive hypermultiplets on  $S^3$  as an example in which we have the confinement solution and other solutions. We find that in the large  $N$  limit with  $N \gg k$  and  $\frac{km}{N}$  finite and large, the solution associated with confinement phase is expected to give the dominant contribution.

First, we will consider the case in which the Chern-Simons level is vanishing. Here, the matrix model is given by

$$Z = \frac{1}{N!} \int d^N a \delta\left(\sum_i a_i\right) \prod_{i>j}^N \frac{4 \sinh^2 \pi(a_i - a_j)}{(2 \cosh \pi(a_i - a_j + m) 2 \cosh \pi(a_i - a_j - m))^{N_f}}, \quad (\text{B.1.1})$$

where  $\delta(\sum_i a_i)$  denotes the condition of  $SU(N)$ . This matrix model converges when we take  $N_f \geq 2$ . Then, we take  $N_f \geq 2$ . The saddle-point equation of this matrix model is difficult to solve analytically. However, we can find a numerical solution of the saddle-point equation. we find two solutions of the saddle-point equation, one of which is associated with confinement phase. The other solution is the real valued one while the confinement solution is complex valued. These two types of solution are showed in figure B.1 and B.2. We find that the free energy for the real solution is smaller than that for the confinement one. Then, the confinement phase cannot be realized in the large  $N$  limit. We will show some numerical values of the free

energy for the two solutions in the following tables<sup>†1</sup>:

	$m_a = 1$	$m_a = 2$	$m_a = 5$	$m_a = 8$
$N_f = 2$	49746	94563	233023	372313
$N_f = 3$	83582	160235	337392	632638
$N_f = 5$	148258	287081	699586	1125850
$N_f = 10$	306535	600494	1486380	2379170

Table B.1: The free energies correspond to the real solution.

	$m_a = 1$	$m_a = 2$	$m_a = 5$	$m_a = 8$
$N_f = 2$	61742	123947	310557	497168
$N_f = 3$	92844	186150	466066	745982
$N_f = 5$	155047	310557	713310	1243610
$N_f = 10$	310555	621575	1554630	2487680

Table B.2: The free energies correspond to the confinement solution.

Thus, the numerical results strongly suggest that the confinement solution is not the dominant saddle-point solution in any regions of  $m$  and  $N_f$ . However, naively considering, in the infinite mass limit the theory become pure  $SU(N)$  SYM since the matter fields become decoupled and then the supersymmetry phase could appear. As we discussed for  $\mathcal{N} = 4$  case, in Chapter 1 of Part II, this naive expectation is not always true. This is because the naive discussion of decoupling is based on the assumption that the theory is on the origin of the Coulomb branch. In fact, the numerical results suggest that the dominant solution of the saddle-point equation does not correspond to the origin of the Coulomb branch of the flat space. We will discuss this from the numerical result with the case  $N_f \geq 3$  in the next subsection.

### B.1.1 The dominant saddle-point solutions

As we discussed in Chapter 1 of Part II, it is plausible to consider that in the large  $N$  limit the specific point of the Coulomb branch is selected. This means that in the large  $N$  limit we can argue which massive hypermultiplets are effectively massless based on the saddle-point solution.

Let us consider the meaning of the real solution we introduced above. Our numerical results has shown that when we take mass sufficiently large, the real valued saddle-point solution splits

---

<sup>†1</sup>The free energy is estimated by the saddle-point approximation with the numerical solution obtained here.

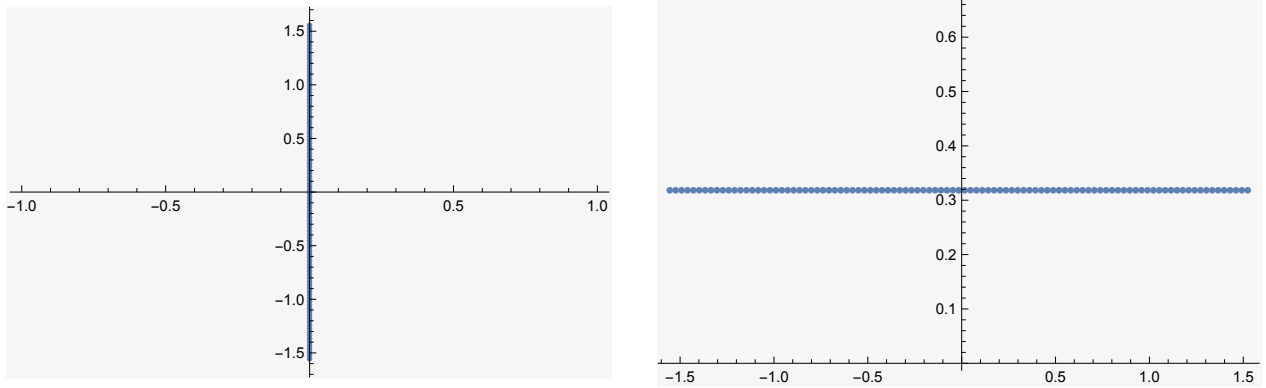


Figure B.1: The left figure shows the numerical solution which corresponds to the confinement phase plotted on the Complex plane with the parameters  $(N, N_f, m) = (100, 3, 8)$ . The solution actually lies on the Imaginary axis. The right one shows the density function of it. We can check that the solution does not depend on the parameters. (These figures are cited from [4].)

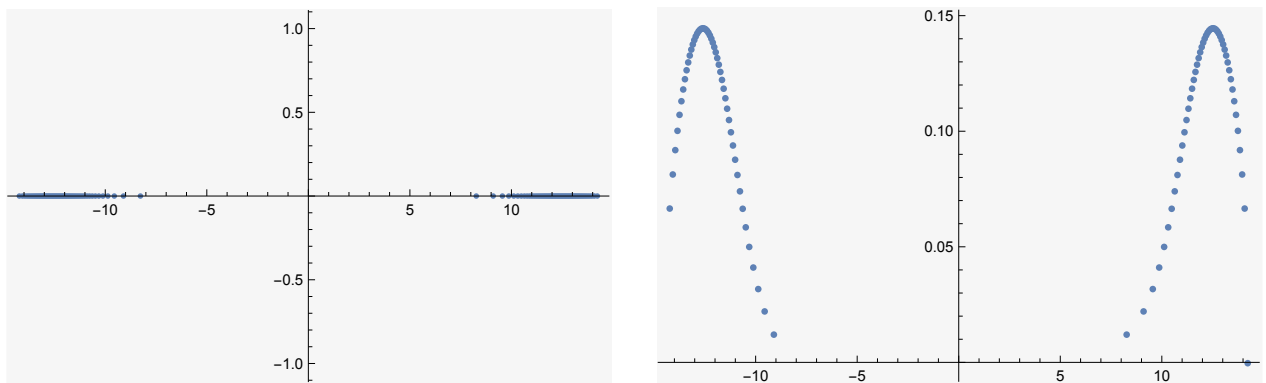


Figure B.2: The left figure shows the other numerical solution plotted on the Complex plane with  $(N, N_f, m) = (100, 3, 8)$ . The solution actually lies on the real axis. The right one shows the density function of it. (These figures are cited from [4].)

into two parts and the half of the  $N$  eigenvalues are distributed around  $-\frac{m}{2}$  and the others are around  $\frac{m}{2}$ . This solution means that a non-trivial point of the Coulomb branch is selected in the large  $N$  limit. Following from the same consideration in Section 3, we can determine the corresponding point of the Coulomb branches of the original  $SU(N)$  theory on the flat space as:

$$\sigma = \left( \begin{array}{c|c} -\frac{m}{2} \mathbf{1}_{\frac{N}{2} \times \frac{N}{2}} & \mathbf{0} \\ \hline \mathbf{0} & \frac{m}{2} \mathbf{1}_{\frac{N}{2} \times \frac{N}{2}} \end{array} \right). \quad (\text{B.1.2})$$

Then, it is natural to expect that the gauge group  $SU(N)$  is broken to  $S[U(\frac{N}{2}) \times U(\frac{N}{2})]$  and the  $N_f$  massive adjoint hypermultiplets become effectively massless around this vacuum.

For  $k = 0$  case, we have found that the massive multiplets cannot simply decouple so

that the theory becomes in the SUSY breaking phase as we found in 3 that a good theory cannot become a bad theory since the effectively massless multiplets appear and the non-trivial superconformal fields theory is realized in the infinite mass limit on  $S^3$ .

In the next subsection, we propose the theory where the confinement solution is the dominant saddle-point solution by adding the Chern-Simons term to the theory considered here. With the CS term, the eigenvalues feel the central force in the sense that we regard the saddle-point equation as the E.O.M of the mechanics of the eigenvalues. Then, the eigenvalues tend not to be split and the solution is forbidden.

## B.1.2 A theory in which confinement solution is dominant

Here, we consider the  $SU(N)$  Chern-Simons Yang-Mills theory with  $N_f$  massive adjoint hypermultiplets. The matrix model is given by

$$Z = \frac{1}{N!} \int d^N a \delta\left(\sum_i^N a_i\right) e^{i\pi k \sum_i a_i^2} \prod_{i>j}^N \frac{4 \sinh^2 \pi(a_i - a_j)}{(2 \cosh \pi(a_i - a_j + m) 2 \cosh \pi(a_i - a_j - m))^{N_f}}. \quad (\text{B.1.3})$$

The saddle-point equation is

$$0 = 2ik a_i + 2 \sum_{j \neq i} \coth \pi(a_i - a_j) - N_f \sum_j (\tanh \pi(a_i - a_j + m) + \tanh \pi(a_i - a_j - m)) + \mu, \quad (\text{B.1.4})$$

where the first term of the R.H.S of the above equation is from the Chern-Simons term and causes the central force in the real and imaginary parts of the saddle-point equation. With the help of the Chern-Simons term the split type solution no longer can exist.

We will argue that the confinement solution is dominant for the large  $N$  limit with  $N \gg k$  with  $\frac{km}{N}$  finite and large. To do this in detail we repeat the same argument in the previous subsection. The saddle-point equation under the assumption that the eigenvalues are distributed around two points  $\pm \frac{m}{2}$  becomes as

$$0 = 2i \frac{k}{N} \left( \lambda_i - \frac{m}{2} \right) + \left( \frac{N_f}{2} - 1 \right) + \frac{2}{N} \sum_{j \in I_-} \coth \pi(\lambda_i - \lambda_j) - \frac{N_f}{N} \sum_{j \in I_+} \tanh \pi(\lambda_i - \tilde{\lambda}_j) + \mu, \quad i \in I_-, \quad (\text{B.1.5})$$

$$0 = 2i \frac{k}{N} \left( \tilde{\lambda}_i + \frac{m}{2} \right) + \left( 1 - \frac{N_f}{2} \right) + \frac{2}{N} \sum_{j \in I_+} \coth \pi(\tilde{\lambda}_i - \tilde{\lambda}_j) - \frac{N_f}{N} \sum_{j \in I_-} \tanh \pi(\tilde{\lambda}_i - \lambda_j) + \mu, \quad i \in I_+. \quad (\text{B.1.6})$$

Here, we consider a strong 't Hooft coupling limit  $\frac{k}{N} \ll 1$  and  $\frac{m}{N} \ll 1$  in order to make the confining solution valid. When a combination of the parameters  $\frac{km}{N}$  is small, then the Chern-Simons term can be neglected and the split type solution is valid. When  $\frac{km}{N} = \mathcal{O}(N^0)$ , the solution should be deformed. Then, assuming that  $\frac{km}{N}$  is large, we expect the split type solution cannot exist. We will not explicitly determine how large  $\frac{km}{N}$  should be for the confinement phase to be realized because it is difficult analytically. The numerical analysis shown below suggests that the critical value of  $km/N$  is in  $2 \lesssim km/N \lesssim 4$ . In figure 4, we show the density functions of some examples for these saddle-point solutions.

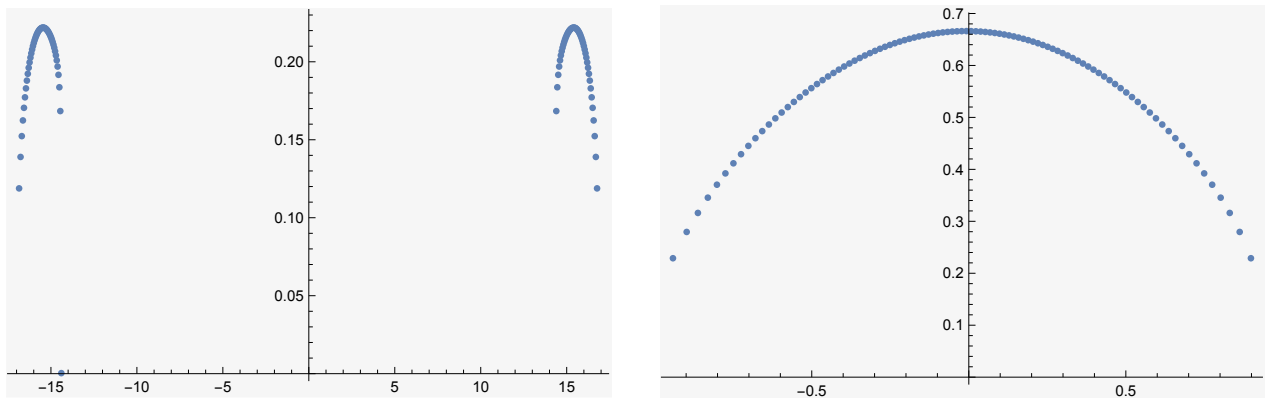


Figure B.3: These figure show that density functions of the real part of saddle-point solution for  $N = 100$ . The left one is with parameter  $(k, m_a) = (10, 10)$ . The right one is with parameter  $(k, m_a) = (150, 10)$ . The horizontal line means the value of the real part of the eigenvalue. (These figures are cited from [4]).

To show the behavior of the solution as the Chern-Simons level become large we summarize the value of the Wilson loop  $W_R$  (2.6.31) and the free energy  $-\log |Z|$  from the numerical analysis in the following tables:

These values are evaluated by the saddle-point approximation with the solution numerically obtained. The result has shown the value of the Wilson loop is drastically changed for  $20 \lesssim k \lesssim 40$  when  $N = 100, m = 10$ . The numerical analysis also suggests that the solution of the saddle-point equation no longer splits in this region although we still call this the split type solution. The solution sits around the origin when  $k$  is bigger than 30, however, the solution looks different from the confinement solution, but have similar structures with one associated with confinement phase. <sup>†2</sup> When  $k \geq 30$ , we have found only the solutions independent on the mass, which also become close to the weak 't Hooft solution as the Chern-Simons level  $k$  becomes large <sup>†3</sup>. However, the value of the Wilson loop which is evaluated by the each of the

<sup>†2</sup>For  $k = 30$ , the value of  $-\log |Z|$  for the split solution seems to be strange. We expect that there are some accidental reasons for this singular behavior because  $N$  is finite.

<sup>†3</sup>Our claim is subtle because this argument is based on the numerical analysis of the saddle-point equation.

$(N, m) = (100.10)$	$W_R$	$-\log  Z $
$k = 10$	$2.60356 \times 10^{15} - 2.87161 \times 10^{15}i$	834190
$k = 20$	$11.3867 - 0.10577i$	965491
$k = 30$	$4.29052 \times 10^{14} - 2.57048 \times 10^{15}i$	53126
$k = 40$	$22.56929 - 3.50511i$	940792
$k = 50$	$-0.914496 + 0.185339i$	935889
$k = 60$	$-3.46485 - 3.57006i$	939455
$k = 70$	$1.0154 + 0.434397i$	935684

Table B.3: The value of Wilson loop and free energy corresponding to the split solution discussed in the previous subsection from numerical analysis.

$(N, m) = (100.10)$	$W_R$	$-\log  Z $
$k = 10$	$-0.000341459 - 1.60786i$	932650
$k = 20$	$-0.00133768 - 3.21552i$	932824
$k = 30$	$-0.00289594 - 4.82279i$	933113
$k = 40$	$-0.00484618 - 6.42953i$	933518
$k = 50$	$0.0468883 - 7.95619i$	933976
$k = 60$	$0.0197115 - 9.61648i$	934642
$k = 70$	$-0.075207 - 8.80006i$	934371

Table B.4: The value of Wilson loop and free energy corresponding to the confinement type saddle solution (5.3.6) from numerical analysis.

two solutions is  $\mathcal{O}(N^0)$  which means there are some cancellations in  $\text{Tr}_R$  in the definition of the Wilson loop in the fundamental representation. This is nothing but a characteristic property of the confinement phase.

In the tables, we also showed the  $F = -\log |Z|$ . The values for the two different solutions are almost the same except  $k = 10$ , for which the density function splits for one solution. Thus, we cannot say which solution is dominant because the  $1/N$  corrections will be important. In order to decide which solution is dominant, we need to compute them numerically for larger  $N$ . We hope to do it in near future.

we note that we have assumed that the probe approximation of the Wilson loop is appropriate in this numerical computations. Indeed, the values of  $F$  are much larger than the values

---

However, we can confirm that the behavior of the solution of the saddle-point equation changes around  $k = 30$  and we could not find any counterexample.

of the logarithm of the Wilson loop. This fact justifies the probe approximation.



# Appendix C

## Appendix for Chapter 6

### C.1 Exact computation of $Z(N, k, 0, \zeta_2)$

In this appendix we explain details on how to compute  $Z(N, k, 0, \zeta_2)$  for integer  $k$ .

#### C.1.1 Exact partition function for finite $(N, k)$

We can also evaluate the exact values of the partition function for finite  $(N, k)$  by a slight generalization [77, 78] of the technique employed in the ABJM theory [79, 80]. We will find a good agreement with both results.

we compute the partition function for some finite  $(N, k)$  by the technique used in [77]. We start with the partition function written in the Fermi gas formalism

$$Z(N, k, 0, \zeta_2) = \frac{1}{N!} \int \frac{d^N x}{(2\pi)^N} \det_{i,j} \langle x_i | \hat{\rho}(\hat{q}, \hat{p}) | x_j \rangle, \quad (\text{C.1.1})$$

where  $[\hat{q}, \hat{p}] = i\hbar$  with  $\hbar = 2\pi k$  and<sup>†1</sup>

$$\hat{\rho} = \sqrt{\frac{1}{2 \cosh \frac{\hat{q}}{2}}} \frac{e^{\frac{2i\zeta_2}{k} \hat{p}}}{2 \cosh \frac{\hat{p}}{2}} \sqrt{\frac{1}{2 \cosh \frac{\hat{q}}{2}}}. \quad (\text{C.1.2})$$

If we consider the generating function of the partition function or equivalently the grand partition function  $\sum_{N=0}^{\infty} z^N Z(N)$ , we can show that it is written as the following Fredholm determinant

$$\sum_{N=0}^{\infty} z^N Z(N) = \text{Det}(1 + z\hat{\rho}) \equiv \exp \left[ \sum_{n=1}^{\infty} \frac{(-1)^{n-1}}{n} z^n \text{Tr} \hat{\rho}^n \right]. \quad (\text{C.1.3})$$

---

<sup>†1</sup>For a later convenience we have symmetrized the density matrix by another similarity transformation from (4.3.11).

Comparing the coefficient of  $z^N$  on the both sides, we find that the partition function  $Z(N)$  is determined by  $\text{Tr } \widehat{\rho}^n$  with  $n \leq N$ , as

$$Z(1) = \text{Tr } \widehat{\rho}, \quad Z(2) = \frac{1}{2}(\text{Tr } \widehat{\rho})^2 - \frac{1}{2} \text{Tr } \widehat{\rho}^2, \quad Z(3) = \frac{1}{6}(\text{Tr } \widehat{\rho})^3 - \frac{1}{2} \text{Tr } \widehat{\rho} \text{Tr } \widehat{\rho}^2 + \frac{1}{3} \text{Tr } \widehat{\rho}^3, \quad \dots \quad (\text{C.1.4})$$

We can compute  $\text{Tr } \widehat{\rho}^n$  by completely the same way as that in the case of R-charge deformation [77]. First we notice that the matrix element  $\langle x | \widehat{\rho} | y \rangle$  has the following structure

$$\langle x | \widehat{\rho} | y \rangle = \frac{1}{2 \cosh \frac{x}{2}} \frac{1}{2k \cosh \frac{x-y+4\pi\zeta_2}{2k}} = \frac{E(x)E(y)}{k(\alpha M(x) + \alpha^{-1}M(y))}, \quad (\text{C.1.5})$$

with

$$E(x) = \frac{e^{\frac{x}{2k}}}{\sqrt{2 \cosh \frac{x}{2}}}, \quad M(x) = e^{\frac{x}{k}}, \quad \alpha = e^{\frac{2\pi\zeta_2}{k}}. \quad (\text{C.1.6})$$

For  $\alpha = 1$ , this form is in the range of application of Tracy-Widom's lemma [94] which has been very powerful tool to systematically compute  $\text{Tr } \widehat{\rho}^n$  in various M2-brane theories without masses [80, 95–102]. We can easily extend it to general  $\alpha$  as follows. The structure (C.1.5) can be expressed as a quasi-commutation relation for  $\widehat{\rho}$

$$\alpha \widehat{M} \widehat{\rho} + \alpha^{-1} \widehat{\rho} \widehat{M} = \widehat{E} | 0 \rangle \rangle \langle \langle 0 | \widehat{E}, \quad (\widehat{E} = E(\widehat{q}), \quad \widehat{M} = M(\widehat{q})), \quad (\text{C.1.7})$$

where  $|p\rangle\rangle$  is momentum eigenstate satisfying

$$\langle x | x' \rangle = 2\pi\delta(x - x'), \quad \langle \langle p | p' \rangle \rangle = 2\pi\delta(p - p'), \quad \langle x | p \rangle = \frac{1}{\sqrt{k}} e^{\frac{ixp}{\hbar}}, \quad \langle \langle p | x \rangle = \frac{1}{\sqrt{k}} e^{-\frac{ixp}{\hbar}}. \quad (\text{C.1.8})$$

This relation can be generalized straightforwardly for  $\widehat{\rho}^n$  as

$$\alpha^n \widehat{M} \widehat{\rho}^n - (-1)^n \alpha^{-n} \widehat{\rho} \widehat{M} = \sum_{\ell=0}^{n-1} (-1)^\ell \alpha^{n-1-2\ell} \widehat{\rho}^\ell \widehat{E} | 0 \rangle \rangle \langle \langle 0 | \widehat{E} \widehat{\rho}^{n-1-\ell}. \quad (\text{C.1.9})$$

This implies that we can compute the matrix element of  $\widehat{\rho}^n$  from two sets of functions  $\phi_\ell(x)$  and  $\psi_\ell(x)$  as

$$\langle x | \widehat{\rho}^n | y \rangle = \frac{E(x)E(y)}{\alpha^n M(x) - (-1)^n \alpha^{-n} M(y)} \sum_{\ell=0}^{n-1} (-1)^\ell \phi_\ell(x) \psi_{n-1-\ell}(y), \quad (\text{C.1.10})$$

where

$$\phi_\ell(x) = \alpha^{-\ell} \langle x | \widehat{E}^{-1} \widehat{\rho}^\ell \widehat{E} | 0 \rangle \rangle, \quad \psi_\ell(x) = \alpha^\ell \langle \langle 0 | \widehat{E}^{-1} \widehat{\rho}^\ell \widehat{E} | x \rangle \rangle = \phi_\ell(x) |_{\alpha \rightarrow \alpha^{-1}}. \quad (\text{C.1.11})$$

We can show that the function  $\phi_\ell(x)$  satisfies the following recursion relation

$$\begin{aligned}\phi_{\ell+1}(x) &= \int \frac{dy}{2\pi} \frac{1}{E(x)} \alpha^{-1} \rho(x, y) E(y) \phi_\ell(y) \\ &= \int \frac{dy}{2\pi k} \frac{1}{e^{\frac{y}{k}} + \alpha^2 e^{\frac{y}{k}} e^{\frac{y}{2}} + e^{-\frac{y}{2}}} e^{\frac{y}{k}} \phi_\ell(y),\end{aligned}\tag{C.1.12}$$

as well as  $\psi_\ell(x)$ . In app. C.1, we explain how to practically solve the recursion relation for integer  $k$  while their details are slightly different between odd  $k$  and even  $k$  cases. According to the algorithm, we have computed  $Z(N, k, 1, \zeta_2)$  by Mathematica for  $(k = 1, N \leq 12)$ ,  $(k = 2, N \leq 9)$ ,  $(k = 3, N \leq 5)$ ,  $(k = 4, N \leq 5)$  and  $(k = 6, N \leq 4)$ . In app. C.2, we explicitly write down a part of the results and also compare them with the result of saddle-point approximation (4.3.29).

### Even $k$

If  $k \in 2\mathbb{N}$ , we can introduce a new variable  $u = e^{\frac{x}{k}}$  to rewrite the integration (C.1.12) as

$$\phi_{\ell+1}(u) = \frac{1}{2\pi} \int_0^\infty dv \frac{v^{\frac{k}{2}}}{(v + \alpha^2 u)(v^k + 1)} \phi_\ell(v).\tag{C.1.13}$$

If we assume that  $\phi_\ell(u)$  can be expanded as the following finite series (inductively correct)

$$\phi_\ell(u) = \sum_{j \geq 0} \phi_\ell^{(j)}(u) (\log u)^j, \quad (\phi_\ell^{(j)}(u) \text{ are some rational functions of } u)\tag{C.1.14}$$

we can compute the integration (C.1.13) as [80]

$$\begin{aligned}\phi_{\ell+1}(u) &= \frac{1}{2\pi} \sum_{j \geq 0} \left[ -\frac{(2\pi i)^j}{j+1} \int_\gamma \frac{v^{\frac{k}{2}}}{(v + \alpha^2 u)(v^k + 1)} \phi_\ell^{(j)}(v) B_{j+1} \left( \frac{\log^{(+)} v}{2\pi i} \right) \right] \\ &= \frac{1}{2\pi} \sum_{j \geq 0} \left[ -\frac{(2\pi i)^{j+1}}{j+1} \sum_{w \in \text{poles}} \text{Res} \left[ \frac{v^{\frac{k}{2}}}{(v + \alpha^2 u)(v^k + 1)} \phi_\ell^{(j)}(v) B_{j+1} \left( \frac{\log^{(+)} v}{2\pi i} \right), v \rightarrow w \right] \right].\end{aligned}\tag{C.1.15}$$

Here  $\log^{(+)}$  is logarithm function with the branch cut located on  $\mathbb{R}^+$  and the integration contour  $\gamma$  is as depicted in figure C.1. The poles to be collected in the step  $\phi_\ell \rightarrow \phi_{\ell+1}$  are at most

$$\begin{aligned}v &= -\alpha^2 u, \\ v &= \alpha^{-2a} e^{\frac{\pi i(2b+1)}{k}}, \quad (a = 0, 1, \dots, \ell; b = 0, 1, \dots, k-1),\end{aligned}\tag{C.1.16}$$

which can be seen from the same argument as in [77].

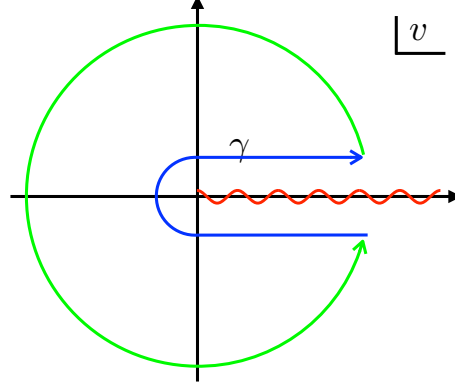


Figure C.1: The integration contour  $\gamma$  in (C.1.15) (blue) and the deformed contour to use the Cauchy theorem (green). The cut of  $\log^{(+)}$  is depicted by wavy red line. (This figure is cited from our paper [3].)

After obtaining  $\phi_\ell$  for  $\ell = 0, 1, \dots, n-1$ , we can compute  $\text{Tr } \widehat{\rho}^n$  by

$$\begin{aligned} \text{Tr } \widehat{\rho}^n &= \frac{1}{2\pi(\alpha^n - (-1)^n \alpha^{-n})} \int_0^\infty du \frac{u^{\frac{k}{2}-1}}{u^k + 1} \Psi_n(u) \quad \left( \Psi_n(u) = \sum_{\ell=0}^{n-1} (-1)^\ell \phi_\ell(u) \psi_{n-1-\ell}(u) \right) \\ &= \frac{1}{2\pi(\alpha^n - (-1)^n \alpha^{-n})} \sum_{j \geq 0} \left[ -\frac{(2\pi i)^{j+1}}{j+1} \sum_{w \in \text{poles}} \text{Res} \left[ \frac{u^{\frac{k}{2}-1}}{u^k + 1} \Psi_n^{(j)}(u) B_{j+1} \left( \frac{\log^{(+)} u}{2\pi i} \right), u \rightarrow w \right] \right], \end{aligned} \quad (\text{C.1.17})$$

where  $\Psi_n = \sum_{j \geq 0} \Psi_n^{(j)}(u) (\log u)^j$  and *poles* are (at most)

$$u = \alpha^{-2a} e^{\frac{\pi i(2b+1)}{k}}. \quad (a = -(n-1), -(n-2), \dots, n-1; b = 0, 1, \dots, k-1) \quad (\text{C.1.18})$$

### Odd $k$

For odd  $k$ , we define  $u = e^{\frac{x}{2k}}$  to obtain the following formulas

$$\phi_{\ell+1}(u) = \frac{1}{\pi} \sum_{j \geq 0} \left[ -\frac{(2\pi i)^{j+1}}{j+1} \sum_{v \in \text{poles}} \text{Res} \left[ \frac{1}{v^2 + \alpha^2 u^2} \frac{v^{k+1}}{v^{2k} + 1} \phi_\ell^{(j)}(v) B_{j+1} \left( \frac{\log^{(+)} v}{2\pi i} \right), v \rightarrow w \right] \right], \quad (\text{C.1.19})$$

where  $\phi_\ell^{(j)}(u)$  are the rational functions given by  $\phi_\ell(u) = \sum_{j \geq 0} (\log u)^j \phi_\ell^{(j)}(u)$  and the poles to be collected are

$$v = \pm i \alpha u,$$

$$\begin{aligned}
v &= \alpha^{-2a} e^{\frac{\pi i(2b+1)}{2k}}, \quad \left( a = 0, 1, \dots, \left[ \frac{\ell}{2} \right]; b = 0, 1, \dots, 2k-1 \right) \\
v &= \alpha^{-(2a+1)} e^{\frac{\pi i b}{k}}. \quad \left( a = 0, 1, \dots, \left[ \frac{\ell-1}{2} \right]; b = 0, 1, \dots, 2k-1 \right)
\end{aligned} \tag{C.1.20}$$

The traces of  $\widehat{\rho}^n$  can be computed as

$$\text{Tr} \widehat{\rho}^n = \frac{1}{\pi(\alpha^n - (-1)^n \alpha^{-n})} \sum_{j \geq 0} \left[ -\frac{(2\pi i)^{j+1}}{j+1} \sum_{w \in \text{poles}} \text{Res} \left[ \frac{u^{k-1}}{u^{2k} + 1} \Psi_n^{(j)}(u) B_{j+1} \left( \frac{\log^{(+)} v}{2\pi i} \right), u \rightarrow w \right] \right] \tag{C.1.21}$$

where  $\psi(u) = \sum_{\ell=0}^{n-1} (-1)^\ell \phi_\ell(u) \psi_{n-1-\ell}(u) = \sum_{j \geq 0} (\log u)^j \Psi_\ell^{(j)}(u)$  and the poles are

$$\begin{aligned}
u &= \alpha^{2a} e^{\frac{\pi i(2b+1)}{2k}}, \quad \left( a = -\left[ \frac{n-1}{2} \right], -\left[ \frac{n-1}{2} \right] + 1, \dots, \left[ \frac{n-1}{2} \right]; b = 0, 1, \dots, 2k-1 \right), \\
u &= \alpha^{\pm(2a+1)} e^{\frac{\pi i b}{k}}. \quad \left( a = 0, 1, \dots, \left[ \frac{n-2}{2} \right]; b = 0, 1, \dots, 2k-1 \right)
\end{aligned} \tag{C.1.22}$$

## C.2 Exact expressions for $Z(N, k, 0, \zeta_2)$

The technique introduced in sec. C.1.1 allows us to compute the partition function of the mass deformed ABJM theory  $Z(N, k, 0, \zeta_2)$  with  $\zeta_1 = 0$  and for small integers  $N, k$ . We have computed  $Z(N, k, 0, \zeta_2)$  for  $(k=1, N \leq 12)$ ,  $(k=2, N \leq 9)$ ,  $(k=3, N \leq 5)$ ,  $(k=4, N \leq 5)$  and  $(k=6, N \leq 4)$ . Here we display the first few results ( $\alpha = e^{2\pi\zeta_2/k}$ ).

$$\begin{aligned}
Z(1, 1, 0, \zeta_2) &= \frac{\alpha}{2(1+\alpha^2)}, \quad Z(2, 1, 0, \zeta_2) = -\frac{\zeta_2 \alpha^3}{(1+\alpha^2)(1-\alpha^4)}, \\
Z(3, 1, 0, \zeta_2) &= \frac{\alpha^5(1+12\zeta_2\alpha - \alpha^2)}{8(1+\alpha^2)(1-\alpha^4)(1+\alpha^6)}, \quad \dots
\end{aligned} \tag{C.2.1}$$

$$\begin{aligned}
Z(1, 2, 0, \zeta_2) &= \frac{\alpha}{4(1+\alpha^2)}, \quad Z(2, 2, 0, \zeta_2) = \frac{\zeta_2^2 \alpha^4}{(1-\alpha^4)^2}, \\
Z(3, 2, 0, \zeta_2) &= \frac{\alpha^7(-1+4\zeta_2^2 + (2+32\zeta_2^2)\alpha^2 + (-1+4\zeta_2^2)\alpha^4)}{32(1+\alpha^4)(1-\alpha^4)^2(1+\alpha^6)}, \quad \dots
\end{aligned} \tag{C.2.2}$$

$$Z(1, 3, 0, \zeta_2) = \frac{\alpha}{6(1+\alpha^2)},$$

$$Z(2, 3, 0, \zeta_2) = \frac{\alpha^4(1+(1+4\zeta_2)\alpha + 4\zeta_2\alpha^2 + (-1+4\zeta_2)\alpha^7\alpha^3 - \alpha^4)}{12(1+\alpha)(1+\alpha^2)(1-\alpha^3)(1+\alpha^6)},$$

$$Z(3, 3, 0, \zeta_2) = -\frac{\alpha^8}{18\sqrt{3}(1+\alpha^6)^3(1-\alpha^6)}(2 + \sqrt{3}\zeta_2 - 3\sqrt{3}\alpha + (4 - 2\sqrt{3}\zeta_2)\alpha^2 + 3\sqrt{3}\zeta_2\alpha^4 + (-4 - 2\sqrt{3}\zeta_2)\alpha^6 + 3\sqrt{3}\alpha^7 + (-2 + \sqrt{3}\zeta_2)\alpha^8), \quad \dots \quad (\text{C.2.3})$$

$$Z(1, 4, 0, \zeta_2) = \frac{\alpha}{8(1+\alpha^2)}, \quad Z(2, 4, 0, \zeta_2) = \frac{\alpha^4(1 + (-2 - 8\zeta_2^2)\alpha^2 + \alpha^4)}{64(1+\alpha^4)(1-\alpha^4)^2},$$

$$Z(3, 4, 0, \zeta_2) = \frac{\alpha^9}{256(1-\alpha^2)^2(1+\alpha^2)^2(1+\alpha^4)^2(1+\alpha^6)(1+\alpha^8)}(5 + 8\zeta_2 + 4\zeta_2^2 + (-7 + 8\zeta_2)\alpha^2 + (5 - 8\zeta_2 + 4\zeta_2^2)\alpha^4 + (-6 - 32\zeta_2^2)\alpha^6 + (5 + 8\zeta_2 + 4\zeta_2^2)\alpha^8 + (-7 - 8\zeta_2)\alpha^{10} + (5 - 8\zeta_2 + 4\zeta_2^2)\alpha^{12}), \quad \dots \quad (\text{C.2.4})$$

$$Z(1, 6, 0, \zeta_2) = \frac{\alpha}{12(1+\alpha^2)}, \quad Z(2, 6, 0, \zeta_2) = \frac{\alpha^4(1 - 9\alpha^2 + 8(2 + 3\zeta_2^2)\alpha^4 - 9\alpha^6 + \alpha^8)}{432(1-\alpha^4)(1-\alpha^{12})},$$

$$Z(3, 6, 0, \zeta_2) = \frac{\alpha^9}{5184(1+\alpha^2)^2(-1+\alpha^6)^2(1+\alpha^6)(1+\alpha^{12})}(1 + (-54 - 32\sqrt{3}\zeta_2 - 24\zeta_2^2)\alpha^2 + (-15 - 64\sqrt{3}\zeta_2)\alpha^4 + (30 - 32\sqrt{3}\zeta_2 + 96\zeta_2^2)\alpha^6 + (76 + 192\zeta_2^2)\alpha^8 + (30 + 32\sqrt{3}\zeta_2 + 96\zeta_2^2)\alpha^{10} + (-15 + 64\sqrt{3}\zeta_2)\alpha^{12} + (-54 + 32\sqrt{3}\zeta_2 - 24\zeta_2^2)\alpha^{14} + \alpha^{16}), \quad \dots \quad (\text{C.2.5})$$

## C.2.1 Comparison with saddle-point approximation

Let us compare the exact partition function (C.2.1)-(C.2.5) with the result of the saddle-point approximation (4.3.29). In figure C.2 we plot the difference between two results

$$F_{\text{saddle-exact}} = \frac{\pi\sqrt{2k}}{3} \sqrt{1 + \frac{16\zeta_2^2}{k^2}} N^{\frac{3}{2}} - (-\log Z(N, k, 0, \zeta_2)) \quad (\text{C.2.6})$$

for  $k = 1, 2, 3, 4, 6$  and  $\zeta_2 = 1$ . The plot indicates  $F_{\text{saddle-exact}} \sim \sqrt{N}$  for large- $N$ , hence the leading part of the two results ( $\sim N^{3/2}$ ) agree with each other.

We can make a more refined comparison between the exact results and large- $N$  expansion as follows. First we notice that the saddle-point approximation (4.3.29) agree with the following expression in the large- $N$  limit

$$Z_{\text{pert}} = e^A C^{-\frac{1}{3}} \text{Ai}[C^{-\frac{1}{3}}(N - B)] \quad (\text{C.2.7})$$

where

$$C = \frac{2}{k\pi^2(1 + \frac{16\zeta_2^2}{k^2})}, \quad B = \frac{k}{24} - \frac{1}{6k} + \frac{1}{2k(1 + \frac{16\zeta_2^2}{k^2})},$$

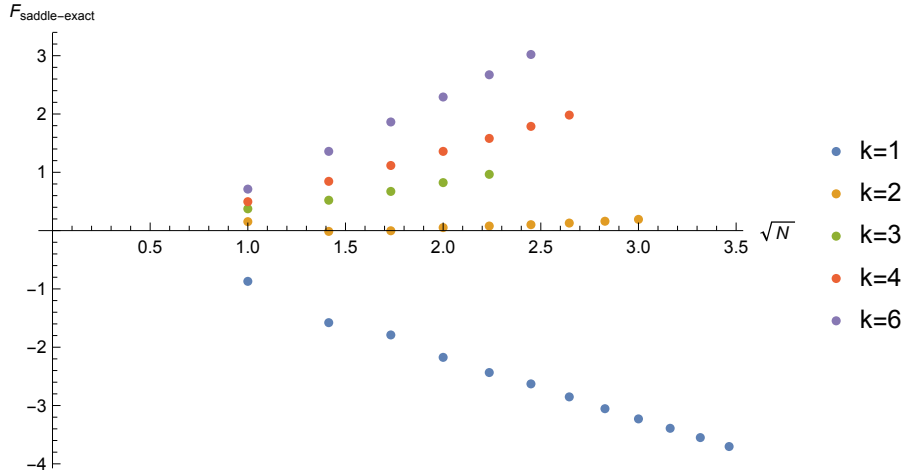


Figure C.2: Plot of  $F_{\text{saddle-exact}}$  (C.2.6) for  $k = 1, 2, 3, 4, 6$ ,  $\zeta_2 = 1$ . This is cited from our paper [3].

$$A = \frac{2A_{\text{ABJM}}(k) + A_{\text{ABJM}}(k + 4i\zeta_2) + A_{\text{ABJM}}(k - 4i\zeta_2)}{4}, \quad (\text{C.2.8})$$

which is obtained from the partition function of the ABJM theory with R-charge deformation by ignoring the large- $N$  non-perturbative effects ( $e^{-\sqrt{N}}$ ) and replacing the real deformation parameters  $\xi, \eta$  formally as  $\xi \rightarrow 0$ ,  $\eta \rightarrow 4i\zeta_2/k$  (see eq(1.4) in [77]). By comparing the numerical values of (C.2.1)-(C.2.5) and (C.2.7) we find good agreement. As an example, in figure C.3 we display the comparison of the free energy for  $\zeta_2 = 1$ .

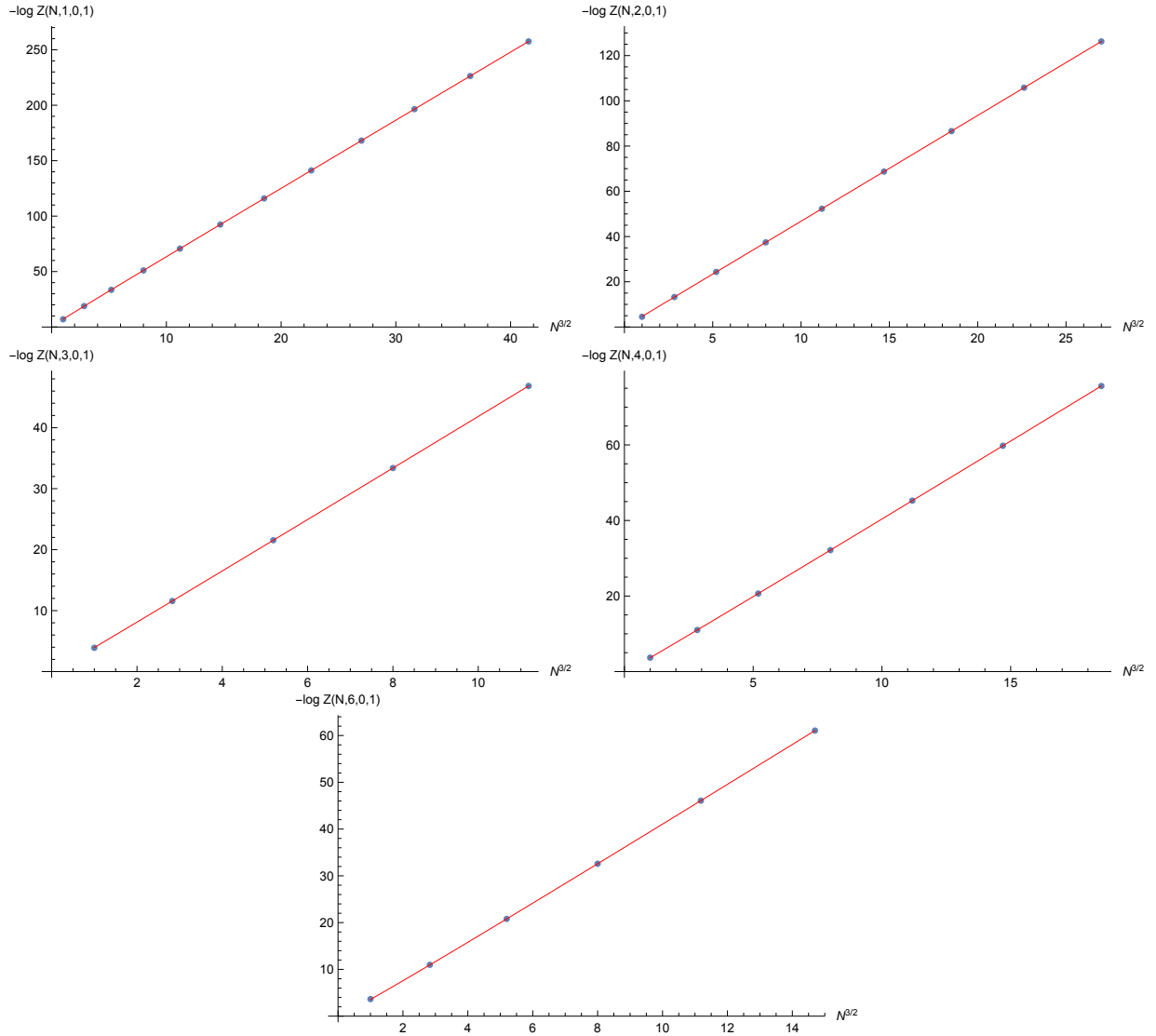


Figure C.3: Blue points: exact values of  $-\log Z(N, k, 0, \zeta_2)$  (C.2.1)-(C.2.5); Red line:  $-\log Z_{\text{pert}}(N)$  (C.2.7).



# Bibliography

- [1] T. Nosaka, K. Shimizu and S. Terashima, “Large  $N$  behavior of mass deformed ABJM theory,” *JHEP* **1603**, 063 (2016) [arXiv:1512.00249 [hep-th]].
- [2] T. Nosaka, K. Shimizu and S. Terashima, “Mass Deformed ABJM Theory on Three Sphere in Large  $N$  limit,” *JHEP* **1703** (2017) 121 [arXiv:1608.02654 [hep-th]].
- [3] M. Honda, T. Nosaka, K. Shimizu and S. Terashima, “Supersymmetry Breaking in a Large  $N$  Gauge Theory with Gravity Dual,” arXiv:1807.08874 [hep-th].
- [4] K. Shimizu and S. Terashima, “Supersymmetry Breaking Phase in three-dimensional Large  $N$  Gauge Theories,” *JHEP* **1811** (2018) 064 [arXiv:1809.03670 [hep-th]].
- [5] K. Shimizu, “Aspects of Massive Gauge Theories on Three Sphere in Infinite Mass Limit,” *JHEP* **1901** (2019) 090 [arXiv:1809.03679 [hep-th]].
- [6] R. D. Pisarski, “Chiral Symmetry Breaking in Three-Dimensional Electrodynamics,” *Phys. Rev. D* **29**, 2423 (1984).
- [7] T. Appelquist, D. Nash and L. C. R. Wijewardhana, “Critical Behavior in (2+1)-Dimensional QED,” *Phys. Rev. Lett.* **60**, 2575 (1988).
- [8] T. Appelquist and D. Nash, “Critical Behavior in (2+1)-dimensional QCD,” *Phys. Rev. Lett.* **64**, 721 (1990).
- [9] E. Witten, “String theory dynamics in various dimensions,” *Nucl. Phys. B* **443** (1995) 85 [hep-th/9503124].
- [10] O. Aharony, O. Bergman, D. L. Jafferis and J. Maldacena, “ $N=6$  superconformal Chern-Simons-matter theories, M2-branes and their gravity duals,” *JHEP* **0810** (2008) 091 doi:10.1088/1126-6708/2008/10/091 [arXiv:0806.1218 [hep-th]].
- [11] A. Barranco and J. G. Russo, “Large  $N$  phase transitions in supersymmetric Chern-Simons theory with massive matter,” *JHEP* **1403**, 012 (2014) [arXiv:1401.3672 [hep-th]].

- [12] J. G. Russo, G. A. Silva and M. Tierz, “Supersymmetric U(N) Chern-Simons-Matter Theory and Phase Transitions,” Commun. Math. Phys. **338**, no. 3, 1411 (2015) [arXiv:1407.4794 [hep-th]].
- [13] L. Anderson and K. Zarembo, “Quantum Phase Transitions in Mass-Deformed ABJM Matrix Model,” JHEP **1409**, 021 (2014) [arXiv:1406.3366 [hep-th]].
- [14] L. Anderson and J. G. Russo, “ABJM Theory with mass and FI deformations and Quantum Phase Transitions,” JHEP **1505**, 064 (2015) [arXiv:1502.06828 [hep-th]].
- [15] J. G. Russo and M. Tierz, “Quantum phase transition in many-flavor supersymmetric QED<sub>3</sub>,” Phys. Rev. D **95**, no. 3, 031901 (2017) [arXiv:1610.08527 [hep-th]].
- [16] L. Anderson and N. Drukker, “More Large  $N$  limits of 3d gauge theories,” J. Phys. A **50**, no. 34, 345401 (2017) [arXiv:1701.04409 [hep-th]].
- [17] L. Anderson and M. M. Roberts, “Mass deformed ABJM and  $\mathcal{PT}$  symmetry,” arXiv:1807.10307 [hep-th].
- [18] L. Santilli and M. Tierz, “Phase transitions and Wilson loops in antisymmetric representations in Chern-Simons-matter theory,” arXiv:1808.02855 [hep-th].
- [19] N. Seiberg, “Electric - magnetic duality in supersymmetric nonAbelian gauge theories,” Nucl. Phys. B **435**, 129 (1995) [hep-th/9411149].
- [20] D. Gaiotto and E. Witten, “Supersymmetric Boundary Conditions in N=4 Super Yang-Mills Theory,” J. Statist. Phys. **135**, 789 (2009) [arXiv:0804.2902 [hep-th]].
- [21] A. Kapustin, B. Willett and I. Yaakov, “Nonperturbative Tests of Three-Dimensional Dualities,” JHEP **1010**, 013 (2010) [arXiv:1003.5694 [hep-th]].
- [22] J. Bagger and N. Lambert, “Modeling Multiple M2’s,” Phys. Rev. D **75** (2007) 045020 [hep-th/0611108].
- [23] A. Gustavsson, “Algebraic structures on parallel M2-branes,” Nucl. Phys. B **811** (2009) 66 [arXiv:0709.1260 [hep-th]].
- [24] J. Bagger and N. Lambert, “Gauge symmetry and supersymmetry of multiple M2-branes,” Phys. Rev. D **77** (2008) 065008 [arXiv:0711.0955 [hep-th]].
- [25] J. Bagger and N. Lambert, “Comments on multiple M2-branes,” JHEP **0802** (2008) 105 [arXiv:0712.3738 [hep-th]].

- [26] S. Kim, “The Complete superconformal index for  $N=6$  Chern-Simons theory,” Nucl. Phys. B **821** (2009) 241 Erratum: [Nucl. Phys. B **864** (2012) 884] doi:10.1016/j.nuclphysb.2012.07.015, 10.1016/j.nuclphysb.2009.06.025 [arXiv:0903.4172 [hep-th]].
- [27] M. K. Benna, I. R. Klebanov and T. Klose, “Charges of Monopole Operators in Chern-Simons Yang-Mills Theory,” JHEP **1001**, 110 (2010) doi:10.1007/JHEP01(2010)110 [arXiv:0906.3008 [hep-th]].
- [28] A. Gustavsson and S. J. Rey, “Enhanced  $N=8$  Supersymmetry of ABJM Theory on  $R^{*8}$  and  $R^{*8}/Z(2)$ ,” arXiv:0906.3568 [hep-th].
- [29] O. K. Kwon, P. Oh and J. Sohn, “Notes on Supersymmetry Enhancement of ABJM Theory,” JHEP **0908**, 093 (2009) doi:10.1088/1126-6708/2009/08/093 [arXiv:0906.4333 [hep-th]].
- [30] D. Bashkirov and A. Kapustin, “Supersymmetry enhancement by monopole operators,” JHEP **1105**, 015 (2011) doi:10.1007/JHEP05(2011)015 [arXiv:1007.4861 [hep-th]].
- [31] O. Aharony, A. Hanany, K. A. Intriligator, N. Seiberg and M. J. Strassler, “Aspects of  $N=2$  supersymmetric gauge theories in three-dimensions,” Nucl. Phys. B **499**, 67 (1997) [hep-th/9703110].
- [32] B. Assel and S. Cremonesi, “The Infrared Physics of Bad Theories,” SciPost Phys. **3**, no. 3, 024 (2017) /SciPostPhys.3.3.024 [arXiv:1707.03403 [hep-th]].
- [33] B. Assel and S. Cremonesi, “The Infrared Fixed Points of 3d  $\mathcal{N} = 4$   $USp(2N)$  SQCD Theories,” arXiv:1802.04285 [hep-th].
- [34] J. de Boer, K. Hori and Y. Oz, “Dynamics of  $N=2$  supersymmetric gauge theories in three-dimensions,” Nucl. Phys. B **500** (1997) 163 [hep-th/9703100].
- [35] E. Witten, “Supersymmetric index of three-dimensional gauge theory,” In \*Shifman, M.A. (ed.): The many faces of the superworld\* 156-184 [hep-th/9903005].
- [36] K. Intriligator and N. Seiberg, “Aspects of 3d  $N=2$  Chern-Simons-Matter Theories,” JHEP **1307**, 079 (2013) [arXiv:1305.1633 [hep-th]].
- [37] K. Hosomichi, K. M. Lee, S. Lee, S. Lee and J. Park, “ $N=5,6$  Superconformal Chern-Simons Theories and M2-branes on Orbifolds,” JHEP **0809**, 002 (2008) doi:10.1088/1126-6708/2008/09/002 [arXiv:0806.4977 [hep-th]].

- [38] R. C. Myers, “Dielectric branes,” JHEP **9912** (1999) 022 doi:10.1088/1126-6708/1999/12/022 [hep-th/9910053].
- [39] I. Bena and N. P. Warner, “A Harmonic family of dielectric flow solutions with maximal supersymmetry,” JHEP **0412** (2004) 021 doi:10.1088/1126-6708/2004/12/021 [hep-th/0406145].
- [40] H. C. Kim and S. Kim, “Supersymmetric vacua of mass-deformed M2-brane theory,” Nucl. Phys. B **839** (2010) 96 doi:10.1016/j.nuclphysb.2010.06.002 [arXiv:1001.3153 [hep-th]].
- [41] S. Cheon, H. C. Kim and S. Kim, “Holography of mass-deformed M2-branes,” arXiv:1101.1101 [hep-th].
- [42] J. Gomis, D. Rodriguez-Gomez, M. Van Raamsdonk and H. Verlinde, “A Massive Study of M2-brane Proposals,” JHEP **0809**, 113 (2008) doi:10.1088/1126-6708/2008/09/113 [arXiv:0807.1074 [hep-th]].
- [43] H. Nastase, C. Papageorgakis and S. Ramgoolam, “The Fuzzy  $S^2$  structure of M2-M5 systems in ABJM membrane theories,” JHEP **0905**, 123 (2009) [arXiv:0903.3966 [hep-th]].
- [44] G. Festuccia and N. Seiberg, “Rigid Supersymmetric Theories in Curved Superspace,” JHEP **1106** (2011) 114 [arXiv:1105.0689 [hep-th]].
- [45] N. Hama, K. Hosomichi and S. Lee, “SUSY Gauge Theories on Squashed Three-Spheres,” JHEP **1105** (2011) 014 [arXiv:1102.4716 [hep-th]].
- [46] K. Hosomichi, “A Review on SUSY Gauge Theories on  $S^3$ ,” doi:10.1007/978-3-319-18769-3\_10 arXiv:1412.7128 [hep-th].
- [47] V. Pestun *et al.*, “Localization techniques in quantum field theories,” J. Phys. A **50** (2017) no.44, 440301 [arXiv:1608.02952 [hep-th]].
- [48] N. A. Nekrasov, “Seiberg-Witten prepotential from instanton counting,” Adv. Theor. Math. Phys. **7** (2003) 5, 831 doi:10.4310/ATMP.2003.v7.n5.a4 [hep-th/0206161].
- [49] V. Pestun, “Localization of gauge theory on a four-sphere and supersymmetric Wilson loops,” Commun. Math. Phys. **313** (2012) 71 doi:10.1007/s00220-012-1485-0 [arXiv:0712.2824 [hep-th]].
- [50] A. Kapustin, B. Willett and I. Yaakov, “Exact Results for Wilson Loops in Superconformal Chern-Simons Theories with Matter,” JHEP **1003** (2010) 089 [arXiv:0909.4559 [hep-th]].

- [51] D. L. Jafferis, “The Exact Superconformal R-Symmetry Extremizes Z,” JHEP **1205** (2012) 159 [arXiv:1012.3210 [hep-th]].
- [52] N. Hama, K. Hosomichi and S. Lee, “Notes on SUSY Gauge Theories on Three-Sphere,” JHEP **1103** (2011) 127 [arXiv:1012.3512 [hep-th]].
- [53] J. Källén and M. Zabzine, “Twisted supersymmetric 5D Yang-Mills theory and contact geometry,” JHEP **1205** (2012) 125 [arXiv:1202.1956 [hep-th]].
- [54] K. Hosomichi, R. K. Seong and S. Terashima, “Supersymmetric Gauge Theories on the Five-Sphere,” Nucl. Phys. B **865** (2012) 376 [arXiv:1203.0371 [hep-th]].
- [55] F. Benini and S. Cremonesi, “Partition Functions of  $\mathcal{N} = (2, 2)$  Gauge Theories on  $S^2$  and Vortices,” Commun. Math. Phys. **334** (2015) no.3, 1483 [arXiv:1206.2356 [hep-th]].
- [56] F. Benini and W. Peelaers, “Higgs branch localization in three dimensions,” JHEP **1405** (2014) 030 [arXiv:1312.6078 [hep-th]].
- [57] M. Fujitsuka, M. Honda and Y. Yoshida, “Higgs branch localization of 3d  $\mathcal{N} = 2$  theories,” PTEP **2014** (2014) no.12, 123B02 [arXiv:1312.3627 [hep-th]].
- [58] A. Kapustin, B. Willett and I. Yaakov, “Nonperturbative Tests of Three-Dimensional Dualities,” JHEP **1010** (2010) 013 [arXiv:1003.5694 [hep-th]].
- [59] B. Willett and I. Yaakov, “N=2 Dualities and Z Extremization in Three Dimensions,” arXiv:1104.0487 [hep-th].
- [60] A. G. Bytsko and J. Teschner, “Quantization of models with non-compact quantum group symmetry: Modular XXZ magnet and lattice sinh-Gordon model,” J. Phys. A **39**, 12927 (2006) doi:10.1088/0305-4470/39/41/S11 [hep-th/0602093].
- [61] Y. Hatsuda, “ABJM on ellipsoid and topological strings,” JHEP **1607**, 026 (2016) doi:10.1007/JHEP07(2016)026 [arXiv:1601.02728 [hep-th]].
- [62] C. Closset, T. T. Dumitrescu, G. Festuccia, Z. Komargodski and N. Seiberg, “Contact Terms, Unitarity, and F-Maximization in Three-Dimensional Superconformal Theories,” JHEP **1210**, 053 (2012) [arXiv:1205.4142 [hep-th]].
- [63] C. Closset, T. T. Dumitrescu, G. Festuccia, Z. Komargodski and N. Seiberg, “Comments on Chern-Simons Contact Terms in Three Dimensions,” JHEP **1209**, 091 (2012) [arXiv:1206.5218 [hep-th]].

- [64] C. Closset, T. T. Dumitrescu, G. Festuccia and Z. Komargodski, “Supersymmetric Field Theories on Three-Manifolds,” JHEP **1305**, 017 (2013) [arXiv:1212.3388 [hep-th]].
- [65] K. A. Intriligator and N. Seiberg, “Mirror symmetry in three-dimensional gauge theories,” Phys. Lett. B **387** (1996) 513 [hep-th/9607207].
- [66] V. Niarchos, “Seiberg dualities and the 3d/4d connection,” JHEP **1207**, 075 (2012) [arXiv:1205.2086 [hep-th]].
- [67] I. Yaakov, “Redeeming Bad Theories,” JHEP **1311**, 189 (2013) [arXiv:1303.2769 [hep-th]].
- [68] O. Aharony, S. S. Razamat, N. Seiberg and B. Willett, “3d dualities from 4d dualities,” JHEP **1307**, 149 (2013) [arXiv:1305.3924 [hep-th]].
- [69] A. Amariti, “A note on 3D  $\mathcal{N} = 2$  dualities: real mass flow and partition function,” JHEP **1403**, 064 (2014) [arXiv:1309.6434 [hep-th]].
- [70] A. Giveon and D. Kutasov, “Seiberg Duality in Chern-Simons Theory,” Nucl. Phys. B **812**, 1 (2009) [arXiv:0808.0360 [hep-th]].
- [71] M. Tierz, “Wilson loops and free energies in 3d  $\mathcal{N} = 4$  SYM: exact results, exponential asymptotics and duality,” arXiv:1804.10845 [hep-th].
- [72] Y. Fyodorov and B. Khoruzhenko, “A few remarks on colour-flavour transformations, truncations of random unitary matrices, Berezin reproducing kernels and Selberg-type integrals, ” J. Phys. A **40**, 669-700, (2007) [arXiv:math-ph/0610045].
- [73] D. Z. Freedman and S. S. Pufu, “The holography of  $F$ -maximization,” JHEP **1403** (2014) 135 doi:10.1007/JHEP03(2014)135 [arXiv:1302.7310 [hep-th]].
- [74] D. L. Jafferis, I. R. Klebanov, S. S. Pufu and B. R. Safdi, “Towards the F-Theorem:  $N=2$  Field Theories on the Three-Sphere,” JHEP **1106**, 102 (2011) [arXiv:1103.1181 [hep-th]].
- [75] C. P. Herzog, I. R. Klebanov, S. S. Pufu and T. Tesileanu, “Multi-Matrix Models and Tri-Sasaki Einstein Spaces,” Phys. Rev. D **83**, 046001 (2011) [arXiv:1011.5487 [hep-th]].
- [76] M. Marino and P. Putrov, “ABJM theory as a Fermi gas,” J. Stat. Mech. **1203** (2012) P03001 doi:10.1088/1742-5468/2012/03/P03001 [arXiv:1110.4066 [hep-th]].
- [77] T. Nosaka, “Instanton effects in ABJM theory with general R-charge assignments,” JHEP **1603** (2016) 059 doi:10.1007/JHEP03(2016)059 [arXiv:1512.02862 [hep-th]].
- [78] K. Okuyama and S. Zakany, “TBA-like integral equations from quantized mirror curves,” JHEP **1603** (2016) 101 doi:10.1007/JHEP03(2016)101 [arXiv:1512.06904 [hep-th]].

- [79] C. A. Tracy and H. Widom, “Proofs of two conjectures related to the thermodynamic Bethe ansatz,” *Commun. Math. Phys.* **179** (1996) 667 doi:10.1007/BF02100102 [solvent/9509003].
- [80] P. Putrov and M. Yamazaki, “Exact ABJM Partition Function from TBA,” *Mod. Phys. Lett. A* **27** (2012) 1250200 doi:10.1142/S0217732312502008 [arXiv:1207.5066 [hep-th]].
- [81] A. Grassi and M. Marino, *JHEP* **1502** (2015) 115 doi:10.1007/JHEP02(2015)115 [arXiv:1403.4276 [hep-th]].
- [82] Y. Hatsuda, M. Honda and K. Okuyama, “Large  $N$  non-perturbative effects in  $\mathcal{N} = 4$  superconformal Chern-Simons theories,” *JHEP* **1509**, 046 (2015) doi:10.1007/JHEP09(2015)046 [arXiv:1505.07120 [hep-th]].
- [83] S. Terashima, “On M5-branes in  $N=6$  Membrane Action,” *JHEP* **0808**, 080 (2008) [arXiv:0807.0197 [hep-th]].
- [84] C. Closset, H. Kim and B. Willett, “Supersymmetric partition functions and the three-dimensional A-twist,” *JHEP* **1703**, 074 (2017) doi:10.1007/JHEP03(2017)074 [arXiv:1701.03171 [hep-th]].
- [85] C. Closset, H. Kim and B. Willett, “Seifert fibering operators in 3d  $\mathcal{N} = 2$  theories,” arXiv:1807.02328 [hep-th].
- [86] I. Affleck, J. A. Harvey and E. Witten, “Instantons and (Super)Symmetry Breaking in (2+1)-Dimensions,” *Nucl. Phys. B* **206**, 413 (1982). doi:10.1016/0550-3213(82)90277-2
- [87] C. Toldo and B. Willett, “Partition functions on 3d circle bundles and their gravity duals,” *JHEP* **1805**, 116 (2018) doi:10.1007/JHEP05(2018)116 [arXiv:1712.08861 [hep-th]].
- [88] D. Gang and N. Kim, “Large  $N$  twisted partition functions in 3d-3d correspondence and Holography,” arXiv:1808.02797 [hep-th].
- [89] O. Bergman, A. Hanany, A. Karch and B. Kol, “Branes and supersymmetry breaking in three-dimensional gauge theories,” *JHEP* **9910**, 036 (1999) [hep-th/9908075].
- [90] K. Ohta, “Supersymmetric index and s rule for type IIB branes,” *JHEP* **9910** (1999) 006 doi:10.1088/1126-6708/1999/10/006 [hep-th/9908120].
- [91] T. Morita and V. Niarchos, “F-theorem, duality and SUSY breaking in one-adjoint Chern-Simons-Matter theories,” *Nucl. Phys. B* **858**, 84 (2012) [arXiv:1108.4963 [hep-th]].

- [92] T. Suyama, “Supersymmetry Breaking in Chern-Simons-matter Theories,” *JHEP* **1207** (2012) 008 doi:10.1007/JHEP07(2012)008 [arXiv:1203.2039 [hep-th]].
- [93] T. Suyama, “Supersymmetry Breaking and Planar Free Energy in Chern-Simons-matter Theories,” arXiv:1405.7469 [hep-th].
- [94] C. A. Tracy and H. Widom, “Proofs of two conjectures related to the thermodynamic Bethe ansatz,” *Commun. Math. Phys.* **179**, 667 (1996) doi:10.1007/BF02100102 [solv-int/9509003].
- [95] Y. Hatsuda, S. Moriyama and K. Okuyama, “Exact Results on the ABJM Fermi Gas,” *JHEP* **1210**, 020 (2012) doi:10.1007/JHEP10(2012)020 [arXiv:1207.4283 [hep-th]].
- [96] Y. Hatsuda, S. Moriyama and K. Okuyama, “Instanton Effects in ABJM Theory from Fermi Gas Approach,” *JHEP* **1301**, 158 (2013) doi:10.1007/JHEP01(2013)158 [arXiv:1211.1251 [hep-th]].
- [97] S. Matsumoto and S. Moriyama, “ABJ Fractional Brane from ABJM Wilson Loop,” *JHEP* **1403**, 079 (2014) doi:10.1007/JHEP03(2014)079 [arXiv:1310.8051 [hep-th]].
- [98] M. Honda and K. Okuyama, “Exact results on ABJ theory and the refined topological string,” *JHEP* **1408**, 148 (2014) doi:10.1007/JHEP08(2014)148 [arXiv:1405.3653 [hep-th]].
- [99] Y. Hatsuda and K. Okuyama, “Probing non-perturbative effects in M-theory,” *JHEP* **1410**, 158 (2014) doi:10.1007/JHEP10(2014)158 [arXiv:1407.3786 [hep-th]].
- [100] S. Moriyama and T. Nosaka, “Partition Functions of Superconformal Chern-Simons Theories from Fermi Gas Approach,” *JHEP* **1411**, 164 (2014) doi:10.1007/JHEP11(2014)164 [arXiv:1407.4268 [hep-th]].
- [101] S. Moriyama and T. Nosaka, “Exact Instanton Expansion of Superconformal Chern-Simons Theories from Topological Strings,” *JHEP* **1505**, 022 (2015) doi:10.1007/JHEP05(2015)022 [arXiv:1412.6243 [hep-th]].
- [102] S. Moriyama, S. Nakayama and T. Nosaka, “Instanton Effects in Rank Deformed Superconformal Chern-Simons Theories from Topological Strings,” *JHEP* **1708**, 003 (2017) doi:10.1007/JHEP08(2017)003 [arXiv:1704.04358 [hep-th]].
- [103] K. Okuyama, “A Note on the Partition Function of ABJM theory on  $S^3$ ,” *Prog. Theor. Phys.* **127** (2012) 229 doi:10.1143/PTP.127.229 [arXiv:1110.3555 [hep-th]].



- [104] J. G. Russo and G. A. Silva, “Exact partition function in  $U(2) \times U(2)$  ABJM theory deformed by mass and Fayet-Iliopoulos terms,” JHEP **1512** (2015) 092 doi:10.1007/JHEP12(2015)092 [arXiv:1510.02957 [hep-th]].
- [105] M. Hanada, M. Honda, Y. Honma, J. Nishimura, S. Shiba and Y. Yoshida, “Numerical studies of the ABJM theory for arbitrary N at arbitrary coupling constant,” JHEP **1205** (2012) 121 doi:10.1007/JHEP05(2012)121 [arXiv:1202.5300 [hep-th]].
- [106] N. Drukker, M. Marino and P. Putrov, “Nonperturbative aspects of ABJM theory,” JHEP **1111**, 141 (2011) doi:10.1007/JHEP11(2011)141 [arXiv:1103.4844 [hep-th]].
- [107] A. Cagnazzo, D. Sorokin and L. Wulff, “String instanton in AdS(4) x CP\*\*3,” JHEP **1005**, 009 (2010) doi:10.1007/JHEP05(2010)009 [arXiv:0911.5228 [hep-th]].
- [108] T. Morita and V. Niarchos, “F-theorem, duality and SUSY breaking in one-adjoint Chern-Simons-Matter theories,” Nucl. Phys. B **858** (2012) 84 doi:10.1016/j.nuclphysb.2012.01.003 [arXiv:1108.4963 [hep-th]].
- [109] M. Marino, “Lectures on localization and matrix models in supersymmetric Chern-Simons-matter theories,” J. Phys. A **44**, 463001 (2011) [arXiv:1104.0783 [hep-th]].
- [110] Brézin, C. Itzykson, G. Parisi and J. B. Zuber, “Planar Diagrams,” Commun.Math. Phys. (1978) 59: 35.
- [111] T. Suyama, “On Large N Solution of N=3 Chern-Simons-adjoint Theories,” Nucl. Phys. B **867** (2013) 887 [arXiv:1208.2096 [hep-th]].
- [112] B. R. Safdi, I. R. Klebanov and J. Lee, “A Crack in the Conformal Window,” JHEP **1304**, 165 (2013) [arXiv:1212.4502 [hep-th]].